TRANSPORTATION RESEARCH
RECORD

No. 1478

Materials and Construction

Concrete and Concrete Pavement Construction

A peer-reviewed publication of the Transportation Research Board

TRANSPORTATION RESEARCH BOARD
NATIONAL RESEARCH COUNCIL

NATIONAL ACADEMY PRESS
WASHINGTON, D.C. 1995

Transportation Research Record 1478
ISSN 0361-1981
ISBN 0-309-06116-4
Price: $27.00

Subscriber Category
IIIB materials and construction

Printed in the United States of America

Sponsorship of Transportation Research Record 1478

GROUP 2—DESIGN AND CONSTRUCTION OF TRANSPORTATION FACILITIES
Chairman: Michael G. Katona, U.S. Air Force Armstrong Laboratory

Concrete Section
Chairman: H. Celik Ozyildirim, Virginia Department of Transportation

Committee on Performance of Concrete
Chairman: Steven A. Ragan, U.S. Army Corps of Engineers Waterways Experiment Station
Jamshid M. Armaghani, M. Arockiasamy, Philip D. Cady, William P. Chamberlin, Glenn William De Puy, Philip H. DeCabooter, John W. Figg, Robert J. Girard, Kenneth C. Hover, Joseph F. Lamond, James W. Mack, Richard C. Meininger, Roger P. Northwood. John T. Paxton, V. Ramakrishnan, John Ryell, David Stark, Joyce M. Susa, Richard Edwin Weyers

Committee on Mechanical Properties of Concrete
Chairman: S. P. Shah, Northwestern University
Shuaib Ahmad, Archie F. Carter, Jr., Mark E. Felag, Robert J. Girard, W. Charles Greer, Jr., James D. Grove, Lloyd E. Hackman, Louis A. Kuhlmann, Joseph F. Lamond, Colin Lobo, V. M. Malhotra, Edward G. Nawy, Steven A. Ragan, V. Ramakrishnan, Masood Rasoulian, Gary L. Robson, M. Reza Salami, Charles F. Scholer, Raymond J. Schutz, James M. Shilstone, Sr., Parviz Soroushian, Michael M. Sprinkel, D. Gerry Walters, Dan G. Zollinger

Committee on Admixtures and Cementitious Materials for Concrete
Chairman: V. Ramakrishnan, South Dakota School of Mines
Milton D. Anderson, P. Balaguru, Tom Blackstock, Bernard C. Brown, John W. Bugler, W. Barry Butler, Ramon L. Carrasquillo, Edward Gannon, Jose Garcia, Robert Douglas Hooton, Chao-Lung Hwang, Daniel P. Johnston, Kamal Henri Khayat, Louis A. Kuhlmann, Clifford N. MacDonald, Stella L. Marusin, Frances A. McNeal, Yoshihiko Ohama, P. Paramasivam, D. V. Reddy, John J. Schemmel, A. Haleem Tahir, Suneel N. Vanikar, Ming L. Wang, Thomas G. Weil, David A. Whiting, Robert C. Zellers

Construction Section
Chairman: Donn E. Hancher, University of Kentucky

Committee on Portland Cement Concrete Pavement Construction
Chairman: Sanford P. Lahue, American Concrete Pavement Association
Curt A. Beckemeyer, Archie F. Carter, Jr., Yves Charonnat, Lawrence W. Cole, Michael I. Darter, Howard J. Durham, John E. Eisenhour, Jr., Ronald M. Guntert, Jr., Jim W. Hall, Jr., Ira J. Huddleston, Lon S. Ingram, Carlos Kraemer, Louis R. Marais, John E. McChord, Jr., Dennis A. Morian, Wayne F. Murphy, Theodore L. Neff, M. Lee Powell III, Carl W. Rapp, Terry W. Sherman, William L. Trimm, Steven L. Tritsch, Dan G. Zollinger

Transportation Research Board Staff
Robert E. Spicher, Director, Technical Activities
Frederick D. Hejl, Engineer of Materials and Construction
Nancy A. Ackerman, Director, Reports and Editorial Services
Marianna Rigamer, Oversight Editor

Sponsorship is indicated by a footnote at the end of each paper. The organizational units, officers, and members are as of December 31, 1994.

Transportation Research Record 1478

Contents

Foreword

The papers in this volume deal with various facets of concrete technology and concrete pavement construction. They should be of interest to state and local construction, design, materials, and research engineers as well as contractors and material producers.

The first six papers address concrete materials technology. Leek et al., Roy et al., Mokhtarzadeh et al., and Pleau et al. report on high-performance concrete. Signore and Roesler discuss the use of fiber optic sensing techniques to examine transportation materials and facilities. Abou-Zeid et al. report on the use of Type C fly ash and limestone in silicious sand-gravel concrete to minimize durability problems in Kansas.

The last seven papers address concrete pavement construction. Cole and Okamoto, Smith and McWaters, Reed, and Jones and Hermann discuss designing for quality construction of concrete pavements. Hall reports on early strength testing of concrete cores and cylinders. Wade et al. discuss the monitoring of European concrete pavements. Cramer et al. discuss the effect of optimizing total aggregate gradation on Wisconsin portland cement concrete pavements.

PART 1

Concrete

Specification and Production of Durable Reinforced Concrete

DARRELL S. LEEK, ANN M. HARPER, AND CHRISTOPHER R. ECOB

A durability design method that has been used to quantify the requirements for reinforced concrete is described. It specifies the data required and decisions that need to be taken to achieve the specified performance. Codes and standards currently used for design are insufficient to ensure the long-term durability of structures in aggressive environments. Specific environmental data are a prerequisite for the modeling processes used to predict the performance of different mix designs. Selecting suitable materials is vital to ensure that performance is achieved and may necessitate that the concrete producer adopt more stringent performance requirements than those demanded by the specification. Mix design trials must consider the performance aspects of the specification and particular site characteristics. In extremely severe environments, concrete alone may not be sufficient to ensure durability performance, and additional protective measures may be necessary.

Quantitative analysis based on the measurement of physical properties has been used in the structural design of reinforced concrete for many years. Durability design, however, has been largely empirical, based on standards and codes that have been modified only in response to increasing numbers of structural failures (*1*). Although this approach may be satisfactory for conventional structures in normal environments, it is inappropriate for major structures in unusually severe environments.

To determine the likely mechanisms of deterioration, quantitative design of reinforced concrete for durability must be based on (a) the assessment of the design life requirements of the structure and (b) the thorough characterization of internal and external environments to which it will be subjected.

With the ever increasing costs of construction, the required durability of structures (i.e., the time before an item fails or requires unacceptable expenditure on maintenance to sustain performance) is also increasing. The current British Standard (BS) for structural concrete, BS 8110 (*2*), has an implicit design life of 60 years. Highway structures designed in accordance with the U.K. Department of Transport specification (*3*) have an expected life of 120 years, and recent examples of structures in North America are required to be durable for 100 years.

To quantify local concentrations of acidic gases and depassivating ions, and so forth, reliable environmental data can only be obtained from systematic site investigation. The risk of attack can then be characterized for each structural element. It is essential not to ignore or underestimate the synergism of deteriorating factors, for example, the release of bound chlorides by the carbonation of the cement paste.

The properties of the concrete constituents should be considered in terms of their individual performance and their collective effects on the structure. For example, cement with a high alkali content and a reactive aggregate may, individually, perform adequately as concreting materials; however, the combination of the two may prove disastrous. The thermal behavior of the concrete and the possible incompatibility of the components can also have a major influence on the overall durability of a structure.

Predictions of the time to structural damage can be made by modeling different concrete mix designs with varying proportions of mix constituents, total porosity, depth of cover and so forth. Thus the properties required to limit the ingress of these aggressive substances into concrete can be evaluated and the likely long-term performance of the structure more accurately predicted.

In extremely aggressive environments, the use of concrete alone may not be sufficient to ensure that the required design life is achieved. In such cases it is necessary to enhance the durability of the concrete and any embedded steel reinforcement by influencing the factors that control the rate of deterioration. The design and use of very low-permeability, high-resistivity concrete limit the magnitude of corrosion currents that can pass between adjacent bars. Experimental work (*4*) has shown that the application of nonconductive coatings to either the concrete or the reinforcement provides a physical barrier to aggressive species. The use of coated reinforcement can also limit the size and distribution of active sites, with corrosion only able to initiate at imperfections.

The approach described in this paper was developed over many years from specifying and testing high-quality concrete. It establishes the specific requirements for structures in particular environments. It does not provide general requirements for all structures because this may result in (a) over-specification in benign environments, which would be costly for the contractor, or (b) underspecification in aggressive environments, which could be very expensive for the structure owner. The strategy described here was adopted for the design and specification of concrete on major projects around the world, including the Channel Tunnel (U.K.), Storebaelt Tunnel (Denmark), St. Clair River Tunnel (U.S.-Canada), and the Lantau Fixed Crossing (Hong Kong).

DETERIORATION OF REINFORCED CONCRETE

Most reinforced concrete around the world performs adequately and gives few problems. A few structures have deteriorated as a result of either the action of aggressive components from the external environment or incompatibility of the particular mix constituents. Problems can arise as a result of incomplete or inaccurate site investigation, poor design, badly specified concrete, poor workmanship, and a range of other factors. The mechanisms of deterioration are primarily chemico-physical (i.e., a chemical reaction with the formation of products greater in volume than the reactants producing physical effects, such as cracking and spalling) and occur in three discrete stages, as shown in Figure 1 (*5*).

Mott MacDonald Ltd., Special Services Division, St. Anne House, 20–26 Wellesley Road, Croydon, Surrey, England CR9 2UL.

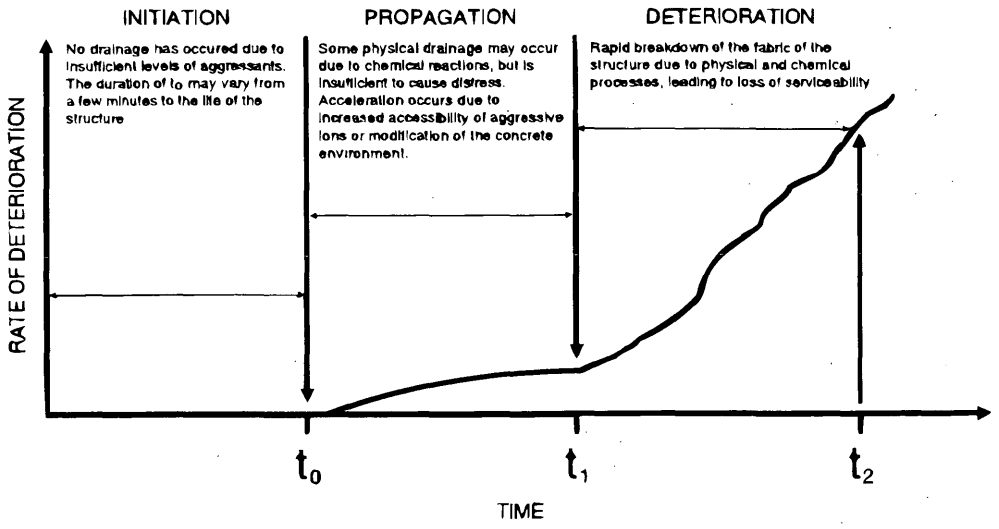

FIGURE 1 General model of the chemico-physical deterioration of concrete.

- Stage 1: Initiation (t_0)—Concentration of aggressive species is insufficient to initiate any chemical reactions, or the chemical reaction is occurring slowly. No physical damage has occurred. The duration of t_0 may vary from a few minutes to the design life of the structure.
- Stage 2: Propagation (t_1)—Chemical reactions begin or are continuing. Some physical damage may occur, but it is insufficient to cause distress. Acceleration of the deterioration process usually occurs during this stage because of increased accessibility of aggressive ions or modification of the concrete environment.
- Stage 3: Deterioration (t_2)—Breakdown of the fabric of the structure is rapid. The combined effects of the physical and chemical processes are of sufficient severity that the structure is no longer serviceable (failure occurs), and major remedial work or, in extreme cases, demolition is required.

Deterioration may occur as a result of a number of mechanisms on which a large body of literature already exists (*6,7*). These mechanisms include

- Corrosion of reinforcement because of chloride ions, carbonation, and change in the rebar environment (e.g., impinging cracks);
- Sulfate attack of concrete;
- Soft water or acid attack of concrete;
- Alkali aggregate reaction (AAR);
- Other aggregate quality problems, such as popouts, abrasion resistance, and D-cracking;
- Thermal incompatibility of concrete components;
- Shrinkage; and
- Frost damage.

The factors must be considered during design and specification(*8*).

SPECIFICATION OF CONCRETE

Current Methods of Design and Specification for Durability

The design and specification of most structural concrete is carried out in accordance with codified recommendations based on past experience and accepted good practice at the time of writing. Therefore innovative techniques and materials can only be incorporated after relatively long periods and as experience of their successful application increases.

The requirements for a durable concrete mix design, primarily in terms of strength, are detailed and many other properties that influence durability are ignored in works by the British Standards Institution (*2,9*). Water to cement (w-c) ratio, minimum cement content, and depth of cover to reinforcement are defined for concrete in relation to various grades of environmental exposure from mild to extreme. The inability of this system always to work satisfactorily, particularly in severe environments, is demonstrated by the number of structures that fail within their design life.

Fundamental questions concerning rates of deterioration in a given environment, such as the rate of penetration of aggressive species, cannot be predicted using this approach. It is therefore not possible to reliably estimate the duration of each stage of deterioration and hence obtain the likely maintenance-free life of the structure.

The properties of individual components are often covered by their own standards, which occasionally conflict with codes for the specification of concrete. For example, BS 12:Ordinary Portland Cement (*10*) allows concrete to contain up to 0.1 percent Cl^- by mass, while BS 8110 states that for prestressed concrete, the maximum allowable Cl^- concentration is 0.1 percent by mass of cement. This makes compliance with the specification difficult, or impossible, to achieve.

By specifying fixed levels of aggressive ions that may be incorporated in the concrete, it is possible for the initiation stage in the deterioration process to be completely eliminated. For example, the level of acid-soluble chloride necessary to initiate the corrosion of reinforcement in OPC concrete is widely regarded as being 0.4 percent (by mass of cement), yet this is specified as the maximum allowable level in accordance with BS 8110. American Concrete Institute (ACI) codes (*11*) permit only 0.2 percent acid-soluble chloride in conventional reinforced concrete, thus extending the duration of the initiation period and increasing the time to first damage of the structure.

The use of inappropriate standards for the design of structures has also led to problems of concrete durability. In the United Kingdom, the use of BS 8007 (*12*) to limit crack widths in structures designed

to retain aqueous liquids has frequently been specified for the design of structures that retain aggressive liquids, although the standard clearly states that it is not applicable for use with such fluids.

Although there are clearly problems associated with the use of codes and standards, this approach works reasonably well for everyday, nonaggressive environments. Where structures of major importance are to be exposed to severe environments, a different approach must be adopted based on the detailed classification of the environment and the fundamental properties of the structural materials.

Characterisation of Service Environment

Current British Standards classify the service environment of the concrete into five groups based on exposure to moisture, chloride, and frost action. This type of approach, classifying environments on moisture content and exposure to deicing salts, seawater, and chemical attack, with or without freezing is followed elsewhere (*13*). However, none of these parameters is quantified in terms of concentration or number of cycles of action. Quantification of environmental parameters is essential if durability design is to be successful. The classification of environments for acid and sulfate attack by the U.K. Building Research Establishment (BRE) (*7*) partly satisfies this requirement in that five classes and two subclasses are defined with relation to the concentrations of aggressive anions and cations present in the soil or groundwater. ACI (*14*) also follows this type of approach by specifying for exposure classes related to sulfate concentration and recommends suitable cement types for use in them.

This type of approach should also be followed to classify environments for other potential mechanisms of deterioration. Rigorous site investigation must be undertaken to collect the necessary specific data on groundwater compositions and other environmental factors, for example:

- Ionic concentrations in the ground, groundwater, and atmosphere;
- pH of groundwater, hydrostatic pressure, and any rate of flow data;
- Temperature variation, including numbers of freezing cycles;
- Relative humidity variation;
- Rainfall; and
- Presence of organic compounds.

These factors will vary from site to site. For example, the principal durability considerations for the Channel Tunnel were sea water strength chloride ion concentrations [approximately 18,000 mg/l (ppm)] and a maximum hydrostatic pressure of 2 bar (equivalent to 20 m of water). The initial investigations for the St. Clair River Tunnel indicated the possibility of very high concentrations of chloride ions in the strata adjacent to the tunnel, up to 175,000 mg/l (ppm) were reported. The Tsing Ma suspension bridge (Lantau Fixed Crossing) was to operate in warm saline conditions, 19,000 mg/l (ppm), with temperature varying from 7°C to 35°C (see Figure 2) and to have a number of large concrete pours. Also of importance is the orientation of a particular structure on a site and the influence of design in the inadvertent formation of corrosive microenvironments where, for example, high concentrations of aggressive ions accumulate.

The internal environment likely to occur within the structure when it is in service also affects the durability of the concrete. For example, the concrete lining of a tunnel may be cool and water saturated at the extrados and hot and dry (e.g., Channel tunnel, 40°C, 25 percent RH) at the intrados. The concrete should be designed to accommodate both of these environments. The behavior of concrete in structures with environments similar to those expected (particularly the internal environment) should be examined to obtain basic performance data.

Factors That Affect Concrete Durability

Concrete can be thought of as a four-component system consisting of aggregate, cement paste, void space (porosity), and pore solution that fully or partially fills the void space. The durability of good-

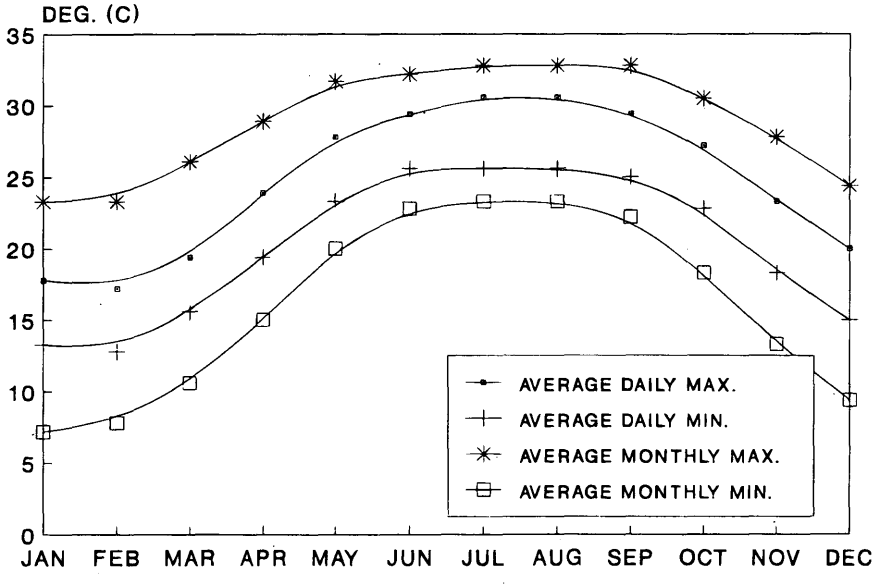

FIGURE 2 Climatic data for Hong Kong.

quality concrete is dominated by the paste fraction, pore solutions, and void space, with the aggregate remaining largely inert. The physical structure of the cement paste consists of a complex interlocking network of crystalline and gel phase material with spaces (pores) within and between them. The pore solution is primarily an alkaline solution with a pH generally of more than 12.4. It is this alkalinity that provides the means by which steel reinforcement is protected through the stabilization of a passive oxide film on the metal surface.

The bulk of the concrete acts as a physical barrier to the ingress of aggressive ions from the external environment. Ions can migrate into concrete by a number of mechanisms (*15*), such as

- Permeation under a pressure gradient,
- Diffusion across a chemical gradient in both the liquid and gaseous states,
- Capillary suction (sorption), and
- Wetting and drying cycles.

Ionic movement through solids is extremely slow; hence the factors that influence the rate of transport are concerned with the void space within the paste matrix. The paste density, (i.e., quantity of hydrates per unit volume) determines the porosity, permeability, pore size distribution, and pore tortuosity. All of these factors influence the rate of migration, as does the degree of water saturation of the concrete. Gaseous aggressants migrate more slowly through the liquid phase in water-filled pores than in the gaseous state through open pores.

The rate of migration of ions through concrete can be described by appropriate coefficients that depend on the physical properties of the paste and that can be used to model the ingress processes. The composition of the paste and pore fluid influences the rate and extent of deleterious chemical reactions by limiting the quantities of reactants or adjusting the reaction conditions, or both, such that some reactions are not thermodynamically favorable.

The final feature that determines durability is the strength of the concrete, particularly its tensile strength. The higher the tensile strength of the concrete the more resistant it will be to the stresses generated by the deleterious reactions.

Modeling Concrete Behavior

Figure 3 shows the stages that must be undertaken when modeling concrete to arrive at a rational basis for specification. The design life requirement of the structure must be clearly established so that the time period over which the model must be run can be established.

The site investigation will provide the basic starting data to quantify the external environment and identify the mechanisms of deterioration that are likely to occur. Initial parameters for the concrete can then be selected, including quantities of mix constituents, w-c ratio, and appropriate coefficients of diffusion, permeability, and so forth. The physical dimensions of the element concerned are also important. The model can then be run to establish the performance of the particular mix in relation to the site environment. By varying the concrete parameters, it is possible to establish the minimum requirements of the concrete to achieve the required durability.

One example of this type of approach is the CHLORPEN program, which models the ingress of chloride ions into concrete and evaluates the time to initiation of corrosion. The principal factors that affect the rate of penetration of chloride ions into concrete are the coefficients of diffusion, permeability, and the rate of evaporation from an exposed internal face. The processes described by Fick and D'Arcey's laws are mathematically modeled in a series of incremental time steps into the concrete, which is divided into a number of lamina of fixed material properties. A typical plot of the output based on a simple diffusion process is shown in Figure 4.

Where chlorides originate from deicing salts, the number of applications and quantity of chloride applied during each freezing cycle are also important. On particularly sensitive structures, where chloride-based deicers have been prohibited, the extent of carryover from the use of chloride deicers must also be considered. On a U.K. submarine tunnel road deck, chloride concentrations of up to 26,000 mg/l (ppm) have been recorded at distances of 2 km (1.2 mi) from the boundary of chloride deicer use after each application.

Initiation of corrosion is assumed to occur when the level of chloride reaches 0.4 percent by mass of cement. From the output data for a design life of 120 years before initiation occurs, two options become apparent: (a) the depth of cover can be specified for a concrete with a fixed diffusion coefficient or (b) the diffusion coefficient of the concrete can be specified for a fixed depth of cover. In the St. Clair River Tunnel, the cover to the extrados reinforcement was fixed; therefore the diffusion coefficient was specified to achieve the maximum resistance to chloride penetration. A value of 600×10^{-15} m^2/s was selected as being achievable in production. Measured values from trial mix designs of less than 350×10^{-15} m^2/s were reported.

Once the durability of the concrete has been determined, the materials selection process to achieve the desired properties can begin. It is important to establish the behavior of the proposed mix (particularly its thermal properties) to minimize the likelihood of early thermal cracking and to establish the curing regime and stripping times of formwork. Modeling can also be used to establish the likely thermal behavior of concrete mixes with respect to boundary conditions (Figure 5). This shows the effect of varying the boundary conditions (formwork type and period before striking) on the thermal behaviour of a 70 percent ggbs mix proposed for use in the cable anchorage of a suspension bridge. Where boundary conditions are fixed (e.g., concrete cast against the ground) the effects of varying the mix design can be simulated.

Modeling is a powerful predictive tool, but there are limitations. Some processes are almost impossible to model because of a lack of basic data on the nature of the process or the high variability in behavior. A good example is AAR, where a number of different processes operate simultaneously and are sensitive to the chemical and physical environment. In such cases it is necessary to rely on codified rules to minimize the risk (*16*).

MIX DESIGN

When designing the concrete, the contractor who is to produce the concrete must initially consider the detailed requirements of the specification and the site to simultaneously satisfy all the specification requirements, including the durability and structural properties. A program of trial mixes that clearly identifies principal performance criteria to be evaluated, particularly in areas where onerous or unusual requirements occur, must be undertaken. After the important parameters that must be achieved have been established, an assessment of the particular site requirements, the local materials available, and alternative reserve supplies should be made.

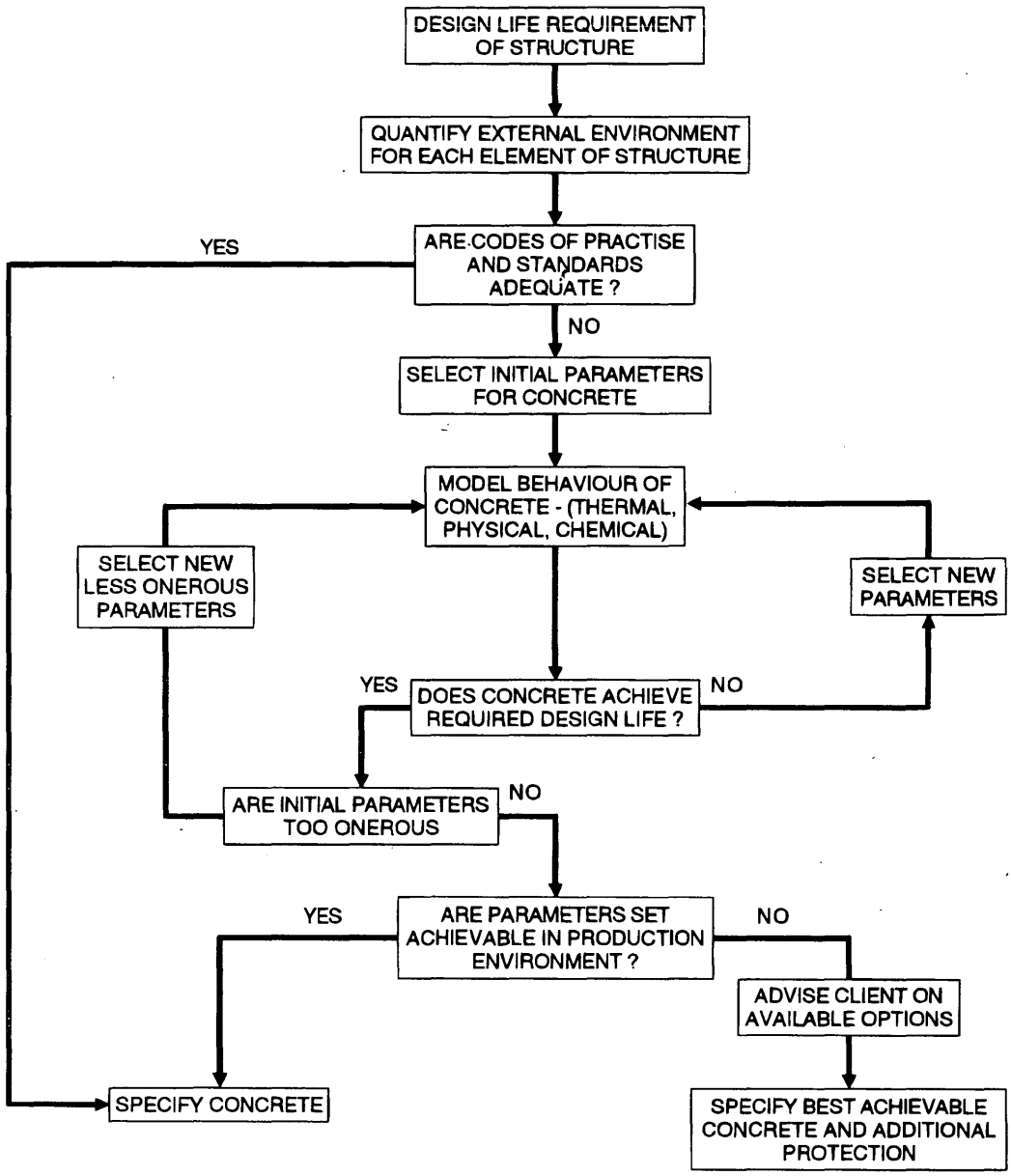

FIGURE 3 Flowchart of the modeling process leading to the specification of concrete.

SPECIFICATION REQUIREMENTS

The specification should be studied to identify all the requirements that must be met and those likely to be the most difficult to achieve. The study should distinguish between compliance tests (to achieve specified values) and reference tests (where data on particular properties are required, but no minimum values must be achieved).

Time and resource implications of the testing specified, particularly where the contractor is unfamiliar with the test methods specified or long-term data are required, must be considered and a suitable program for conducting the testing developed. Some durability tests (e.g., diffusion resistance) may require extended test periods [3 to 4 months in some cases (*15*)]. It is essential that this be recognized and sufficient time allowed for all the testing to be completed and the results evaluated before construction begins.

SITE REQUIREMENTS

With the examination of the specification requirements, the individual site requirements need to be identified, particularly the types and volumes of concrete required, the earliest date by which each mix design is needed, and any special requirements of the mix for construction (e.g., pumping or placing characteristics.)

The site requirements must be carefully linked to the requirements in the specification and the testing program so that sufficient

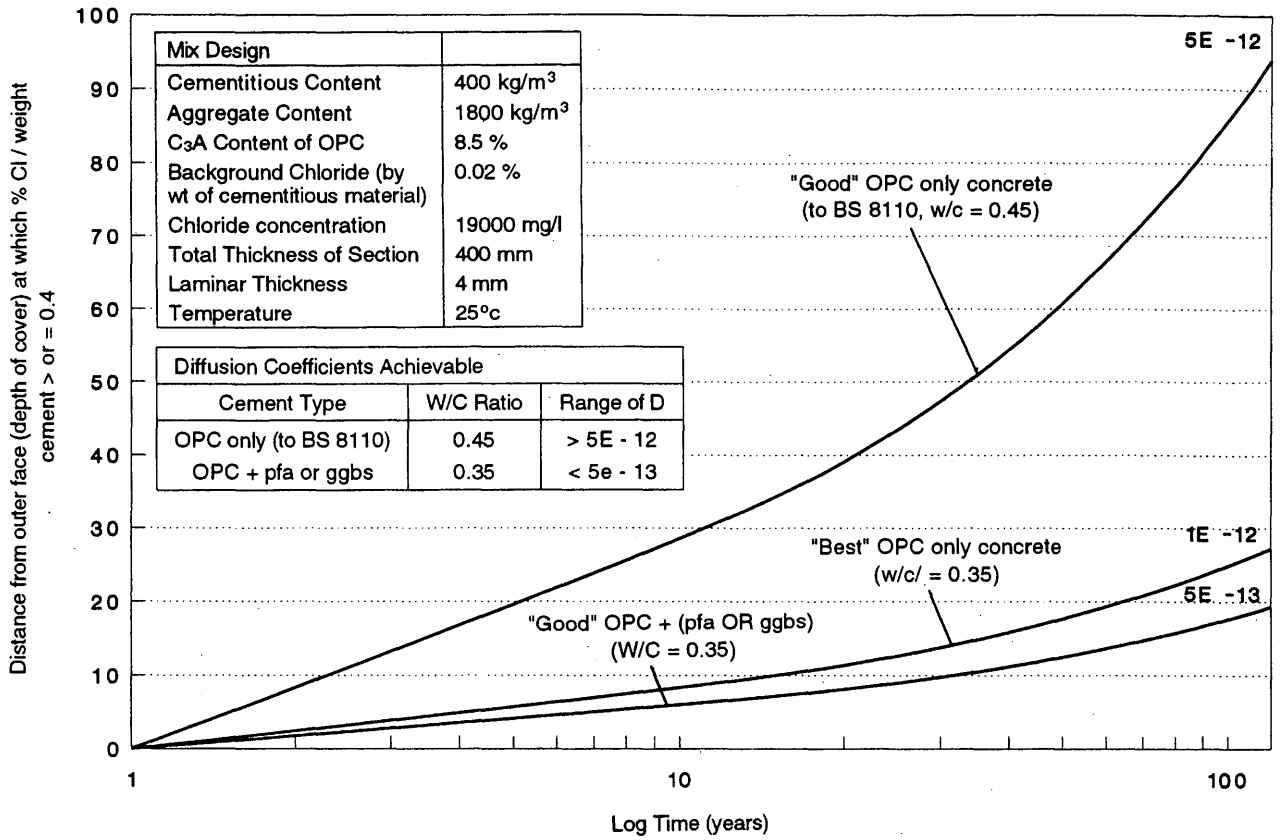

FIGURE 4 Effect of diffusion coefficient (D) on depth of penetration of 0.4 percent Cl^- (by mass of cement) front (example is for concrete immersed in seawater, no external pressure).

time is allowed, before construction begins, to carry out all the necessary testing and reporting and gain approval for the use of the concrete before it is required in the structure.

MATERIALS SELECTION FOR DURABILITY

The component materials must be selected with care to ensure that the required performance level can be achieved and maintained. This necessitates considering the specification and collection of technical data on a wide range of material types and sources. It should be noted that the specification will define only minimum acceptable values and that the performance requirements of the concrete may necessitate the use of materials with superior qualities. It may therefore be necessary for the contractor to impose limits on some materials properties that are tighter than those required by the specification (e.g., the use of a tighter grading curve on aggregates or the selection of admixtures to reduce the effects of retardation.) Selection is also influenced by the availability of the required quantities of each material of the necessary quality at the delivery rates required by the construction program, handling and storage on site, and cost. A short list of materials considered to be suitable can then be established. This list can also be used to determine technical performance.

It is important to optimize the performance of the individual and the materials combinations, particularly when considering their synergistic effects—using cements with a high-lime saturation factor with pozzolanic materials and the effects of aggregate properties, cleanliness, shape, grading, on the development of the cement paste microstructure.

It is possible to produce concretes with a wide range of properties: from what would be considered normal concrete to mixes that, if carefully produced, will offer a high degree of durability. Quality assurance testing of materials throughout the duration of the contract should be undertaken to ensure that the requirements are consistently maintained.

MIX DESIGN TRIALS

Trials are essential to ensure that the specified properties can be achieved in a cost-effective manner. The mix design process must consider the factors that have the most influence over the specified parameters and design a series of trial mixes accordingly. With respect to durability against deterioration because of aggressive species in the environment, these factors are likely to be

- Minimizing voids and cracks (including micro-cracking),
- Ensuring good bond between the aggregate and the cementitious paste,
- Minimizing the porosity of the paste fraction, and
- Minimizing the paste fraction in the concrete (this is likely to be the path for the ingress of aggressive ions as dense aggregate is generally considered to be effectively impermeable).

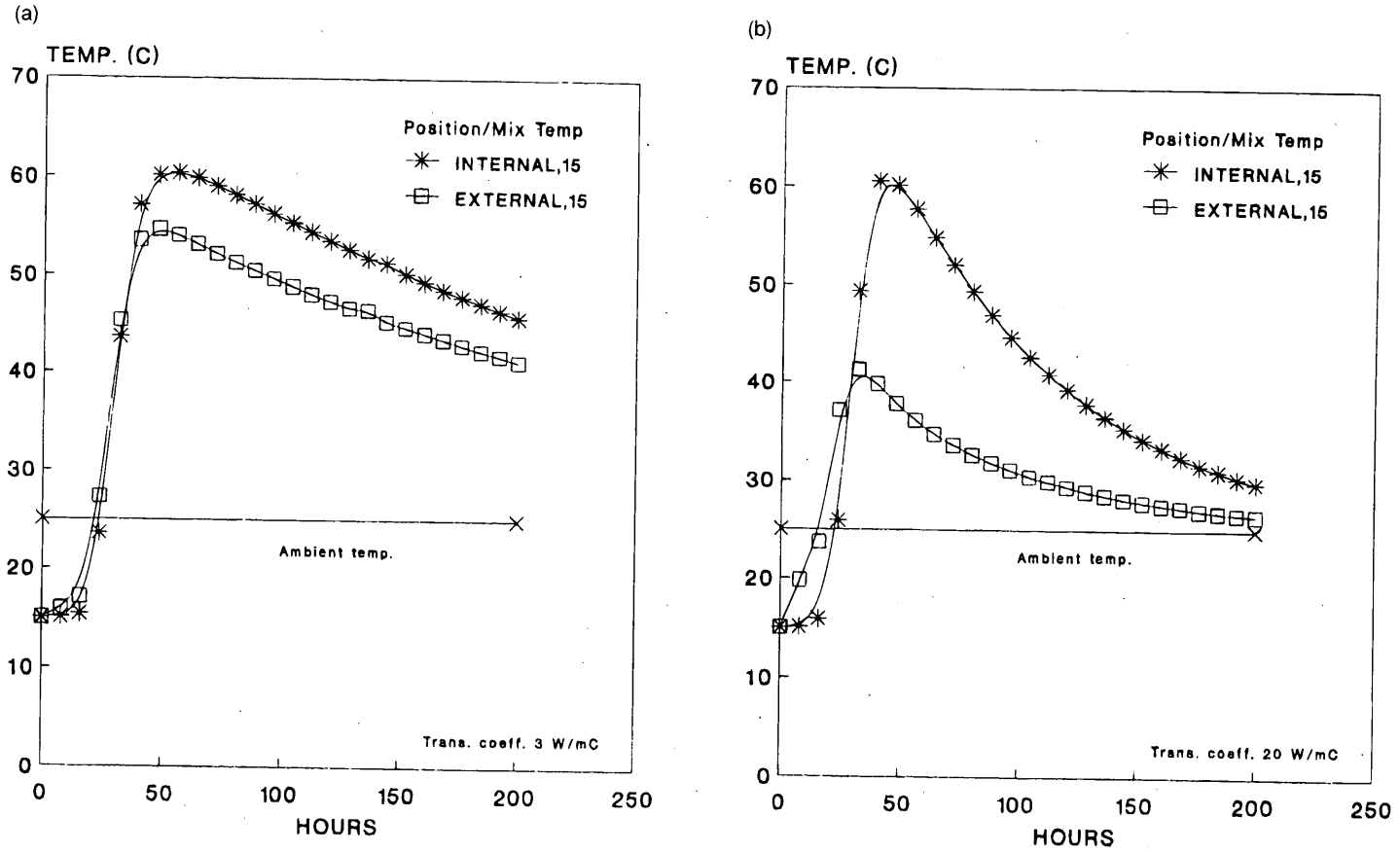

FIGURE 5 Modeling of thermal behavior of the interior and surface of concrete [examples are for a mix with a cementitious content of 400 kg/m^3, 70 percent ggbs with (*a*) extended period before striking shutters and (*b*) early striking of shutters].

The mix design should therefore adopt constituent materials and practices consistent with achieving these requirements. The use of cement replacement materials or pozzolans—such as fly ash, ground granulated blast-furnace slag (ggbs), or micro-silica—results in densification of the cement paste and modification of the long-term pore size distribution, and provides long-term hydration characteristics (*17*). The water-to-cementitious ratio adopted should be as low as practicable to minimize the porosity of the paste (but sufficiently high to prevent self-desiccation). The use of admixtures, such as plasticizers and superplasticizers, is beneficial in enabling high-workability mixes to be produced while retaining low water-to-cementitious ratios. However, other side effects, such as retardation of setting, must also be considered. The selective processing of constituent materials can improve properties that hinder workability and increase water demand, particularly aggregate shape and grading. Workability is important in the overall durability of an element by ensuring that uniform good compaction can be achieved, especially where complicated reinforcement cages are to be used.

Materials that improve some aspects of durability performance may increase the risk of deterioration from others, such as the use of pozzolanic materials to reduce porosity, and may reduce the scaling resistance of concrete exposed to deicing salts. It is important that all the results of the durability testing be considered holistically to select the most appropriate mix design for the particular application.

ADDITIONAL PROTECTIVE MEASURES

There are particularly severe environments where concrete alone will not be sufficiently durable to achieve the required design life. In such the cases, additional protective measures will need to be specified. Many systems are becoming available to improve the durability of reinforced concrete structures, including the following:

- Thermosetting and thermoplastic coatings to reinforcement;
- Coatings to the surface of the concrete;
- Admixtures to modify the structure of the cement paste, improving its resistance to the ingress of aggressive ions;
- Admixtures that modify the corrosion processes;
- Modification of the external environment, such as by cladding; and
- Cathodic protection.

These techniques all have advantages and disadvantages in service and may not be universally applicable. Specialist advice must always be sought before implementing the measures.

CONCLUSIONS

The approach described has been used to specify concrete for long-term durability on major projects around the world. By using this method it is possible to predict with a high degree of accuracy the likely behavior of different concrete mix designs in a wide range of aggressive environments. It is also possible to predict the thermal behavior of the concrete during mixing, pouring, and setting. A rational basis for the durability requirements can be established, and concrete of the appropriate standard and properties can be specified. Appropriate materials and testing to verify performance can then be selected and investigated. Testing the structure while in service may also be undertaken to verify the predictions of long-term performance. Where concrete alone will not be sufficiently durable, additional protective measures may be specified; however, these measures should not be routinely used without specialist advice.

REFERENCES

1. Leek, D. S., and M. J. Walker. A Review of the Research and Recommendations Regarding Chloride Associated Reinforcement Corrosion in the United Kingdom and United States of America. In *Corrosion Damaged Concrete: Assessment and Repair*, (P. Pullar-Strecker, ed.), CIRIA, Butterworths, 1988, pp. 79–97.
2. *Structural Use of Concrete, Parts 1 and 2*. HMSO, BS 8110: Parts 1 and 2. British Standards Institution, 1985.
3. *Specification for Highway Works*. U.K. Department of Transport, HMSO, 1992.
4. Leek, D. S., B. M. Stewart, and C. R. Ecob. The Corrosion Behaviour of Epoxy Coated Reinforcement and its Relationship to Service Life in Concrete. *UK Corrosion '90*, Institute of Corrosion, Vol. 3, 1990, pp. 27–36.
5. Lambert, P., and J. G. M. Wood. Improving Durability by Environmental Control. *5th International Conference on Durability*, RILEM/BRE, Brighton, England. Nov. 1990.
6. Wood, J. G. M. Predicting Future Decay in Concrete Structures. *Henderson Colloquium on Design Life of Structures*, IABSE, British Group, Pembroke College, Cambridge, England, July 1990.
7. *Sulphate and Acid Resistance of Concrete in the Ground*. Building Research Establishment, Digest 363, July 1991.
8. Wood, J. G. M., A. M. Harper, and D. S. Leek. Specification for Major Projects. *9th International Conference on Alkali Aggregate Reaction*, Concrete Society, July 1992, pp. 1113–1121.
9. *Eurocode 2: Design of Concrete Structures. Part 1. General Rules and Rules for Buildings*. British Standards Institution, DD ENV, 1992–1–1, 1992.
10. *Ordinary Portland Cement*. British Standards Institution, BS 12, 1991.
11. *Corrosion of Metals in Concrete. Manual of Concrete Practice, Part 1*. American Concrete Institute, ACI 222.R–89.
12. *Design of Concrete Structures for Retaining Aqueous Liquids*. British Standards Institution, BS 8007, 1987.
13. *Concrete: Performance, Production and Compliance Criteria*. British Standards Institution, DD ENV 206, 1992.
14. *Guide to Durable Concrete. Manual of Concrete Practice, Part 1*. American Concrete Institute, ACI 201.2R–92.
15. Wood, J. G. M., J. R. Wilson, and D. S. Leek. Improved Testing for Chloride Ingress Resistance of Concretes and Relation of Results to Calculated Behaviour. *3rd International Conference on Deterioration and Repair of Reinforced Concrete in the Arabian Gulf*, BSE, Oct. 1989, pp. 427–441.
16. *Alkali-Silica Reaction, Minimising the Risk of Damage to Concrete*. Concrete Society Technical Report 30, Oct. 1987.
17. Mehta, P. K. Pozzolanic and Cementitious By-Products in Concrete—Another Look. *3rd International Conference on Fly Ash, Silica Fume, Slag and Natural Pozzolans in Concrete*, ACI SP–114, 1989, pp. 1–44.

Publication of this paper sponsored by Committee on Performance of Concrete.

Superior Microstructure of High-Performance Concrete for Long-Term Durability

DELLA M. ROY, MICHAEL R. SILSBEE, SCOTT SABOL, AND BARRY E. SCHEETZ

Recent advances in using calculated packing diagrams to optimize cement and concrete materials offer the promise of superior product characteristics achieved by increased packing efficiency. A high packing efficiency with adequate mixing and placing techniques results in the formation of a fine microstructure that results in low permeability. The low permeability causes increased resistance to aggressive forces from the environment, which together enhance its long-term durability. The favorable interaction among physical and chemical phenomena gives rise to better long-term performance, whether the application is structural, chemical (such as in waste management), or a combination (as in highway concrete).

High-performance concrete has been defined (*1*) as concrete in which some or all of the following properties have been enhanced:

- Ease of placement and compaction,
- Long-term mechanical properties,
- Early-age strength,
- Toughness,
- Volume stability, and
- Extended life in severe environments.

High strength is not necessarily a criterion for high-performance concrete, although many high-performance concretes exhibit superior mechanical properties. Three of the six criteria are concerned with the long-term behavior or durability of the concrete. Transport of fluids into or out of the pore structure of hardened concrete is the principal mechanism responsible for the deterioration of concrete (*2*). The transport of fluids and accompanying dissolved ionic species in hardened concrete may be considered in terms of permeability.

This paper focuses on high-performance cementitious materials designed for durability. First, some of the fundamentals of porosity and permeability of cementitious systems and their relation to durability are examined. Then, factors that control the porosity and permeability in concretes are discussed. Finally, the effect of packing on properties, such as chloride permeability, is treated.

POROSITY AND PERMEABILITY IN HARDENED CEMENTITIOUS SYSTEMS

Assuming negligible volume change on curing, the total volume of a hardened portland cement paste will be the sum of the volumes of the anhydrous cement, water, and any entrapped air, or

$$V_t = V_s + V_l + V_a$$

where

V_t = total volume,
V_s = volume of anhydrous portland cement,
V_l = volume of liquid (water), and
V_a = volume of any entrapped air.

Another way of expressing V_t is

$$V_t = (W_s/\rho_s + W_l/\rho_l) + V_a$$

where

W_s = mass of anhydrous cement,
ρ_s = density of anhydrous cement,
W_l = mass of water, and
ρ_l = density of water.

Assuming $\rho_l = 1$, then

$$V_t = (W_s/\rho_s + W_l) + V_a$$

Each gram of anhydrous portland cement will combine chemically with approximately 0.25 g of water during hydration. Therefore, V_t becomes

$$V_t = [1.25W_s/\rho_h + (W_l - 0.25W_s)] + V_a$$

Where ρ_h = density of the hydrated solid.

The total volume of the pores in the hydrated cement pastes is then

$$V_p = (W_l - 0.25W_s) + V_a$$

As early as 1886 (*3*) the effect of water content on the strength of hardened concrete was recognized. The volume of pores thus calculated represents the capillary porosity, gel porosity, and entrapped air. From these three sources of porosity, only the capillary porosity will contribute to the fluid permeability of the hardened cement paste.

Ideally, the flow through a hardened portland cement paste may be expressed as

$$F/A = K\mu/(L \cdot \Delta P)$$

Pennsylvania State University, Materials Research Laboratory, University Park, Pa. 16802. Current affiliation of S. Sabol: Transportation Research Board, National Research Council, 2101 Constitution Avenue, N.W., Washington, D.C. 20418.

where

F = flow (L/sec),
A = cross-sectional area (m^2),
L = thickness of specimen (m),
K = permeability coefficient (m^2),
μ = viscosity of permeating fluid ($N \cdot sec/m^2$), and
ΔP = mean pressure (N/m^2).

For a cement paste it was concluded (*4,5*) that it was possible to block the capillary porosity with cement gel if the water-to-cement ratio in the paste is low. The limiting water-to-cement ratio required to block fluid flow is a function of curing time. At a ratio of 0.7, times of approximately 1 year are required; at a ratio of 0.4, the time required for the cement gel to block the capillary pores may be only 3 days.

A characteristic pore size is determined by mercury intrusion porosimetry was defined (*6*). The characteristic pore size was defined as the maximum on the derivative of the volume intruded versus pressure curve (dV/dP). A linear relationship between the log of the characteristic pore size and permeability was found. However, the coefficient of variation for the relationship was large (approximately 50 percent). More recent studies (7–9) have shown that a log-normal distribution or mixtures of log-normal distributions may be used to describe the pore structure of hardened cementitious materials. These studies defined a characteristic diameter based on the moment, $<D^2>$, of the log-normal distribution. The relationship between the characteristic diameter and permeability was found to be (*10*):

$$k = (f/32)p<D^2>$$

where

k = permeability,
f = fraction of connected porosity, and
p = porosity.

When the total porosity decreases and commonly the median pore size decreases, the rate-controlling mechanism for movement of ions through hardened cement pastes transforms from fluid flow to diffusion. The controlling relationship then obeys Fick's law:

$$\text{rate of diffusion} = -D\frac{dc}{dx}$$

where D is the diffusion coefficient, and dc represents a concentration gradient over distance dx.

DURABILITY

Table 1 lists the principal mechanisms that contribute to the shortening of the service life of hardened concretes. These degradation mechanisms can be classified into two categories—thermo-mechanical and chemical—although there is some interaction and overlapping of the two. The mechanisms highlighted in boldface type require a mass transport of ionic or molecular species into or out of the cementitious matrix. This transport occurs via movement through the conduits that connect the exterior of the concrete to the interior (that is, the system of pores). Therefore, both the total number of pores and the pore size distribution are important in controlling the performance of the concrete and hence its durability.

The preceding section discussed the formation of porosity. To develop durable concrete formulations, one must address the methods of modifying the total porosity and the pore size distribution by advanced placement procedures and proper selection of the constituents of the formulations based on particle size distributions and chemistry.

CONTROL OF POROSITY AND PERMEABILITY IN CONCRETES

Chemical Effects on Porosity and Permeability

The use of low water-to-solids (w-s) ratio formulations and mineral admixtures to increase the durability of hardened cementitious systems is well documented (*2,11–13*). With the proper selection of

TABLE 1 Degradation Processes

Thermo-mechanical	*Chemical*
	sulfate
pressure/temperature alteration of phase stability	**-- calcium**
freezing and thawing cycling	**-- magnesium**
wet and dry cycling	**-- sodium**
cracking	**chloride**
-- drying shrinkage	**carbonation**
-- metal corrosion	**alkali aggregate reaction**
-- stresses due to temperature changes	**leaching**
-- carbonation	
-- physical loading	

reactive mineral admixtures, a fair degree of control can be exercised over the performance of the concrete. Figure 1 demonstrates the effect of w-s, high-range water-reducing admixture (HRWRA), and mineral admixtures on porosity development in cementitious pastes.

Ground granulated (glassy) blast-furnace slag as an ingredient of the cement paste that can replace significant amounts of the portland cement has been developed and is currently a commercial product. The commonly accepted mechanism for hydrating slag is by activating the very finely ground glassy slag by portland cement hydration products, which results in a slow initial hydration reaction. Figure 2 contrasts mercury-intrusion porosimetry results obtained on freeze-dried specimens of an ordinary portland cement (OPC) paste and a 60:40 slag: OPC-blended cement paste both cured under identical conditions at 45°C for 14 days with a w-s of 0.4. The data, presented as the differential *dV/dP*, show that the OPC possesses a pore distribution that centers at about 12.5 nm, the so-called critical pore radius. In contrast, the blended slag cement reveals a pore-size distribution with a very broad maximum weakly centered at about 3.5 nm and extending from 12.5 to 2.0 nm. Figure 3 is a replot of these data in a cumulative pore volume form showing that both specimens had approximately the same total porosity (within about 5 to 6 percent) but distinctly different pore size distributions. In this example, the reactive additional ingredient (slag) has the characteristic of hydrating at a much slower rate, resulting in a significantly reduced pore size distribution, and at the same time not adversely affecting the 28-day mechanical properties of the concrete. Any number of other materials have the potential of performing similarly.

Degradation due to steel corrosion induced by chloride penetration is a common cause of concrete structure failures. Many

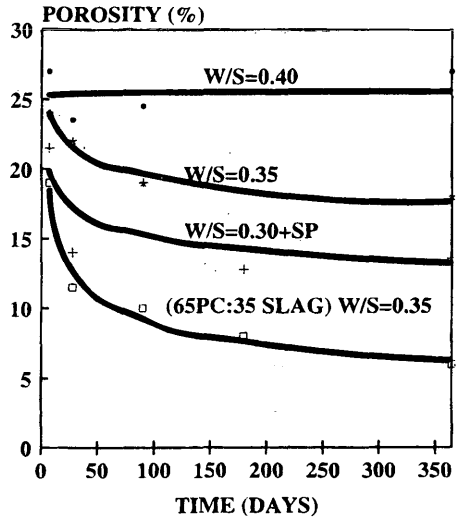

FIGURE 1 Effect of W/S (HRWRA) and mineral admixtures on porosity development in cementitious pastes (*13*).

investigations have been performed on the movement of chlorides through hardened cement pastes (*2,6,14–19*). In view of applications to radioactive waste management, the movement of Cs+ and Cl− ions through hardened cement pastes prepared using a variety of w-s and various slags and mineral admixtures was studied (*13*). Typical results for the diffusion of Cl ions are summarized in Table 2. Decreasing the w-s from 0.40 to 0.35 resulted in a decrease in the effective diffusion coefficient from 110 to 75.1 [($\times 10^{13}$) (m^2/sec)].

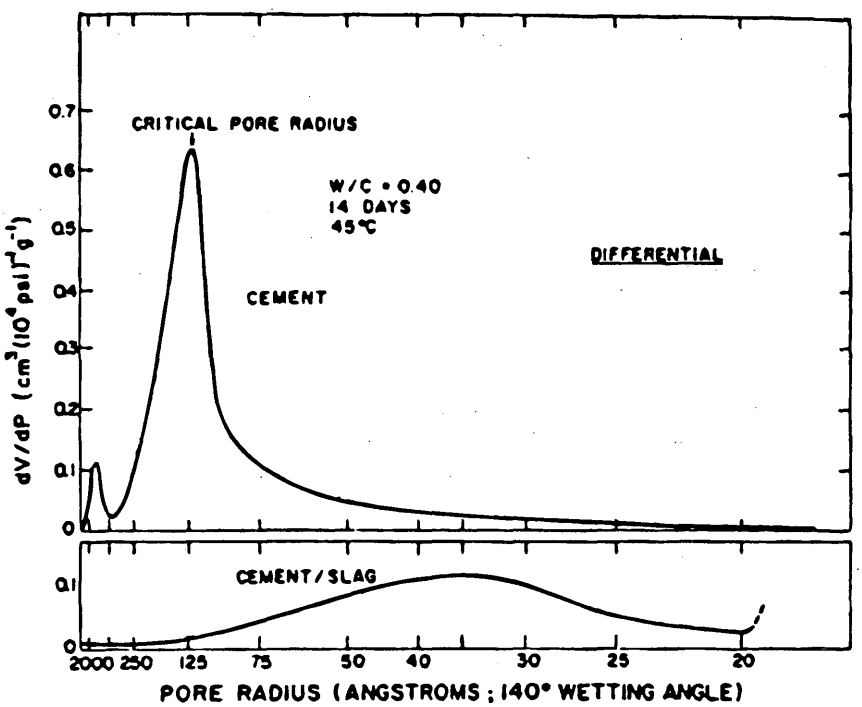

FIGURE 2 Comparison of mercury intrusion porosimetry results obtained on freeze-dried specimens of OPC and 60:40 slag (OPC blended cement both cured under identical conditions at 45°C for 14 days with w-s ratio of 0.4).

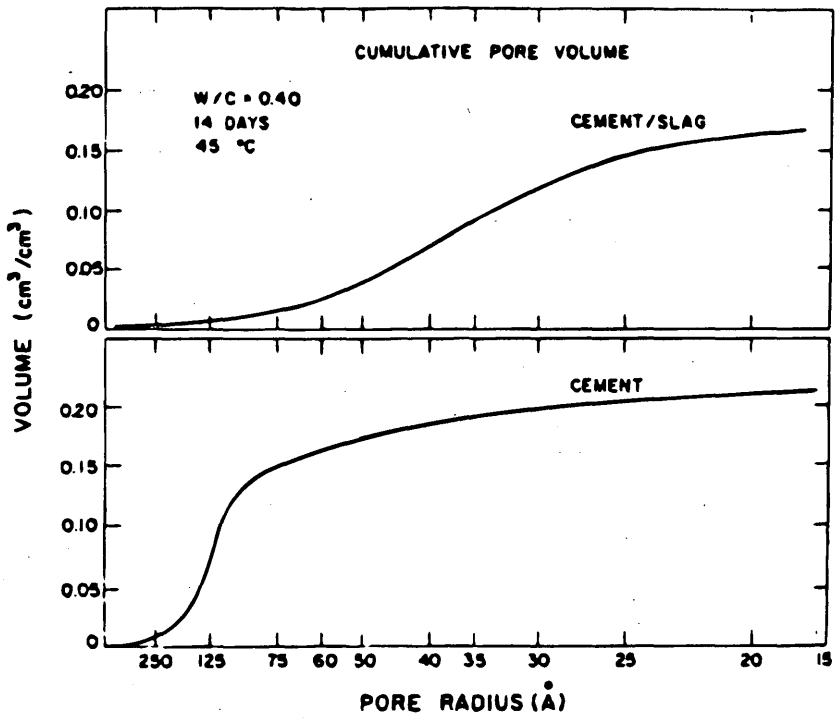

FIGURE 3 Replot of data in Figure 2 in cumulative pore volume form showing that both specimens had approximately same total porosity (within about 5 to 6 percent) but distinctly different pore size distributions.

Lower water contents result in lower total porosity and a more tortuous pore system. The addition of a small amount of a HRWRA further decreased the diffusion coefficient at the same w-s. Blast-furnace slag and silica fume proved the most effective in reducing the diffusion coefficient as compared with an OPC paste from 75.1 to 9.62 to 4.35, respectively. The effectiveness of blast-furnace slag and silica fume was attributed to increased calcium-silica-hydrate (C-S-H) production resulting in a filling of the pores. In both cases, using an HRWRA resulted in still a further decrease in the diffusion coefficient. The use of a low calcium fly ash as a mineral admixture proved much less effective in reducing chloride diffusion. The lower effectiveness of the fly ash as compared with slag and silica fume was attributed to the lesser reactivity of the lower calcium ash. Other studies (*14,17–19*) have shown similar results. Although the total porosity and median pore size remain the same as compared to OPC at normal curing temperatures, the reduction in the diffusion coefficient has been attributed to an increased number of finer pores. High-calcium content fly ashes have generally been found to be more effective at reducing chloride diffusion at early ages. Fly ashes have been shown to be more effective at elevated temperatures presumably as a result of higher reaction rates leading to increased C-S-H production. The results suggest that with elevated temperature curing or after a long curing time fly ash may still be an effective tool for reducing chloride diffusion (*16*).

Physical Effects on Porosity and Permeability

An integral part of the porosity that occurs in cementitious systems is attributable to the voids created among the dry components of the

TABLE 2 Effective Diffusion Coefficients for Cl^- in Water-Saturated Pastes at 25°C on Samples Cured for 28 Days at 25°C before Testing (*13*)

PASTE	W/S	D_{Cl^-}(X10^{13}) (m^2/sec)
OPC	0.40	110
OPC	0.35	75.1
OPC	0.35+SP*	60
OPC	0.30+SP	56.9
35% OPC + 65% SLAG	0.35	9.62
35% OPC + 65% SLAG	0.30+SP	8.61
90% OPC + 10% SILICA FUME	0.40	4.35
90% OPC + 10% SILICA FUME	0.35+SP	2.9
70% OPC + 30% FLY ASH	0.35	55.8
70% OPC + 30% FLY ASH	0.30+SP	43.8

* *with HRWRA addition*

formulation as well as the morphology of the individual components. Studies performed in Denmark (*11*) and the United States (*12*) demonstrated that significant improvement in mechanical properties of portland cement systems could be achieved using an approach based on the proper selection of concrete components to maximize space filling. The development of densified small particle (DSP) cements resulted in low interconnected porosity, very high compressive strengths, and a variety of additional outstanding properties, least of which is the retention of compressive strengths in thermal application in excess of 600°C that is about 65 percent of room temperature values (*20*).

A computer algorithm that has been used to help calculate concrete formulations with maximal density has been described (*9,21,22*). The algorithm requires as input size distributions and tap densities of the individual components. The size distributions for the fine components, such as cement, are determined using x-ray sedimentation techniques and for the coarse components by dry sieving. The tap density is determined by packing the dry component in a column with vibration. The bulk or tap density is then calculated based on the weight of the sample and the volume occupied in the column. The code is the implementation of two models reported in the open literature; one for large particles [Toufar model (*23*)] and one for small particles [(Aim model (*24*)].

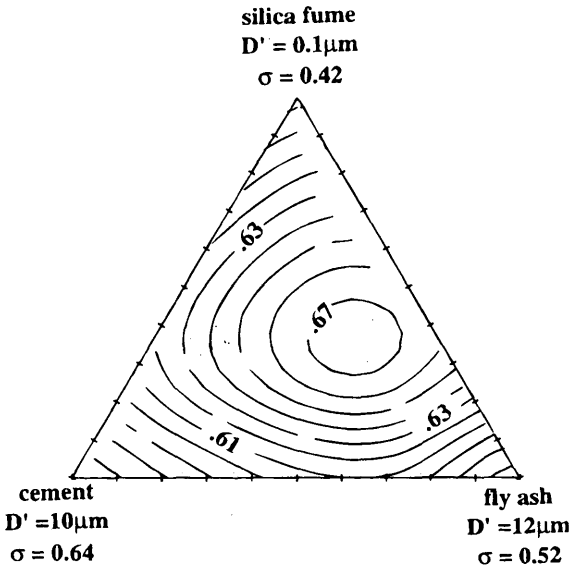

FIGURE 4 Packing diagram blend of 37.5, 19.0, and 9.5mm size-numbered coarse aggregate with input from Table 5.

Use of Reactive Mineral Admixtures and Tailored Aggregate Mixtures.

Increasingly large numbers of concrete formulations are being proportioned with some form of reactive mineral admixture. Each component of the concrete formulation—cement, fine, and coarse aggregate—can in turn be optimized to ensure the densest possible formulation. Caution must be exercised when using this approach. The densest formulation may not be desirable, and its use must be tempered by practical knowledge of reactivity and desired physical properties. Figure 4 represents the use of one such packing diagram for blending cementitious constituents in a concrete. Table 3 summarizes the input data used to generate Figure 4.

Maximum packing for this example suggests an optimal blending, which is summarized in Table 4. As can be seen, the maximum packing density does not necessarily correspond to where one would normally select a cementitious blend; it contains slightly more silica fume and less fly ash than desirable from the standpoint of chemistry and rheology. Figure 5 is a comparable packing diagram blend of 37.5 mm, 19.0 mm, and 9.5 mm size-numbered coarse aggregate with input from Table 5.

ASTM C 33—Standard Specification for Concrete Aggregates

Using the dry packing model allows for a critical evaluation of the existing size-number designation grading requirements. It also facilitates analysis of the effects of those gradings on subsequent dependent specifications, such as ACI 211.11. This analysis should enhance the quality control in the production of high-performance concrete.

Analysis of the grading requirements for coarse aggregates contained in Table 2 of ASTM C 33 (Figure 6) was carried out in the

TABLE 3 Input Data for Packing Calculation of Cementitious Components

	characteristic size* (μm)	tap density
silica fume	0.1	0.42
cement	10	0.64
fly ash	12	0.52

* determined from the D50 value.

TABLE 4 Optimal Packing for Cementitious Components

	density (Mg/m^3)	volume percent	mass percent
silica fume	2.1	22	16
cement	3.1	72	79
fly ash	2.35	6	5

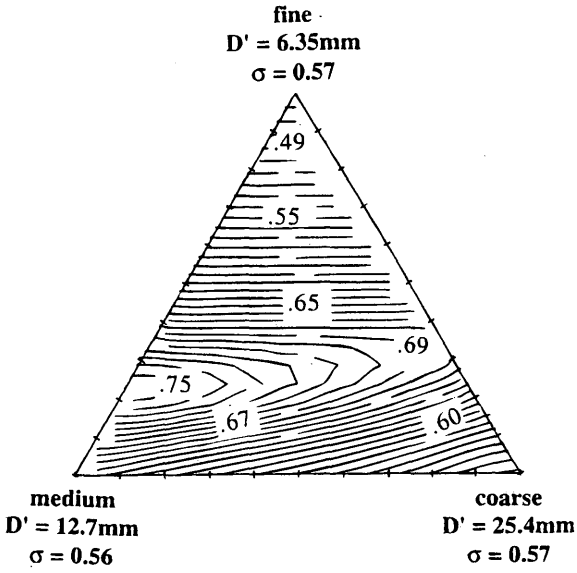

FIGURE 5 Use of packing diagram for blending of cementitious constituents in concrete. Table 3 summarizes input data used to generate this figure.

following manner. For each size-number designation, five different combinations of the size fractions were developed. One combination emphasized the largest allowable aggregate sizes for a size-number. The second combination emphasized the aggregate size in the middle-size ranges for the same specified size-number. A third combination consisted of the highest percentage allowable for the smallest aggregate in the size-number designation, with minimum of medium- or large-sized aggregate. The fourth combination resulted from combining of the largest and the smallest size-number fractions, but minimizing the percentage from the medium sizes. The final combination was developed using the mean value of the existing allowable percentages in each of the size-fraction designations.

These five combinations were input into the packing algorithm, and plots of iso-densities were determined for a concrete formulation consisting of cement and fine and coarse aggregate. Coarse aggregate was chosen as the variable for this study because of its greater influence on the binary packing of the fine and coarse aggregate (*25*).

It was observed that some of the combinations described for each size-number designation resulted in poor packing density characteristics and therefore in poorer concretes. These poor packing characteristics within a size-number designation include combinations that (a) result in a noticeably lower maximum packing density than other combinations, (b) result in very small regions of comparable packing density, or (c) have gradients in packing density in the directions of increasing or decreasing volume percentages of fine or coarse aggregate, or all. This final characteristic would result in little tolerance for error in aggregate proportioning during the batching process that could lead to large changes in the concrete and therefore affect the initial and final concrete properties.

An encouraging outcome of the study is noted in all of the combinations within a size-numbered designation. There is a certain arbitrary level of packing that is the same in value and roughly in the same area and location for all of the combinations evaluated. An example of this phenomenon is demonstrated by comparing the shaded regions of panels (a), (b), and (c) of Figure 7. Note that although the maximum packing density value and position are different for all three combinations, the density plateau labeled 0.87 is generally the same in area, shape, and position for all three. This similarity suggests that, in practice, this iso-density limit would be the lowest level of packing expected regardless of the proportioning of size fractions in the coarse aggregate size-number (based on these combinations of concrete components). It is only the characteristics of the packing densities above this "base level" that are affected by the various combinations analyzed here. Although these observations could result in improvements to the use of coarse aggregates in concrete, it is reassuring that the packing model helps to explain the generally acceptable results obtained using the current ASTM C 33 gradings.

Effects of Natural Versus Manufactured Aggregates on Packing Density

The efficiency with which the dry constituents of a concrete formulation can be assembled depends on the morphology of the particles. Angularity and aspect ratio are not specifically measured for input into the packing model described elsewhere (*9,22*) but are indirectly included in the tap density. An aggregate that meets the C 33 grading guidelines and has been prepared by crushing, when contrasted with a similar aggregate that occurs naturally and does not require crushing, will exhibit different packing behavior. An angular to subangular aggregate will not pack as densely as its rounded to subrounded counterpart. Figure 8 contrasts the differences in packing that are calculated for a no. 8 manufactured limestone aggregate with the same cement and fine aggregate prepared from a rounded natural quartz aggregate. The differences in dry packing for these two systems can be as much as 8 to 10 volume percent.

Effect of Packing on Chloride Permeability

The effect of packing density on durability and, in particular, transport properties of species into or out of the concrete is reflected in measurements such as that of chloride permeability. Some experimental studies were undertaken to evaluate this effect. The chloride permeability of concrete specimens was measured by monitoring the net charge (coulombs) passing in 6 hr through a cylinder

TABLE 5 Input Data for Packing Calculation of Coarse Aggregate

	characteristic size (mm)	*tap density*
fine	6.35	0.57
medium	12.7	0.56
coarse	25.4	0.57

Size Number	Nominal Size (Sieves with Square Openings)	Amounts Finer than Each Laboratory Sieve (Square-Openings), Weight Percent												
		4 in. (100 mm)	3½ in. (90 mm)	3 in. (75 mm)	2½ in. (63 mm)	2 in. (50 mm)	1½ in. (37.5 mm)	1 in. (25.0 mm)	¾ in. (19.0 mm)	½ in. (12.5 mm)	⅜ in. (9.5 mm)	No. 4 (4.75 mm)	No. 8 (2.36 mm)	No. 16 (1.18 mm)
1	3½ to 1½ in. (90 to 37.5 mm)	100	90 to 100	...	25 to 60	...	0 to 15	...	0 to 5	...	...	...	...	...
2	2½ to 1½ in. (63 to 37.5 mm)	...	...	100	90 to 100	35 to 70	0 to 15	...	0 to 5	...	...	...	...	...
3	2 to 1 in. (50 to 25.0 mm)	...	...	...	100	90 to 100	35 to 70	0 to 15	...	0 to 5	...	...	...	...
357	2 in. to No. 4 (50 to 4.75 mm)	...	...	...	100	95 to 100	...	35 to 70	...	10 to 30	...	0 to 5	...	...
4	1½ to ¾ in. (37.5 to 19.0 mm)	...	...	...	...	100	90 to 100	20 to 55	0 to 15	...	0 to 5	...	...	...
467	1½ in. to No. 4 (37.5 to 4.75 mm)	...	...	...	...	100	95 to 100	...	35 to 70	...	10 to 30	0 to 5	...	...
5	1 to ½ in. (25.0 to 12.5 mm)	...	...	...	...	...	100	90 to 100	20 to 55	0 to 10	0 to 5	...	...	...
56	1 to ⅜ in. (25.0 to 9.5 mm)	...	...	...	...	...	100	90 to 100	40 to 85	10 to 40	0 to 15	0 to 5	...	...
57	1 in. to No. 4 (25.0 to 4.75 mm)	...	...	...	...	...	100	95 to 100	...	25 to 60	...	0 to 10	0 to 5	...
6	¾ to ⅜ in. (19.0 to 9.5 mm)	...	...	...	...	...	...	100	90 to 100	20 to 55	0 to 15	0 to 5	...	...
67	¾ in. to No. 4 (19.0 to 4.75 mm)	...	...	...	...	...	...	100	90 to 100	...	20 to 55	0 to 10	0 to 5	...
7	½ in. to No. 4 (12.5 to 4.75 mm)	...	...	...	...	...	...	...	100	90 to 100	40 to 70	0 to 15	0 to 5	...
8	⅜ in. to No. 8 (9.5 to 2.36 mm)	...	...	...	...	...	...	...	...	100	85 to 100	10 to 30	0 to 10	0 to 5

FIGURE 6 Table 2 of ASTM C 33.

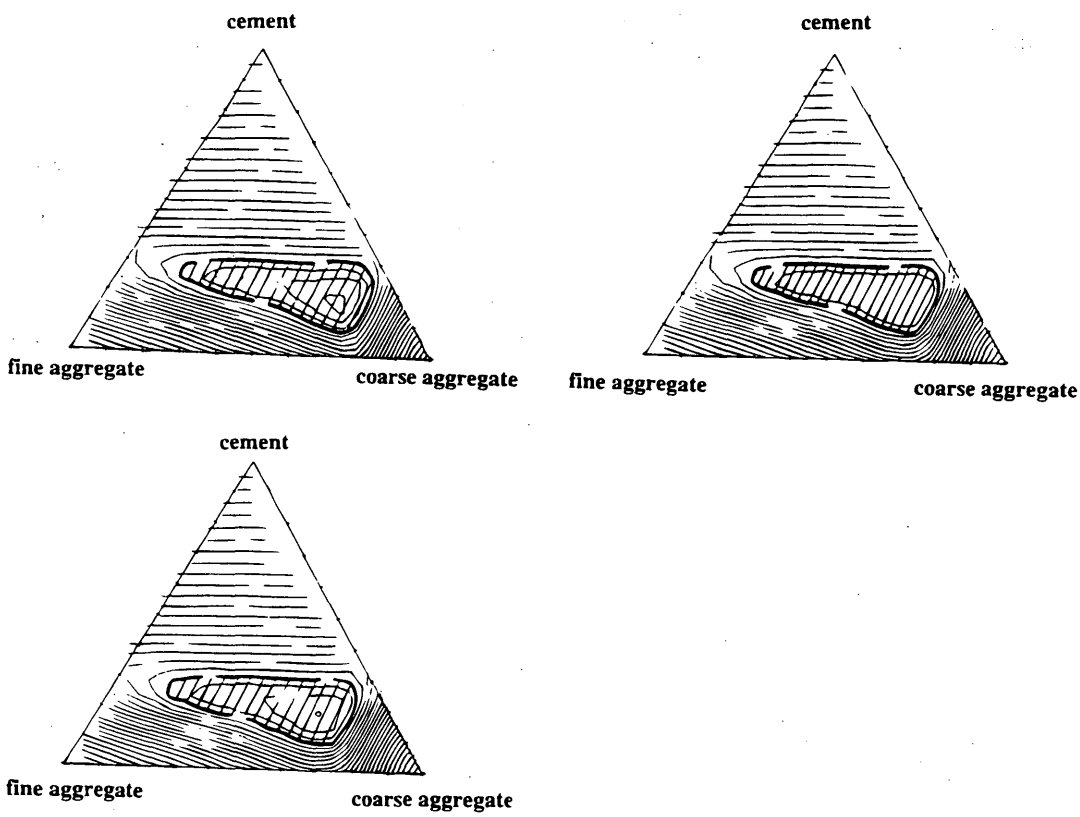

FIGURE 7 Dry packing calculation of cement, fine aggregate, and coarse aggregate with varying proportions of sizes within coarse aggregate.

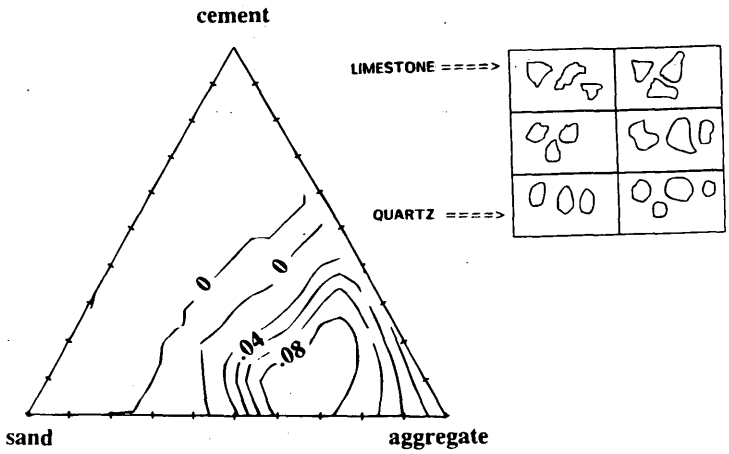

FIGURE 8 Difference between iso-density lines for two concretes composed of cement, sand, and no. 8 coarse aggregate. Differences expressed present effects on packing density between angular, manufactured limestone and natural, subround morphology of quartz aggregate.

(95.25ϕ× 51 mm) mounted in a cell with two compartments, filled with NaCl and NaOH solutions, under the influence of 60 V dc electrical potential (AASHTO T–277). The samples were preconditioned by vacuum saturation before measurement. An example of typical results is given in Figure 9, where concretes having higher packing density (in this case, higher proportions of coarse or fine aggregate, all other factors kept constant) showed a lower chloride transport rate. In general, the concrete samples formulated, based on the packing code, have the highest possible packing density and lowest porosity of their ingredients showed the minimum chloride permeability (*26,27*).

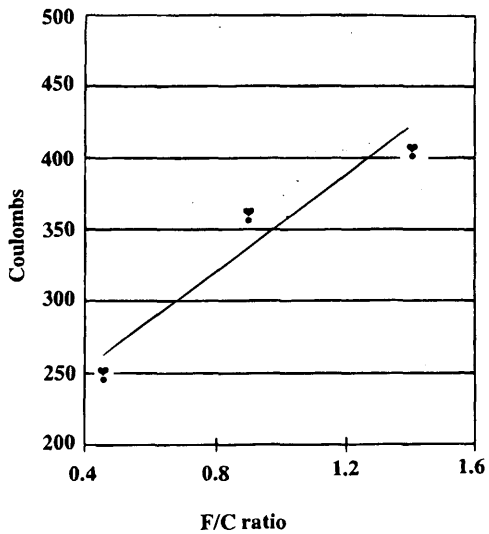

FIGURE 9 Chloride permeability of concrete specimens as measured by monitoring net charge (coulombs) passing in 6 hr through cylinder (95.25ϕ × 51 mm) mounted in cell with two compartments (filled with NaCl and NaOH solutions) under influence of 60 V dc electrical potential (AASHTO T–277).

SUMMARY

Major advances have been made in the development of cementitious materials having superior properties. Such materials have been produced with widely ranging compositions, and their potential applications in modern technology are challenging. High-performance cementitious materials include the very strong, high-density materials of the pressed macro-defect-free (MDF), (DSP), or alkali-activated varieties; their superior properties may be achieved by using either special processing conditions optimal combinations of materials components, or both (*9,21,22*). However, high-performance also includes the ability to predict and achieve long-term durability. The nature of the microstructure of these materials is an important key to such predictability.

This paper has focused on the accomplishments in high-performance cementitious materials with respect to durability. The achievement of dense particle packing, development of a dense microstructure, fine pore structure, superior transport properties, and the relationship among them are critical to high performance and to its understanding and prediction. Additional focus in this important area is critical and will provide new knowledge that will open further horizons in the development of high-performance concrete materials for many applications, especially for the national infrastructure.

ACKNOWLEDGMENTS

The authors acknowledge the support of National Science Foundation (NSF) grant DMR88–12824, the National Academy of Sciences/National Research Council Strategic Highway Research Program grant SHRP–C–201, and NSF grant MSS–91–23239.

REFERENCES

1. *High-performance Construction Materials and Systems: An Essential Program for America and Its Infrastructure*, Civil Engineering Research Foundation, 1993, pp. 20–21.

2. Roy, D. M., Relationships Between Permeability, Porosity, Diffusion and Microstructure of Cement Pastes, Mortar, and Concrete at Different Temperatures *Proc., Materials Research Society Symposium* (L. R. Roberts and J. P. Skalny, eds.). Vol. 137, 1989, pp. 179–189.
3. Neville, A. M. *Properties of Concrete*, 3rd ed. Pitman Publishing Inc., Marshfield, Mass., 1981.
4. Powers, T. C., L. E. Copeland, J. C. Hayes, and Mann, H. M. Permeability of Portland Cement Paste. *Proc., Journal of American Concrete Institute*, Vol. 51; No. 3, 1954, pp. 285–298.
5. Powers, T. C., L. E. Copeland, and H. M. Mann. *Journal for the Portland Cement Association Research and Development Laboratories*, Vol. 1, No. 2, 38, 1959.
6. Nyame, B., and J. Illston. Capillary Pore Structure and Permeability of Hardened Cement Paste. *Proc., 7th International Congress of the Chemistry of Cement*, Vol. 3, 1980, pp. VI–181–185.
7. Shi, D., P. Brown, and S. Kurtz, A Model for the Distribution of Pore Sizes in Cement Paste. *Proc., Materials Research Symposium*, (L. R. Roberts and J. P. Skalny, eds.) Vol. 137, 1989, pp. 23–24.
8. Shi, D., W. Ma, and P. W. Brown, Lognormal Simulation of Pore Evolution During Cement and Mortar Hardening. *Scientific Basis for Nuclear Waste Management*, Vol. 13, Materials Research Society, 1990, pp. 143–148.
9. Roy, D. M., B. E. Scheetz, R. I. A. Malek, and D. Shi. *Concrete Component Packing Handbook*. Supplemental Report 1, SHRP–C–624, Washington, D.C., 1993.
10. Brown, P. W., D. Shi, and J. P. Skalny. Porosity Permeability Relationships. Appendix, Roy, D. M., et al. *Concrete Microstructure Porosity and Permeability*, Supplemental Report 5, SHRP–C–628 SHRP, National Academy of Sciences, Washington, D.C., 1993.
11. Bache, H. H. *Densified Cement/Ultra-Fine Particle-Based Materials*. Cement Beton Laboratory Internal Report 40, CBL, 1981.
12. Scheetz, B. E., J. M. Rizer, and M. Hahn, U.S. Patent No. 4,505,753. 1985.
13. Kumar, A. *Diffusion and Pore Structure Studies in Cementitious Materials*. Ph.D. thesis. Pennsylvania State University, University Park, Pa., 1985.
14. Malek, R. I. A., D. M. Roy, and Y. Fang. Pore Structure, Permeability, and Chloride Diffusion in Fly Ash- and Slag-Containing Pastes and Mortars. *Proc., Materials Research Symposium*, Vol. 137 (L. R. Roberts and J. P. Skalny, eds.), 1989, pp. 403–410.
15. Kumar, A., and D. M. Roy. *Cement and Concrete Research 16*, 1986, pp. 74–78.
16. Li, S., and D. M. Roy. Investigation of Relations Between Porosity, Pore Structure, and Cl Diffusion of Fly Ash and Blended Cement Pastes. *Cement and Concrete Research 16*, 1986, pp. 749–759.
17. Smolcyzk, H. G. State of Knowledge on Chloride Diffusion in Concrete. *Betonwerk und Fertigteil-Technik*, Vol. 12, Germany, 1984.
18. Ushiyama, H., and S. Goto. Diffusion of Various Ions in Hardened Portland Cement Paste. *Proc. 6th International Congress on Chemistry of Cement*, Vol. 2, No. 1, Moscow, Russia, 1974, pp. 331–337.
19. Goto, S., and D. M. Roy. Diffusion of Ions through Hardened Cement Pastes. *Cement and Concrete Research 11*, No. 5, 1981, pp. 751–757.
20. Wise, S., J. A. Satkowski, B. E. Scheetz, J. M. Rizer, M. L. Mackenzie, and D. D. Double. The Development of High Strength Cementitious Tooling/Molding Materials. *Very High Strength, Cement-Based Materials*, Vol. 42 (J. Francis Young, ed.) Materials Research Society, Pittsburgh, Pa., 1985, pp. 245–252.
21. Roy, D. M., P. W. Brown, D. Shi, B. E. Scheetz, and W. Ma. Concrete Microstructure Porosity and Permeability. Supplemental Report 5, SHRP–C–628, SHRP, National Academy of Sciences, Washington, D.C., 1993.
22. Roy, D. M., B. E. Scheetz, and M. R. Silsbee. Processing of Optimized Cements and Concretes via Particle Packing. *MRS Bulletin*, Materials Research Society, Pittsburgh, Pa., 1993, pp. 45–49.
23. Toufar, W., M. Born, and E. Klose. Freeberger Forschungsheft, A559 (VEB Deutschen Verlag fur Grundslaffindustrie), Germany, 1967.
24. Aim, R. B., and P. LeGoff. *Powder Technol*, Vol. 1 1967/1968, pp. 281–290.
25. Roy, D. M., P. D. Cady, S. A. Sabol, and P. H. Licastro. *Concrete Microstructure: Recommended Revisions to Test Methods*. SHRP–C–339. SHRP, National Academy of Sciences, Washington, D.C., 1993.
26. Roy, D. M., and G. M. Idorn. *Concrete Microstructure*. SHRP–C–340. SHRP, National Academy of Sciences, Washington, D.C., 1993.
27. Malek, R. I. A. Effects of Particle Packing and Mix Design on Chloride Permeability of Concrete. *Proc., 9th International Congress on Chemistry of Cement*, Vol. V, National Council for Cement and Building Materials, New Delhi, India, 1992, pp. 143–149.

Publication of this paper sponsored by Committee on Performance of Concrete.

Mechanical Properties and Durability of High-Strength Concrete for Prestressed Bridge Girders

ALIREZA MOKHTARZADEH, ROXANNE KRIESEL, CATHERINE FRENCH, AND MARK SNYDER

Results from a comprehensive laboratory investigation on the application of high-strength concrete to the production of precast/prestressed bridge girders are presented. The portion of the laboratory investigation described consisted of producing high-strength concrete with a variety of cementitious materials (portland cement, silica fume, and fly ash) in different proportions and made with five different types of coarse aggregate. Some specimens were moist cured in saturated-limewater at 23°C; others were heat cured in an environmental chamber at 65°C to simulate the accelerated curing technique typically used by precast/prestressed plants. The hardened concrete specimens were tested for compressive strength, modulus of elasticity, tensile strength, modulus of rupture, shrinkage, creep, absorption potential (as an indirect indicator of permeability), and freeze-thaw durability.

An extensive investigation is under way at the University of Minnesota to study the application of high-strength concrete to prestressed bridge girder production. High-strength concrete is defined as concrete with a 28-day compressive strength in excess of 41 MPa. The objective of the study is to obtain information on production techniques, mechanical properties, and durability of high-strength concrete in general and to provide recommendations for using these concretes in manufacturing precast/prestressed bridge girders. Test variables include total amount and composition of cementitious material [portland cement, fly ash (FA), and silica fume (SF)], type and brand of cement, type of silica fume (dry-densified and slurry), type and brand of high-range water-reducing admixture, coarse-to-fine aggregate ratio, type of aggregate, aggregate gradation, maximum aggregate size, and curing. Tests are being conducted to determine the effects of these variables on changes in compressive strength and modulus of elasticity over time, splitting tensile strength, modulus of rupture, creep, shrinkage, absorption potential [as an indirect indicator of permeability (*1*)], and freeze-thaw durability. Also being investigated are the effects of test parameters such as mold size, mold material, and end condition. Nearly 7,000 specimens have been cast from approximately 150 mixes over a period of 3 years (*2,3*).

This paper presents results from a portion of the study (20 mixes) for which total cementitious material content, water-to-cementitious material ratio, and coarse-to-fine aggregate ratio were held constant at 445 kg/m^3, 0.30, and 1.5, respectively. Four different cementitious material combinations were investigated: reference mix (portland cement only) and three comparison mixes containing 20 percent FA, 7.5 percent SF, and a combination of 20 percent FA with 7.5 percent SF. For the three comparison mixes, the fly ash and silica fume were incorporated as replacements for portland cement on an equal weight basis. Five different types of locally obtained coarse aggregates were used in this phase of the investigation: round gravel (RG), partially crushed gravel (PCG), crushed granite (GR), and a high-absorption (LS–H) and a low-absorption (LS–L) crushed limestone. From each concrete batch, both heat- and moist-cured specimens were investigated.

Department of Civil Engineering , University of Minnesota, 122 Civil Engineering Building, 500 Pillsbury Drive, S.E., Minneapolis, Minn. 55455–0220.

MATERIALS

The cementitious material comprised low-alkali ASTM C150 Type III portland cement, ASTM C618 Class C fly ash, and silica fume slurry.

All the aggregates were obtained from local sources and washed in the laboratory. The coarse aggregates had a nominal maximum particle size of 13 mm. The natural coarse sand used in all mixes had a fineness modulus of 2.80. According to Minnesota Department of Transportation specifications, the maximum allowable absorption capacity for Class B aggregates (crushed quarry or mine rock) is 1.7 percent to ensure durable performance of concrete superstructures (*4*). Absorption capacities of the aggregates used in the study were 0.50 percent for the fine aggregate, 1.11 percent for the RG, 1.39 percent for the PCG, 1.00 percent for the granite, 2.05 percent for the LS–H (used in the reference and 7.5 percent silica fume mixes), 2.97 percent for the LS–H (used in the 20 percent fly ash and combination of 20 percent FA with 7.5 percent SF mixes), and 1.50 percent for the LS–L. The reason for listing two absorption capacities for the high-absorption limestone is that the aggregate was obtained at two different times from the same source.

A modified naphthalene sulfonate high-range water-reducer (superplasticizer) was used in varying quantities (13 to 23 mL/kg of cement) to attain a target slump of 100 to 150 mm. No air-entraining agents were used in the mixes, in conformance with typical precast girder production.

The moisture content of the aggregates and the water content of the SF slurry and superplasticizer were considered in proportioning the mix water. The mix proportions per cubic meter of concrete, as batched, are given in Table 1.

FABRICATION AND CURING PROCEDURES

For each mix investigated, all specimens were cast from a single batch. The mixing and curing was conducted in the Structural Labo-

TABLE 1 As-Batched Mix Proportions per Cubic Yard of Concrete

Mix	Coarse Aggr* (kg)	Fine Aggr* (kg)	Cement (kg)	Fly Ash (kg)	Silica Fume Slurry+ (kg)	Water∇ (kg)	HRWRΔ (g)
RG	1120	747	445	0	0	129	5569
RG w/FA	1112	742	356	89	0	129	5569
RG w/SF	1110	740	412	0	70	95	5569
RG w/FA&SF	1104	736	323	89	70	95	5569
PCG	1139	760	445	0	0	129	5569
PCG w/FA	1133	755	356	89	0	129	5569
PCG w/SF	1130	753	412	0	70	95	5569
PCG w/FA&SF	1124	749	323	89	70	95	5569
GR	1125	749	445	0	0	129	5569
GR w/FA	1117	746	356	89	0	129	5569
GR w/SF	1116	744	412	0	70	95	5569
GR w/FA&SF	1109	739	323	89	70	95	5569
LS-H	1147	765	445	0	0	129	5569
LS-H w/FA	1139	760	356	89	0	129	5569
LS-H w/SF	1138	759	412	0	70	95	5569
LS-H w/FA&SF	1130	753	323	89	70	95	5569
LS-L	1142	761	445	0	0	129	5569
LS-L w/FA	1135	756	356	89	0	129	5569
LS-L w/SF	1133	755	412	0	70	95	5569
LS-L w/FA&SF	1126	751	323	89	70	95	5569

* Values listed are for SSD moisture condition. Water was proportioned to compensate for actual moisture content of aggregates at time of mixing.
+ Silica Fume Slurry includes water weight (Solids: 659 kg/m^3 ; Water: 683 kg/m^3).
∇Water weight corresponding to SSD aggregate condition, adjusted for the amount of water in silica fume slurry and HRWR.
Δ Nominal amount of HRWR which was then adjusted (increased or decreased) during the mixing process to achieve the desired slump range of 100 to 150 mm.

ratory at the University of Minnesota. A 0.3-m^3 fixed-drum mixer powered by an electric motor was used to mix all of the concrete batches. Specimens cast from each mix included thirty-eight 100 × 200 mm and six 150 × 300 mm cylinders for compression tests (compressive strength and modulus of elasticity tests), three 150 × 300 mm cylinders for splitting tensile strength tests, four 150 × 150 × 610 mm beams for modulus of rupture tests, two 100 × 250 mm cylinders for shrinkage tests, and two 100 × 200 mm cylinders for absorption potential tests. Two 100 × 250 mm cylinders were cast from 14 of the mixes for creep studies. Four beams 76 × 102 × 406 mm were cast from 17 of the mixes for freeze-thaw durability testing. These quantities reflect that at least two duplicate specimens were fabricated to establish every test data point by averaging the results.

Mixing

Following evaluation of a few trial batches, the standard laboratory mixing and batching procedures recommended by ASTM C192 were modified slightly to allow an easy and uniform production technique. The mixing procedure followed these steps:

1. Spray interior of mixer with water. Empty the mixer and drain it.
2. Load the mixer with all coarse aggregate and half of the mixing water. Mix for ½ min.
3. Stop the mixer and allow the coarse aggregate to soak in the water for 10 min.
4. Turn on the mixer and add sand, cementitious material, remaining water, and high-range water-reducer. Mix for 5 min.
5. Stop the mixer for 1 min. Evaluate the workability. Add additional high-range water-reducer (up to a total of 23 mL/kg of cement), if needed.
6. Turn on the mixer for an additional 3 min.
7. Perform a final slump test and discharge the concrete into a clean, moist, metal bin and cast the specimens.

For each mix, slump and air contents were measured according to ASTM C143 and C173 (volumetric method) procedures, respectively. Results are given in Table 2 along with the 28-day compressive strengths of the heat- and moist-cured 100 × 200 mm specimens.

Casting and Curing

One day before mixing, the insides of all molds were lightly oiled with form coating oil. Molds were filled and manually rodded in accordance with the provisions of ASTM C192. All high-strength concrete specimens were cast in plastic molds except for the flexural modulus and freeze-thaw beams, which were cast in heavy-gauge reusable steel molds.

A 1460 L curing tank equipped with a thermostatically controlled electric heater was used to moist-cure concrete specimens. The specimens to be moist-cured were placed into the 23°C saturated-limewater bath immediately after casting. To avoid damage to the

TABLE 2 Air Contents, Slumps, and 28-Day Compressive Strengths

Mix	air content (%)	slump (mm)	f'c, heat-cured (MPa)	f'c, moist-cured for 7 days (MPa)	f'c, moist-cured for 28 days (MPa)
RG	1.5	127	77	98	91
RG w/FA	2.5	140	75	91	82
RG w/SF	1.5	70**	89	105	100
RG w/FA&SF	1.5	140	79	103	102
PCG	1.5	13*	89	111	104
PCG w/FA	2.0	89**	86	104	104
PCG w/SF	1.5	89**	99	113	108
PCG w/FA&SF	2.0	76**	91	114	110
GR	1.5	44*	87	99	98
GR w/FA	1.5	102	81	99	98
GR w/SF	1.5	NR	97	120	115
GR w/FA&SF	1.0	102	90	104	111
LS-H	1.5	152	104	118	114
LS-H w/FA	1.0	114	86	98	98
LS-H w/SF	NR	102	115	116	118
LS-H w/FA&SF	1.5	152	96	109	107
LS-L	1.5	38*	112	120	111
LS-L w/FA	1.0	102	98	101	103
LS-L w/SF	2.0	114	113	127	121
LS-L w/FA&SF	1.0	NR	111	124	110

*It was not possible to achieve the desired slump range of 100 to 150 mm without exceeding the maximum superplasticizer dosage of 23 ml per kilogram of cement (12282 g/m^3 of concrete).
NR Indicates measurement not recorded.
**For these mixes, adequate workability was achieved without meeting target slump range of 100 to 150 mm.

young specimens, molds were stripped after 48 hr (instead of 24 ± 8 hr, as specified by ASTM C192). The specimens were immediately returned to the saturated-limewater bath where they remained until testing, except the freeze-thaw beams, which were moist cured for 7 days.

To simulate the accelerated heat-curing process typical of precast/prestressed concrete manufacturers, an electronically controlled environmental chamber was used. The temperature in the chamber was varied according to the following procedure: 3 hr at room temperature (preset period after casting), temperature increased to 65°C over the next 2.5 hr, temperature held constant for 12 hr, and specimens returned to room temperature over 2 hr. To prevent loss of moisture from the fresh concrete, the surface of each heat-cured specimen was covered immediately after casting with a piece of plastic wrap held in place by a rubber band. The heat-cured specimen molds were stripped after 24 hr. These specimens were then stored in air in the laboratory until testing.

EXPERIMENTAL PROGRAM TO INVESTIGATE MECHANICAL PROPERTIES

All compression tests, splitting tensile strength tests, and modulus of rupture tests were conducted using an MTS Model 810 Material Testing System. The system has a dual capacity of 534 or 2,670 kN (tension or compression) and can be programmed to operate in either load or displacement control modes. For compression tests, the load was continuously applied to the specimens by moving the top spherical bearing block at a rate of 1.3 mm/min (displacement control mode).

The splitting tensile strength tests and flexural modulus tests were conducted under the load control mode with the 534 kN capacity of the testing machine selected. Specimens were loaded at a rate of 75.5 kN/min and 8 kN/min for splitting tensile strength and modulus of rupture tests, respectively. These loading rates corresponded to a stress increase of 1.03 MPa/min. The ASTM C496 (specification for

splitting tensile strength test) and ASTM C78 (specification for third-point loading flexural strength test) specified ranges for loading rates are 0.69 to 1.38 MPa/min and 0.86 to 1.21 MPa/min, respectively.

An aluminum compressometer, similar in principle to conventional compressometers used for standard cylinders, was built to measure Young's modulus of elasticity for 100 × 200 mm cylinders. A linear variable differential transformer (LVDT) with a maximum range of ±0.254 mm was mounted on this device to measure the sum of deformations of two diametrically opposite gauge lines. The gauge length for the axial deformation measurements was 100 mm. A conventional compressometer with a gauge length of 200 mm, equipped with a dial gauge, was used to measure Young's modulus of elasticity for the 150 × 300 mm cylinders. The 100 × 200 mm and 150 × 300 mm test cylinders were preloaded to 67 kN and 134 kN, respectively, and unloaded before testing for Young's modulus of elasticity. This initial loading and unloading was performed to ensure proper seating of the fixture on the test specimen.

The results of mechanical tests of compression strength and Young's modulus of elasticity changes with respect to time, splitting tensile strength, and modulus of rupture follow. Tests to investigate creep and shrinkage are still in progress.

Compression Tests

In this portion of the study, compression tests were conducted on 100 × 200 mm cylinders at different ages to study strength-time and elastic modulus-time relationships. For heat-cured specimens, tests were conducted at 1, 28, 182, and 365 days. Moist-cured specimens were tested at 28, 182, and 365 days (results are reported for data available up to 182 days). Compression tests on companion 150 × 300 mm cylinders were also conducted (at 1 and 28 days for heat-cured and 28 days for moist-cured specimens) to study size effects. All compression test specimens were capped using a high-strength sulfur-based capping compound.

Compressive Strength Change with Time

Table 3 summarizes the ranges of compressive strengths obtained for all mixes in this part of the study. Also shown in Table 3 are ratios of 1-day and 182-day strengths relative to 28-day strengths. These data indicate that the heat-cured specimens did not gain much compressive strength after 28 days. However, on average, 182-day-old continuously moist-cured specimens achieved compressive strengths that averaged approximately 10 percent greater than those measured at 28 days.

The effect of curing on strength gain over time for the LS–H reference mix is shown in Figure 1. In addition to the data described in this portion of the study (which are represented by filled symbols), additional data are included from the main body of tests (lines). The lines shown in the figure represent data obtained from identical mixes (except aggregate gradation) tested at more frequent intervals (1, 14, 28, 56, and 182 days). At early ages, the heat-cured specimens developed higher strengths (which is why heat-curing is used in precasting operations with short turnaround times on casting beds). At later ages (20 to 60 days), the strengths of the moist-cured specimens catch up with and then surpass those of the heat-cured specimens. This can be attributed to the continued hydration of cement in the moist-cured specimens and the reduced rate of hydration in the heat-cured specimens during the laboratory storage portion of their curing.

Figure 2 shows the effect of aggregate type on strength gain. In comparing the compressive strength of concrete made with crushed limestone (LS–H and LS–L) versus RG, the concrete made with limestone aggregates achieved higher compressive strengths. Crushed limestone particles showed a very strong bond with cement paste, and the plane of fracture in the limestone concrete crossed through many coarse aggregate particles. In contrast, the smooth surface of RG particles resulted in a relatively poor bond with cement paste, and the plane of fracture passed around all but the smaller coarse aggregate particles. Compressive strengths of the mixes using GR and PCG were between those of the limestone and

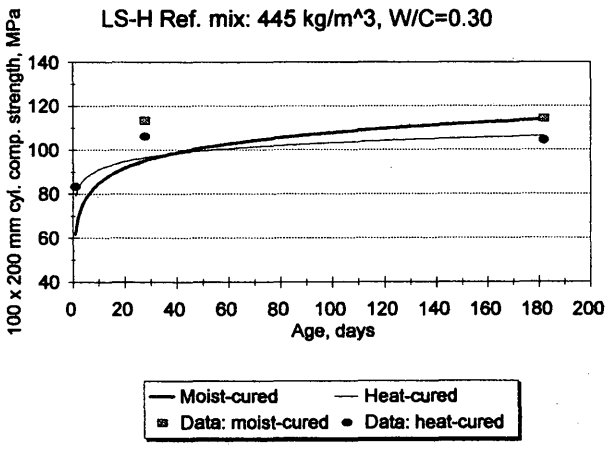

FIGURE 1 Effect of curing on strength gain with time.

TABLE 3 Compressive Strength Change with Time

	Heat-Cured	Moist-Cured
1-day Compressive Strength, MPa	44 - 101	-
28-day Compressive Strength, MPa	58 - 116	70 - 119
182-day Compressive Strength, MPa	63 - 117	87 - 122
Ratio of 1-day to 28-day Strength	mean: 0.84 SD: 0.06	-
Ratio of 182-day to 28-day Strength	mean: 1.00 SD: 0.04	mean: 1.10 SD: 0.09

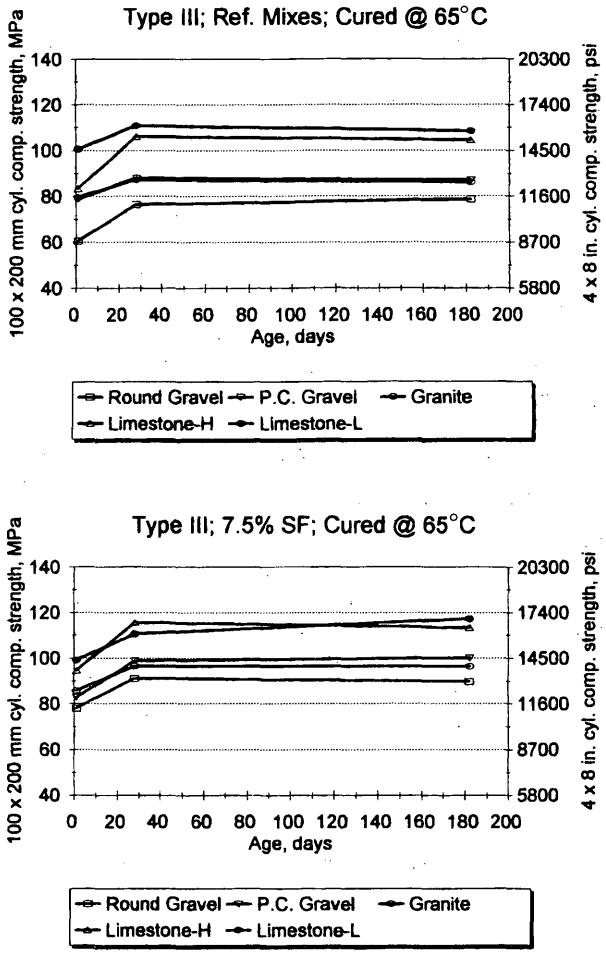

FIGURE 2 Effect of type of aggregate on strength development: reference mixes (*top*) and mixes containing 7.5 percent SF (*bottom*).

RG mixes. The PCG mix failures were attributed to the flaky physical nature of the aggregate. Mineralogical characteristics of the specific granite used were suspected to be the reason for the relatively poor performance of high-strength concrete made with granite.

The difference between the top and bottom of Figure 2 is the cementitious material composition represented (the reference mix versus the 7.5 percent SF replacement by weight of cement mix). The replacement of cement by 7.5 percent SF improved the concrete compressive strength at all ages. In particular, silica fume increased the compressive strength of RG concrete. This can be attributed to the improved bond between the round gravel and the cement paste. More fractured aggregate particles were observed in tests of the RG mix containing silica fume than were observed in the reference mix tests. Moist-curing enhanced the benefit obtained from including silica fume.

Effects of replacement of cement by 20 percent FA, 7.5 percent SF, and the combination of 20 percent FA with 7.5 percent SF on heat-cured high-strength concrete made with GR are shown in Figure 3. For crushed granite, the concrete compressive strength of the 7.5 percent SF mix was highest followed by compressive strengths of the reference concrete and the concrete made with the combination of 20 percent FA with 7.5 percent SF. Concrete mixes containing 20 percent fly ash exhibited the lowest compressive strengths at all ages (to 182 days). The same trend with respect to cementitious material composition was observed for the concretes made with other types of aggregates and curing.

Modulus of Elasticity

The modulus of elasticity was measured after 1 (heat-cured specimens only), 28, and 182 days. Figures 4 and 5 show comparisons of the modulus of elasticity and compressive strengths measured on both 100 × 200 and 150 × 300 mm cylinders relative to equations given in American Concrete Institute (ACI) 318 and proposed by ACI High-Strength Committee 363 (*5,6*). It is clear that for high-strength concrete, the ACI 318 equation overestimates the measured modulus of elasticity of 150 × 300 mm cylinders. Comparing the top and bottom of Figure 5 it is observed that heat-cured specimens exhibited slightly lower moduli of elasticity at any given strength than the moist-cured cylinders.

Of particular interest is the change of modulus of elasticity with time. The initial modulus of elasticity is important to the precast/prestressed industry for investigating effects such as elastic shortening. The later age modulus of elasticity can be used to predict prestress

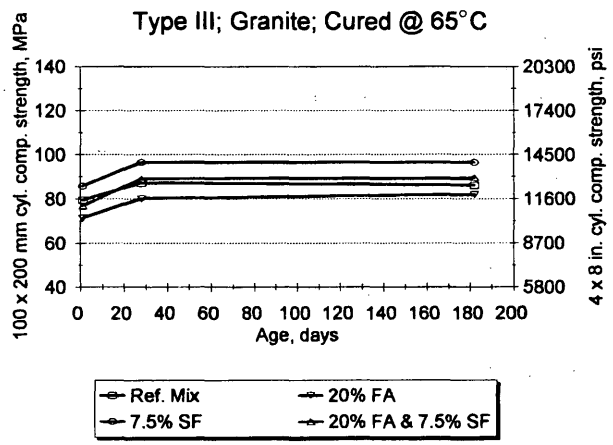

FIGURE 3 Effect of replacement of cement by 20 percent FA and 7.5 percent SF.

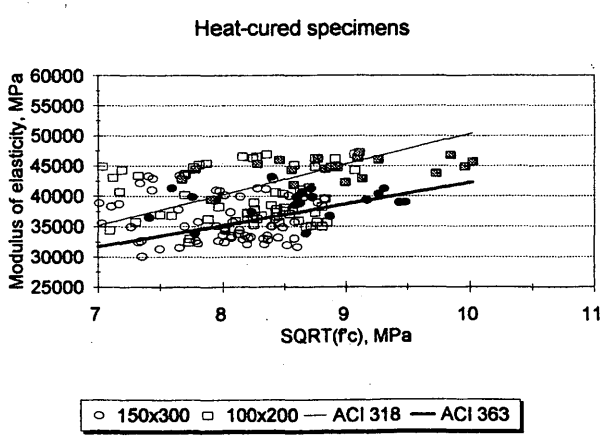

FIGURE 4 1-day modulus of elasticity versus ACI 318 and 363 equations.

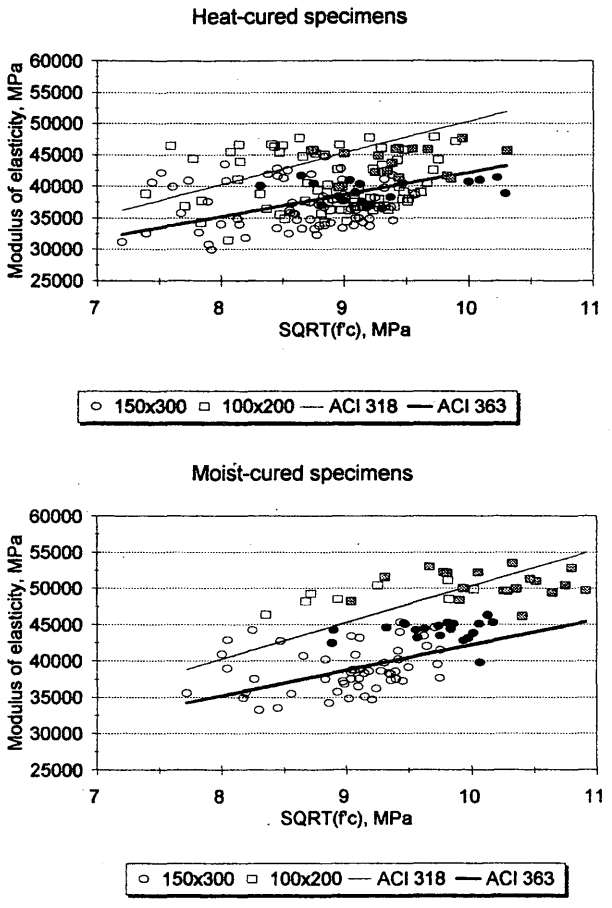

FIGURE 5 28-day modulus of elasticity versus ACI 318 and 363 Equations: heat-cured specimens (*top*) and moist-cured specimens (*bottom*).

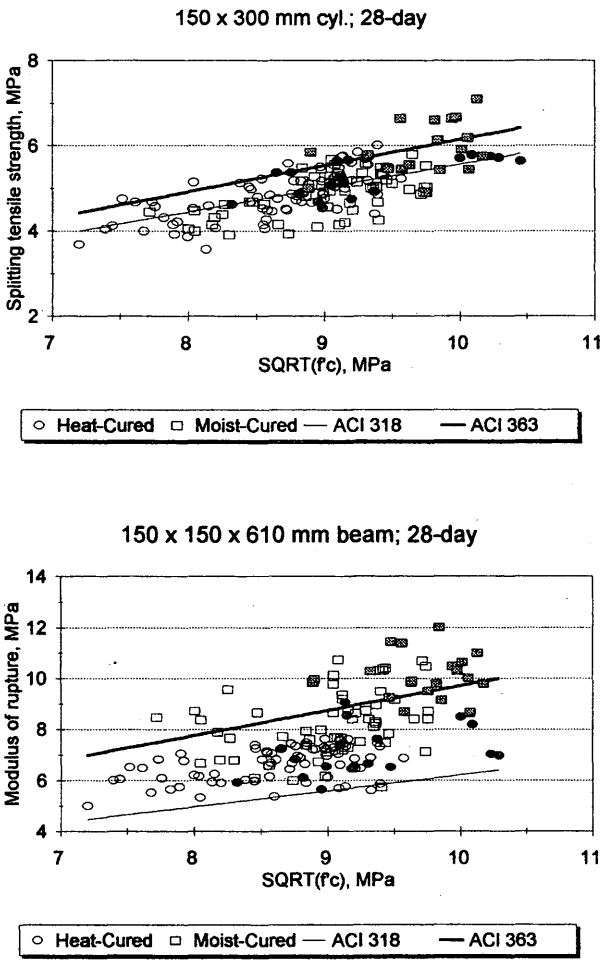

FIGURE 6 Splitting tensile strength test results (*top*) and modulus of rupture test results (*bottom*).

losses and deflection of bridge girders. The results obtained from this study indicate that the 1-day modulus of elasticity measured on heat-cured 100 × 200 mm or 150 × 300 mm cylinders was approximately 98 percent of the 28-day modulus of elasticity value. The modulus of elasticity of the heat- and moist-cured 100 × 200 mm cylinders at 182-days were approximately 96 and 106 percent of their 28-day modulus of elasticity values, respectively.

Tensile Strength

Data obtained for splitting tensile strength of both heat-cured and moist-cured cylinders 150 × 300 mm were more closely predicted by the ACI 318 equation than the proposed ACI 363 relationship. Figure 6 (top) shows results from splitting tensile strength tests conducted on cylinders 150 × 300 mm at 28-days.

Modulus of Rupture

Figure 6 (bottom) shows modulus of rupture test results for heat-cured and moist-cured specimens relative to equations proposed by ACI 318 and ACI 363. Data obtained for modulus of rupture of heat-cured specimens ranged between values predicted by ACI 318 and ACI 363 equations. From this figure, it is evident that the type of curing significantly affected the modulus of rupture test results, with moist-cured samples exhibiting higher flexural strengths. The modulus of rupture of moist-cured specimens was adequately predicted by the ACI 363 proposed equation.

EXPERIMENTAL PROGRAM TO INVESTIGATE FREEZE-THAW DURABILITY

To investigate the durability of high-strength concrete, freeze-thaw studies were conducted on 17 of the mixes in general accordance with ASTM C666 Procedure B (rapid freezing in air and thawing in water). An exception to the standard test procedure was made to investigate the effect of curing on freeze-thaw durability. The standard procedure requires freeze-thaw specimens to be cast and continuously moist cured for 14 days before placing them in the freeze-thaw testing machine. To investigate curing effects, specimens were either heat cured or moist cured for a limited amount of time before being stored in a relatively constant temperature and humidity environment for approximately 6 months. This procedure was intended to simulate casting and aging of cast-in-place and precast/prestressed members before exposing them to freeze-thaw conditions. Other variables investigated were aggregate type and cementitious material composition.

Specimen Preparation and Test Procedure

Four beams 76 × 102 × 406 mm were cast from each mix following ASTM C192 procedures. Manual rodding was used as the method of consolidation. (Measured slumps and air contents are given in Table 2.) As mentioned previously, no air-entraining agents were used to emulate the production of precast/prestressed bridge girders.

Two of the freeze-thaw beam specimens were heat cured, and two were moist cured in a saturated-limewater bath for 7 days. Following the specified curing period, the specimens were placed in an environment of relatively constant temperature and humidity (23°C and 50 percent relative humidity). At 189 days, the specimens were placed in a constant temperature bath at 4.5°C for a period of 21 days before the start of freeze-thaw testing. The 3-week period of immersion was to enable at least partial saturation of the concrete beam specimens before freezing and thawing. This was considered a severe condition because bridge girders are not typically maintained in a saturated moisture condition. Following the 21-day immersion in the constant temperature bath, the first set of concrete beam specimens and some beams from subsequent mixes were placed on a chest freezer and kept at an approximately constant temperature (−18°C) until calibration of the new freeze-thaw testing machine was completed. The calibration was performed in accordance with ASTM C666, which specifies storage of the specimens in a frozen condition if the sequence of freezing and thawing is interrupted. The lengths of time the specimens were kept frozen varied from 0 to 41 days and are provided in Table 4, along with the freeze-thaw test results.

Companion cylindrical specimens 100 × 200 mm were tested to determine absorption potential, which serves as an indirect indicator of concrete permeability (*1*). These specimens were heat cured at 65°C or moist cured for 28 days, as described. After the specified curing period, the specimens were stored in an environment of 23°C and 50 percent relative humidity until they were 56 days old. They were then submerged in water and the weight gain measured with respect to time. This test was still in progress at the time this paper was written; measurements at 105 days are given in Table 4.

Results

The specimens were removed from the freeze-thaw testing machine at intervals conforming to the requirements of ASTM C666; measurements were taken to evaluate deterioration. Changes in specimen weight and length were monitored, and the specimen fundamental transverse frequency was measured in accordance with the ASTM C215, Impact Resonance Method. The relative dynamic modulus (RDM) of elasticity of each specimen was calculated using the fundamental transverse frequency measurements. ASTM C666 requires that the testing of each specimen continue until it has been subjected to 300 freeze-thaw cycles or until it has reached a failure criterion, whichever occurs first. ASTM defines possible failure criteria as the relative dynamic modulus of elasticity reaching 60 percent of the initial modulus or, optionally, a 0.10 percent length expansion. In this study, both failure criteria were considered, and the specimens were removed from the freeze-thaw testing machine when the relative dynamic modulus of elasticity reached 50 percent of the initial modulus.

The average number of cycles after which the failure criteria were met and the corresponding average durability factors (DF) for each pair of specimens are given in Table 4. The number of cycles to observed failure is given for the relative dynamic modulus and the length expansion failure criteria. As can be seen in the table, there is generally a strong correlation between the two failure criteria for all but the limestone aggregate mixes; in which case, the length expansion or dilation criterion was generally reached much more quickly than the relative dynamic modulus criterion. This may be because of the relative inability of the more porous limestone to restrain dilations of the cement mortar when compared with concrete containing the harder gravel and granite aggregates.

The DF for the heat- and moist-cured specimens are plotted in Figure 7 *top* and *bottom*, respectively. The results shown in these figures are grouped according to aggregate type and cementitious material composition.

The following DF scale to evaluate frost-resistant performance was proposed (*7*): concrete with a DF less than 40 is probably unsatisfactory for frost resistance, concrete with a DF between 40 and 60 is of doubtful performance, and concrete with a DF greater than 60 is probably satisfactory for frost resistance. This scale was used to evaluate the effects of curing condition, aggregate type, and cementitious composition. These evaluations follow.

Effect of Curing Condition

Figure 7 *top* and *bottom* indicates that the moist-cured specimens generally exhibited better freeze-thaw durability than the heat-cured specimens. Moist-curing allows continuous hydration of the cementitious materials, developing a less permeable pore structure. The hydration in heat-curing is limited by the amount of mix water. Microcracking could also develop on drying, weakening the strength of the transition zone between the aggregate and the cement paste. These factors result in increased permeability. In the instances in which the heat-cured specimens performed better, the durability factors were less than 25 for the heat- and moist-cured specimens (unsuitable for frost resistance). Both heat- and moist-cured specimens performed satisfactorily (DF > 60) for all LS–L mixes, although moist-curing appeared to provide better durability.

These observations on the effect of curing condition correlate well with the results of the absorption potential tests in which the moist-cured specimens consistently absorbed less water than the heat-cured specimens.

Effect of Aggregate Type

The low-absorption limestone specimens consistently performed the best of all of the mixes (reference, 7.5 percent SF, and combination of 20 percent FA with 7.5 percent SF) for both types of curing, with DFs ranging from 61 to 98. Several of the LS–L specimens endured more than 1,500 freeze-thaw cycles without failing (the RDM criterion) before they were removed from the freeze-thaw testing machine. The moist-cured LS–H and PCG reference mixes also exhibited satisfactory performance. The RG and granite specimens performed the poorest (DF < 15). The order of performance, with the exception of the limestone aggregate specimens, was consistent with the results of the absorption tests. In other words, the limestone specimens exhibited the highest absorption but showed the best performance. Improved performance of the other mixes correlated with reduced absorption.

The good performance of the limestone may be attributed to the surface texture of the aggregate. Angular, rough-surfaced aggregates develop a better bond with the cement mortar, strengthening

TABLE 4 Freeze-Thaw Durability and Absorption Potential Test Results

Mix	Days Frozen Prior to Testing	Cycles to Observed RDM Failure *Length Change Failure*		Durability Factor		Absorption @ 105 days* (% weight)	
		Heat-cured	Moist-cured	Heat-cured	Moist-cured	Heat-cured	Moist-cured
RG	18	34 *34*	80 *80*	5	14	1.27	0.67
RG w/FA	41	26 *30*	85 *85*	5	15	1.62	0.73
RG w/SF	32	34 *34*	26 *30*	6	5	0.78	0.52
RG w/FA&SF	27	48 *41*	26 *26*	7	7	1.10	0.72
PCG	4	71 *62*	1507+(346) *1507+(346)*	12	97	1.20	0.71
PCG w/FA	4	55 *48*	201 *180*	10	40	1.54	0.75
PCG w/SF	0	30 *26*	26 *26*	4	2	0.93	0.61
PCG w/FA&SF	0	68 *58*	35 *38*	12	6	0.87	0.70
GR	0	46 *30*	52 *48*	9	9	1.58	0.78
GR w/FA	0	53 *53*	59 *62*	10	11	1.43	0.82
GR w/SF	0	30 *30*	20 *20*	3	2	0.88	0.59
GR w/FA&SF	0	53 *53*	19 *22*	10	4	1.10	0.69
LS-H	13	469(149) *59*	1507+ *1507(1132)*	66(30)	97	1.59	0.78
LS-H w/FA&SF	6	119 *62*	26 *26*	24	5	1.25	0.98
LS-L	0	1520+ *1520+(1166)*	1520+ *1520+*	96	98	1.35	0.80
LS-L w/SF	0	640 *229*	1510+ *420(240)*	77	81	0.93	0.71
LS-L w/FA&SF	0	308 *161*	1366 *116*	61	71	0.94	0.77

*Test in progress.

+Indicates that the specimens have not yet failed the relative dynamic modulus test.

( ) Indicates value for companion specimen if different.

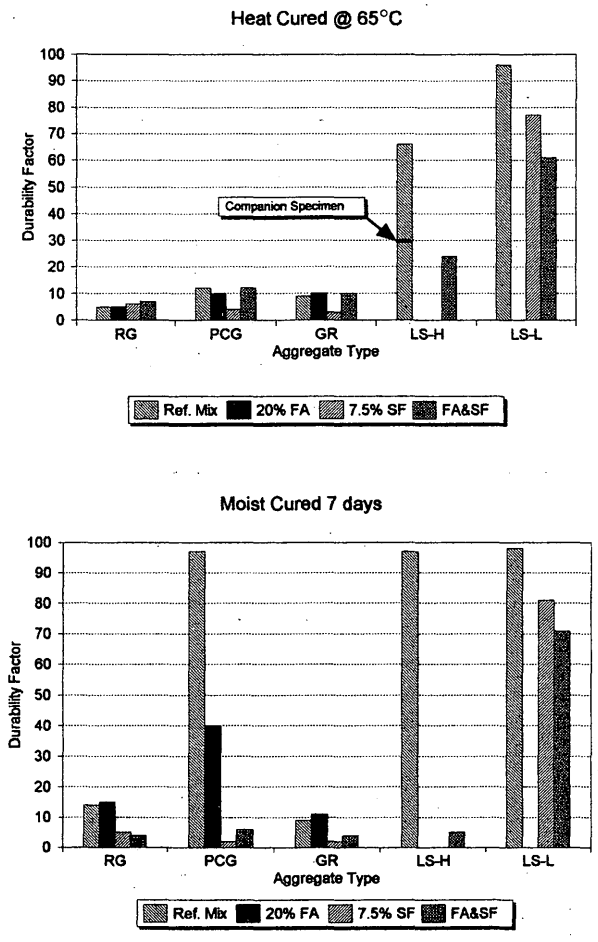

FIGURE 7 Freeze-thaw cycle durability: heat-cured specimens (*top*) and moist-cured specimens (*bottom*).

the transition zone between the paste and aggregate. A weak transition zone could result in microcracking around the aggregates. This theory is supported by the performances of the PGG and RG specimens. When mix composition is held constant, the PCG (with the more angular, rough-surfaced particles) generally exhibited better freeze-thaw durability (see Table 4). For example, the reference concrete mixes made with PCG and RG resulted in durability factors of 12 and 5, respectively.

Although the limestone specimens achieved high durability factors, they generally failed the length expansion test quite early compared with the RDM criterion. The dilation of the limestone mixes that failed the ASTM criteria ranged from 0.20 to 0.38 percent at RDM failure. As previously mentioned, the large dilations observed may be because of the relative inability of the more porous limestone to restrain the expanding cement mortar. The low-absorption limestone reference mix, however, exhibited excellent freeze-thaw durability in terms of both RDM and dilation, withstanding over 1,100 cycles without failing.

Effect of Cementitious Composition

Comparing the results in the *top* and *bottom* of Figure 7, it can be seen that the reference mixes generally performed the best for any given aggregate type. For the moist-cured specimens, the reference mixes prepared using limestone and PCG achieved DFs in excess of 90. The heat-cured limestone reference mixes also generally exhibited satisfactory performance.

For both heat- and moist-cured specimens of the low-absorption limestone, the good performance of the reference mixes was followed by the performances of 7.5 percent SF and the combination of 20 percent FA with 7.5 percent SF mixes. Similar results were seen in the heat- and moist-cured LS–H mixes in which the reference mix exhibited better durability than the 20 percent FA with 7.5 percent SF combination mix.

For the remaining three aggregates (RG, PCG, GR), the effect of variations in cementitious composition strongly correlated with curing condition. All of the heat-cured specimens exhibited poor durability (DF = 3 to 12). When moist-curing was used, the reference and fly ash mixes performed much better than those containing silica fume, especially for the PCG.

The absorption tests have shown that the FA specimens typically absorbed the most water, followed by the reference mix specimens. The SF specimens absorbed the least water, with the silica fume and fly ash with FA combination specimens exhibiting similar performance (with a slightly higher absorption observed for the specimens containing the combination of fly ash with silica fume). There was no apparent correlation between the absorption (indirect permeability measurement) and the durability factor.

Relationship of Compression Strength to Durability

Plots of durability factors versus 28-day compressive strengths of the heat- and moist-cured (7 day) 100 × 200 mm specimens are shown in Figure 8 *top* and *bottom*, respectively. Figure 8 (*top*) appears to show a strong correlation between compressive strength and durability factor for the heat-cured specimens, but on closer examination it can be seen that the relationship is strongly influenced by aggregate type. This is more clearly shown in Figure 8 (*bottom*) for the moist-cured specimens. Data in both figures indicate that for a given aggregate type for which a range of concrete strengths was produced (e.g., for GR, range in f'c of 81 to 120 MPa) little change in durability factor was observed.

The mechanisms that produced the observations and results described will be more fully investigated when analyses of the water pore and air void systems have been completed. This work is now under way.

Ongoing Research

Tests are being performed on the freeze-thaw concrete beams in accordance with ASTM C457 to measure the air void system of the hardened concrete and to determine the mechanism of failure in each case. Additional mixes will be tested to explore reasons for the failures and to identify potential improvements. Additional mixes will also be cast to compare the effects of curing in accordance with ASTM C666 (a 14-day moist cure) with the curing method used in this study. Three mixes are also being repeated to determine the effect, if any, of the period of freezing before testing on the observed durability performance. Two mixes that performed poorly in the study are being remixed with the addition of an air-entraining agent to assess its effect on improving the concrete durability results and to better quantify the durability of the various coarse aggregate sources.

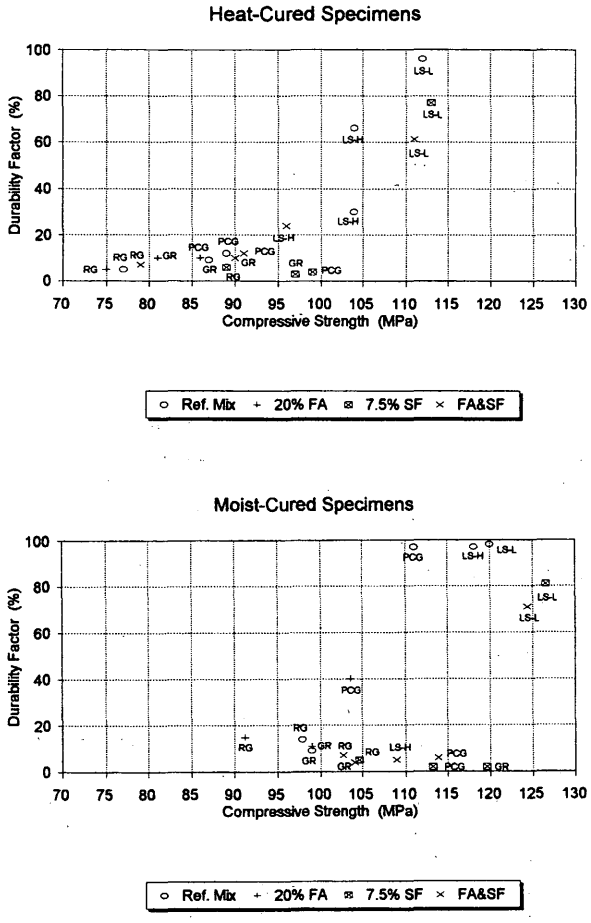

FIGURE 8 Durability factor versus 28-day compressive strength: heat-cured specimens (*top*) and moist-cured specimens (*bottom*).

SUMMARY

Preliminary results of a study of the mechanical characteristics and freeze-thaw durability of high-strength concrete were presented. Over 7,000 specimens have been cast and tested. The results described focus on a portion of the tests in which the total amount of cementitious material, water-to-cementitious material ratio, and coarse-to-fine aggregate ratio was held constant. Variables investigated include cementitious material composition, aggregate type, and curing condition. Results indicate that it is possible to develop non–air-entrained high-strength concrete with superior mechanical properties and freeze-thaw durability characteristics using local aggregate sources. In particular, the limestone reference mixes (without the addition of fly ash and silica fume) offered excellent mechanical and durability characteristics.

ACKNOWLEDGMENTS

This research investigation was conducted under the joint sponsorship of the Minnesota Prestress Association, Minnesota Department of Transportation, University of Minnesota Center for Transportation Studies, Precast/Prestressed Concrete Institute, and National Science Foundation Grant NSF/GER–9023596–02. The authors also acknowledge the generous donations of materials and equipment from Lehigh Cement Company; Holnam, Inc.; National Minerals Corporation; J. L. Shiely Company; Edward Kraemer & Sons, Inc.; Meridian Aggregates; W. R. Grace & Co.; Cormix Construction Chemicals; and Elk River Concrete Products.

REFERENCES

1. Burg, R.G., and B.W. Ost. Engineering Properties of Commercially Available High-Strength Concretes. *PCA Research and Development Bulletin RD104T.* Portland Cement Association, Skokie, Ill., 1992.
2. French, C.W., and A. Mokhtarzadeh. High Strength Concrete: Effects of Curing and Test Procedures on Short Term Compressive Strength. *PCI Journal,* Vol. 38, No. 3, May-June 1993, pp. 76–87.
3. French, C., A. Mokhtarzadeh, T. Ahlborn, and R. Leon. *Applications of High-Performance Concrete to Prestressed Concrete Bridge Girders.* Paper submitted to the International Workshop on Civil Infrastructure Systems, Taipei, Taiwan, Jan. 1994.
4. Minnesota Department of Transportation. *Standard Specifications for Construction,* 1988 ed. St. Paul, Minn. 1988.
5. *Building Code Requirements for Concrete, 318–89* (Rev. 1992). American Concrete Institute, Committee 318, Detroit, Mich., 1992.
6. *State-of-the-Art Report on High-Strength Concrete, 363R–92.* American Concrete Institute, Committee 363, Detroit, Mich., 1992.
7. Neville, A.M. *Properties of Concrete.* Pitman Publishing Ltd., London, England, 1975.

The views expressed herein are those of the authors and do not necessarily reflect the views of the sponsors.

Publication of this paper sponsored by Committee on Performance of Concrete.

Influence of Pumping on Characteristics of Air-Void System of High-Performance Concrete

R. PLEAU, M. PIGEON, A. LAMONTAGNE, AND M. LESSARD

The results of an experimental study in which a high-performance air-entrained concrete mixture (water-cement ratio = 0.29; 28-day average compressive strength of 75 MPa) was pumped at the job site horizontally and vertically are presented. Concrete specimens were taken before and after pumping. The specimens were subjected to the ASTM C 457 microscopical determination of the characteristics of the air-void system. The size distribution of the air voids was also recorded using a computer-assisted image analysis system. The study results indicate that pumping can reduce the total air content and increase the air-void spacing factor. It was observed that the loss of air is mainly due to a very significant decrease of the number of small air voids (<100 μm in diameter); the number of larger voids is very little modified. This suggests that the frost durability may be more detrimentally affected than it first appears, when only the air content and the spacing factor are considered. It was also found that the loss of small air voids is more important for vertical pumping than for horizontal pumping, probably because the pumping pressure involved is higher. A mechanism is proposed to explain the observed effect of pumping on the characteristics of the air-void system.

Field experience indicates that pumping often reduces the total air content in air-entrained concrete (*1–4*), which can possibly have a detrimental influence on the frost resistance. The air loss is generally small (i.e., 1 to 2 percent, but it can also be significant (i.e., greater than 4 percent). Lowering the air content generally yields a higher value of the air-void spacing factor, but very little data are available on the influence of pumping on the value of the spacing factor. Three mechanisms can explain the loss of air during pumping (*4*):

- Dissolution of air into the mixing water as a result of the higher solubility at a higher pressure,
- Vacuum effect occurring when the concrete falls in the descending portion of the hose, and
- Impact when the concrete drops from a given height at the end of the hose.

Previous work indicates that for ordinary concretes the decrease of the total air content is mainly due to the last two mechanisms. However, a recent study by Elkey et al. (*4*) clearly indicates that the first mechanism (dissolution of air) can cause a significant reduction in the total number of voids contained per unit volume even without a significant reduction of the total air content.

The necessity of air entrainment to protect high-performance concretes (HPCs) against freezing and thawing cycles is still disputed. It is clear, however, that many HPCs require at least a minimum amount of entrained air to be frost resistant (*5,6*), which means that these concretes could be detrimentally affected by a loss of air due to pumping. No data have been found on the influence of pumping on the air-void system of HPC. The aim of the present study was to provide such data.

R. Pleau, School of Architecture, Laval University, Québec, Canada G1K 7P4. M. Pigeon and A. Lamontagne, Department of Civil Engineering, Laval University, Québec, Canada G1K 7P4. M. Lessard, Department of Civil Engineering, University of Sherbrooke, Sherbrooke, Québec, Canada J1K 2R1.

TEST PROGRAM

The test program was conducted during the construction of a highway bridge built with an HPC having a water-cement ratio of 0.29 and a 28-day average compressive strength of 75 MPa. The specified composition of the concrete mixture is given in Table 1. At the job site, the fresh concrete was discharged and pumped directly into the formwork. Two series of concrete specimens (from two distinct batches) were prepared. In the first series, the concrete was pumped horizontally over a distance of approximately 20 m. In the second series, the concrete was pumped to a height of about 20 m before being discharged 5 to 7 m lower. In both series, specimens were prepared immediately before and after pumping. All concrete specimens were subjected to the ASTM C 457 microscopical examination (modified point count method) to assess the characteristics of the air-void system in the hardened concrete. For each specimen, 3,200 point counts were regularly spaced along a line of traverse of 240 cm covering a surface of 144 cm^2. The size distributions of the air-void circular sections seen under the microscope were also recorded using a computer-assisted image analysis system. For each specimen, the sections having a diameter smaller than 300 μm were measured and counted on 50 images covering a total surface of 2.84 cm^2.

A numerical method described elsewhere (*7,8*) was used to determine the size distribution of the air voids contained in a unit volume of concrete and the flow length (i.e., the distance between a point chosen at random into the cement paste and the boundary of the nearest air void). The flow length (Q) is similar to the Philleo factor (*9*), and it physically corresponds to the distance that freezable water must travel to reach an escape boundary during freezing. It is closely related to the frost resistance of concrete (*8*) and provides a much better evaluation of the efficiency of the air-void system than the commonly used ASTM C 457 spacing factor.

TEST RESULTS

The air content measured in the fresh concretes (ASTM C 231) and the characteristics of the air-void system in the hardened concretes

TABLE 1 Specified Composition of the Concrete Mixture

Water (kg/m³)	Cement* (kg/m³)	Fine Aggr. (kg/m³)	Coarse Aggr. (kg/m³)	Super-plasticizer (L/m³)	Air-Entraining Agent (mL/m³)	Set-Retarding Admixture (mL/m³)
130	450	700	1000	7.5	300 to 350	450

* Portland cement with silica fume (7% by weight)

(ASTM C 457) are presented in Table 2. This table indicates that the air content measured in the fresh concrete before pumping was almost the same for the two concrete batches (5.9 versus 6.4 percent). It also shows that a small air loss (0.9 and 0.4 percent) occurred during the transportation from the plant to the job site. That the air contents measured in the hardened concrete are lower than those measured in the fresh concrete is not uncommon, but it could suggest that some loss of air occurred from the time of casting to the final set of cement paste.

For the specimens subjected to horizontal pumping, the data in Table 2 show that the air content measured in the hardened concrete before pumping (4.3 percent) is relatively low. The air-void system, however, can be considered excellent because the specific surface of the air voids is very high (33.6 mm^{-1}), and the spacing factor (160 μm) is much lower than the maximum value of 230 μm recommended by the Canadian Standard CSA A23.1 (*10*). After pumping the air content is approximately the same (4.7 versus 4.3 percent), but the specific surface decreases significantly (from 33.6 to 23.1 mm^{-1}) and the spacing factor increases to a value (225 μm), very close to the 230 μm limit.

For the specimens subjected to vertical pumping, the data in Table 2 show that, even if the air content before pumping is significantly higher than in the specimens subjected to horizontal pumping (5.6 versus 4.3 percent), the specific surface is much smaller (21.8 versus 33.6 mm^{-1}), and the spacing factor is significantly higher (205 versus 160 μm). Nevertheless, the air-void system before pumping can still be considered satisfactory. Table 2 indicates however that after vertical pumping the air-void system is not satisfactory because the air content drops from 5.6 to 3.6 percent, the specific surface remains approximately the same (21.6 versus 21.8 mm^{-1}), and the spacing factor increases from 205 μm to 265 μm, a value clearly over the 230 μm limit. It is interesting to note that this increase in the spacing factor is similar to that due to horizontal pumping.

Figures 1 and 2 show the size distributions of air-void sections per unit surface of concrete observed under the microscope for the concrete specimens subjected to horizontal and vertical pumping, respectively. According to the data in these figures, which were obtained with the image analysis system, pumping reduces the number of air-void sections having a diameter smaller than 100 μm, but the size distribution of the larger sections is little modified. This effect is more important when concrete is subjected to vertical pumping instead of horizontal pumping.

Figures 3 and 4 show the size distributions of air voids for the concrete specimens subjected to horizontal and vertical pumping, respectively, as obtained from the mathematical relationship between the size distribution of a system of spheres randomly dispersed in a volume and the projection of this system on a planar surface (*7*). According to the data in these figures, horizontal pumping only slightly reduces the number of air voids smaller than 100 μm in diameter, but vertical pumping reduces the number of voids smaller than 100 μm significantly. It can be seen in Figure 4 that the number of voids smaller than 50 μm becomes extremely small after vertical pumping.

Figures 5 and 6 show the statistical distribution of the flow length as computed assuming that all the air voids are randomly dispersed throughout the cement paste. As mentioned previously, this flow length corresponds physically to the distance between a point chosen at random in the cement paste and the boundary of the nearest air void. The area under the curve from 0 to any given flow length value is equal to the probability that the flow length is smaller or equal to that value. The total area under the curve is obviously equal to 1.0 because the probability that the flow length is smaller than infinity is 100 percent. According to these test results, horizontal

TABLE 2 Air Content in Fresh Concrete (ASTM C 231) and Characteristics of the Air-Void System in Hardened Concrete (ASTM C 457)

		Fresh Concrete	Hardened Concrete		
		Air Content (%)	Air Content (%)	Specific Surface (mm^{-1})	Spacing Factor (μm)
Horizontal pumping	At plant	6.8	—	—	—
	Before pumping	5.9	4.3	33.6	160
	After pumping	6.1	4.7	23.1	225
Vertical pumping	At plant	6.8	—	—	—
	Before pumping	6.4	5.6	21.8	205
	After pumping	4.8	3.6	21.6	265

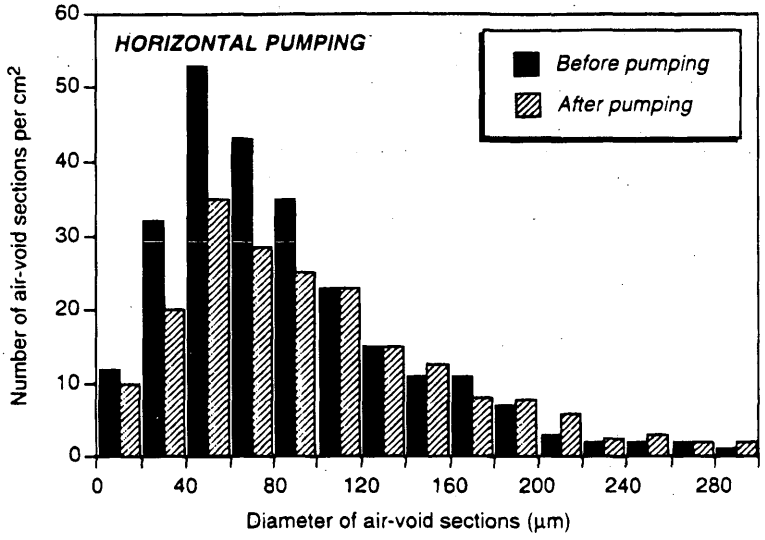

FIGURE 1 Size distributions of sections of air voids observed under microscope for specimens subjected to horizontal pumping.

pumping only slightly increases the probability of having a higher flow length, but vertical pumping has a more significant influence. After vertical pumping, a significant fraction of the cement paste is located much farther from the nearest air void.

Table 3 summarizes the characteristics of the air-void system of the various specimens when only the air voids smaller than 300 μm in diameter are taken into account. In this table, the flow length is associated with a probability level of 98 percent (i.e., only 2 percent of the cement paste is located at a distance larger than this value from the perimeter of the nearest air void). Although for the specimens subjected to horizontal pumping, the number of air voids is reduced by about 25 percent (31,400 to 23,900 voids/cm^3), the characteristics of the air-void system (air content and flow length) are not significantly modified. However, for the specimens subjected to vertical pumping, the number of voids per cm^3 of concrete and the air content are roughly reduced to half of their initial values, and the flow length increases by about 75 percent (from 175 to 305 μm).

DISCUSSION OF RESULTS

The test results described are interesting in many ways. First, they indicate that in certain cases pumping can have a small effect (as it was found for horizontal pumping) or sometimes a significant detrimental effect (as it was found for vertical pumping) on the characteristics of the air-void system. Second, they provide valuable information on the mechanisms of air loss due to pumping and the influence of various parameters. Third, they point the way to further research to understand

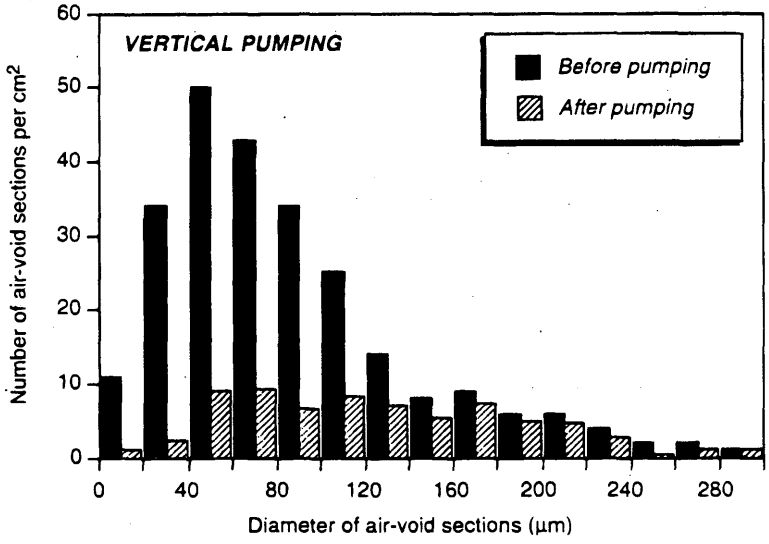

FIGURE 2 Size distributions of sections of air voids observed under microscope for specimens subjected to vertical pumping.

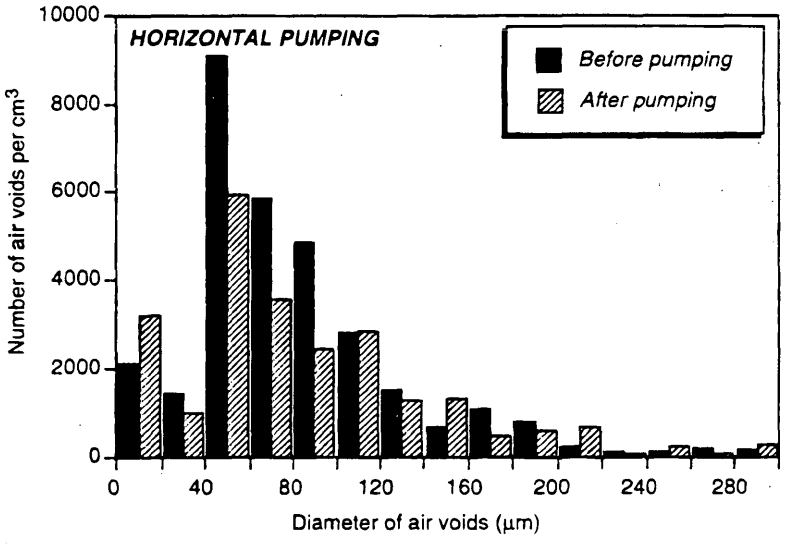

FIGURE 3 Size distributions of air voids obtained for specimens subjected to horizontal pumping.

and predict the influence of pumping on the characteristics of the air-void system and thus on the frost durability of concrete.

Field experience and laboratory investigations indicate that, most of the time, the loss of air during pumping is mainly due to the falling of concrete. In the pumping hose, falling creates a vacuum effect, and air voids can also break when concrete violently hits the formwork or the concrete already in place (*1–3*). The lowering of the falling height and the adding of an elbow pipe in the descending part of the pumping hose were found to be two efficient ways to attenuate this problem. It appears clear, however, that the loss of air caused by the falling of concrete is mainly because of the loss of large air voids, whereas the number of small air voids (<300 μm in diameter) is little affected. The pressure inside an air void is inversely proportional to its diameter. This pressure is roughly equal to the atmospheric pressure (≈100 kPa) inside the larger voids, but it can reach values as high as 250 kPa inside the smaller ones (≈10 μm in diameter) (*11*). It follows that, because of their higher internal pressure, smaller air voids are less vulnerable to the vacuum or the breaking mechanism. Even if the air losses due to these mechanisms are annoying for the site engineer, it is unlikely that they significantly influence the real spacing of the air voids and, consequently, the frost resistance of concrete.

The dissolution of air in the surrounding mixing water appears to be a more important concern. Because the pumping pressures used at job sites typically range from 1,500 to 3,000 kPa and because the solubility of air increases linearly with the pressure, the rate of dissolution of air is dramatically increased during the pumping of concrete. The dissolution process affects the smaller air voids more than

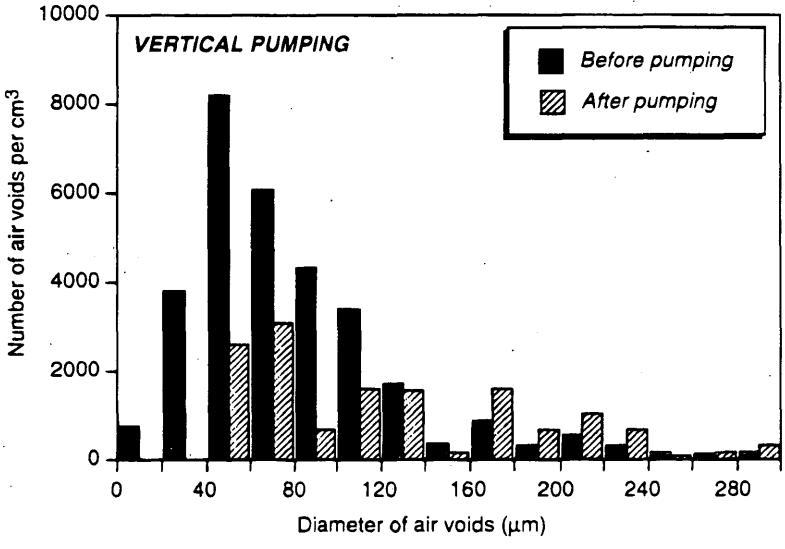

FIGURE 4 Size distributions of air voids obtained for specimens subjected to vertical pumping.

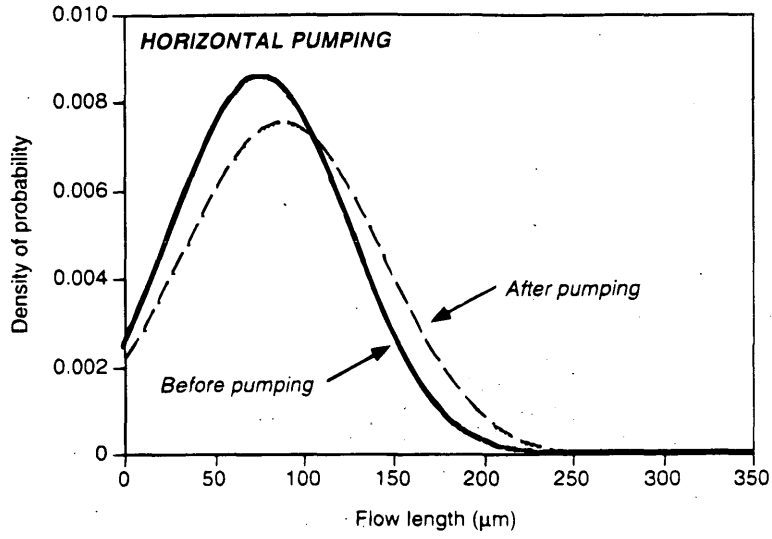

FIGURE 5 Statistical distributions of flow length obtained for specimens subjected to horizontal pumping.

the larger ones because their specific surface is higher (which speeds up the exchanges at the gas-liquid interface) and because their initial volume is smaller. At the end of the pumping hose, the pressure is released, the mixing water becomes oversaturated in air and, consequently, part of the dissolved air comes back into the existing voids. Assuming that the pressure was not high enough or was not applied long enough for the air in the smaller air voids to be completely dissolved, the number of voids per unit volume will remain almost unchanged even though the final air content could be a little lower than the initial value (if the dissolved air is not fully recovered). In such a case, the real spacing of air voids will be little modified, and thus the frost durability of concrete will not be significantly affected. However, if the pressure is sufficiently high or if this pressure is maintained for a sufficiently long period of time, it is likely that all the air voids having a diameter smaller than some critical value will be completely dissolved. In that case, the number of air voids per unit volume of concrete will be significantly reduced during pumping. When the pumping pressure is released, the dissolved air will mainly ingress into the existing voids (because this requires less energy than forming new air voids), and the small air voids that were completely dissolved during pumping will not be recovered. Consequently, the real spacing of the air voids will be significantly increased, and the frost durability of concrete will be reduced.

The mechanisms described, which are considered responsible for the loss of air during pumping, are supported by the test results presented. Even if the pumping pressures were not recorded at the job

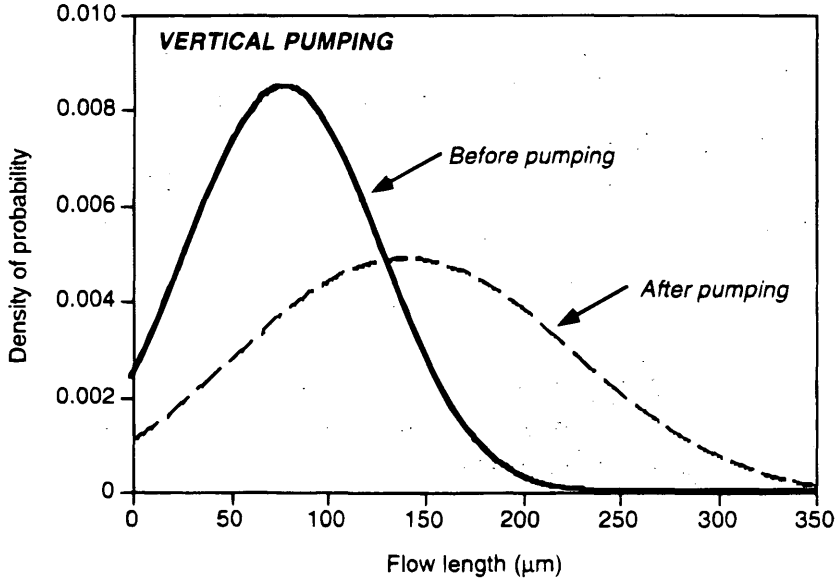

FIGURE 6 Statistical distributions of flow length obtained for specimens subjected to vertical pumping.

TABLE 3 Characteristics of the Air-Void System for Voids Having a Diameter Smaller than 300 μm as Obtained From Image Analysis

		Air Content (%)	Specific Surface (mm^{-1})	Spacing Factor (μm)	Number of Voids (nbr/cm^3)	Flow Length (μm)
Horizontal pumping	Before pumping	2.0	42.9	170	31 400	170
	After pumping	2.1	37.5	190	23 900	195
Vertical pumping	Before pumping	2.0	42.0	175	30 900	175
	After pumping	1.1	40.0	235	13 500	305

site, it is clear that the vertical pumping of concrete requires a higher pressure than horizontal pumping. It appears that, when the concrete was pumped horizontally, the pressure was not high enough to completely dissolve the smaller air voids (see Figure 3). Thus, the characteristics of the air-void system were little modified (see Figure 5 and Table 3), and the frost durability was not significantly influenced. However, when the same concrete was pumped vertically, almost all the air voids having a diameter smaller than 50 μm completely disappeared (see Figure 4). Even if the corresponding air loss was relatively small (0.9 percent according to Table 3), the number of voids per unit volume of concrete decreased dramatically (see Table 3), and the real spacing of the air voids increased significantly (see Figure 6 and Table 3). This increase is detrimental to the frost resistance.

A recent laboratory study by Elkey et al. (*4*) corroborates these findings. It was found that the pumping of concrete lowers the total air content, increases the spacing factor, and, most important, yields a coarser void-size distribution (as obtained by recording the chords intercepted according to the ASTM C 457 linear traverse method). It was also found that the differences were more important when the pumping pressure was increased or the pressure was applied for a longer time. Finally, it was observed that concretes having a higher initial air content are less detrimentally influenced by pumping, which is consistent with the mechanism described (if concrete initially contains more small voids, a higher pressure or a longer period of time, or both, will be required to completely dissolve them).

It is obvious from the data presented that the measurement of the air content alone cannot provide a good assessment of the influence of pumping on the quality of the air-void system. It is also clear, considering the data in Tables 2 and 3, that even the microscopical determination of the characteristics of the air-void system in hardened concrete according to ASTM C 457 (although it generally yields significant data concerning the frost resistance) cannot provide a precise assessment of the influence of pumping on the quality of the air-void system. Table 2 indicates that when concrete was subjected to either horizontal or vertical pumping, the spacing factor increased by approximately 60 μm, which represents an increase of roughly 33 percent in both cases. Table 3 indicates, however, that the flow length (which is a better estimate of the real spacing of the air voids) increased only from 170 to 195 μm in the case of horizontal pumping, but from 175 to 305 μm in the case of vertical pumping (i.e., an increase of approximately 75 percent). The simplifying assumptions underlying the ASTM C 457 method are such that the large voids (those larger than 200 or 300 μm) have an exaggerated influence on the test results. The spacing factor is thus less sensitive to the disappearance of the small voids than to the disappearance of the larger ones.

CONCLUSIONS

The results presented in this paper, which are based on tests performed on HPC, indicate that it is possible to explain the influence of pumping on the characteristics of the air-void system in terms of simple physical concepts. The detrimental influence of pumping is due to the dissolution of the smaller air voids in the mixing water and is a function of the pressure. It is also a function of the length of time during which this pressure is applied (*4*). The results further show that the ASTM C 457 method is not sufficiently precise to assess correctly the influence of pumping. More research is needed to determine the influence of the mixture composition (normal concrete versus HPC) and the air-entraining agent and to determine the relationships among the pressure, the length of time during which it is applied, the concrete properties, and the loss of the small air voids.

ACKNOWLEDGMENTS

The authors are grateful to the Natural Sciences and Engineering Research Council of Canada; Handy Chemicals from Laprairie, Québec; and Euclid Admixture from Saint-Hubert, Québec, for their financial support.

REFERENCES

1. Yingling, J., G. M. Mullings, and R. D. Gaynor. Loss of Air Content in Pumped Concrete. *Concrete International,* Vol. 14, No. 10, Oct. 1992, pp. 57–61.
2. Hoppe, J. Air Loss in Free-Falling Concrete, Queries on Concrete. *Concrete International*, Vol. 14, No. 6, June 1992.
3. Gorsha, R. P. Air Loss in Free-Falling Concrete, Queries on Concrete. *Concrete International*, Vol. 14, No. 8, Aug. 1992, pp. 71–72.
4. Elkey, W., D. Jannssen, and K. C. Hover. *Concrete Pumping Effects on Entrained Air-Voids*. Technical Report, Research Project T9233, Task 21. Washington State Transportation Center, June 1994.
5. Gagné, R., P. C. Aïtcin, M. Pigeon, and R. Pleau. The Frost Durability of High Performance Concretes. In *High Performance Concrete: from Material to Structure* (Chapman and Hall, eds.), London, England, 1991, pp. 250–261.
6. Whiting, D. Durability of High-Strength Concrete, *Proc., Katharine and Bryant Mather International Conference on Concrete Durability*, American Concrete Institute Special Publication SP–100, Atlanta, Ga., 1987, pp. 169–183.
7. Pleau, R., and M. Pigeon. The Use of the Flow Length Concept to Assess the Efficiency of Air Entrainment With Regards to Frost Durability: Part I—Description of the Test Method. Submitted for publication in *Cement, Concrete, and Aggregates.*

8. Pleau, R., M. Pigeon, J. L. Laurençot, and R. Gagné. The Use of the Flow Length Concept to Assess the Efficiency of Air Entrainment With Regards to Frost Durability: Part II—Experimental Results. Submitted for publication in *Cement, Concrete, and Aggregates*.
9. Philleo, R. E. A Method for Analyzing Void Distribution in Air-Entrained Concretes. *Cement, Concrete, and Aggregates*, Vol. 5, No. 2, Winter 1983, pp. 128–130.
10. CAN3–A23.1–M90 Standard: Concrete Materials and Methods of Concrete Construction Canadian Standard Association, Rexdale, Ontario, Canada, 1994.
11. Hover, K. C. Analytical Investigation of the Influence of Bubble Size on the Determination of Air Content in Fresh Concrete. *Cement, Concrete, and Aggregates*, Vol. 10, No. 1, Summer 1988, pp. 29–34.

Publication of this paper sponsored by Committee on Performance of Concrete.

Using Fiber-Optic Sensing Techniques To Monitor Behavior of Transportation Materials

JAMES M. SIGNORE AND JEFFERY R. ROESLER

Although not new to the communications or manufacturing area, fiber-optic sensors are only recently being applied to civil engineering structural evaluation. These sensors offer enormous potential within the transportation field to examine and characterize strain behavior in commonly used materials. Fiber-optic sensing research efforts conducted during the past 2 years on three materials relevant to the transportation industry are documented: portland cement concrete, steel, and asphalt concrete. Portland cement mortar beams were tested to determine the rate and magnitude of shrinkage. Impending fractures in steel structures may be avoided by real-time sensing, thereby minimizing potential safety problems. Steel beams were loaded to measure bending strains, as a precursor to beam crack detection. Finally the lateral strain behavior of axially loaded asphalt emulsion aggregate mixture (EAM) cylinders was studied. The EAM Poisson ratio was determined. Findings comparable with those calculated from theory, found in the literature, and obtained with traditional sensing techniques are presented. Whereas this fiber-optic sensing methodology offers great potential, the reliability and viability of this new measurement technique must be further assessed. This research advances the development and use of this innovative technology.

Although traditionally used for communications purposes, fiber optics show considerable promise as strain sensors. These sensors have been used primarily to evaluate composite materials (*1,2*). Progress is beginning to be made in the use of fiber-optic sensors in civil engineering. The evaluation of crack formation and propagation in concrete beams has also been researched (*3,4*). Stresses and strains present in concrete specimens under load were also investigated (*5–7*).

In this research, fiber-optic sensing techniques were used to test and characterize the behavioral properties of three transportation materials: portland cement concrete (mortar), steel, and asphalt emulsion aggregate mixtures (EAMs). The shrinkage strains associated with mortar beams, the bending strains of a loaded steel beam, and the lateral deformation of EAM cylinders subjected to compressive loads were studied. An additional intent of this research was to verify the viability of fiber-optic sensors in civil engineering.

RESEARCH OBJECTIVE

The objective of this research was to use innovative fiber-optic sensing methods to evaluate nondestructively three transportation materials and to assess the practicality of using fiber-optic sensing techniques in this domain. Specifically the study objectives were to

- Determine the total amount (and rate) of internal shrinkage strain that a mortar beam undergoes at certain critical points in its cross section during the curing process.
- Determine bending strains within a steel beam subjected to load.
- Determine the lateral strain associated with rutting and fatigue evaluation that EAM cylinders undergo when subjected to static compressive loads.

EXPERIMENTAL PROGRAM

This research involved blending several engineering disciplines. To ensure that the sensors were accurately evaluating the material characteristics, knowledge of optical fibers and the host materials is necessary. Brief descriptions of pertinent background information and the procedures followed in this study are presented to help the reader understand fiber-optic sensing methodologies.

Optical Fibers as Strain Sensors

Basics

Optical fibers consist of a central core and cladding surrounded by a protective jacket (Figure 1). The core and cladding are typically silica glass, and the jacket is usually a polymeric material. In manufacture of the fiber, the core and cladding are drawn together as a filament from a single piece of molten glass called the preform. This preform is an enlarged version of the fiber that exhibits the same general physical properties as those desired in the final product. The cladding is doped with trace elements or impurities to give it a higher index of refraction than the core, which allows for light transmission through the core via total internal reflection as shown in Figure 1. The polymeric (or other material, such as metal or ceramic) jacket is applied to the fiber after it is drawn from the preform and provides protection to the core and cladding.

The light that propagates through the fiber is sent by a laser or light emitting diode and detected by a photodetector. Associated peripheral electronics adjust the laser output and process the signals produced by the photodetector. By analyzing the signal outputs, fiber strains and host material changes can be determined.

Civil Engineering Department, University of Illinois at Urbana-Champaign, 1208 NCEL, MC–250, Urbana, Ill. 61801.

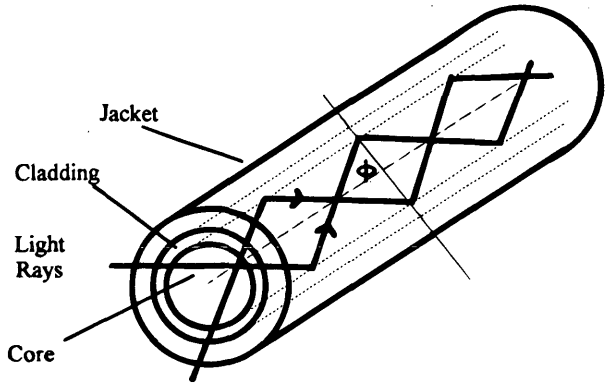

FIGURE 1 Optical fiber and light transmission.

Issues and Concerns

Three issues dealing with the use of fiber optics as sensors need to be addressed. These issues are often ignored or assumptions are made to minimize their influence in previous literature. The first issue is the potential for slippage or loss of bond at the core or cladding and jacket interface. The core or cladding is the active sensing region of the fiber, and any slippage with the jacket will result in erroneous test data because the jacket is bonded to the host material. Tests performed in this study confirmed that there is adequate bond present to assume a full bond. This assumption implies that any strain transferred to the jacket along the fiber length must also be transferred to the glass core. Concerns have arisen in the literature about the capabilities of given jacket materials to transfer stresses and strains adequately; hence the proper choice of jacket material is important (*8*).

The second issue is the bond between the fiber jacket and the host material. For this research, adequate bond between the fiber and concrete matrix, fiber and steel, and fiber and asphalt must be present. One approach taken to ensure that adequate bond exists is to use a cement paste coating on the fiber before embedding it into the concrete (*4*). Most of the remaining literature on the subject does not address this issue. In early attempts it was difficult to obtain consistent and reliable bond between the optical fiber and the mortar, thereby yielding errant results. A novel technique was developed to ensure bond between the fiber and the mortar, resulting in a dramatically increased repeatability and consistency of results. Beads of epoxy were formed along the length of the fiber to protrude into the mortar matrix similar to deformed rebars (Figure 2). This ensured a strong bond between the mortar and the fiber so that strain could be transferred to the fiber jacket without slip between the mortar and the fiber jacket. Fortunately, the loss of bond in localized areas is not critical to measuring the total strain.

For bonding to the steel beams and EAM specimens, a combination of surface roughness and selected epoxies were used to ensure ample bonding. Previous experimentation with various epoxies and host material surface conditions provided the knowledge of which epoxies and surface conditions result in the most accurate and consistent measurement values.

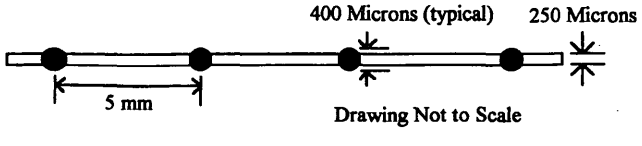

FIGURE 2 Epoxy microbeading details.

The third issue deals with fiber-optic survivability under demanding conditions. Although this study consisted of laboratory experiments, appropriate fiber materials that can withstand harsh environments such as temperature extremes, moisture, and dynamic or static fatigue as well as ways to best protect the fibers from impact damage were investigated. Some existing literature deals with these concerns because fiber failure is a major concern in the telecommunications industry as well as in sensor development (*9,10*).

Sensing Techniques

Several different methods of fiber-optic sensing are now in use. One method is monitoring light polarization, which deals with examining the character of the light as it progresses through a fiber (*11*). As a fiber is stressed transversely, the fiber deforms and the relative polarization of the light changes locally. These changes can then be correlated to the applied pressures. Another technique measures the relative phase of light waves exiting a fiber (*11*). The phase change experienced by the light, as a result of fiber perturbation, is indicative of the strain experienced by the fiber. In addition, changes in the intensity of light propagating through a fiber indicate the degree of stress, strain, or bending within a fiber (*5*). Light intensity diminishes as fibers are bent into curves or are stressed transversely. This decrease in light output can then be correlated to material deformations. In optical time domain reflectometry (OTDR), the relative transit times for light sent through a fiber are monitored, and time changes are indicative of fiber strain (*12*). An OTDR may also be used to measure light intensity.

Because the primary concern in this study was to determine length changes, OTDR was the most applicable and practical technique to use. The instrument used was a very high-speed, high-resolution OTDR that could measure fiber length changes or locate fiber breaks to within 0.1 mm. The OTDR injects a laser pulse into a fiber and detects changes in laser pulse transit time through a fiber that has experienced strain or refractive index change, whether by applied load or temperature change (*12*). These changes in light transit time are converted into length changes by accounting for the speed of light, temperature variation, and material density changes. Note that the density of the core increases during shrinkage and decreases during elongation. This density change affects the speed of light within the fiber, which can then be related to shrinkage or bending strain. Light travels at a speed of c/n through the fiber, where n is the index of refraction of the fiber, typically around 1.5, and c is the speed of light (3E8 m/sec). This research graded index used multimode fibers with a 100-micron core diameter and 140-micron cladding diameter. The graded index of refraction profile of the fiber core minimizes light pulse dispersion by progressively slowing down the light as it nears the fiber core axis. This enables the light, which travels along many reflected paths within the fiber, to arrive at the fiber end more coherently.

Two OTDR sensing techniques were used in this research. The first sensing technique used in this research was far-end reflection time measurement, as illustrated in Figure 3. Light was sent through the fiber under test, and the time it took to traverse the fiber and return to the detector was noted. Subsequent readings were taken, and changes in this "transit time" due to perturbations of the material under test reflected changes in fiber/beam length. An increase

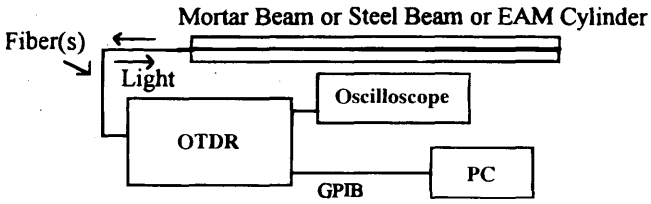

FIGURE 3 Original test setup.

in transit time would reflect a corresponding increase in fiber length and therefore material strain.

The second sensing technique used was a more elaborate technique known as "fiber re-entrant loops" (*12*) (Figure 4). As in previous experiments, the fiber was inserted longitudinally through or around the specimen, but this time the laser sensing pulse was circulated through the fiber many times via a fiber coupler. An important benefit of this technique was that, because the accuracy of the sensing equipment was limited for a given gauge length, increasing the gauge length increased the strain resolution. In the re-entrant loop technique, each circulation effectively increased the sensing length by an additional beam length or EAM specimen circumference. For example, five circulations afforded a fivefold increase in strain resolution over the far end reflection technique.

Fiber-Optic Sensing Studies and Discussion

Concrete Shrinkage

Concrete shrinkage typically presents an unpredictable and undesirable problem during the design and construction of concrete structures such as buildings and pavements. Concrete maturity and overall shrinkage vary widely depending on the curing conditions and type of mixture. Although the shrinkage characteristics of concrete measured at the surface have been extensively reported in the literature (*13–19*), the measurement of the internal shrinkage of concrete has been limited (*20*) and lacks conclusive results. Having the capability to know a priori the internal shrinkage for a given mixture and curing conditions would be an extremely valuable tool for the design engineer. This information could be used to better understand crack formation in concrete and how to control this problem.

Sixteen concrete beams were produced for this experimental study. The specimens were made of mortar paste consisting of Type I cement, sand, and water at a weight ratio of 1:1:0.4. The fineness modulus of the sand was 2.55. The beams were 760 mm (30 in.) long with 50 mm (2 in.) by 50 mm (2 in.) square cross sections. Precision forms were made to ensure that the fibers were placed exactly along the axis of each beam at three locations in the beam cross section. The outside fibers (A and C) were 12 mm (0.5 in.) from the edge and centered in the vertical direction, and the third fiber (B) was placed exactly in the center of the beam (Figure 5). The specimens were removed from the forms 24 hr after casting. Baseline readings were then taken, and the specimens were placed in a controlled environment at 55°C (130°F) and less than 10 percent relative humidity to facilitate shrinkage.

Two different methods were investigated to ensure correct fiber placement within the beams. The first method was to feed the fiber through a long hypodermic steel tube placed within the mortar (*21*). Once the fiber is fed through the tube, the tube is carefully pulled out. The second method developed as part of this research was to place the mortar around pretensioned fibers and then thoroughly vibrate the form to promote bond between the mortar and the fibers (Figure 6).

Pull-out tests performed on the beams indicated that the tensioning method was preferred over the hypodermic steel tube. The bleeding effect seen around the void left by the steel tube resulted in weak, unbonded spots along the fiber. The second method, although more difficult and fiber-breakage prone, yielded solid and continuous bonds in this experiment. It was realized that in situations with larger aggregate concrete the tensioning method was preferable if good bond could somehow be ensured. These tests were performed before developing the epoxy microbead procedure, so either of the procedures could have been implemented in this study.

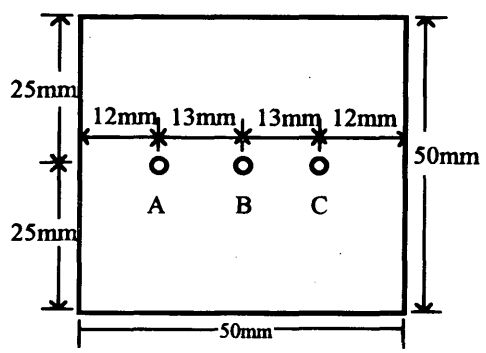

FIGURE 5 Mortar beam cross section.

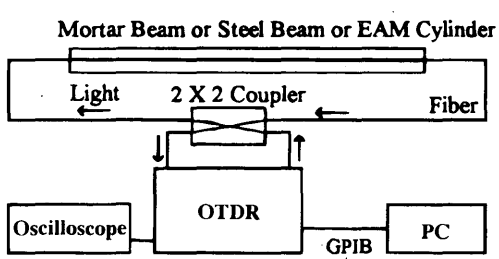

FIGURE 4 Re-entrant loop setup.

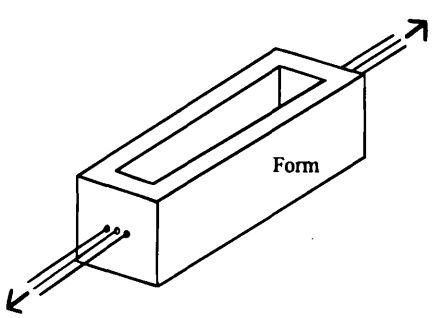

FIGURE 6 Fiber placement and tensioning.

With these fibers placed longitudinally along the entire length of the beam, the total strain in the beam could be determined. A major advantage of this technique was that the entire beam length was the gauge length. Attempts have been made to evaluate internal shrinkage by using embedded strain transducers. However, the intrusive wires and gauges only give values of local shrinkage over a minimal gauge length, not of regional or total deformations (*20*). Concrete surface shrinkage can be determined relatively easily using commonly available gauges; however, correlation of internal shrinkage from surface shrinkage is not an accurate approach. To date, this approach has met with limited success because the free surface boundary conditions cause moisture loss associated with plastic shrinkage, whereas internal shrinkage (drying shrinkage) is attributed to loss of interlayer water in the cement paste (*15*).

The magnitude of the ultimate shrinkage for each of the 16 beams tested is presented in Table 1. The values shown are the average readings from the three fibers embedded in each beam. As was typical in dealing with mortar, there was variation in the ultimate shrinkage. This variation typically was no more than 15 percent from the mean and followed no particular trends. Figure 7 shows a representative plot of shrinkage versus time. Fibers A and C are those fibers located 12 mm (0.5 in.) from the edge of the beam, and fiber B is the center fiber. The internal shrinkage strains shown are similar to results obtained in other experiments (*14*). The shrinkage results also appear realistic as a function of time. Mortar shrinkage was found to be 0.2 to 0.3 percent at a relative humidity of less than 20 percent and determined an ultimate shrinkage at 0 percent relative humidity of 0.32 percent (*14*). In this study, a mean shrinkage of 0.25 percent (2,517 microstrain) was determined (Table 1). Discrepancies can be attributed to the use of a lower water-to-cement ratio in this experiment and that surface shrinkage was measured with a dial gauge comparator (*14*).

The shrinkage at the center of the beam can be compared with that nearer the edge. As expected, the internal shrinkage at the center was less than that at the edges. The outside two fibers (A and C) showed similar results throughout the experimental program. It is well-known that the specimen size and shape affect the measured ultimate shrinkage of concrete, especially when the dimensions are less than 100 mm (4 in.) (*16,17*). Although the specimen cross section used in this study was only 50 mm (2 in.) by 50 mm (2 in.), the results shown in Figure 7 show that there is a difference between internal and near-surface shrinkage in the mortar beams. These preliminary results indicate the possibility of a moisture gradient present in the mortar.

TABLE 1 Mortar Beam Shrinkage Results Summary

Beam #	Ultimate Shrinkage Average of 3 Fibers (Microstrain)
1	2300
2	3100
3	*
4	*
5	2000
6	1900
7	2800
8	2900
9	2700
10	2700
11	2300
12	2000
13	2800
14	2800
15	2200
16	2000
Mean	**2517**
Standard Dev.	405

Steel Bending Strain

Structural members weakened through deterioration pose a safety problem for state and federal highway agencies. As the design lives of bridges are reached or exceeded, early detection of structural weaknesses that result in increased failure potential become more critical. Detection of strained or cracked members before their structural usefulness diminishes to the point of bridge collapse could be an enormous benefit in terms of lives and dollars saved. Research is underway to evaluate procedures for sensing strains and crack formation in reinforced concrete structures (*22,23*) and bridges (*24*). The goal of this research is to measure bending strains in loaded steel beams.

Optical fibers were affixed to a steel beam, which was then loaded for the purpose of measuring bending strains. For initial assessment of the sensing capability, a simply supported beam configuration was used (Figure 8). The beam was 9.5 mm (0.375 in.) thick by 51 mm (2 in.) wide, with a span of 2.2 m (88 in.). The fibers were epoxied onto the tensile side of the beam. Three strain gauges were added at the L/4 points of the beam for additional verification of the bending strains.

For various loads, bending strains were measured. The fiber-optic sensing system was able to detect the integrated or total strain along the entire beam. This measured strain was compared with beam theory predictions and the readings from the strain gauges on the beam. Typical test results are shown in Figure 9. Predictions within 5 percent of theoretical predictions were common for small strains with slight decreases in accuracy at much higher strains. However, both the optical-fiber system and resistive strain gauges produced comparable results throughout the study. Of note is that the test results show linear strain behavior similar to that theoretically predicted and shown by the strain gauges. Additional refinement of the measurement and bonding techniques are underway to further increase accuracy. A significant outcome of this study was that fiber-optic sensing techniques were extremely repeatable, with minimal variation between readings.

To fully use these sensors in a field environment, suitable epoxies or fiber bonding methods, or both, that can withstand harsh weather conditions are necessary. Methods of isolating or protecting the fibers from impact damage are also needed. The fibers must be capable of functioning under severe conditions, such as fatigue and temperature cycling. To implement a real-time sensing system on a field structure, there must be a monitoring system that includes a signal to indicate whether a structural problem exists. Each of these system concerns is under investigation.

Asphalt EAM Deformation

Much of the knowledge about EAM behavior is based on simple mechanical measurements. Knowledge of the lateral straining char-

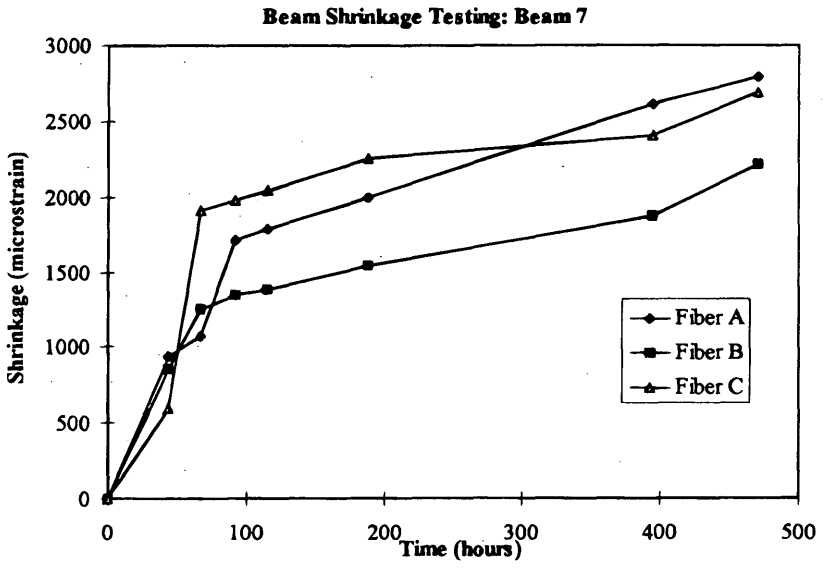

FIGURE 7 Representative shrinkage plot.

acteristics of EAM under load is an important feature in assessing the rutting and fatigue performance of the material. In this research, fiber-optic methods were used to determine the Poisson ratio (horizontal strain/vertical strain) for EAM samples.

The testing of EAM specimens with fiber-optic sensors is a completely new concept, and this study is the first such application the authors have found on this subject. Fibers were affixed about the perimeter of the cylindrical samples, and the subsequent circumferential deformation of the sample under load was measured. Figure 10 illustrates the setup for this test. The samples under test were 305 mm (12 in.) long with a diameter of 152 mm (6 in.). Only static loading of the sample was evaluated. It is hoped that the behavior under dynamic loading can be addressed as the fiber-sensing technique develops.

The Poisson ratio was determined by relating the horizontal and vertical strain in the material. Unlike current methods used to measure horizontal deformation, which only assess the deformation in one plane, the fiber sensor allows for a complete assessment of horizontal deformation entirely around the sample. For these tests, vertical deformations were incremented in 1.25 mm (0.05 in.) steps and were limited to 6mm (0.25 in.) to maintain linear elastic behavior in the specimen. Vertical and horizontal strains were recorded at each increment. The experimentally determined Poisson ratios were 0.44 for the first sample and 0.35 for the second sample. Although these measured Poisson ratios are not exact, they are close to the accepted values of 0.40 ± for EAM specimens. The test procedure was simple to conduct.

FIBER OPTICS VERSUS TRADITIONAL SENSORS

This paper has shown that fiber-optic sensors can give comparable results to existing measurement techniques, such as strain gauges. The use of fibers to directly measure total internal strains and strains in large structures has promise because global estimates are not extrapolated from local measurements. Fiber optics have proved their viability in the laboratory as a research tool. However, fiber-optic sensing is delicate, and there is only limited structural application, much of which has inconclusive results. This sensing technique is presently impractical for widespread field use because of the cost of the equipment and peripheral items. As technology progresses, along with the use of other less expensive techniques, fiber-optic sensing should become competitive.

SUMMARY AND CONCLUSIONS

Research efforts using fiber-optic sensing procedures in the civil engineering field are just beginning. These sensors offer great potential for evaluating commonly used transportation materials and structures in a nondestructive manner. In this study, the strain characteristics of cement mortar beams, steel beams, and emulsion aggregate mixtures were examined with success. This research has shown that fiber-optic sensors produce repeatable and accurate measurements under a variety of conditions. The test results compare favorably with existing techniques. Fiber-optic sensors also

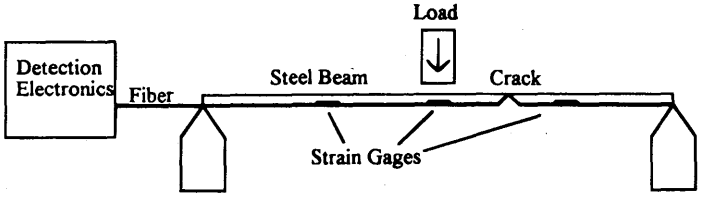

FIGURE 8 Typical steel beam testing configuration.

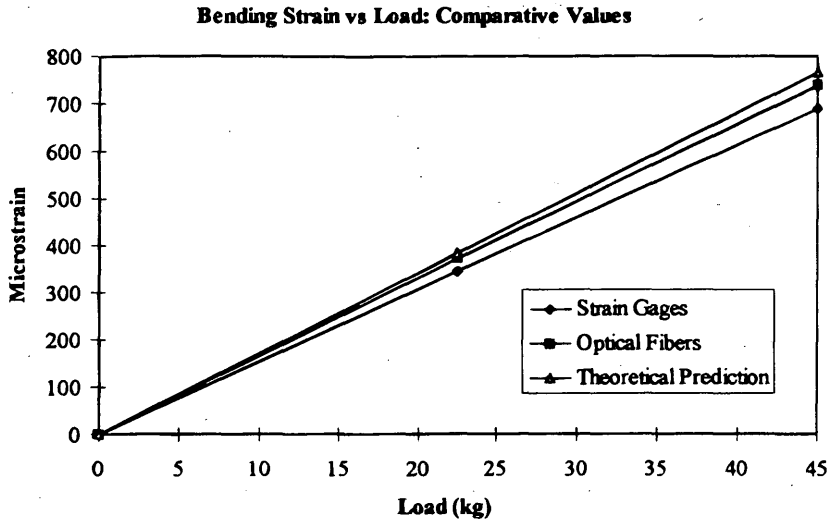

FIGURE 9 Steel beam bending strain.

offer the advantages of being immune to electromagnetic interference and can measure total or integrated strain as well as point strain. To fully use the capability of these sensors, however, further work must be performed relating to long-term sensor reliability and survivability.

The internal shrinkage of mortar beams was monitored. Methods were developed to ensure that the measured internal shrinkage strains were accurate through a full bond between the mortar and the optical fiber, and the fiber core and the jacket. The shrinkage strains measured for the mortar specimens of 0.25 percent were similar to results reported in the literature. It was shown that the use of fiber-optic sensors may be used internally in a cement-based material to provide excellent real-time results.

Fiber-optic sensors were applied to steel beams to sense bending strains due to static loads. The results were both accurate and consistent. Research efforts on larger-scale projects that would include crack detection would be an important next step. Eventually with refinement, this technique should allow for real-time monitoring of high-risk field structures, statically and dynamically.

The first use of fiber-optic sensors on EAM samples resulted in the measurement of Poisson's ratio. This technique may be used to further corroborate mechanically derived Poisson values. The results of these initial tests indicate that further research toward additional applications is promising.

These positive research findings suggest that fiber-optic sensors have many applications in civil engineering. Examples of possible

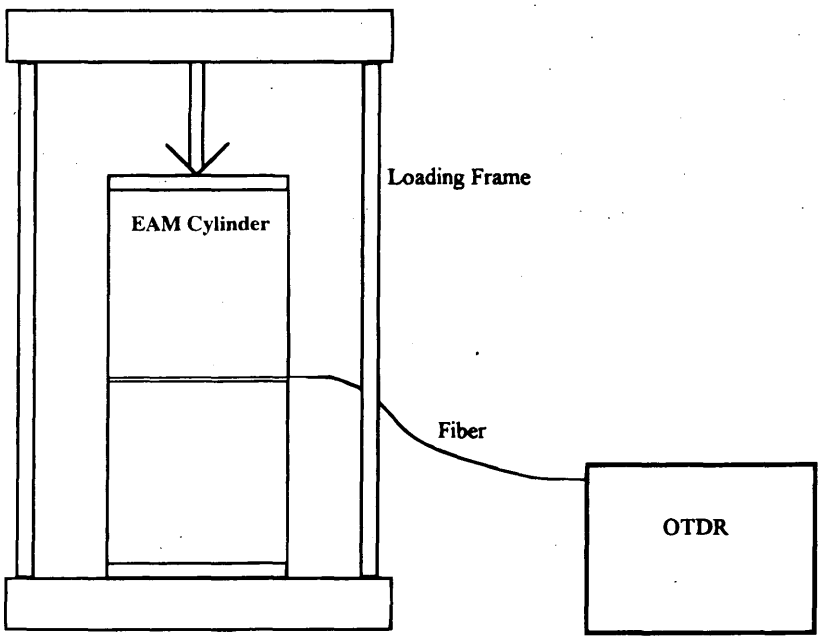

FIGURE 10 EAM deformation testing.

applications include long-term concrete shrinkage and creep monitoring, concrete and steel crack initiation and propagation, and monitoring the growth of the fracture process zone. In addition, real-time information on static and dynamic loading and displacements of in situ structures, such as buildings and pavements, may be obtained.

ACKNOWLEDGMENTS

This project was funded through a research grant from the Association of American Railroads. The authors would like to thank Basors Barry Dempsey, Ernest Barenberg, and David Lange of the Civil Engineering Department of the University of Illinois for their consultations during this research.

REFERENCES

1. Claus, R. O., K. D. Bennett, A. M. Vengsarkar, and K. A. Murphy. Embedded Optical Fiber Sensors for Materials Evaluation. *Journal of Nondestructive Evaluation*, Vol. 8, No. 2, 1989, pp. 135–145.
2. Meisseler, H. J., and R. Wolff. Experience with Fiber Composite Materials and Monitoring with Optical Fiber Sensors. *Proc., Advanced Composite Materials in Civil Engineering Structures*, ASCE, 1991, pp. 167–181.
3. Rossi, P., and F. LeMaou. New Method for Detecting Cracks in Concrete Using Fiber Optics. *Materials and Structures (RILEM)*, Vol. 22, No. 122, Nov. 1989, pp. 437–442.
4. Ansari, F., and R.K. Navalurkar. Kinematics of Crack Formation in Cementitious Composites by Fiber Optics. *Journal of Engineering Mechanics, ASCE*, Vol. 119, No. 5, May 1993, pp. 1048–1061.
5. Nanni, A., C. C. Yang, K. Pan, J. Wang, and R. Michael. Fiber-Optic Sensors for Concrete Strain/Stress Measurement. *ACI Materials Journal*, May-June 1991, pp. 257–264.
6. de Vries, M., M. Nasta, and R. Claus. Fatigue Loaded Fiber Optic Strain Gages Performance in Reinforced Concrete Structures, prepublication from authors, 1993.
7. Huston, D., P. Fuhr, P. Kajenski, and D. Snyder. Concrete Beam Testing with Optical Fiber Sensors. *Nondestructive Testing of Concrete*, pp. 61–69.
8. Dasgupta, A., and J. S. Sirkis. Importance of Coatings to Optical Fiber Sensors Embedded in 'Smart' Structures. *AIAA Journal*, Vol. 30, No. 5, May 1992, pp. 1337–1343.
9. Saifi, M. A. Long-Term Fiber Reliability. *Fiber Optic Reliability: Benign and Adverse Environments IV*, SPIE Vol. 1366, 1990, pp. 58–70.
10. Biswas, D. R. Strength and Fatigue of Optical Fibers at Different Temperatures. *Fiber Optic Reliability: Benign and Adverse Environments IV*, SPIE Vol. 1366, 1990, pp. 71–76.
11. Grossman, B., T. Alavie, F. Ham, J. Franke, and M. Thursby. Fiber-Optic Sensor and Smart Structures Research at Florida Institute of Technology. *Fiber Optic Smart Structures and Skins II*, SPIE Vol. 1170, 1989, pp. 123–135.
12. Zimmermann, B. D., R. O. Claus, D. A. Kapp, and K. A. Murphy. Fiber-Optic Sensors Using High-Resolution Optical Time Domain Instrumentation Systems. *Journal of Lightwave Technology*, Vol. 8, No. 9, Sept. 1990, pp. 1273–1277.
13. Bryant, A. H., and C. Vadhanavikkrt. Creep, Shrinkage-Sized, and Age at Loading Effects. *ACI Materials Journal*, Vol. 84, No. 2, March-April 1987, pp. 117–123.
14. Hansen, W., and J. A. Almudaiheem. Ultimate Drying Shrinkage of Concrete-Influence of Major Parameters. *ACI Materials Journal*, Vol. 84, No. 3, May-June 1987, pp. 217–223.
15. Mindness, S., and J. F. Young. *Concrete*, Prentice-Hall, Inc., Englewood Cliffs, N.J., 1981.
16. Almudaiheem, J. A., and W. Hansen. Effect of Specimen Size and Shape on Drying Shrinkage of Concrete. *ACI Materials Journal*, Vol. 84, No. 2, March-April 1987, pp. 130–135.
17. Kraai, P. P. Proposed Field Test for Drying Shrinkage of Concrete. *Concrete Construction*, Vol. 29, July 1984, pp. 663–665.
18. Smadi, M. M., F. O. Slate, and A. H. Nilson. Shrinkage and Creep of High, Medium, and Low Strength Concretes, Including Overloads. *ACI Materials Journal*, Vol. 84, No. 3, May-June 1987, pp. 224–234.
19. Bazant, Z. P., F. H. Wittmann, and J. K. Kim. Statistical Extrapolation of Shrinkage Data. *ACI Materials Journal*, Vol. 84, No. 1, Jan.-Feb. 1987, pp. 20–34.
20. Chaallal, O., B. Benmokrane, and G. Balling. Drying Shrinkage Strains: Experimental Versus Codes. *ACI Materials Journal*, Vol. 89, No. 3, May-June 1992, pp. 263–266.
21. Mendez, A., and T. F. Morse. Overview of Optical Fiber Sensors Embedded in Concrete. *Fiber Optic Smart Structures and Skins V*, SPIE Vol. 1198, 1992, pp. 123–136.
22. Ansari, F. Nondestructive Testing of Concrete: Real-Time Condition Monitoring of Concrete Structures by Embedded Optical Fibers. In *Nondestructive Testing of Concrete Elements and Structures*, 1992, pp. 49–59.
23. Wolff, R. Applications with Optical Fiber Sensor Systems for Monitoring Prestressed Concrete Structures. *Structures Congress Abstracts*, American Society of Civil Engineers, 1990, pp. 94–95.
24. Miesseler, H., and R. Lessing. Monitoring of Load Bearing Structures with Optical Fiber Sensors. *Proc., IABSF Symposium*, 1989, pp. 853–858.

Publication of this paper sponsored by Committee on Mechanical Properties of Concrete.

Use of ASTM Type-C Fly Ash and Limestone in Sand-Gravel Concrete

MOHAMED NAGIB ABOU-ZEID, JOHN B. WOJAKOWSKI, AND STEPHEN A. CROSS

Serious damage in concrete structures worldwide has been attributed to alkali-aggregate reactions. Field and laboratory work has demonstrated that silicious aggregates in wide regions in the midwestern United States can yield concrete with durability problems. This is the case for some sand-gravel aggregates in Kansas. To minimize durability problems, pozzolans, such as fly ash, and limestone have been suggested for use in concrete mixtures involving such aggregates. The use of two ASTM type-C fly ashes as 15 percent replacement of portland cement is evaluated. Also, the use of limestone (sweetener) from two sources as a 30 percent weight replacement of the sand-gravel is investigated. Thirty concrete mixtures were prepared with a water-to-cementitious materials ratio of 0.51. Eight approved and unapproved types of sand-gravel aggregates from different areas in Kansas were used. Concrete beams were cast and tested to determine the change in lengths and the modulus of rupture. Test results indicate that mixtures made with the two fly ashes have higher expansion and lower modulus of rupture when compared with mixtures containing no fly ash. Of the 16 concrete mixtures made with fly ash 15 failed to meet Kansas Department of Transportation specifications. The mixtures made with unapproved sand gravel and limestone had lower expansion and higher modulus of rupture when compared with concrete made with approved aggregates with no fly ash.

For the past 5 decades, deleterious chemical reactions between aggregates and cement paste in concrete have been observed. One of the most common forms of such reactions is that between some active silica ingredients that may exist in aggregates and the alkalis in cement, known as the alkali-silica reaction. This reaction results in an alkali-silicate gel that is characterized by a tendency to increase in volume (*1*). The reaction can lead to localized volume changes, cracking, pop-outs, loss of strength, and dislocation of structures (*2*). In some extreme cases, complete destruction of the concrete may occur (*2–4*). Severe alkali-aggregate reaction problems have been reported in several countries worldwide, including Japan, the United States, England, and Canada. In the United States, such problems are mostly associated with aggregates from the West and Southwest, as well as Kansas, Nebraska, Iowa, Alabama, and Georgia (*4*). Most of those aggregates contain significant amounts of volcanic and opaline materials known to be potentially alkali reactive (*5*).

More than 2 decades ago, the use of pozzolanic materials was suggested to minimize the problems associated with alkali-aggregate reactions. Fly ash, a pozzolanic by-product material from burning coal, is being used on a wide scale worldwide for that purpose. However, the chemical and physical properties vary significantly from one fly ash source to another. Therefore, the performance of concrete is affected by the characteristics and dosage of the fly ash used. It has been reported that certain dosages of some fly ash types do not minimize the alkali-aggregate reaction and can even exacerbate the problem (*6,7*). For that reason, use of fly ash (or any other pozzolans) is not recommended to reduce alkali-aggregate reaction unless its ability has been confirmed through testing.

The use of limestone as partial replacement of sand-gravel aggregate in concrete has been suggested to enhance concrete performance. The Kansas Department of Transportation (KDOT) Standard Specifications (*8*) allows the use of limestone (as a sweetener) in all sand-gravel concrete and requires limestone use if the sand-gravel aggregate is from an unapproved source.

M. N. Abou and S. A. Cross, Department of Civil Engineering, University of Kansas, Lawrence, Kans. 66045. J. B. Wojakowski, Kansas Department of Transportation, Topeka, Kans. 66611.

OBJECTIVE AND SCOPE

The work presented in this paper is part of an ongoing study carried out by KDOT to determine the effect of using fly ash in sand-gravel concrete. This study was undertaken to investigate the possibility of using two locally available type-C fly ashes and two limestones in sand-gravel concrete.

Concrete mixtures were prepared using sand-gravel aggregates from approved and unapproved sources in Kansas. Fly ash from two sources was used as 0 and 15 percent replacements, by weight, of portland cement. Limestone (as a sweetener) was used as a 30 percent replacement, by weight, of the sand-gravel aggregate in concrete made with unapproved aggregates. The concrete mixtures were evaluated by performing KDOT's wetting and drying test (*9*). In this test, concrete beams are prepared, and the change in length as well as the modulus of rupture are measured and evaluated.

MATERIALS

Cement

Type II portland cement (Ash Grove brand) was used. The cement had a specific gravity of 3.15 and a specific surface area (blaine fineness) of 3,780 cm^2/g. The Bogue compounds of the cement were as follows: C_3S = 53.1 percent, C_2S = 21.7 percent, C_3A = 7.7 percent, and C_4AF = 9.5 percent. The alkali content (as Na_2O equivalent) is 0.50 percent. The chemical analysis of the cement is provided in Table 1.

Fly Ash

Two type-C fly ashes, produced at two Kansas power plants (Jeffrey and LaCygne), were used. The specific surface areas of the two ashes (blaine fineness) are 3,760 and 4,200 cm^2/g, respectively. The alkali contents of the two fly ashes are (as Na_2O equivalent) 0.84

TABLE 1 Chemical Analysis of Portland Cement and Fly Ashes Used

Component	Portland Cement	F-1 fly ash (Jeffrey)	F-2 fly ash (LaCygne)
SiO_2	21.54	28.84	30.87
Al_2O_3	4.88	21.73	23.61
Fe_2O_3	3.12	5.16	3.94
CaO	64.07	31.75	30.88
MgO	2.23	6.76	5.52
SO_3	2.34	3.49	3.30
Na_2O	0.32	0.94	1.03
K_2O	0.28	0.15	0.18
L.O.I.	1.20	0.44	0.10

and 1.04 percent, respectively. The chemical analyses of the two fly ashes used are provided in Table 1. [Note: the two fly ashes (Jeffrey and LaCygne) will be referred to, respectively, as F–1 and F–2 in this paper.]

Aggregates

Sand-gravel aggregates from eight sources in Kansas were used. Five of these sand-gravel aggregates were from approved sources, and three were from unapproved sources. All eight aggregates were used in concrete mixtures made with and without fly ash. Limestone from two sources was used with the unapproved aggregates by replacing 30 percent of the sand-gravel with an equal weight of limestone.

Water

City of Topeka municipal water was used as the mixing water in the concrete mixtures.

TEST PROCEDURE

Concrete beams were prepared and tested for change in length and modulus of rupture in accordance with the KDOT Standard Specifications for Wetting and Drying Test of Total Mixed Aggregate Concrete (*9*).

Fifteen concrete mixtures were prepared using each of the five approved aggregates with 0 and 15 percent replacement, by weight, of cement with the two type-C fly ashes. Similarly, nine concrete mixtures were prepared using each of the three unapproved aggregates with 0 and 15 percent fly ash (from two sources). Six concrete mixtures were prepared using the three unapproved aggregates by replacing 30 percent of the sand-gravel aggregate with an equal weight of limestone (from two sources). All mixtures had a water-to-cement ratio of 0.51 and yielded a slump of 50 to 75 mm (2 to 3 in.). The identification of each mixture and the constituent materials for each mixture are presented in Table 2.

To perform the wetting and drying test, concrete beams were prepared and subjected to a scheme of wetting and drying. After casting, the beams were cured for 7 days in a moist room (curing room), followed by a 21-day air-drying period at room temperature, then submerged in water for 2 days. Beam lengths were then measured after 30 days. Three beams are moist-cured an additional 30 days and tested for flexural strength. The rest of beams were subjected to cycles of oven-heating for 8 hr at a temperature of 53.5°C, followed by 15.75 hr of being submerged in water at room temperature. Cycles (oven heating and water submerging) were carried out every working day, otherwise beams were kept in a water bath.

Beam lengths were measured at 60, 120, 240, 300, and 365 days. The changes in beam lengths were calculated using the 30-day beam lengths as the initial value for comparisons. Flexural tests were performed at 60 and 365 days, and the modulus of rupture calculated.

RESULTS

The result of the percentage of increase in length after 180 and 365 days and the modulus of rupture after 60 and 365 days are presented in Table 3 and illustrated in Figures 1 through 4. The results of the compressive strength of modified cubes after 60 and 365 days are also presented in Table 3.

The results (illustrated in Figure 1) show that the average percentage of increase in length for the concrete mixtures made with approved aggregates with no fly ash after 365 days (mixture nos. 1, 4, 7, 10, and 13) was 0.041. (Note: the maximum percentage of increase allowed by the specifications is 0.070 percent.) Also, the percentage of increase in length for the individual mixtures was less than the maximum allowed by the specifications. However, the average percentage of increase for mixtures made with approved aggregates with 15 percent F–1 fly ash (mixture nos. 2, 5, 8, 11, and 14) was 0.076 percent, which exceeds the maximum value allowed by the specifications (0.070). Also, the results of two of the five

TABLE 2 Composition of Concrete Mixtures Used in This Study

Mixture I.D.	Fly Ash		Sand-Gravel		Limestone	
	Percent	Source	Source	Approval	Percent	Source
1	0	-	Westhoff	Yes	0	-
2	15	Jeffrey (F-1)	Westhoff	Yes	0	-
3	15	LaCygne (F-2)	Westhoff	Yes	0	-
4	0	-	Blue River	Yes	0	-
5	15	Jeffrey (F-1)	Blue River	Yes	0	
6	15	LaCygne (F-2)	Blue River	Yes	0	-
7	0	-	Mueller	Yes	0	-
8	15	Jeffrey (F-1)	Mueller	Yes	0	-
9	15	LaCygne (F-2)	Mueller	Yes	0	-
10	0	-	Gaither	Yes	0	-
11	15	Jeffrey (F-1)	Gaither	Yes	0	-
12	15	LaCygne (F-2)	Gaither	Yes	0	-
13	0	-	Smith	Yes	0	-
14	15	Jeffrey (F-1)	Smith	Yes	0	-
15	15	LaCygne (F-2)	Smith	Yes	0	-
16	0	-	Moore	No	0	-
17	15	Jeffrey (F-1)	Moore	No	0	-
18	15	LaCygne (F-2)	Moore	No	0	-
19	0	-	Moore	No	30	Walker
20	0	-	Moore	No	30	Hallet
21	0	-	St. Francis	No	0	-
22	15	Jeffrey (F-1)	St. Francis	No	0	-
23	15	LaCygne (F-2)	St. Francis	No	0	-
24	0	-	St. Francis	No	30	Walker
25	0	-	St. Francis	No	30	Hallet
26	0	-	J&R	No	0	-
27	15	Jeffrey (F-1)	J&R	No	0	-
28	15	LaCygne (F-2)	J&R	No	0	-
29	0	-	J&R	No	30	Walker
30	0	-	J&R	No	30	Hallet

mixtures were well above the maximum value. Similarly, the average percentage of increase for mixtures made with 15 percent F–2 fly ash (mixture nos. 3, 6, 9, 12, and 15) was 0.071 percent, with two of the five mixtures exceeding the maximum allowed by the specifications. Thus, the mixtures made with fly ash yielded a higher percentage of increase in length than those with no fly ash.

The average percentage of increase in length for concrete beams made with unapproved sand-gravel aggregates with 0 percent fly ash and no limestone (mixture nos. 16, 21, and 26) was 0.075. (Note: as expected, the percentage of increase is higher for mixtures made with unapproved aggregates than for those made with approved aggregates.) The average percentage of increase for mixtures made with the unapproved sand-gravel aggregates with F–1 fly ash (mixture nos. 17, 22, and 27) was 0.204, and the average percentage of increase for mixtures made with F–2 fly ash (mixture nos. 18, 23, and 28) was 0.171. The concrete made with both ashes clearly exceeds the maximum value allowed by the specifications. In contrast, concrete mixtures made with unapproved sand-gravel aggregates with 30 percent of the aggregate replaced by a limestone sweetener (mixture nos. 19, 20, 24, 25, 29, and 30) yielded an average percentage of increase of 0.030, which is well below the maximum in the specifications. Also, all individual mixtures yielded a percentage of increase in length less than the maximum allowed by the specifications (as shown in Figure 2).

The average modulus of rupture after 365 days for mixtures made with approved aggregates with no fly ash was 4.6 MPa (666 psi), which exceeds the minimum value allowed by the specifications [Note: The specification minimum is 3.8 MPa (550 psi).] However, the two average values for mixtures made with the same aggregates but with 15 percent F–1 and F–2 fly ash were 3.1 and 3.2 MPa (451 and 461 psi), respectively. Also, all mixtures made with fly ash, except for one, failed to meet the minimum specification requirements, as shown in Figure 3.

Mixtures made with unapproved aggregates with no limestone or fly ash had an average modulus of rupture of 3.4 MPa (487 psi) after 365 days. The average modulus of rupture for mixtures involving F–1 and F–2 fly ashes were 1.8 and 2.3 MPa (254 and 337 psi), respectively. Also, all of those mixtures, except one, yielded moduli of rupture that were significantly less than the minimum allowable value. On the other hand, mixtures involving the use of limestone had an average modulus of rupture of 4.8 MPa (708 psi), which represents the highest value for the sets of mixtures evaluated in this study.

DISCUSSION OF RESULTS

The results illustrate that the use of the two type-C fly ashes introduces an increase in concrete expansion. For example, the average percentage of expansion of the mixtures made with approved sand-gravel aggregates increased by more than 85 percent when 15 percent of the portland cement is replaced by the F–1 fly ash. (Note:

TABLE 3 Results of Wetting and Drying Test

Mixture I.D.	Change in Length		Modulus of Rupture		Compressive Strength	
	180 Days (%)	365 days (%)	180 Days (psi)	365 days (psi)	180 Days (psi)	365 days (psi)
1	0.035	0.036	670	720	5870	6560
2	0.038	0.062	632	505	5380	5510
3	0.047	0.067	609	450	5270	5290
4	0.033	0.038	679	582	5960	6620
5	0.038	0.069	560	443	5390	5410
6	0.058	0.058	573	515	5280	5870
7	0.036	0.049	674	626	6160	5440
8	0.040	0.093	605	419	5400	5260
9	0.036	0.080	570	381	5570	5470
10	0.031	0.042	612	680	4700	5930
11	0.042	0.093	566	427	5310	5020
12	0.042	0.096	528	367	5020	5070
13	0.033	0.400	644	720	5920	6890
14	0.031	0.062	593	459	5110	5430
15	0.031	0.055	634	590	5950	6170
16	0.033	0.051	639	532	5350	6170
17	0.069	0.158	562	240	4720	4100
18	0.076	0.196	588	279	5200	4620
19	0.029	0.029	664	679	5140	5560
20	0.029	0.033	643	673	5070	5420
21	0.040	0.116	620	372	5720	5550
22	0.089	0.371	567	154	5280	4040
23	0.062	0.251	580	227	5560	4320
24	0.031	0.031	680	695	5970	6630
25	0.029	0.033	627	702	5600	5860
26	0.033	0.058	650	557	5960	6580
27	0.033	0.082	609	368	5340	5240
28	0.040	0.065	658	506	5850	5630
29	0.020	0.025	719	743	5820	6420
30	0.025	0.031	670	758	5440	6110

the average percentage of increase in length for mixtures with 0 and 15 percent F–1 fly ash was 0.041 and 0.076, respectively.) Also, the use of the two fly ashes in this study resulted in a significant decrease in the modulus of rupture. For example, the average modulus of rupture for the concrete mixtures made with approved aggregates decreased by more than 32 percent when 15 percent of the cement was replaced by the F–1 fly ash. [Note: the two average moduli for mixtures with 0 and 15 percent fly ash were 4.6 and 3.1 MPa (666 and 451 psi), respectively.] The deterioration of concrete quality expressed by the higher percentage of increase in length and the lower modulus of rupture for the mixtures made with the two fly ashes was so significant that all those concrete mixtures, except for the one made with approved aggregate, failed to meet the specifications.

On the basis of those results, it is clear that replacing 15 percent of the portland cement by either of the two type-C fly ashes has a detrimental effect on the durability of the concrete. It has been reported by many investigators that the role played by pozzolans (such as slag, fly ash, and silica fume) in controlling the alkali-aggregate reaction depends on several parameters, including the chemical composition of the pozzolan used (fly ash in this study), the portland cement used, and the dosage of the pozzolan in the mix (*10–13*). In addition, it has been reported (*2*) that there is a pessimum dosage for the replacement of cement by type-C fly ash at which fly ash does not help control the alkali-aggregate reaction. The pessimum dosage can be discussed in the light of earlier work (*5,14*) as the dosage at which a definite alkali content is reached and that this alkali content would produce the maximum expansion in concrete. This expansion, however, would progressively decrease at higher and lower alkali contents (fly ash dosages). In that sense, it is not surprising that the behavior of fly ash concrete changes drastically as a function of fly ash dosage. In fact, it has been shown that a dosage of 15 percent replacement of cement by fly ash causes an increase in concrete expansion, and a dosage of 40 percent results in a significant decrease in expansion (improvement) when both are compared with concrete with no fly ash (*2*). Therefore, it should be emphasized that the results discussed in this study are associated with the parameters involved in this work. It is also recommended that the work presented in this study be extended to evaluate other fly ash replacement dosages. In fact, another study involving a higher percentage of fly ash replacement has been initiated by KDOT.

Clearly, the mixtures made with unapproved sand-gravel aggregates fail to meet the standard specifications as expressed by their relatively high percentage of increase in length or their relatively low moduli of rupture, or both. Yet, a significant improvement in

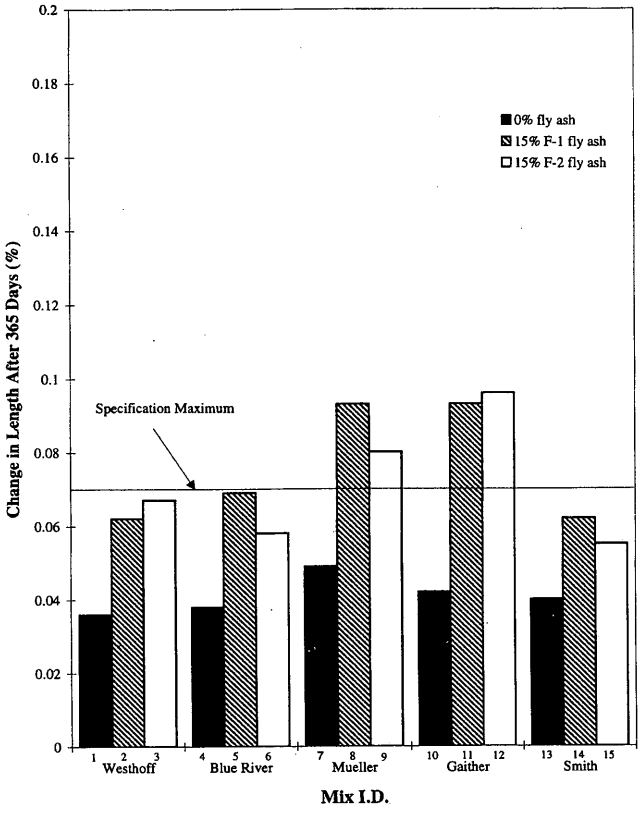

FIGURE 1 Change in length of specimens made with approved aggregates.

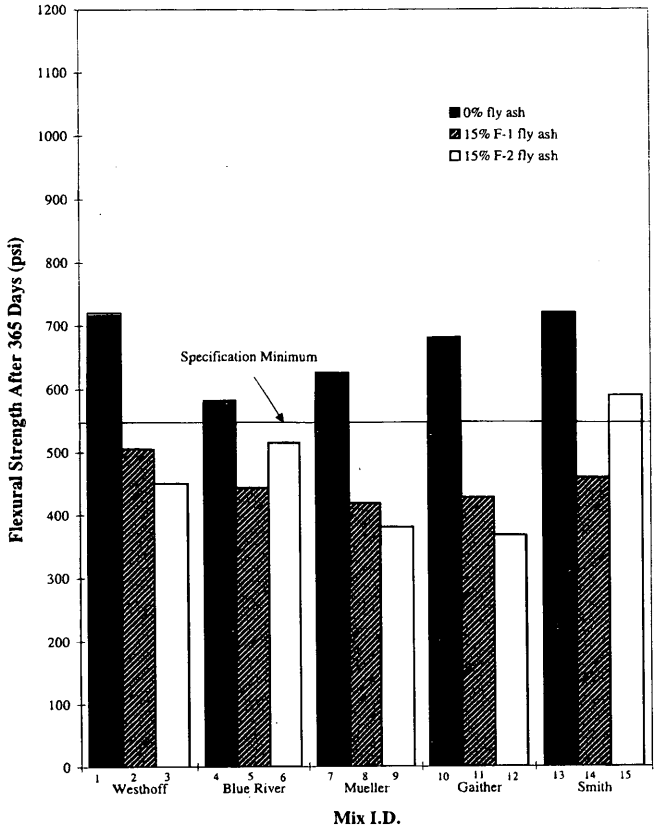

FIGURE 3 Modulus of rupture of specimens made with approved aggregates.

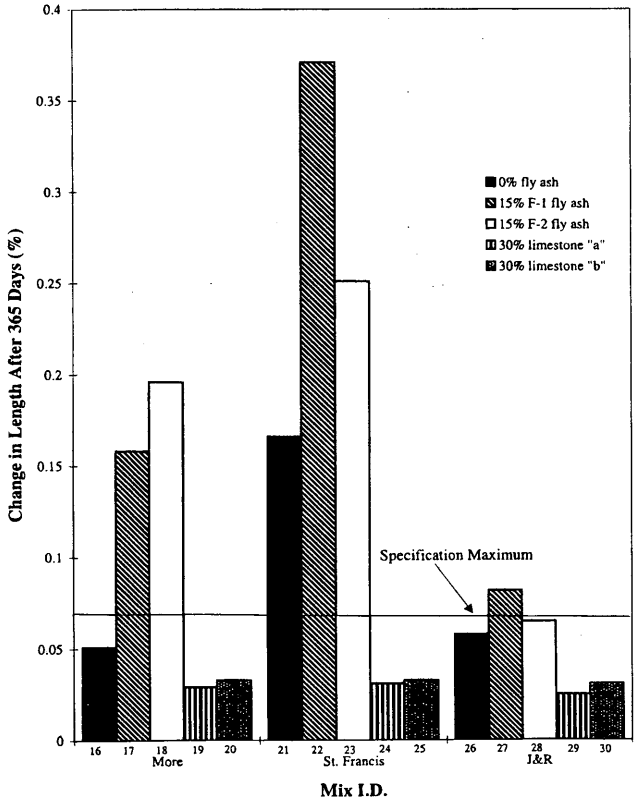

FIGURE 2 Change in length of specimens made with unapproved aggregates.

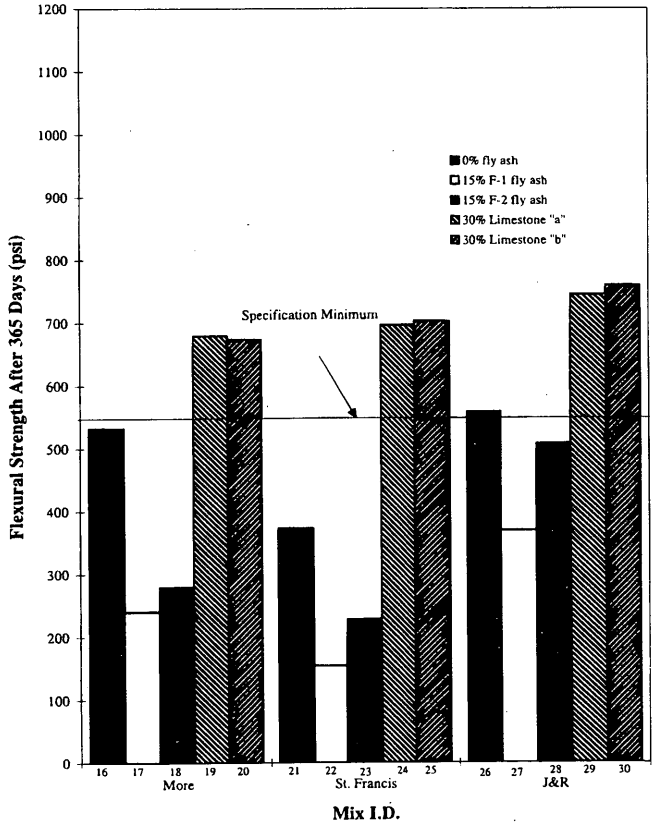

FIGURE 4 Modulus of rupture of specimens made with unapproved aggregates.

concrete performance is observed when 30 percent of the aggregate is replaced with limestone. For example, the average percentage of increase in length for the concrete made with unapproved aggregates with no limestone (sweetener) is 0.075 percent, whereas an average of 0.028 percent is obtained when limestone is used (63 percent decrease). The average modulus of rupture for mixtures made with unapproved aggregate is 3.4 MPa (487 psi) and an average of 4.9 MPa (708 psi) is obtained when limestone is used (a 45 percent increase). All individual mixtures made with unapproved sand-gravel aggregates and limestone sweetener met the requirements of the standard specifications. It is interesting that most of the mixtures made with the three unapproved aggregate types and limestone yielded significantly better results than the mixtures made with approved aggregates. This points out the effectiveness of the use of limestone in minimizing alkali-aggregate reaction problems.

CONCLUSIONS AND RECOMMENDATIONS

On the basis of the data obtained and the parameters involved in this study, the following conclusions and recommendations are warranted:

- The use of the three unapproved sand-gravel aggregates resulted in concrete of inferior durability. Therefore, the mix design should be adjusted by selecting other constituent materials or changing the mix proportions before allowing their use.
- The replacement of 15 percent of portland cement by an equal weight of either of the two type-C fly ashes used in this study resulted in concrete of higher expansion and lower modulus of rupture when compared with concrete with no fly ash.
- The use of limestone sweetener is an effective method to minimize the expansion of sand-gravel concrete. Furthermore, the use of limestone sweetener in concrete made with unapproved sand-gravel aggregates, in most cases, yields concrete of superior quality than concrete made with approved aggregate (with no fly ash or limestone). Further research should be carried out to evaluate the optimum dosages, types of limestone, and the economic aspects of its use to enhance the durability of sand-gravel concrete.

REFERENCES

1. Neville, A. M. *Properties of Concrete*. Pitman Publishing Inc., Marshfield, Mass., 1983.
2. Lee, C. Effects of Alkalies in Class C Fly Ash. *Proc., 3rd International Conference on the Use of Fly Ash, Silica Fume, Slag and Natural Pozzolans in Concrete*, Vol. 1, Norway, 1989, pp. 417–441.
3. Diamond, S. A Review of Alkali-Silica Reaction and Expansion Mechanisms. *Cement and Concrete Research*, Vol. 5, 1975, pp. 329–346.
4. Mindess, S., and F. Young. *Concrete*. Prentice-Hall, Inc., Englewood Cliffs, N.J., 1981.
5. Hadley, D. W. Field and Laboratory Studies on the Reactivity of Sand-Gravel Aggregates. *Journal of the Portland Cement Association Research and Development Laboratories*, Jan. 1968.
6. Kansas Department of Transportation Internal Report. Bureau of Materials and Research, Topeka, Nov. 1985.
7. Kobayashi, S., Y. Hozumi, T. Nakano, T. Yanagida. Study on the Effects of the Quality of Fly Ash for Controlling Alkali-Aggregate Reaction. *Proc., 3rd International Conference on the Use of Fly Ash, Silica Fume, Slag and Natural Pozzolans in Concrete*, Vol. 1, Norway, 1989, pp. 403–415.
8. Requirements for Sweetened Basic Aggregates. Kansas Department of Transportation Standard Specifications, 1980 ed. Sec. 1100, Subsec. 1102(b)(2), Topeka, 1980.
9. Wetting and Drying Test of Total Mixed Aggregate Concrete. Kansas Department of Transportation Standard Specifications, 1980 ed., Sec. 1100, Subsec. 1116(t), Topeka, 1980.
10. Perry, C., and J. E. Gillott. The Feasibility of Using Silica Fume to Control Concrete Expansion Due to Alkali-Aggregate Reactions. *Durability of Building Materials*, Vol. 3, No. 2, Nov. 1985, pp. 133–146.
11. Alasali, M. M., Alkali-Aggregate Reaction in Concrete: Investigation of Concrete Expansion from Alkali Contributed by Pozzolans or Slag. *Proc., 3rd International Conference on the Use of Fly Ash, Silica Fume, Slag and Natural Pozzolans in Concrete*, Vol. 1, Norway, 1989, pp. 431–451.
12. Hobbs, D. W. Expansion due to Alkali-Silica Reaction and the Influence of Pulverized fuel Ash. *Proc., 5th International Conference on Alkali-Aggregate Reaction in Concrete, Cape Town, South Africa*, March-April 1981.
13. Kawamura, M., K. Takemoto, and S. Hasaba. Effects of Pozzolanic Additive on Alkali-Silica Reaction in Mortar Made with Two Types of Opaline Reactive Aggregates. *CAJ Review*, 1984, p. 92.
14. Vivian, H.E. Studies in Cement-Aggregate Reaction, Part XIII. The Effect of Added Sodium Hydroxide on the Tensile Strength of Mortar. *Bulletin 256*, Commonwealth Scientific and Industrial Research Organization, Melbourne, Australia, 1950, pp. 48–52.

Publication of this paper sponsored by Committee on Admixtures and Cementitious Materials for Concrete.

PART 2

Concrete Pavement Construction

Flexural Strength Criteria for Opening Concrete Roadways to Traffic

LAWRENCE W. COLE AND PAUL A. OKAMOTO

After a concrete pavement is placed, a period of time is required for the concrete to gain strength. The pavement can be opened to traffic only after it has achieved adequate strength. Various criteria have been used for opening concrete roadways to traffic. Most criteria are based on the accumulated judgment of specifying agencies or other authorities. Little or no engineering analysis exists to substantiate most opening-to-traffic criteria currently in use. Rational criteria for opening concrete pavements to traffic are presented. On the basis of Miner's hypothesis of accumulated fatigue, flexural strength opening criteria are presented for concrete roadways (municipal and highway) subjected to construction and public traffic. The criteria are appropriate for new construction, reconstruction, and concrete overlays except bonded concrete overlays.

In many cases, traditional concrete paving practices will meet the needs of the specifying agency, contractor, and motoring public. However, increasing traffic volumes and public demand often require pavement construction to be accelerated as much as possible. Accelerated concrete pavement construction techniques (*1*) can meet these needs. This is often referred to as "fast track" concrete paving. Minimizing the time a roadway is out of service or accelerating new construction is the objective of fast track concrete paving.

SELECTION OF OPENING-TO-TRAFFIC CRITERIA

After the pavement is placed, a period of time is required for the concrete to gain strength. The pavement can be opened to traffic, both construction and public traffic, only after it has achieved adequate strength.

Various criteria have been used for opening to traffic. Generally, opening to traffic has been based on a minimum time requirement or a minimum concrete strength requirement. In some cases, a combination of time and strength is specified. Most criteria are based on the accumulated judgment of specifying agencies and other authorities. Little or no engineering analysis exists to substantiate opening-to-traffic criteria currently in use.

Report Objectives

This report presents rational criteria for opening concrete roadways to traffic. The criteria presented are based on flexural strength and apply to new construction, reconstruction, and concrete overlays, except bonded concrete overlays. (Criteria for opening bonded concrete overlays to traffic are not discussed in this report.) The criteria presented are appropriate for conventional and accelerated (fast track) paving projects.

L. W. Cole, American Concrete Pavement Association, 3800 N. Wilke Road, Suite 490, Arlington Heights, Ill. 60004. P.A. Okamoto, Construction Technology Laboratories, Inc., 5420 Old Orchard Road, Skokie, Ill. 60077.

Strength or Time?

Criteria for opening concrete roadway pavements to traffic have generally been based on time or strength. In some cases a combination of strength and time is used. Time to opening, whether measured in hours or days, is the most convenient criterion. Time is easily measured and, therefore, less debatable. More elaborate methods are required to determine the in-place strength of concrete.

Time alone, however, is insufficient to predict concrete pavement strength. The ability of a given pavement to carry anticipated loads is a function of the strength of the concrete. Time, as a measurement criterion for opening to traffic, is used as an indirect method of estimating concrete strength. The general relationship between time at early ages (less than 28 days) and strength is well-known (see Figure 1).

The rate of concrete strength gain is affected by a number of factors other than time, including

- Water-to-cement ratio,
- Properties of cement (composition and fineness),
- Aggregate properties,
- Presence or absence of admixtures and pozzolans,
- Concrete temperature,
- Consolidation, and
- Curing conditions.

Any or all of these factors can vary under field conditions. To account for these factors and the known imprecision of using time alone as an estimate of in-place concrete strength, pavement designers have often taken a conservative approach to establishing time-to-opening requirements for concrete pavements.

Strength as Opening-to-Traffic Criterion

If strength is used as an opening-to-traffic criterion, many of the uncertainties of estimating concrete strengths based solely on time are eliminated. Field methods to estimate the in-place concrete strengths are more direct methods for determining when to open a pavement to traffic. In-place concrete strength, not time, is the better criterion for opening pavements to traffic.

Determining In-Place Concrete Flexural Strength

The concrete pavement's in-place flexural strength can be determined by nondestructive testing (NDT) measurements of the pavement, such as

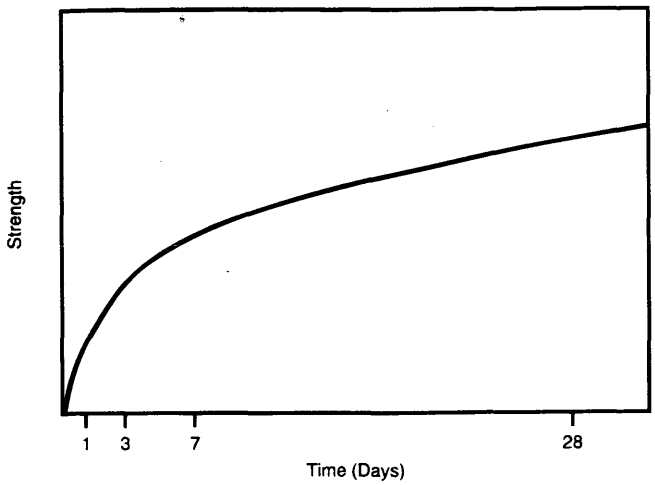

FIGURE 1 General relationship between concrete strength and time (5).

- Maturity methods (ASTM C 1074),
- Pulse velocity method (ASTM C 597),
- Pullout method (ASTM C 900), and
- Breakoff method (ASTM C 1150).

Generally, these nondestructive measurements are correlated to compressive strength as determined by cylinders (ASTM C 39). Correlation to third-point flexural strength can also be made.

A concrete pavements in-place flexural strength can also be determined by concrete cylinders made and stored in the field (ASTM C 31, paragraph 9.3) and tested in compression (ASTM C 39). The compressive strength is correlated to third-point flexural strength. Concrete beams made and stored in the field (ASTM C 31, paragraph 9.3) can also be used to determine the in-place flexural strength (ASTM C 78 and C 293) of concrete pavement.

It is important to note that it is not imperative to use flexural beam testing to determine opening strengths. Instead, compressive strength measurements or NDT measurement can be made, then correlated to third-point flexural strengths. These are often more practical methods to determine opening strengths.

The nondestructive methods, particularly maturity and pulse velocity testing, offer several advantages over cylinder or beam testing:

- Allow a more accurate reflection of the actual conditions in the pavement,
- Require less cumbersome equipment at the field site,
- Eliminate problems associated with making and handling beams and cylinders,
- Allow strength determinations to be made at an earlier age, and
- Allow rapid determination of concrete strength.

Factors Affecting Opening Strength Criteria

Recognizing that strength, not time, is the preferred method of determining opening criteria, the question arises: "What strength is required to open a concrete pavement to traffic?"

The flexural strength required for opening depends on a number of pavement-specific factors:

- Pavement application (new construction, unbonded overlay, concrete overlay of existing asphalt);
- Type, weight, and frequency of anticipated loadings;
- Distance and distribution of loads from edge of pavement;
- Moisture and temperature gradients through the depth of the slab;
- Foundation support characteristics;
- Pavement thickness;
- Concrete modulus of elasticity;
- Presence or absence of tied concrete shoulder or curb and gutter; and
- Longitudinal joint load transfer efficiency.

Accounting for all combinations of these variables to determine the opening strength for a concrete pavement would not be practicable. Defining the values of certain factors, or a range of values of these factors, is necessary if practical opening criteria based on flexural strength are desired.

Pavement Application

The opening criteria differ for various concrete pavement applications because traffic loads induce different critical stresses depending on the application. For typical concrete slabs in new construction and unbonded concrete overlays, it is generally recognized that traffic (wheel) loads cause critical flexural tensile stresses at the bottom of the slab and flexural compressive stresses at the top (*2–4*).

Concrete's tensile strength is significantly less than its compressive strength. The 28-day tensile strength is about 8 to 12 percent of compressive strength (*5*). Therefore, opening criteria based on flexural tensile strength are appropriate for most concrete pavement applications.

Bonded concrete overlays are an exception. In most bonded concrete overlays, the new concrete is generally not in tension from applied traffic loadings. Because bonded overlays are usually thinner than the existing concrete on which they are placed, the concrete overlay is in compression when wheel loads are applied (see Figure 2). The interface bonding the overlay to the existing concrete experiences horizontal shear forces from applied traffic loads.

At early ages, the bonded interface is also subjected to horizontal shear and direct tensile forces caused by temperature and moisture variations through the depth of the overlay (*6*). Therefore, the development of bond strength may be more important to opening bonded overlays to traffic than the overlay's compressive or flexural concrete strength. The criteria presented in this report are not appropriate for bonded concrete overlays.

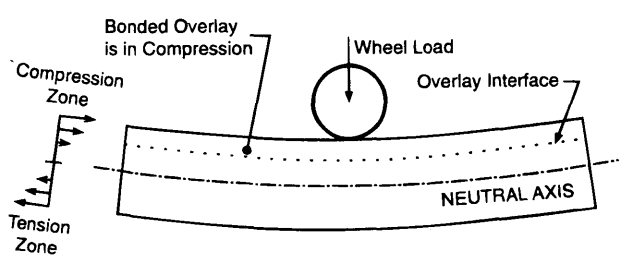

FIGURE 2 Stress distribution in bonded concrete overlay.

BASIS FOR FLEXURAL STRENGTH OPENING CRITERIA

For concrete pavements other than bonded overlays, wheel loads usually cause critical flexural tensile stresses in the bottom of the concrete slab. These stresses can be mathematically calculated. With the stresses known, it is possible to determine the required concrete strength for opening to traffic by applying principles of mechanistic pavement design.

Flexural Fatigue Concept

In concrete pavement design, the most common fatigue-cracking criterion is based on the Miner hypothesis (*7*). Each load application consumes a portion of the pavement's fatigue resistance. The fatigue resistance not consumed by one load is available for repetitions of other loads. The Miner hypothesis can be expressed as

$$\text{Percent Fatigue Damage} = 100\Sigma n/N$$

where n is the expected number of load repetitions of each load and N is the allowable number of load repetitions for each load.

N is determined from established relationships, such as in Figure 3, and n is established from the expected traffic on the pavement. Over the pavement's life, the total fatigue consumed should not exceed 100 percent. By using this hypothesis, it is possible to rationally determine the flexural strength required to open a concrete pavement to traffic.

Traffic Loadings

To determine the required flexural strength for opening to traffic, an estimate of the type, number, and weight of the applied loads is needed. A concrete pavement may be subjected to two general categories of traffic early in its life—construction loads and public traffic loads.

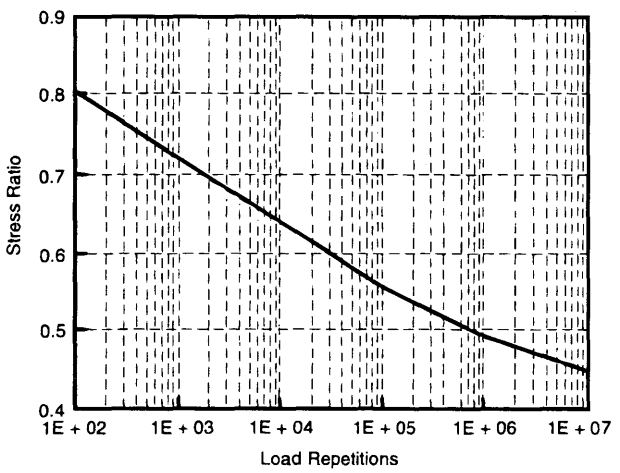

FIGURE 3 Relationship between stress ratio and load repetitions (*2*).

The contractor's equipment causes construction loads. Two types are typical on early-age concrete pavements: span saws for joint construction and trucks for material hauling.

Public traffic includes vehicles normally associated with highway use—automobiles, trucks, and buses. The number and weight of public traffic typically varies depending on the type of roadway. Interstate routes and other highways carrying large numbers of vehicles generally carry greater numbers of heavier loads than municipal streets.

Location of Applied Loads

The location of the applied wheel load has a significant effect on the stress in a concrete pavement. For most conditions, the critical flexural stress occurs when the wheel loads are at the pavement edge, midway between transverse joints (see Figure 4).

The critical flexural stress decreases as the wheel load moves away from the edge of the pavement, eventually reaching an interior slab loading condition. The number of loads expected near the edge of the pavement depends primarily on the following four factors:

- Width of driving lane,
- Type of traffic (construction or public),
- Edge protection (barricades to prevent traffic from dropping off the edge of a newly constructed concrete slab), and
- Presence or absence of curb and gutter.

Moisture and Temperature Gradients

In addition to traffic loading, concrete pavements are also subject to stresses from temperature and moisture differentials through the depth of the slab. Moisture changes, particularly moisture loss from the pavement surface, cause upward concave deformation. This induces compression in the bottom of the slab. This compressive

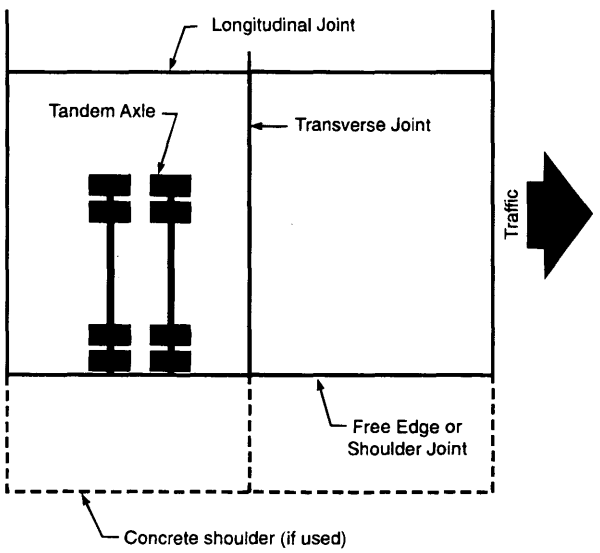

FIGURE 4 Axle load position for critical load repetitions.

stress is subtractive from the critical wheel-load stress. Stresses due to temperature differentials through the depth of the slab can be additive or subtractive from wheel-load stress. During the day, when the top surface is warmer than the bottom, tensile-restraint develops at the slab bottom. During the night, the temperature distribution is reversed and tensile-restraint stresses develop at the slab surface. Usually, the combined effect of moisture and temperature gradients are subtractive from critical mid-panel wheel-load flexural stresses (*2*).

The complex situation of differential conditions at the slab's top and bottom and the uncertainty of the zero-stress position make it difficult to compute these restrained stresses with any degree of confidence or verification. Therefore, for purposes of establishing opening-to-traffic strength criteria, these stresses are considered to be off-setting and are neglected in the analysis.

Foundation Support

The support given to concrete pavements by the subgrade and subbase, where used, affects the flexural strength required to open a pavement to traffic. Subgrade and subbase support is usually defined in terms of the Westergaard modulus of subgrade reaction (k).

ASTM D1196 (*8*) can be used to determine the k-value. However, this test is time consuming and expensive. Methods of correlating approximate k-values to other simpler tests (*2,9*) are adequate for determining opening flexural strength requirements. Higher k-values indicate a stiffer foundation. When other factors are constant, increasing the k-value decreases the wheel-load stress in the concrete pavement (*2*), lowering the flexural strength required for opening to traffic.

Using the concept of effective modulus of subgrade reaction (*2,10*), appropriate k-values can be selected for characterizing foundation support. In this report, effective k-values of 27 MPa/m (100 pci), 54 MPa/m (200 pci), and 136 MPa/m (500 pci) are chosen to represent concrete pavements constructed on compacted natural subgrade, granular subbase, and asphalt or cement stabilized subbase, respectively.

Pavement Thickness

Slab thickness has a significant effect on pavement stresses. Increasing pavement thickness decreases the pavement stress (*2*), lowering the flexural strength required for opening to traffic.

OPENING-TO-TRAFFIC FLEXURAL STRENGTH CRITERIA

Analysis Procedures

An extensive analysis has been made of concrete pavement subjected to traffic loads early in its life (*9*). Flexural stresses were determined with the finite element computer program ILLISLAB (*11*) for a variety of conditions. This early-age fatigue analysis was extensive because stress and strength are related to modulus of elasticity and increase at different rates. The increase in stresses associated with increased modulus of elasticity are offset to various degrees by flexural strength increases.

The relationship between the calculated stress ratio and the number of allowable loads shown in Figure 3 was used where

$$N = 10^{(0.97187 - SR)/0.0828} \quad \text{for } SR > 0.55$$

$$N = \left(\frac{4.2577}{SR - 0.43248}\right)^{3.268} \quad \text{for } 0.45 < SR < 0.55$$

$$N = \text{unlimited} \quad \text{for } SR < 0.45$$

The fatigue analysis was conducted for the following traffic and pavement design conditions:

- Sawing equipment loadings,
- Construction vehicle loadings,
- Traffic channelized away from pavement edge by barricades,
- Traffic allowed to approach free edge of pavement, and
- Tied concrete shoulders or tied adjacent lane.

Complete tables of these analyses can be found elsewhere (*9*). Summaries are presented in Tables 1, 2, 3, 4, and 5 as follows.

Construction Traffic—Span Saw Loading

Analysis was made for a 6575 kg (14,500 lb) span saw applied to a 6.10 × 7.32 m (20 × 24 ft) concrete slab as shown in Figure 5.

Required flexural strengths for span saw operations are shown in Table 1. Fatigue damage was calculated for 10 span saw load applications. The values in the table are based on one-half of 1 percent fatigue consumption. A minimum modulus of rupture a maximum of 1.04 MPa (150 psi) was selected as this relates to the minimum practical flexural strength for sawing joints in concrete pavement (*10*).

TABLE 1 Opening to Construction Traffic—Span Saws

Thickness		k-value		Required Flexural Strength[a]	
mm	(in)	MPa/m	(pci)	MPa	(psi)
150	(6)	27	(100)	1.45	(210)
		54	(200)	1.31	(190)
		136	(500)	1.03	(150)
165	(6.5)	27	(100)	1.31	(190)
		54	(200)	1.10	(160)
		136	(500)	1.03	(150)
180 or greater	(7)	27	(100)	1.03	(150)
		54	(200)	1.03	(150)
		136	(500)	1.03	(150)

[a]From measurements correlated to third-point flexural strength (ASTM C78)

TABLE 2 Opening to Construction Traffic—Construction Vehicles

Thickness		k-value		Required Flexural Strength[a], MPa (psi) Number of 15,400 kg (34 kip) TAL			
mm	(in)	MPa/m	(pci)	10		50	
150	(6)	27	(100)	2.82	(410)	3.17	(460)
		54	(200)	2.48	(360)	2.69	(390)
		136	(500)	2.07	(300)	2.07	(300)
165	(6.5)	27	(100)	2.48	(360)	2.69	(390)
		54	(200)	2.14	(310)	2.41	(350)
		136	(500)	2.07	(300)	2.07	(300)
180	(7)	27	(100)	2.07	(300)	2.34	(340)
		54	(200)	2.07	(300)	2.07	(300)
		136	(500)	2.07	(300)	2.07	(300)
190	(7.5)	27	(100)	2.07	(300)	2.07	(300)
or greater		54	(200)	2.07	(300)	2.07	(300)
		136	(500)	2.07	(300)	2.07	(300)

[a]From measurements correlated to third-point flexural strength (ASTM C78)

TABLE 3 Opening to Public Traffic—Municipal Streets with Barricades (Without Adjacent Concrete Lane or Tied or Integral Curb and Gutter)

Thickness		k-value		Required Flexural Strength in MPa (psi) Estimated ESALs to Design Strength[b]									
mm	(in)	MPa/m	(pci)	100		500		1,000		2,000		5,000	
150	(6)	27	(100)	3.38	(490)	3.72	(540)	3.93	(570)	4.61	(590)	4.34	(630)
		54	(200)	2.82	(410)	3.10	(450)	3.24	(470)	3.38	(490)	3.58	(520)
		136	(500)	2.34	(340)	2.55	(370)	2.67	(390)	2.76	(400)	2.96	(430)
165	(6.5)	27	(100)	2.96	(430)	3.24	(470)	3.38	(490)	3.58	(520)	3.79	(550)
		54	(200)	2.42	(350)	2.67	(390)	2.82	(410)	2.96	(430)	3.10	(450)
		136	(500)	2.07	(300)	2.20	(320)	2.27	(330)	2.41	(350)	2.55	(370)
180	(7)	27	(100)	2.55	(370)	2.82	(410)	2.96	(430)	3.10	(450)	3.31	(480)
		54	(200)	2.14	(310)	2.34	(340)	2.48	(360)	2.55	(370)	2.76	(400)
		136	(500)	2.07	(300)	2.07	(300)	2.07	(300)	2.07	(300)	2.20	(320)
190	(7.5)	27	(100)	2.27	(330)	2.55	(370)	2.62	(380)	2.76	(400)	2.96	(430)
		54	(200)	2.07	(300)	2.07	(300)	2.20	(320)	2.27	(330)	2.41	(350)
		136	(500)	2.07	(300)	2.07	(300)	2.07	(300)	2.07	(300)	2.07	(300)
200	(8)	27	(100)	2.07	(300)	2.27	(330)	2.34	(340)	2.48	(360)	2.62	(380)
		54	(200)	2.07	(300)	2.07	(300)	2.07	(300)	2.07	(300)	2.14	(310)
		136	(500)	2.07	(300)	2.07	(300)	2.07	(300)	2.07	(300)	2.07	(300)

[a]From measurements correlated to third-point flexural strength.
[b]Estimated ESALs that will use the pavement from time of opening until concrete achieves its design (usually 28-day) strength. ESALs are one direction, truck lane.

Construction Traffic—Vehicles

Table 2 presents flexural strength requirements for opening concrete pavements to use by vehicular construction traffic rounded to 0.07 MPa (10 psi).

Table 2 considers typical concrete pavement construction traffic. The most common heavy construction loads are 15,400 kg (34,000 lb) tandem axle load (TAL) dump trucks. Because most construction loads operate away from the pavement edge, all vehicular wheel loads were analyzed at a distance of 0.61 m (2 ft) from the pavement edge. Fatigue consumption from construction vehicles was limited to 1 percent.

A practical minimum flexural strength of 2.07 MPa (300 psi) is shown. This relates to typical concrete pavement flexural strength when joint sawing has been completed (*10*). Construction traffic is usually not allowed on the pavement until joint sawing is completed.

The data in Table 2 can be approximated with the following English unit equation (strengths calculated and the equation derived in English units only):

$$\log(MR) = -1.8425 * \log(t) - 0.0122 * \text{sqrt}(k) + 0.0724 * \log(N) + 4.0870$$
but not less than 300 psi (1)

where

MR = modulus of rupture (flexural strength) in psi (100 psi = 0.689 MPa),
t = slab thickness (in.),
k = modulus of subgrade/subbase reaction (lb/in.^{3}),
N = number of expected TAL trucks, and
R^2 adj = 0.998 for Equation 1.

TABLE 4 Axle Load Distributions (2) Used in Tables 3 and 5

Axle load kg (kips)	Axles per 1000 trucks[a] Table 3 (Municipal streets with barricades)	Table 5 (Highways with barricades)
Single axles		
1,800 (4)		
2,700 (6)		
3,600 (8)	233.60	
4,500 (10)	142.70	
5,400 (12)	116.76	
6,400 (14)	47.76	
7,300 (16)	23.88	57.07
8,200 (18)	16.61	68.27
9,100 (20)	6.63	41.82
10,000 (22)	2.60	9.69
10,900 (24)	1.60	4.16
11,800 (26)	0.07	3.52
12,700 (28)		1.78
13,600 (30)		0.63
14,500 (32)		0.54
15,400 (34)		0.19
Tandem axles		
1,800 (4)		
3,600 (8)	47.01	
5,400 12)	91.15	
7,300 (16)	59.25	
9,100 (20)	45.00	
10,900 (24)	30.74	71.16
12,700 (28)	44.43	95.79
14,500 (32)	54.76	109.54
16,300 (36)	38.79	78.19
18,100 (40)	7.76	20.31
20,000 (44)	1.16	3.52
21,800 (48)		3.03
23,600 (52)		1.79
25,400 (56)		1.07
27,200 (60)		0.57

[a] excluding all two-axle, four-tire trucks

Public Traffic—Types of Roadways

The type of roadway affects the flexural strength criteria for opening concrete pavements to public traffic. Interstate and other highways carry higher volumes of traffic and in most cases larger numbers of heavy vehicles than municipal streets.

Several factors affect the placement of vehicle wheels relative to the pavement edge. Highways may be constructed with widened outside lanes or tied concrete shoulders, or both; municipal concrete streets often have tied or integral curb and gutter sections. Also, for safety purposes, highways and municipal streets often have barricades at the edge of newly constructed lanes to prevent public traffic from driving off the edge.

Number of Loads (Public Traffic)

To determine the required flexural strength to open to public traffic, the expected number of loads must be estimated. Most concrete pavements are designed using a 28-day average flexural strength to represent concrete strength. If concrete pavements are opened in less than 28 days, an estimate of the public traffic on the pavement between time of opening and 28 days is needed.

Pavement designers often use 8,150 kg (18,000 lb) equivalent single-axle loads (ESALs) as a method of estimating traffic (*12*). Therefore, the number of expected ESALs from time of opening until the pavement achieves its design strength is a convenient measure of traffic. A recent survey of highway practices (*13*) determined that 45 state highway agencies specify a 28-day strength (compressive or flexural).

Minimum Flexural Strength for Opening to Public Traffic

Joints in concrete pavements should be constructed before the pavement is opened to public traffic. One study (*10*) indicates that joint sawing operations are usually complete before the pavement

TABLE 5 Opening to Public Traffic—Highways with Barricades (Without Widened Lane or Tied Concrete Shoulder)

Thickness		k-value		Required Flexural Strength[a] in MPa (psi) Estimated ESALs to Design Strength[b]				
mm	(in)	MPa/m	(pci)	100	500	1000	2000	5000
200	(8)	27	(100)	2.55 (370)	2.82 (410)	2.96 (430)	3.10 (450)	3.24 (470)
		54	(200)	2.14 (310)	2.34 (340)	2.41 (350)	2.55 (370)	2.69 (390)
		136	(500)	2.07 (300)	2.07 (300)	2.07 (300)	2.07 (300)	2.14 (310)
215	(8.5)	27	(100)	2.34 (340)	2.55 (370)	2.62 (380)	2.78 (400)	2.96 (430
		54	(200)	2.07 (300)	2.07 (300)	2.20 (320)	2.27 (330)	2.41 (350)
		136	(500)	2.07 (300)	2.07 (300)	2.07 (300)	2.07 (300)	2.07 (300)
230	(9)	27	(100)	2.07 (300)	2.27 (330)	2.41 (350)	2.48 (360)	2.69 (390)
		54	(200)	2.07 (300)	2.07 (300)	2.07 (300)	2.07 (300)	2.20 (320)
		136	(500)	2.07 (300)	2.07 (300)	2.07 (300)	2.07 (300)	2.07 (300)
240	(9.5)	27	(100)	2.07 (300)	2.07 (300)	2.20 (320)	2.27 (330)	2.41 (350)
		54	(200)	2.07 (300)	2.07 (300)	2.07 (300)	2.07 (300)	2.07 (300)
		136	(500)	2.07 (300)	2.07 (300)	2.07 (300)	2.07 (300)	2.07 (300)
250	(10)	27	(100)	2.07 (300)	2.07 (300)	2.07 (300)	2.07 (300)	2.20 (320)
		54	(200)	2.07 (300)	2.07 (300)	2.07 (300)	2.07 (300)	2.07 (300)
		136	(500)	2.07 (300)	2.07 (300)	2.07 (300)	2.07 (300)	2.07 (300)
265	(10.5)	27	(100)	2.07 (300)	2.07 (300)	2.07 (300)	2.07 (300)	2.07 (300)
or greater		54	(200)	2.07 (300)	2.07 (300)	2.07 (300)	2.07 (300)	2.07 (300)
		136	(500)	2.07 (300)	2.07 (300)	2.07 (300)	2.07 (300)	2.07 (300)

[a]From measurements correlated to third-point flexural strength.
[b]Estimated ESALs that will use the pavement from time of opening until concrete achieves its design (usually 28-day) strength. ESALs are one-direction, truck lane.

reaches 2.07 MPa/m (300 psi) flexural strength. While this value may vary depending on aggregate type, weather conditions, and sawing methods, it provides a practical lower limit for opening to public traffic.

Opening to Public Traffic—Municipal Streets

Before municipal streets are opened to public traffic, safety precautions must be taken to prevent vehicles from driving off the new pavement edge. If adjacent lanes or the curb and gutter are not in place, barricades are used.

With barricades, traffic remains at some distance from the pavement edge. In this report, all pavements with barricades were analyzed with wheel loads at a constant distance of 0.61 m (2 ft) from the pavement edge. Opening flexural strength criteria with barricades present, rounded to 0.07 MPa (10 psi), for municipal pavements are presented in Table 3. The tabulated values are for 1 percent fatigue consumption computed with the axle load distribution shown in Table 4.

If adjacent lanes or tied or integral concrete curb and gutter are present, the opening strengths in Table 3 can be reduced by 35 percent [minimum of 2.07 MPa (300 psi)], whether barricades are present or not. For such conditions, appropriate wheel wander (2) was used in the analysis.

The data in Table 3 can be approximated with the following English unit equation (strengths calculated and the equation derived in English units only):

$$\log(MR) = -0.0890 * (t) - 0.2568 * \log(k) + 0.0675 * \log(\text{ESALs}) + 3.5708 \quad \text{but not less than 300 psi} \qquad (2)$$

where

MR = modulus of rupture (flexural strength) in psi (100 psi = 0.689 MPa),
t = slab thickness (in.),
k = modulus of subgrade/subbase reaction (lb/in.^{3}),
ESALs = number of equivalent single-axle loads (18,000 lb) expected on the slab from opening until design strength is obtained, and
R^2 adj = 0.993 for Equation 2.

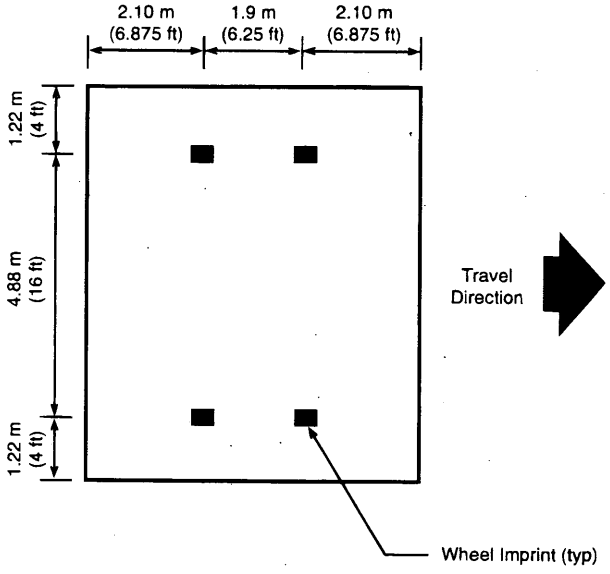

FIGURE 5 Span saw loading.

Opening to Public Traffic—Highways

If adjacent lanes or shoulders are not in place, barricades are used to prevent traffic from driving off the pavement edge. In some highway designs, particularly interstate routes, widened lanes are sometimes used to reduce edge loadings.

Opening criteria for concrete highways with safety barricades in place are presented in Table 5. For Table 5, all wheel loads were analyzed at a constant distance of 0.61 m (2 ft) from the pavement edge. The tabulated values are for 1 percent fatigue consumption computed with the axle load distribution shown in Table 4.

If the highway has a widened truck lane [typically 4.25 m (14 ft) wide] or tied concrete shoulders, the flexural opening strengths in Table 5 can be reduced by 30 percent [minimum of 2.07 MPa (300 psi)], whether or not barricades are present. For such conditions, an appropriate wheel wander (2) was assumed in analysis. If the highway is open to public traffic without widened truck lanes or tied concrete shoulders, barricades should be left in place until the concrete reaches 3.1 MPa (450 psi) flexural strength.

The data in Table 5 can be approximated with the following English unit equation (strengths calculated and the equation derived in English units only):

$$\log(MR) = -0.0873 * (t) - 0.2558 * \log(k) + 0.0635 * \log(\text{ESALs}) + 3.5708 \quad \text{but not less than 300 psi} \tag{3}$$

where

MR = modulus of rupture (flexural strength) in psi (100 psi = 0.689 MPa),
t = slab thickness (in.),
k = modulus of subgrade/subbase reaction (lb/in.^{3}),
ESALs = number of equivalent single-axle loads (18,000 lb) expected on the slab from opening until design strength is obtained, and
R^2 adj = 0.992 for Equation 3.

COMMENTS ON TABLE 4 AND ESALS, AND AN EXAMPLE

In this report, mechanistically based procedures are used to determine flexural strength requirements for opening concrete roadways to traffic. These procedures use the axle-load distributions shown in Table 5. For each 1,000 trucks, the number of expected axles is given in 1,800 kg (2,000 lb) increments (single axle) and 3,600 kg (4,000 lb) increments (tandem axle).

For instance, for every 1,000 trucks on a municipal street, one might expect

- 233.60 single axles weighing 3,600 kg (8,000 lb),
- 142.70 single axles weighing 4,500 kg (10,000 lb),
- 116.76 single axles weighing 5,400 kg (12,000 lb),
- 47.01 tandem axles weighing 3,600 kg (8,000 lb),
- 91.15 tandem axles weighing 5,400 kg (12,000 lb), and
- 59.25 tandem axles weighing 7,300 kg (16,000 lb).

Such load weight distributions can be used to determine the ESALs used in the AASHTO (*12*) procedure for pavement design. Load equivalency factors multiplied by the number of axle loads within a given weight range are totaled to determine total ESALs.

In many cases, however, the axle load distributions are unknown. The pavement design engineer is given only the total number of ESALs or the number of ESALs expected per day on the roadway. Therefore, traffic volumes for opening strength guidelines are presented using ESALs because traffic information is more readily available in this form rather than load weight distribution tables.

To relate expected ESALs to load weight distributions used in the mechanistic analysis, the number of axles equivalent to 1,000 ESALs were computed for the load weight distributions shown in Table 5. The number of axles equivalent to 1,000 ESALs varies slightly with slab thickness and significantly with roadway category (municipal street or highway), as shown in Table 6.

For example, for the municipal street distribution shown in Table 4, it takes about 2,600 trucks to generate 1,000 ESALs. For the highway distribution, about 650 trucks will generate 1,000 ESALs. This is because, in general, highways carry a larger number of heavy trucks than municipal streets.

As an example, consider a municipal street carrying 100 ESALs per day: (a) using the axle load distribution shown in Table 4,

$$100 \text{ ESALs/day} \times (2{,}600 \text{ trucks}/1{,}000 \text{ ESALs}) = 260 \text{ trucks/day}$$

(b) for the highway distribution of Table 4,

$$100 \text{ ESALs/day} \times (650 \text{ trucks}/100 \text{ ESALs}) = 65 \text{ trucks/day}$$

For the highway distribution, 65 trucks will generate 100 ESALs, and 260 trucks of the municipal distribution will generate 100 ESALs.

For the same slab thickness, from a mechanistically based fatigue damage approach, 260 trucks of Table 4 municipal loadings will not cause the same amount of damage as 65 trucks of the highway loadings. Because of the heavier axle loads in the highway distribution, 65 trucks of highway distribution is more damaging than 260 trucks of municipal distribution.

Because 100 ESALs require 65 trucks of highway distribution or 260 trucks of municipal distribution, and, for a specific pavement thickness, 65 highway truck loadings cause more fatigue damage than 260 municipal truck loadings, there will be a difference between the opening-strength criteria for municipal streets and highways for the same slab thickness and ESAL estimate. For example, a 200 mm (8 in.) thick pavement on a granular subbase (k = 54 MPa/m, 200 lb/in.^{3}) expected to carry 2,000 ESALs until design strength is reached can be opened to public traffic at 2.07 MPa (300 psi) when exposed to municipal loadings (Table 3), but should achieve a strength of 2.55 MPa (370 psi) when exposed to highway loadings (Table 5).

CONCLUSION

Throughout the United States a variety of criteria is used to determine whether a newly constructed concrete roadway is capable of carrying construction and public traffic. Although there is inconsistency among specifying agencies, opening criteria are generally based on time, concrete strength, or a combination of time and strength. Through the application of mechanistically based procedures, it is possible to determine flexural strength criteria for opening concrete roadways to traffic. Although it is not possible to account for all combinations of factors affecting opening flexural

TABLE 6 Number of Axle Loads per 100 ESALs

	Number of Axle Loads per 1000 ESALs		
Roadway Category	150 mm (6 in) slab	300 mm (12 in) slab	Average
Municipal/Street	2,564	2,649	2,601
Highway	630	680	655

strength, reasonable values or range of values of these factors can be selected. On the basis of such a selection and analysis, flexural opening strength criteria have been determined for construction and public vehicular traffic on concrete highways and streets. The criteria are appropriate for new construction, reconstruction, and concrete overlays except bonded concrete overlays.

ACKNOWLEDGMENTS

The research reported in this report (*9*) was conducted at Construction Technology Laboratories, Inc., with the sponsorship of the Portland Cement Association (PCA Project Index No. 91–01). Special acknowledgment is due to members of FHWA's Special Project 201 (SP201)—Accelerated Rigid Paving Techniques. SP201 members significantly contributed through reviews and comments.

REFERENCES

1. *Fast Track Concrete Pavements*. TB–004. American Concrete Pavement Association, Arlington Heights, Ill., 1989.
2. Packard, R. *Thickness Design for Concrete Highway and Street Pavements*. EB109. Portland Cement Association, Skokie, Ill., 1984.
3. Salsilli, R., E. Barenberg, and M. Darter. Calibrated Mechanistic Design Procedure to Prevent Transverse Cracking of Jointed Plain Concrete Pavements. *Proc., 5th International Conference on Concrete Pavement Design and Rehabilitation*, Vol. 2, Purdue University, West Lafayette, Ind., April 1993, pp. 71–83.
4. *Thickness Design for Concrete Pavements*. HB35. Portland Cement Association, Chicago, Ill., 1966, p. 6.
5. Kosmatka, S., and W. Panarese. *Design and Control of Concrete Mixtures*. EB001. Portland Cement Association, Skokie, Ill., 1988.
6. Domenichini, L. *Factors Affecting Adhesion of Bonded Concrete Overlays (Abridgment)*. Department of Hydraulics, Transportation and Road Construction, University of Rome, 1986.
7. Miner, M. Cumulative Damage in Fatigue. *Transactions*, Vol. 67, American Society of Mechanical Engineers, 1945, pp. A159–A164.
8. Standard Method for Nonrepetitive Static Plate Load Tests of Soils and Flexible Pavement Components for Use in Evaluation and Design of Airport and Highway Pavements. Designation D1196. American Society for Testing and Materials, Philadelphia, Pa., 1994.
9. Okamoto, P., C. Wu, and S. Tarr. *Opening of Portland Cement Concrete Pavements to Traffic*. R & D Serial No. 2019. Potland Cement Association, Skokie, Ill., 1995.
10. Okamoto, P., P. Nussbaum, and K. Smith. Guideline Recommendations for Timing Contraction Joint Sawing of PCC Highway Pavements. *Proc., 5th International Conference on Concrete Pavement Design and Rehabilitation*, Vol. 2, Purdue University, West Lafayette, Ind., April 1993, pp. 41–45.
11. Tabatabaie, A. M., E. J. Barenberg, and R. E. Smith. Longitudinal Joint Systems in Slip-Formed Rigid Pavements. *Analysis of Load Transfer Systems for Concrete Pavements*, Vol. II, FAA–RD–79–4, Federal Aviation Administration, Washington, D.C., Nov. 1979.
12. *Guide for Design of Pavement Structures*. American Association of State Highway and Transportation Officials, Washington, D.C., 1993, pp. I110–I14.
13. Forsyth, R. *Pavement Structural Design Practices*. NCHRP Synthesis 1989, National Cooperative Highway Research Program, National Academy Press, Washington, D.C., 1993, pp. 26–27.

Publication of this paper sponsored by Committee on Portland Cement Concrete Pavement Construction.

Partnering for Performance—Iowa's Experience with Design and Construction Enhancements for Quality Improvement of Concrete Pavements

GORDON L. SMITH AND BRIAN R. MCWATERS

A strong and proven working relationship among the Iowa Department of Transportation, Iowa's counties and cities, and the Iowa Concrete Paving Association is focused on meeting owners' needs by improving quality of workmanship, product, and innovative techniques. Partnering, a new paradigm for owner and contractor relations that emphasizes up-front team building, clear definition of common objectives, synchronized customs for rapid issue resolution, and joint evaluation of partnership effectiveness, is a popular objective of the 1990s. Construction partnering has existed in a limited form for years, but such relationships have found some difficulty of survival in a system in which the low bidder wins the contract, the taxpayer dollar is at stake, and the government may be sensitive to criticism of not spending the money wisely. Today, new partnering concepts to protect the public interest have been developed by contracting authority and contractor alliances with both parties. Most partnering has been between a contracting authority and contractor with mutual intent to construct a specific project. A more general partnership among the Iowa Department of Transportation, other Iowa contracting authorities, and the Iowa Concrete Paving Association is described. In 1992, Iowa contracting agencies and the concrete paving industry began an Iowa initiative for continuing quality improvement of concrete pavements. Through the Iowa partnership, changes have been made in standard designs, specifications, materials use, and construction techniques to enhance concrete pavement quality.

Over the past several years, much has been written about the evolution of partnering in the field of public highway construction. One definition for partnering describes a new paradigm of owner and contractor relations with emphasis on up-front team building, clear definition of common objectives, synchronized customs for rapid issue resolution, and joint evaluation of partnership effectiveness (*1*). Construction partnering has existed to a limited extent throughout the years, but has found some difficulty of survival in a system in which the low bidder wins the contract, the taxpayer dollar is at stake, and the government may be sensitive to criticism of not spending the money wisely. In the past, there has been a tendency for adverse relationships between the contractor and contracting authority, which some managers thought was beneficial to the owner (*2*).

Today, contracting authorities and industry have become more aware of the total costs of infrastructure and recognize the need to maximize the benefit derived from all administrative and construction dollars spent. It is now necessary to protect the public interest by contracting authority and contractor alliances, with both parties cooperating to achieve different but complementary objectives.

A strong, proven working relationship has developed among the Iowa Department of Transportation (Iowa DOT), Iowa's counties and cities, and the Iowa Concrete Paving Association over many years. This relationship is focused on meeting the owners' needs through quality of workmanship, product, and innovative techniques. In the 1990s, as partners committed to continuing quality improvement of concrete pavements, the construction industry is encouraged to consider changes in design, specifications, and construction procedures that enhance pavement performance.

HISTORICAL BACKGROUND

In 1904, the Iowa legislature passed two laws that have established the responsibility for roadway design, construction, and maintenance in the state. The Iowa State Highway Commission was established, and the supervisors of each county were required to employ a competent engineer to supervise the building of permanent roads. Over the years, legislation has further defined these responsibilities, provided for funding of the roadway network, and broadened the scope to intermodal transportation. The Iowa State Highway Commission became the Iowa Department of Transportation in 1974.

During the early 1900s, Iowa's first concrete city street was built in LeMars, Iowa. It was the second concrete street built in America. The first rural county concrete pavement was constructed near Eddyville, Iowa, in 1911 and from 1913 to 1919 the seedling miles of Iowa's primary highway system were paved with concrete.

A $100 million road bond issue was passed in 1928 to finance the construction of 10,304 km (6,400 mi) of concrete roads connecting main market centers statewide. These major commitments to road building by Iowa contracting agencies and the Iowa concrete paving industry established the foundation for a relationship that would grow through the years (*3*).

The Iowa partnership was highlighted in the late 1940s when a farm-to-market road bill provided major funding for road improvements in the 99 counties. Shortly thereafter, J. Johnson, an Iowa State Highway Commission employee, invented the slipform paving machine. Recognizing the significance of Johnson's machine and responding to the need for an economical method of constructing concrete pavements, Iowa contractors Perkins and Dale refined the Johnson machine and introduced the Quad City

G. L. Smith, Iowa Concrete Paving Association, 8525 Douglas Ave., Suite 38, Des Moines, Iowa 50322. B. R. McWaters, Iowa Department of Transportation, 800 Lincoln Way, Ames, Iowa 50010.

Formless Paver by 1954 (*4*). The slipform paver modernized the industry and allowed concrete to sustain its prominence as an economical, high-performance pavement choice for construction of Iowa's state and county roads and city streets.

The Iowa Concrete Paving Association (ICPA) was founded in 1963 by six Iowa contractors as an organization that would help Iowa agencies design and plan roads and promote the use of concrete, advancing its use in the construction of highways, streets, airfields, and other public improvements. These objectives would be accomplished through product performance, high standards of workmanship, education, research, and innovation.

Today, ICPA's 26 contractor members and 80 allied associates work with Iowa's contracting authorities to provide permanent pavements that serve the public interest.

IOWA PARTNERSHIP

The Iowa partnership for quality and performance has developed through years of cooperation in establishing and reaching mutual goals. Since ICPA's inception, association members and key Iowa DOT staff have gathered annually to review specifications and design standards that may be of concern relative to cost, benefit, and impact on pavement performance. The annual concrete paving workshop in Iowa provides the nation's largest local forum where more than 500 engineers, contractors, and owners gather to explore methods for improving concrete pavement performance through advanced design, materials use, construction techniques, and innovative technology. For 30 years, Iowa contractors, field personnel, agency engineers, and inspectors have been recognized for their outstanding workmanship by a joint ICPA-Iowa DOT awards program at the workshop. Through these traditions of Iowa's partnership, the local contracting agencies and concrete paving industry are recognized as national leaders in the development and implementation of quality enhancements and concrete solutions.

From the slipform development in 1949 to work on high-tech concrete mixes today, many changes in design, materials, and construction techniques have influenced local and national concrete paving technology while improving pavement quality and performance.

The Iowa concrete pavement has evolved over years of experience and varying conditions of service. The agencies have specified jointed reinforced concrete pavement, continuous reinforced concrete pavements, and jointed concrete pavements. Jointed concrete pavement is the preferred design from the specifying agency's and the contractor's perspectives. Jointed concrete pavements without dowels are standard for Iowa's low-volume roads. On the basis of field experience, the design for higher-volume pavements has progressed from no dowels to doweled transverse joints with dowels placed on 30.48-cm (12-in.) centers at 6.10-m (20-ft) intervals (*5*).

Working together, agency and industry personnel have developed standards for keyway spacing and bar size that afford the best constructibility and uniformity of application. Originally, longitudinal tiebar spacing ranged from 30.48 cm (12 in.) to 76.20 cm (30 in.), depending on the width and the thickness of the pavement. After an annual specification meeting, changes were made so that 38.25-cm (15-in.) and 76.20-cm (30-in.) tiebar spacing is standard for keyway in longitudinal joints. The number of bar sizes has been reduced to assist in contractor and supplier inventory control and to minimize confusion in the field.

Joint spacing and dimension standards have been improved to simplify field operations and provide the desired performance. Sealants have been tested to determine the optimum selection for each pavement service level. Today, hot-poured sealants are specified for local, Surface Transportation Program, and primary National Highway System (NHS) pavements. A preformed elastomeric compression seal is specified for transverse joints on interstate pavements.

The Iowa design for four-lane NHS pavements now specifies a widened, 4.27 m (14 ft) outside lane that maximizes pavement performance potential through proven structural advantage. The widened lane is comparable to a tied portland cement concrete paved shoulder, but more economical and easier for the contractor to build.

In 1995, Iowa NHS pavement designs will specify a subbase that extends 0.92 m (3 ft) beyond the edge of the slab. Previous 0.61-m (2-ft) wide padlines did not take full advantage of today's slipform technology. The added subbase width allows for full support of newer paving machine's tracks.

Iowa's first variation of concrete recycling was showcased in 1976 when a composite portland cement concrete and asphalt pavement was recycled. The recycled aggregate was used in the concrete base course of a two-course concrete pavement (*6*). In 1977, concrete pavement was recycled for aggregate in new pavement on projects in Page and Pottawattamie counties (*7*). Although successful, the technique has not been used extensively because many reconstruction candidates were originally built with D-cracking coarse aggregates.

Greene County, Iowa, has used recycled concrete for aggregate in concrete pavement reconstruction on 30.59 km (19 mi) of low-volume roadway constructed since 1985 (*8*). The original Greene County pavements were built using high-durability river aggregates.

With limited funds for reconstruction of an aging Interstate system whose traffic had far exceeded design projections, Iowa began to construct mainline inlays of its Interstate highways in 1979 while maintaining the existing shoulder base. Several changes have improved inlay design and construction. One of the first inlays was constructed one-lane wide with traffic adjacent to the construction zone. Construction difficulties and risk to workers led to construction of two lanes simultaneously with traffic shifted to the other side of the Interstate in a head-to-head configuration. Today, the inside shoulder is completely reconstructed to accommodate construction operations. More than 483 km (300 mi) of two-lane Interstates (I–80, I–35, and I–29) have been reconstructed as concrete inlays and refinements over the past 15 years have provided a constructible, high-performance pavement.

Since 1982, Iowa contractors have recycled existing Interstate pavement as a drainable base course placed before inlay construction. The crushed material provides a drainage layer with a permeability rating of approximately 305 m (1,000 ft) per day. A change in maximum allowable particle size from 12.7 cm (¾ in.) to 5.63 cm (1½ in.) has improved crushing efficiency and material use without compromising the drainage characteristics of the material.

Before 1993, the existing concrete was broken, removed, and hauled to sites near the project, and then crushed, graded, and hauled back to the grade for placement. In 1993 on an I–80 inlay project in central Iowa, the Iowa DOT allowed ICPA contractor Manatt's Inc. to introduce the paradigm system. The innovative recycling system integrated a mobile train of on-grade equipment for breaking, removing, crushing, and placing of the recycled

material. The paradigm reduces the cost of site transportation and processing and eliminates potential safety hazards inherent to off-site hauling. Typical problems of trench construction were also reduced when the recycled material was replaced immediately on the subgrade behind the crushing train (*9*).

Iowa has maintained a role of national leadership in developing concrete solutions for pavement rehabilitation. Concrete overlays are now widely accepted statewide as a rehabilitation alternative. Although Iowa built its first bonded overlay on U.S. 34 in Des Moines County in 1955 (*10*), the modern development of bonded overlay technology began with projects constructed in 1976 on a state highway and two city streets in Waterloo. Today, more than 104.65 km (65 mi) of bonded concrete overlay have been constructed in Iowa on Interstate and primary highways, county roads, city streets, and airport runways and taxiways (*11*). These projects have provided opportunities for research and development in the use of grout for bonding, steel and polypropylene fibers, crack replication, and crack reinforcement.

In 1994, bonded overlays with Fast Track concrete paving were further refined when the Iowa DOT and ICPA contractor Cedar Valley Corporation rehabilitated an existing concrete pavement on Iowa Highway 3 in north central Iowa. Special conditions of this project required traffic to be maintained during the paving operation and returned to all lanes at night. This necessitated half-width paving with a concrete mix that provided center point flexural strength of 2,411.50 kPa (350 psi) in six hr or less. Research on the project includes maturity and pulse velocity testing, bond and temperature relationships, and evaluation of bond when grout is or is not required.

Unbonded overlays soon followed the development of bonded overlays. Experience with stress relief and bond breaker courses constructed with sand seals, slurry seals, and thin asphalt overlays now allows the engineer to design for the condition of the existing roadway. Design guidelines for joints have also been developed from experience, and continued evaluation considers varying thickness designs for performance. Working together, Iowa contractors and contracting authorities have refined unbonded overlay technology and rehabilitated 276.92 km (172 mi) of county roads and airport runways and taxiways (*12*).

Developed as a concrete solution to the ever increasing and recurrent costs of maintaining existing asphalt county roads, whitetopping has become an excellent method for rehabilitating more than 508.76 km (316 mi) of Iowa's county roads and airport runways and taxiways (*13*). The industry and agencies have developed standards for preparing the existing asphalt surface, jointing, and thickness design. An ultra-thin whitetopping research project in Louisville, Kentucky, has confirmed that 5.08-cm (2-in.) and 7.65-cm (3-in.) overlays will carry a significant number of axle loads (*14*). In addition, an Iowa research project in Dallas County suggests that there may be a structural composite action in whitetopping that would support performance of previously unheard of ultra-thin designs (*15*).

Iowa DOT, FHWA, and concrete paving industry worked together in 1994 to design and construct an 11.27-km (7-mi) long paving project that will provide the opportunity to evaluate thin concrete overlays on asphalt. The project is funded in part by moneys allocated in the Intermodal Surface Transportation Efficiency Act of 1992 (Section 6005). Plans called for 65 test sections that consider alternative methods for preparing an existing asphalt surface, using a combination of various concrete thicknesses, plain and fiber reinforced concrete, varying joint spacings, and a typical asphalt overlay.

In response to Iowa's need to complete certain reconstruction or rehabilitation projects in a timely manner while minimizing traffic interruptions, the industry and agencies have worked together since 1986 to develop Fast Track concrete paving. The first major Fast Track project was a bonded overlay and widening project constructed on U.S. 71 in Buena Vista County in 1986 (*16*). In 1988, a major urban highway in Cedar Rapids, Iowa, was constructed with Fast Track II mixes that included a 6-hr concrete maturity for intersections constructed at night and restored to service by 6:00 a.m. (*17*). More than 35 Fast Track projects have been constructed in the state.

Concrete mixes are now designed to meet the demands of the owner or user. Projects, such as the previously mentioned Iowa Highway 3 bonded overlay, provide opportunities to cooperatively evaluate design, materials, and construction techniques that will improve this popular rehabilitation technique.

After considerable discussion between the industry and contracting agencies, Iowa authorities began to offer a smoothness incentive by specification in 1990. Recently, the threshold for incentive was revised from 30.48 cm/1.61 km (12 in./mi) to 17.78 cm/1.61 km (7 in./mi) on the California profilograph (*18*). This change confirms that, despite the contracting industry's initial resistance to a smoothness requirement, the quality of Iowa concrete pavements has improved significantly since the specification's implementation. Incentives provide an opportunity for the better contractors to benefit from their expertise and encourage average contractors to improve their operations to remain competitive. The benefit for the contracting authority is estimated to outweigh the associated cost of incentives.

In 1988, Iowa DOT began to offer incentive payments for pavements constructed in excess of the design thickness, recognizing that thicker concrete enhances expected long-term pavement performance. Before that time, contractors were paid the contract price for design thickness and penalized for short cores. The current statistically based specification rewards the contractor for thickness and uniformity, allowing a maximum achievable incentive at 105 percent of the contract price. Positive response from the contractors indicates that incentives encourage construction of better quality pavement.

SUSTAINING THE IOWA PARTNERSHIP

All good partnerships need to be revitalized periodically with a renewed focus. In 1991, at ICPA's annual business meeting, the Iowa DOT Highway Division Director and Chief Engineer challenged Iowa's concrete paving industry to reach for a higher level of concrete pavement quality. Although the Iowa partnership continues to work, industry may have become complacent in pursuit of old objectives that were not applicable to new demands from the traveling public (the highway user).

In October 1992, ICPA and Iowa DOT entered into a new partnership for Continuing Quality Improvement (CQI). A Quality Advisory Committee was established to (a) identify issues of concern relevant to pavement quality and performance, (b) appoint working groups to study the issues and offer recommendations, and (c) direct the implementation of quality enhancements. In the tradition of quality management, the advisory committee was formed from the owner and top-management levels of the agency and industry. Three contractor and owners; the ICPA Executive Vice President; the Iowa DOT Construction, Materials, and Design

Engineers; and the Deputy Division Administrator for FHWA serve on the advisory committee.

Paramount to the activity of the advisory committee was an immediate understanding that recommendations from the committee would be brought to the appropriate Iowa DOT authorities and the contracting industry for consideration of action.

Among the early objectives established was an intent to consider pavement performance characteristics and the impact that design, specifications, and construction techniques have on quality of the constructed pavement. Four task forces were appointed to address specific quality concerns. Members of the task forces were selected from a broad cross section of contractor and agency personnel at management and field levels of administration, design, materials, and construction. People offering the highest expertise in each subject area were chosen to serve, including experts from other parts of the country. The four task forces have focused on pavement smoothness, paver operations, quality of materials, and concrete mixes. The advisory committee outlined specific objectives for each task force.

The Pavement Smoothness Task Force quickly acknowledged that pavement smoothness was important to pavement performance and the public's perception of pavement quality. In 1994, a revised statistical smoothness specification was implemented for all applicable projects. This specification will be reviewed in the future to evaluate its impact on contractor incentive achievement, performance-related quality, and perceived quality for rural and urban pavements.

One recommendation from the task force has resulted in the revision of a road standard to allow a day's work joint at any location in a pavement panel as long as it is no closer than 1.52 m (5 ft) from a proposed contraction or doweled contraction joint. Another recommendation extends the pavement subbase 1.91 m (3 ft) beyond the edge of pavement to enhance pavement constructibility.

On the basis of discussions of the task force, contracting authorities are asked to set 7.62-m (25-ft) hubs for grade control and contractors are asked to set 4.37-m (12.5-ft) stakes when the rate of change of curve exceeds 2 percent. Contractors also reduce profilograph traces with 0.51-cm (0.2-in.) and 0.0-cm (0-in.) blanking band to evaluate correlation to perceived riding quality. In addition, the ride-related effects of cutting or not cutting wire ties on contraction/dowel (CD) baskets are being reviewed.

Finally, the Pavement Smoothness Task Force supported the construction of a 1993 Iowa pavement research test to evaluate how texture spacing, depth, and direction affect smoothness, skid resistance, and noise in and out of the vehicle.

The Paver Operations Task Force has studied edge slump control, accurate tie bar placement, and consistent and proper concrete consolidation through vibration. The active involvement of several equipment manufacturing representatives and field supervisors familiar with equipment operation was important to the success of the group.

The task force concluded that many edge slump control problems are related to poor communication at the field level. No one told the builder and the inspector why edge control was important. A similar lack of communication was found to be the primary cause for misplaced tie bars. These concerns were referred to the advisory committee for discussion at the annual field training seminar. It is encouraging that, after communicating with the field personnel, the incidence of misplaced tie bars was isolated to two projects in 1993, down from seven in 1992.

Excessive and inconsistent concrete consolidation may have contributed to premature pavement deterioration on isolated projects constructed in Iowa during the past 10 years. Therefore, the Paver Operations Task Force studied the lessons of vibrator frequency, vibrator placement, and mix workability. Guidelines have been developed for vibration and are being revised as more is learned about the effect of vibration on consolidation in slipform paving operations. Communications and transfer of responsibility at the field level should be improved to ensure proper consolidation. The task force has therefore developed field checklists that consistently remind the equipment operators and field management personnel of their obligation to build a high-quality pavement.

One of the primary issues supporting a new initiative for continuing quality improvement was a mutual concern about a recent concrete paving project that exhibited early deterioration. Some type of expansive failure, not unlike alkali silica reaction (ASR), has occurred on a limited number of projects in Iowa. The industry and Iowa DOT considered it essential to identify the cause and act to prevent future occurrences. It was thus quickly agreed that a Materials Quality Task Force would be appointed to review investigations previously conducted by Iowa DOT and further consider issues relative to quality of material and pavement performance.

With information gained from two outside investigations and further in-house research, Iowa DOT concluded that the root cause of the unusual deterioration was not ASR. Additional study is in progress to consider delayed ettringite crystalline growth in the concrete and the integrity of the concrete at time of construction.

As the research continues, the task force has concurred with the Iowa DOT actions that set limits for combined alkali of cementitious material, require use of Type II cement, and direct closer monitoring of air content after placing and finishing. The Materials Quality Task Force is also working with the Concrete Mix Task Force to explore relationships of concrete workability, consolidation, and durability.

The Quality Advisory Committee appointed a Concrete Mix Task Force to study whether the standard Iowa recipe mixes provide an optimum mix for strength, performance, and economy. The task force was directed to explore alternative approaches to mix design. The task force has considered how to improve the quality of mixes economically, discussed the characteristics that truly measure concrete quality, and studied optimization of mixes by using combined aggregate gradations (Shilstone and SHRP Packing Diagram methods). The task force is also involved in projects that will field test the effects of various aggregate gradations; cement contents; and their combined impact on concrete strength, durability, and workability.

The Concrete Mix Task Force has begun exploring parameters for the eventual consideration of a performance-related specification (PRS) for concrete and concrete pavements. This objective responds to a directive from the Quality Advisory Committee to begin transition toward PRS with a goal to be on line in 3 years.

Throughout the CQI endeavor, it has been apparent that communication from top management and engineering to the field needs to be improved to enhance quality of the constructed project. Working with the Quality Advisory Committee, the four task forces have helped create an agenda of quality issues that was discussed at an annual construction season startup seminar for field personnel. Learning from the success of a seminar on joints and joint sealing offered under the cosponsorship of Iowa DOT and ICPA in April 1992, additional seminars addressing concrete pavement quality were offered in 1993 and 1994. Attendance has exceeded 150 at all

meetings, and the support from agencies and contractors has maintained a balance for useful interaction. The seminars will likely be continued.

In 1995, the Quality Advisory Committee will consider interactive cable television as a seminar delivery system, maximizing attendance and minimizing cost.

FUTURE OBJECTIVES

In October 1993, the Quality Advisory Committee renewed its commitment to the quality initiative by participating in a 1-day field tour of Iowa concrete paving projects, new and old. The tour included representatives from the industry and agency and a staff engineer from the American Concrete Pavement Association. The opportunity to share ideas and rekindle a common interest is important to CQJ initiative. An annual event of this nature is anticipated.

Following that field tour, a half-day meeting was held to reflect on the tour and establish direction for the coming year. The challenge to consider and move toward a PRS was a result of that meeting. Over the winter, two meetings were held to focus specifically on PRS issues. FHWA's Office of Technology Applications assisted in this orientation, and the Quality Advisory Committee has now begun to assign tasks relevant to PRS to new working groups. The first PRS group commissioned is a Non-Destructive Testing Task Force.

Another new task force has been assigned to consider constructibility issues relative to urban pavements. The group convened in fall 1994 to focus on specific construction projects.

In other meetings during 1994, the Quality Advisory Committee evaluated the progress and objectives of the four original task force groups. All groups will continue to pursue objectives with the exception of the Paver Operations Task Force, which has completed its assigned tasks. It is not the intent that these groups continue to work for extended terms. By limiting the tasks, it is hoped that the momentum of the quality initiative may be enhanced. This also allows participation by a broad cross section of the combined industry. County engineers, city engineers, and consultants will soon be included on the task forces to ensure that all levels of the governmental and engineering communities are included in the quest for quality improvement.

CONCLUSIONS

Iowa's partnership between contracting agencies and the concrete paving industry is working for continuing quality improvement of pavement design and construction. The cooperative relationship has enabled a strong focus for quality enhancement and expanding technology. The Iowa experience has established improved pavement designs; encouraged development of new approaches to recycling, reconstruction, and resurfacing; initiated development of Fast Track paving, and has confirmed agency and industry commitment to the development of a new generation of performance-related specifications. By using incentives, the PRS will elevate the quality of concrete pavements without detriment to the competitive bid process.

The Iowa initiative for continuing quality improvement has been judged beneficial to the contracting agency and the concrete paving industry. More than 60 individuals representing all facets of the combined industry now meet regularly to work for quality and a more permanent pavement. State and local contracting authorities and the concrete paving industry are committed to the success of the cooperative partnership in Iowa and recommend a similar program to any other contracting agency or industry truly interested in quality improvement of design construction and concrete pavement performance.

REFERENCES

1. Park, R. *Partnering on Construction Projects.* Presented to the Iowa Department of Transportation, Nov. 1992.
2. Tarricone, P. Howdy, Partner. *Civil Engineering Magazine*, March 1992.
3. Given, R. H. *A Former Highway Director's View of Industry and Government Working Together Toward Innovative Technology.* undated.
4. *Iowa's Miracle Machine.* Video Tape, Iowa Department of Transportation, *undated.*
5. *Standard Road Plans.* Iowa Department of Transportation, undated.
6. Bergren, J. V., and R. A. Britson. *Portland Cement Concrete Utilization Recycled Pavement.* Iowa Department of Transportation Office of Materials, undated.
7. Britson, R. A., and G. Calvert. *Recycling of Portland Cement Concrete Roads in Iowa.* Iowa Department of Transportation Office of Materials, undated.
8. *Recycling PCC Pavements, Green County, Iowa.* Iowa Concrete Paving Association, Sept. 1987.
9. *History of Interstate Paving in Iowa, Manatt's Paradigm.* Iowa Concrete Paving Association, 1993.
10. Hutchinson, R. L. *Resurfacing with Portland Cement Concrete.* National Cooperative Highway Research Program 99, Dec. 1982.
11. *Iowa's Bonded PCC Overlays.* Iowa Concrete Paving Association, Aug. 1992.
12. *Iowa's Unbonded PCC Overlays.* Iowa Concrete Paving Association, April 1993.
13. *Iowa's PCC Resurfacing Over Existing Asphalt.* Iowa Concrete Paving Association, Nov. 1993.
14. Risser, Jr., R. J., S. P. LaHue, G. F. Voigt, and J. W. Mack. *Ultra-Thin Concrete Overlays on Existing Asphalt Pavement.* Presented at 5th International Conference on Concrete Pavement Design and Rehabilitation, Purdue University, Ind., April 1993.
15. Grove, J. D., G. K. Harris, and B. J. Skinner. Bond Contribution to Whitetopping Performance on Low-Volume Roads. In *Transportation Research Record 1382*, TRB, National Research Council, Washington, D.C., 1993.
16. Lane, Jr., O. J. *Thin-Bonded Concrete Overlay With Fast Track Concrete.* Iowa Department of Transportation Office of Materials, July 1987.
17. Grove, J. D., K. B. Jones, K.S. Bharil, A. Abdulshafi, and W. Calderwood. Fast Track and Fast Track II, Cedar Rapids, Iowa. In *Transportation Research Record 1282*, TRB, National Research Council, Washington, D.C., 1990.
18. *Standard and General Supplemental Specifications, 1992 Series.* Iowa Department of Transportation, *undated.*

Publication of this paper sponsored by Committee on Portland Cement Concrete Pavement Construction.

Impact of Open-Graded Drainage Layers on the Construction of Concrete Pavements in Illinois

CHRISTINE M. REED

The first portland cement concrete pavement test section constructed by the Illinois Department of Transportation, which included an open-graded drainage layer, was built in 1989. Since the construction of that project, over 30 centerline km (20 centerline mi) of concrete pavements have been built using an open-graded drainage layer. Although the benefits of using open-graded drainage layers to improve concrete pavement performance are widely accepted, the practical impact of the design details on the constructibility of concrete pavements requires additional attention. Examples of problems encountered during the construction of concrete pavements with open-graded drainage layers include placing the open-graded drainage layer, anchoring dowel baskets to the open-graded drainage layer, obtaining a pavement with adequate ride characteristics, and using the open-graded drainage layer to support paving operations. From the experience acquired while constructing several pavements with open-graded drainage layers in Illinois, it is clear that concrete pavements with open-graded drainage layers can be constructed to meet today's high construction standards.

The concept of providing pavements with proper drainage has received a lot of attention in recent years, but this is not a new concept. McAdam, the grandfather of modern highway engineering, understood the importance of providing pavements with proper drainage. In 1820, he stated, "If water passes through a road and fills the native soil, the road, whatever may be its thickness, loses support and goes to pieces" (*1*). Today, 175 years later, drainage is still one of the most important elements to be considered when designing a pavement cross section.

Lately, positive drainage has become a buzz word in the highway engineering community. Typically, positive drainage includes an edgedrain network, an open-graded drainage layer (OGDL), and a separation layer, which prevents the subgrade from infiltrating the drainage layer. In the early 1970s, the Illinois Department of Transportation (IDOT) first used edgedrains in pavements built to Interstate standards, but it was not until the mid 1980s that IDOT initiated studies concerning the use of OGDL with highways (*2,3*). Since the start of these studies, over 30 centerline km (20 centerline mi) of new portland cement concrete (PCC) pavements have been constructed with drainage layers. Over the past 7 years, it has become evident that the construction of PCC pavements with OGDL is different from standard construction techniques. This report details IDOT experience in constructing PCC pavements with OGDL.

Illinois Department of Transportation, Bureau of Materials and Physical Research, 126 East Ash Street, Springfield, Ill. 62704-4766.

PROJECT DESCRIPTIONS

1989 Test Section

The first PCC pavement test section with an OGDL in Illinois was built in 1989 and is just north of Bloomington on I–39. The exact location of this project is shown in Figure 1. The pavement cross section for this project consists of a 275-mm (10.75-in.) hinge jointed PCC pavement. The hinge joint design used doweled and tied joints to construct longer effective pavement slabs with controlled panel cracks. A detail of the hinge joint panel design is included in Figure 2.

The hinge joint pavement was placed on a 100-mm (4-in.) lean concrete subbase. The subgrade was lime modified to a depth of 400 mm (16 in.), and 300-mm (12-in.) geocomposite edgedrains were placed at the shoulder/mainline joint with outlets every 150 m (500 ft). A 150-mm (6-in.) portland cement stabilized OGDL was substituted for the lean concrete subbase for 365 m (1,200 ft) on this project, in the northbound lanes only. A diagram of the complete pavement cross section is included in Figure 3.

The OGDL mix consisted of crushed limestone aggregate, which met the IDOT CA–7 gradation requirements. The IDOT CA–7 gradation is similar to an AASHTO No. 57 gradation. Both gradations are listed in Table 1. The OGDL mix was prepared in a central concrete mix plant and consisted of 167 kg/m^3 (282 lb/yd^3) of portland cement with a water-to-cement ratio of 0.37.

1990 Test Sections

In 1990, the first continuously reinforced concrete (CRC) pavement with OGDL test sections was constructed in Illinois. These test sections are located south of LaSalle/Peru on I–39, as shown in Figure 1. The typical pavement cross section consisted of a 250-mm (10-in.) CRC pavement, which was placed on a 100-mm (4-in.) lean concrete subbase. The subgrade was lime modified 400 mm (16 in.) deep. The 100-mm (4-in.) plastic pipe edgedrains were placed in a sand trench at the shoulder/mainline joint, with outlets every 150 m (500 ft).

The project contains six 300-m (1,000-ft) long test sections. The test sections include three different cross sections with an asphalt cement stabilized OGDL in the northbound lanes and the same three cross sections with a portland cement stabilized OGDL in the southbound lanes. The three cross sections include a 100-mm (4-in.) OGDL placed directly on the lime modified subgrade, a 125-mm (5-in.) OGDL placed directly on the lime modified subgrade, and a 100-mm (4-in.) OGDL placed on a 75-mm (3-in) dense graded

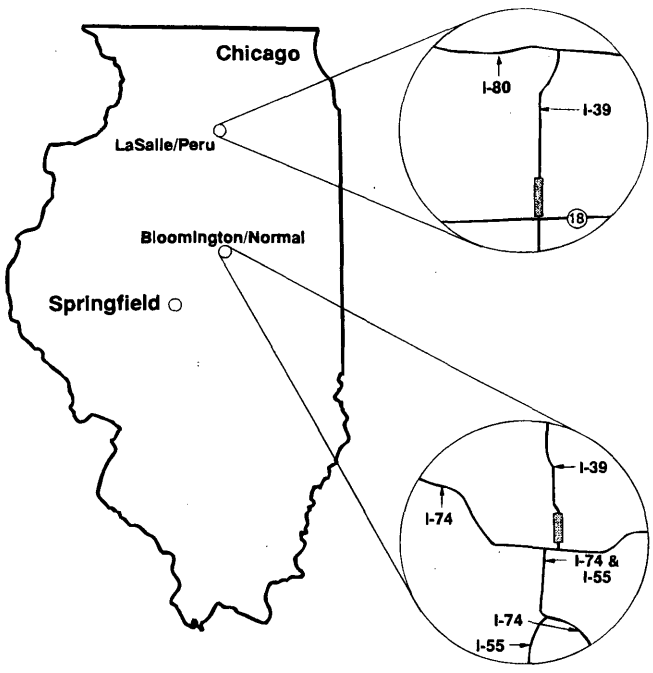

FIGURE 1 Location map of test sections.

aggregate base course, which was placed on the lime modified subgrade. The layout of the test sections is included in Figure 4.

In each test section, the longitudinal edgedrains were placed 1 ft in from the outside edge of the shoulder, because the drainage layer was extended out underneath the shoulders. The top of the edge-drain trench was covered with a geotextile fabric to prevent the sand from infiltrating the drainage layer. The typical cross section for this project is included in Figure 5.

The mix design for the portland cement stabilized OGDL was the same as the mix design used in the 1989 test section. The asphalt cement stabilized OGDL mix design consisted of 2 to 3 percent AC–20 and a crushed limestone aggregate that met the CA–7 gradation requirements. The dense graded aggregate met the IDOT CA–6 gradation requirements listed in Table 1.

1992 Demonstration Project

With the experience acquired while designing and constructing the 1989 and 1990 test sections, the scope of IDOT research was expanded to include using an OGDL on a project 14.5 km (9 mi) long. The location of this project, as shown on Figure 6, is near El Paso on I–39. The typical cross section for this project includes a 250-mm (10-in.) CRC pavement, a 100-mm (4-in.) portland cement stabilized OGDL, a 400-mm (16-in.) lime modified subgrade, and 100-mm (4-in.) pipe edgedrains, which were placed in aggregate backfilled, fabric-wrapped trenches 0.3 m (1 ft) in from the outside edge of the shoulder. A dense graded aggregate separation layer was placed between the OGDL and the lime modified subgrade on the southern portion of the project. On the northern end of the project, the OGDL was placed directly on the lime modified subgrade. A diagram of the typical cross section is included in Figure 7.

The mix design for the portland cement stabilized OGDL consisted of crushed limestone aggregate that met the requirements for the CA–11 gradation (similar to the AASHTO No. 67 gradation), as shown in Table 1 and 142 kg/m^3 (240 lb/yd^3) portland cement. The water-to-cement ratio was 0.50.

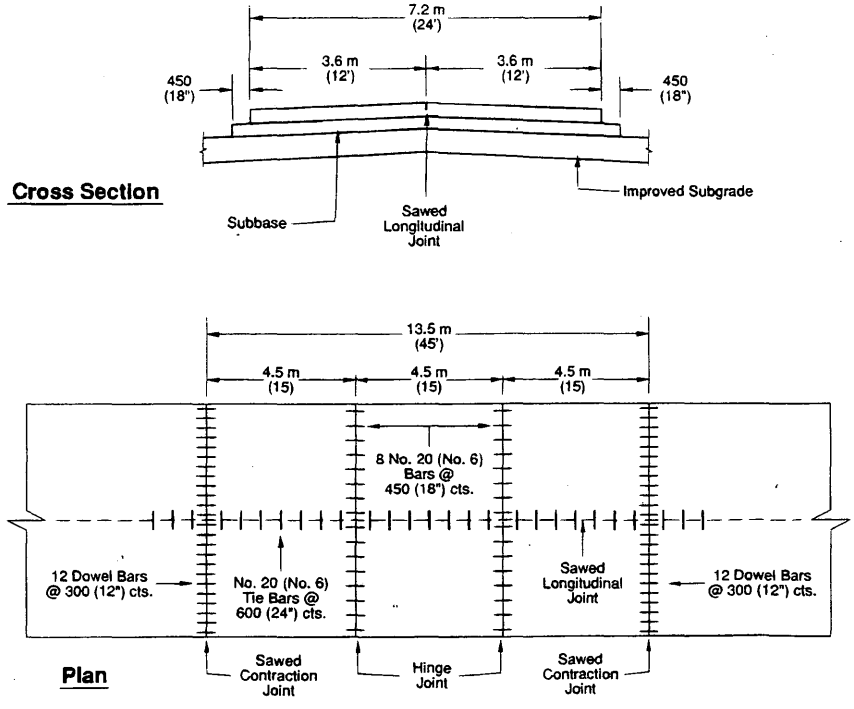

FIGURE 2 Hinge jointed pavement standard.

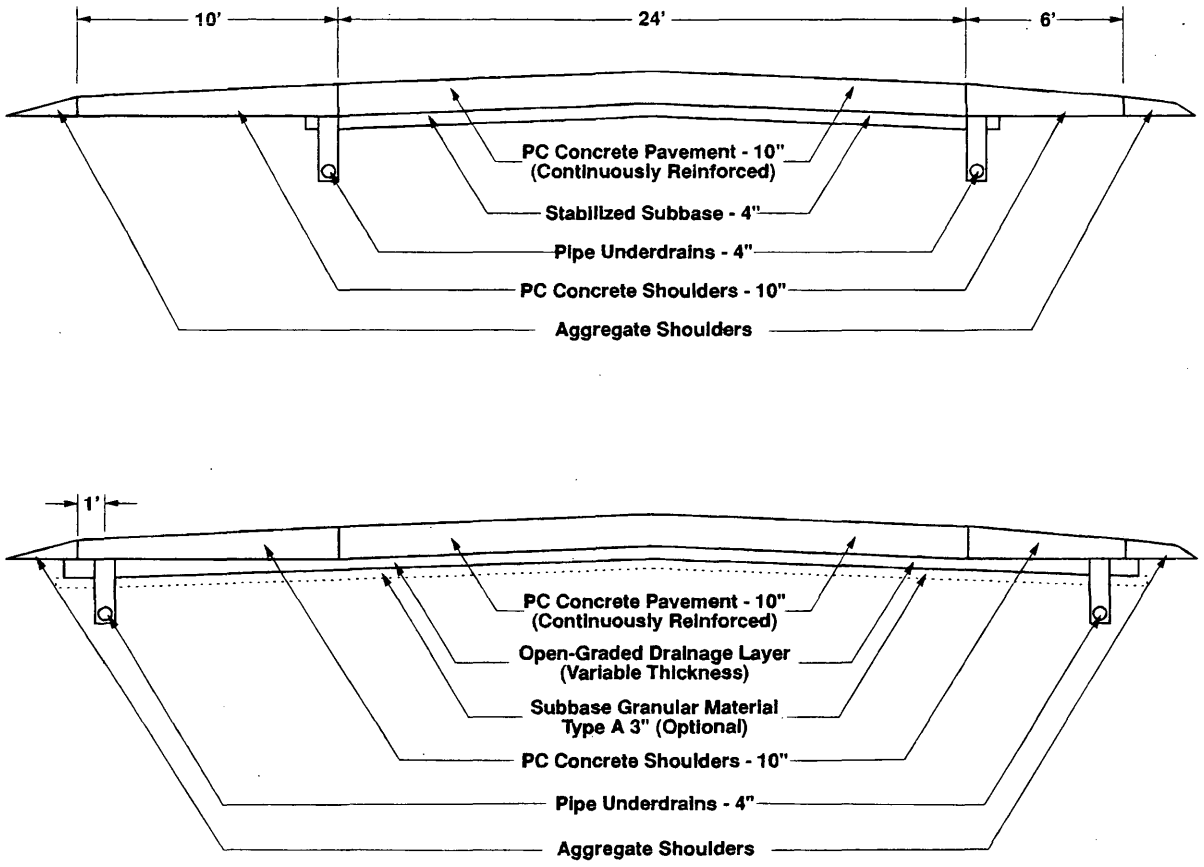

FIGURE 3 1989 test section cross section.

TABLE 1 Aggregate Gradations

	Sieve Size (Percent Passing)								
GRADATION	37.5 mm (1.5 in)	25 mm (1 in)	19 mm (0.75 in)	12.5 mm (0.5 in)	9.5 mm (0.38 in)	4.75 mm (No. 4)	2.36 mm (No. 8)	1.18 mm (No. 16)	75 m (No. 200)
Dense-Graded Aggregate									
CA-6	100	90-100		60-90		30-56		10-40	4-12
CA-10		100	90-100	65-95		40-60		15-45	5-13
Open-Graded Aggregate									
CA-7	100	90-100		30-60		0-10			
AAHSTO No. 57	100	95-100		25-60		0-10	0-5		
CA-11		100	84-100	30-60		0-12		0-6	
AASHTO No. 67		100	90-100		20-55	0-10	0-5		

Reconstruction of I–80

In 1993, IDOT reconstructed a 9.6-km (6-mi) segment of I–80 near Morris, as shown in Figure 6. The typical cross section for this project included a 295-mm (11.5-in.) CRC pavement, a 100-mm (4-in.) portland cement stabilized OGDL, and a 305-mm (12-in.) lime modified subgrade. The 100-mm (4-in.) pipe edgedrains were placed 0.3-m (1-ft) in from the outside shoulder in aggregate backfilled, fabric-wrapped trenches. The typical cross section for this project is the same as the typical cross section for the 1992 demonstration project.

The mix design for the OGDL consisted of recycled concrete crushed to meet the CA–7 aggregate gradation requirements. The portland cement content ranged between 118 and 142 km/m^3 (200 and 240 lb/yd^3), with a water-to-cement ratio of 0.50. A water-reducing additive was added to the mix to ensure that the aggregate was completely coated.

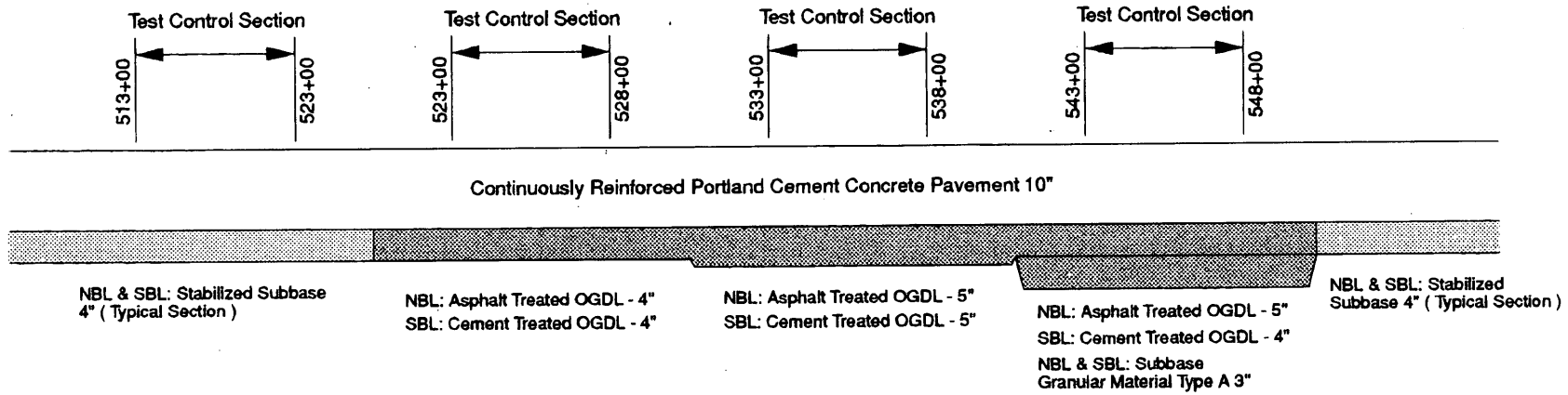

FIGURE 4 1990 test sections layout.

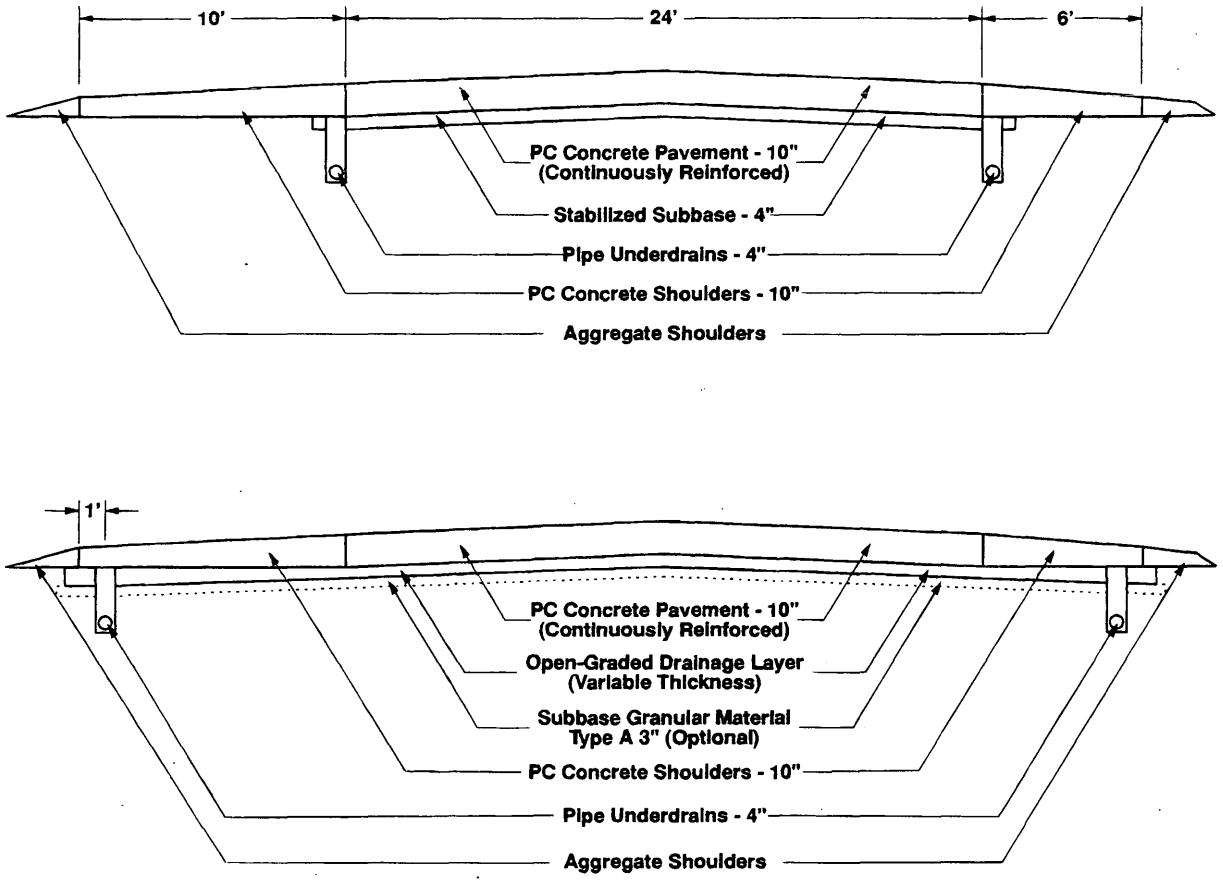

FIGURE 5 1990 test section cross section.

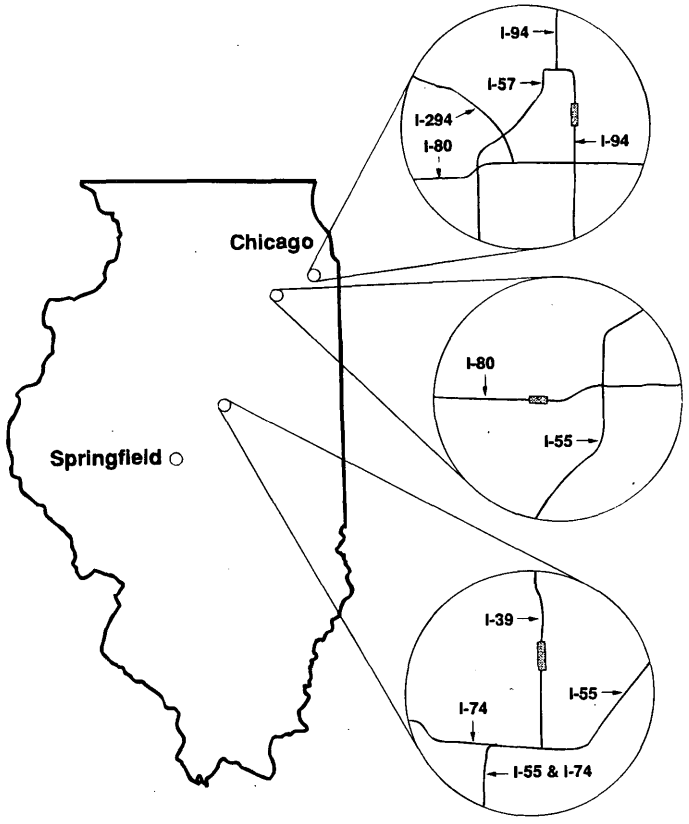

FIGURE 6 Location map of projects.

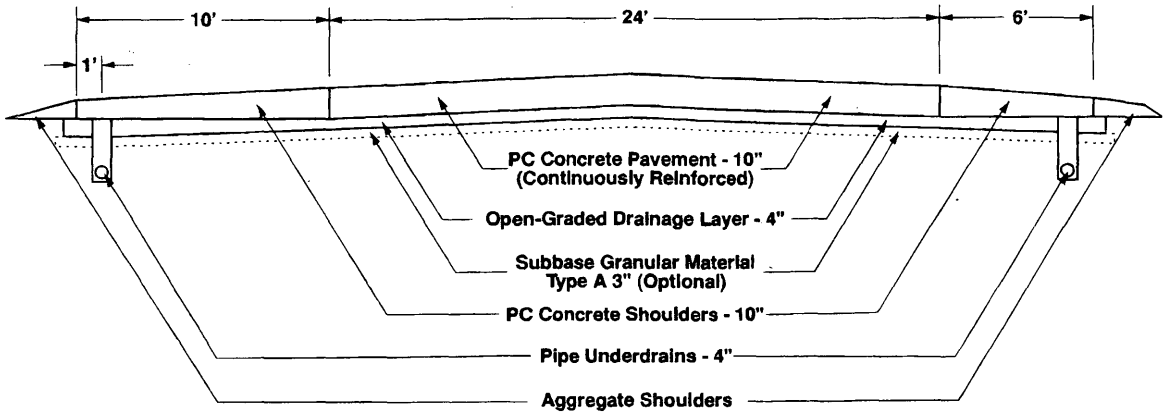

FIGURE 7 1992 demonstration project cross section.

Reconstruction of Calumet Expressway

In 1993, IDOT also reconstructed a segment of the Calumet Expressway in Chicago. The location of this project is shown in Figure 6. The typical cross section for this project included a 320-mm (12.5-in.) CRC pavement, a 100-mm (4-in.) asphalt cement stabilized OGDL, a 305-mm (12-in.) aggregate subbase, and a porous granular embankment subgrade, as shown in Figure 8. The 100-mm (4-in.) pipe edgedrains were placed 460 mm (18 in.) from the shoulder/mainline joint in sand-backfilled trenches, which were wrapped in a geotextile fabric to prevent contamination.

The asphalt cement stabilized OGDL mix consisted of 2.2 percent AC–10 and a crushed limestone aggregate that met the gradation specification for CA–11. The mix also included 0.5 percent anti-strip additive.

CONSTRUCTION EXPERIENCE

OGDL Construction

Portland Cement Stabilized OGDL

Paving Operations During the construction of the 1989 and 1990 test sections, it became evident that a standard concrete paver could not place the harsh portland cement stabilized OGDL mix. The OGDL mix did not flow through the concrete paver, and a standard concrete paver did not have enough power to spread the mix. Because of the slow advancement of the paver, the OGDL started to achieve an initial set before passing through the paver. In these instances, the mix was spread with a backhoe and then placed with the concrete paver. On these first two projects, the pavers broke down many times, resulting in costly construction delays.

As a result of the placement problems encountered on the test sections, IDOT altered the mixture and construction requirements for portland cement stabilized OGDL. The portland cement content requirement was reduced from 167 kg/m^3 (280 lb/yd^3) to 118 to 167 kg/m^3 (200 to 280 lb/yd^3) of mix. The engineer would determine the exact amount of portland cement required to ensure all of the aggregate was coated. In addition, the water-to-cement ratio was increased from 0.37 to 0.50 to increase the workability of the mix. Finally, IDOT required a subgrade planer to place the mix based on the success the Wisconsin Department of Transportation (DOT) was having in placing OGDL to the specified tolerances with a subgrade planer.

These mixture and construction modifications were used for the first time on the construction of the 1992 demonstration project. The modifications had a positive effect on the placement of the drainage layers so that over 1.6 km (1 mi) of 8.2-m-wide (27-ft-wide) OGDL material could be placed in 1 day. A picture of the modified subgrade planer is included in Figure 9.

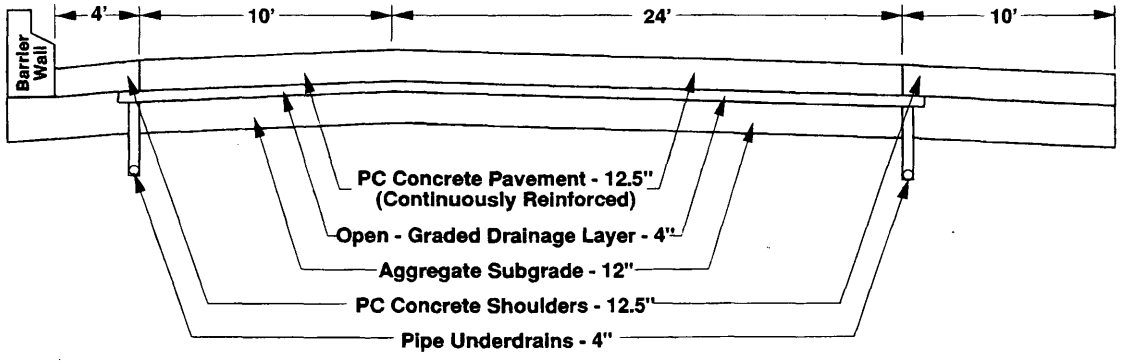

FIGURE 8 Calumet expressway cross section.

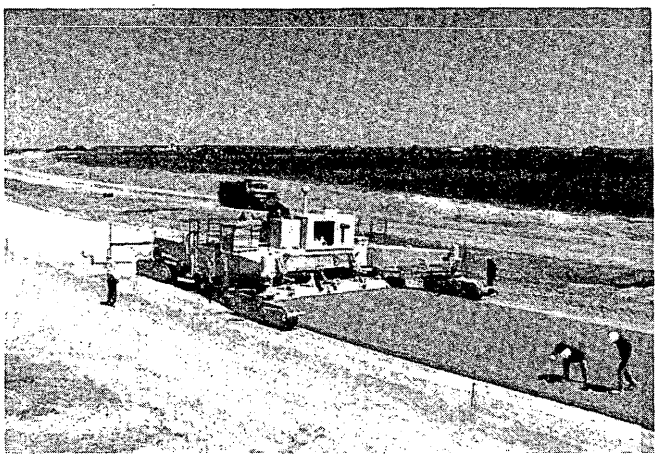

FIGURE 9 Modified CMI.

The changes made to the OGDL mix did not significantly decrease the overall strength of the OGDL. It is interesting that, during the placement of the OGDL on the 1993 reconstruction of I–80, the OGDL was exposed to a heavy rain hours after placement. The OGDL in this area was seen as strong as that which had already cured before the rain.

Compaction Techniques The 1989 and the 1990 test sections were compacted with tandem steel-wheeled rollers. Although the rollers were successful in providing satisfactory compaction of the OGDL material, the rolling operations often resulted in an uneven OGDL surface. The grade control for the PCC pavement is usually taken from the surface of the subbase material in Illinois. As a result, the uneven surface of the rolled OGDL resulted in an uneven pavement surface.

This problem could have been addressed by requiring the grade control for the PCC pavement to be taken off a stringline. This option would restrict the contractor's flexibility during the placement of the PCC pavement, however, which could result in higher PCC pavement costs. To find alternatives, IDOT reviewed the portland cement stabilized OGDL compaction techniques used by other states. Wisconsin DOT did not roll the portland cement stabilized OGDL to achieve compaction; instead, vibratory pans were attached to the subgrade planer to compact the OGDL material. IDOT tried this method on the construction of the 1992 demonstration project. Not only did this technique provide the necessary compaction of the OGDL, but it also provided a very smooth surface to use for grade control during the placement of the PCC pavement. The overall California profilograph rating for the pavement was 4.

Curing The 1989 test section was cured by spraying the portland cement stabilized OGDL with water and then covering it with polyethylene sheets. The OGDL placed on the 1990 test sections was cured with a water spray only. The curing on both projects was not started until late afternoon, long after the first OGDL material was placed. Because of the porous surface of the OGDL, the material that was placed in the morning had already achieved initial set. When the curing was completed, there was no distinguishable difference between the material cured immediately after placement and the material that had achieved initial set before curing.

At the time these observations were made, a paper was published noting that there was no definite benefit from curing an OGDL to achieve stability (*4*). This conclusion, along with IDOT observations, led to the decision not to cure the portland cement stabilized OGDL. The portland cement stabilized OGDL in the 1992 demonstration project and the 1993 I–80 reconstruction project were not cured, and the OGDL on these projects was stable enough to support paving operations without raveling.

Asphalt Cement Stabilized OGDL

Asphalt Cement Stabilized OGDL Mixtures The first time asphalt cement was used to stabilize an OGDL in Illinois was on the construction of the 1990 test section, in the northbound lanes of I–39. During the construction of this project, it was clear that mixing of the OGDL material in the asphalt plant was different from mixing hot mix asphalt concrete. The open nature of the aggregate gradation made it difficult to control the temperatures at the plant. Many of the batches of asphalt cement stabilized OGDL were not well-coated with asphalt cement, and many went to the construction site below the required temperatures.

To address this problem, IDOT reviewed the required mixing temperatures and placement temperatures of the asphalt cement stabilized OGDL. The minimum mixing temperature was 115°C (240°F) and was not lowered because a lower mixing temperature could lead to problems with the stability of the asphalt cement. The minimum placement temperature was lowered to 95°C (200°F) from 110°C (230°F). The OGDL material was open and cooled quickly. Therefore, to achieve a placement temperature of 110°C (230°F), the mixing temperature had to be higher than 115°C (240°F). By lowering the OGDL placement temperature to 95°C (200°F), the mixing temperature could be set to 115°C (240°F), which allowed more control of the mixing operations at the plant.

This new requirement was used on the reconstruction of the Calumet Expressway and resulted in a uniform OGDL mix, which guaranteed that the aggregate was completely coated.

Compaction Techniques The compaction of the asphalt cement stabilized OGDL was achieved by a tandem steel wheeled roller making two passes on the construction of the 1990 test sections. This technique was successful in compacting the OGDL mix but resulted in an uneven OGDL surface. The grade control for the PCC pavement on this project was taken from the surface of the OGDL, which subsequently led to an uneven pavement surface.

Due to the nature of the asphalt cement stabilized OGDL mix, it was clear that the asphalt cement stabilized OGDL could not be compacted with the same techniques as those successfully used on the construction of the portland cement stabilized OGDL on the 1992 demonstration project. Instead, the rolling temperatures for the OGDL were lowered and two rollers instead of one were required to achieve compaction. The first roller served as a breakdown roller and achieved the initial compaction of the OGDL. The second roller made two passes at a lower temperature to smooth the surface of the OGDL. This technique was used on the 1993 reconstruction of the Calumet Expressway and resulted in a smooth pavement surface.

Portland Cement Concrete Pavement Construction

Anchoring Dowel and Hinge Joint Baskets

Typically in Illinois, the dowel and hinge joint bars are set in baskets before paving the PCC pavement. During the construction of the 1989 test section at Bloomington, significant difficulty was encountered when tacking the dowel and hinge joint baskets to the OGDL. In Illinois nails are used to hold the dowel and hinge joint baskets in place. The same nails, however, could not be driven into the portland cement stabilized OGDL. This problem caused construction delays until a pneumatic nailer could be located to drive the nails into the OGDL.

In addition to the problems with driving the nails into the OGDL, the nails that were driven would often pull free from the OGDL. To solve this problem, longer nails were used to secure the dowel and hinge joint baskets.

Concrete Yield

When IDOT first considered using an OGDL on an entire PCC pavement project, there was concern that the porosity of the OGDL surface would drastically reduce the percent of concrete yield, even though research was published that indicated that an OGDL would not have a significant impact on the percentage of concrete yield (*5*). Concrete yield is calculated by subtracting the required quantity of concrete from the used quantity of concrete and dividing that number by the quantity of concrete required. The percentage of concrete yield is calculated by multiplying this value by 100 percent. Typically, on a concrete paving project, the concrete yield is expected to be around +10 percent or less. The additional quantity is due to a combination of concrete that is left in the bottom of the haul trucks, concrete that is added to ensure the required pavement thickness is achieved, concrete that is added to ensure the minimum paving width is achieved, and concrete left in the batching plant.

On the construction of the 14.5-km (9-mi) 1992 demonstration project on I–39, the average concrete yield was 7.1 percent with a standard deviation of 2.48 for 27 days of paving. The average concrete yield for the 1993 reconstruction of I–80 was 9.0 percent with a standard deviation of 4.18 for 31 days of paving. The average concrete yield percentages were weighted by the amount of concrete produced each day. From the information collected on these projects, it is clear that the OGDL has a minimal impact on the concrete yield percentages for projects of considerable length.

OGDL Stability

Before construction of the 1989 test section, there were concerns that the OGDL would not be stable enough to support a paving train. The first test section proved that a CA–7 aggregate gradation, in combination with 127 kg (280 lb) of portland cement and a water-to-cement ratio of 0.37, had the required strength to easily support paving operations.

On the 1992 demonstration project, the portland cement content was reduced to 142 kg/m^3 (240 lb/yd^3), the water-to-cement ratio was increased to 0.50, and the curing requirement was removed. These factors could have combined to result in a weaker OGDL, which might have been incapable of supporting paving operations. For the most part, this was not the case. In isolated instances, the dense graded aggregate base course became saturated and was undrained. The saturated dense-graded aggregate base course failed to provide adequate support to the OGDL during paving operations and resulted in the OGDL fracturing under paving operations. Typical pictures of this problem are included in Figures 10 and 11. This problem can be easily addressed by providing the dense-graded aggregate base course with proper drainage.

CONCLUSIONS

Over the past 7 years, IDOT has acquired extensive experience in constructing PCC pavements with OGDL. As with any new construction material, early attempts at placing an OGDL and the subsequent PCC pavement were successful on a limited basis only. Later attempts were successful as IDOT experience increased. Through the construction of over 30 centerline km (20 centerline mi) of PCC pavements with OGDL, the following items were learned:

- The portland cement stabilized OGDL mix is harsh and must be placed with a subgrade planer or like equipment with the ability to spread the harsh mix the width of the highway.
- The compaction technique used on the OGDL must be capable of providing a smooth surface to reduce the impact that the OGDL has on the overall ride quality of PCC pavement.
- It is not necessary to cure the portland cement stabilized OGDL either to achieve adequate support for paving operations or prevent the OGDL from experiencing problems from inadequate curing, such as raveling.
- Special attention must be directed toward the placement of dowel and hinge joint baskets on the OGDL. Standard construction techniques and materials will not secure the baskets to a portland cement stabilized OGDL.
- The OGDL does not have a large impact on the percentage of concrete pavement yield. The concrete yields on the two largest construction projects built to date were under +10 percent.
- The OGDL has sufficient stability to support paving operations. The only time the OGDL fractured under paving operations is when the dense-graded aggregate base course underneath the OGDL was saturated.

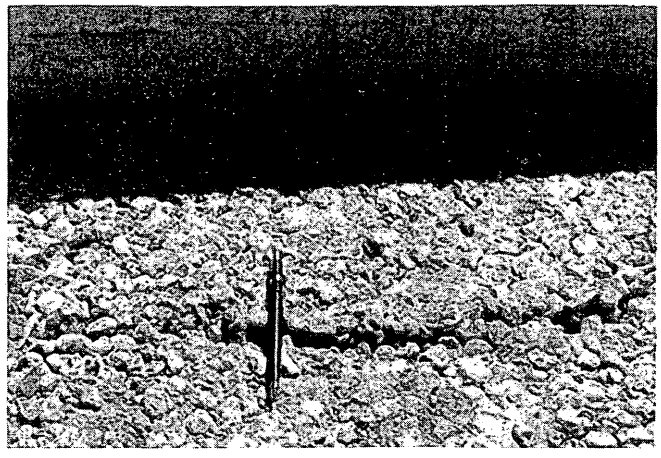

FIGURE 10 Broken OGDL.

FIGURE 11 Broken OGDL.

Experience proves that given proper attention to construction details, PCC pavements can be built to today's standards with an OGDL as part of a positive drainage system. At this time, the pavement sections discussed in this report are too young to provide sufficient data to discern differences in performance between the various OGDL mix designs, placement techniques, and compaction procedures. The impact of these variations on pavement performance will be studied as more information becomes available.

REFERENCES

1. McAdam, J. L. *Report to the London Board of Agriculture.* London, England, 1820.
2. Crovetti, J. A., and B. J. Dempsey. *Pavement Subbases.* Report UILU–ENG–91–2005. Department of Civil Engineering, University of Illinois, May 1992.
3. Reed, C. M. *Design and Construction of Open-Graded Base Courses.* Illinois Department of Transportation, Bureau of Materials and Physical Research, Springfield, Ill. June 1993.
4. Hall, M. *Cement Stabilized Open-Graded Base: Strength Testing and Field Performance Versus Cement Content.* Wisconsin Concrete Pavement Association, Nov. 1990.
5. Cedergren, H. R. *Drainage of Highway and Airfield Pavements.* John Wiley and Sons, Inc., New York, 1974.

Publication of this paper sponsored by Committee on Portland Cement Concrete Pavement Construction.

Concrete Runway Construction Lessons Learned

MICHAEL P. JONES AND FRANK V. HERMANN

The Navy recently administered the construction of a critical Air Force facility—the parallel runway at Clark Air Base in the Philippines. The Pacific Division of the Naval Facilities Engineering Command administered the design and construction of this new runway. The project required construction of a concrete runway 3,200 m (10,500 ft) long by 61 m (200 ft) wide with connecting taxiways and holding aprons, aids to navigation, lighting, storm water drainage, and other facilities. The pavement section included portland cement concrete varying in thickness from 254 mm (10 in.) to 356 mm (14 in.), a 152 mm (6 in.) central plant–mixed cement stabilized base, and a fill subgrade of predominately sandy soils. Features of the design and construction are identified and how these features relate to pavement quality is discussed.

The Navy recently administered construction of a critical Air Force facility; the parallel runway at Clark Air Base in the Philippines. The Pacific Division of the Naval Facilities Engineering Command administered the design and construction of this new runway. The design was prepared by the Honolulu office of the Ralph M. Parsons Co.

The initial construction contract was awarded to the joint venture of the George A. Fuller Co. and Capitol Industrial Construction Groups. A second contract for completion of the project, after default of the joint venture, was awarded to Sundt Corp. of Phoenix, Arizona. Sundt's paving subcontractor was the Coffman Corporation.

The project required construction of a concrete runway 3,200 m (10,500 ft) long by 61 m (200 ft) wide with connecting taxiways and holding aprons, aids to navigation, lighting, storm water drainage, and other facilities. The pavement section consisted of portland cement concrete varying in thickness from 254 mm (10 in.) to 356 mm (14.0 in.), a 152 mm (6 in.) thick central-plant–mixed cement stabilized base, and a fill subgrade of predominately sandy soils. Pavement design was based on Air Force Manual 88–6, Chapter 3 (*1*).

The runway pavement was constructed using a slip form paver 12.2 m (40 ft) wide. Joint spacing was 6.1 m by 6.1 m (20 ft by 20 ft). The longitudinal construction and contraction joints in the thicker central portion of the runway were provided with dowels for load transfer. Longitudinal construction joints in the outer sections were formed with keyways using a metal insert installed by the paving machine. The outermost longitudinal joint was a saw cut joint with deformed tie bars installed to tie the two slabs together. Transverse contraction joints were saw cut with no dowels and therefore relied on aggregate interlock for load transfer. The last three transverse joints at each end of the runway had dowels provided for load transfer.

M. P. Jones, Naval Facilities Engineering Service Center, Building 218, Washington Navy Yard, 901 M Street, S.E., Washington, D.C. 20374-5063. F.V. Hermann, 2333 Kapiolani Boulevard, Suite 2808, Honolulu, Hawaii 96826-4462.

The runway became operational in November 1990. When Mt. Pinatuba erupted nearby in June 1991 covering the entire Air Base with a layer of volcanic ash, the U.S. government closed and vacated the facility. Currently the Philippine government is looking into reopening the facility as an international airport.

LONGITUDINAL CONSTRUCTION JOINTS

Modern concrete paving practices generally result in high-quality finished work. Construction joints, whether constructed with side forms or slip forms, are inherently the weaker portion of the pavement. Variables affecting the concrete mix, including humidity, temperature, water and air content, cement content, and aggregate gradation, result in frequent change in concrete slump. Voids along the sides or excessive edge slump or mortar buildup may occur. Joint edges may be overworked or patched and may contain deficiencies, which can lead to early chipping and spalling, water ponding, and other distress.

On runways, longitudinal joints may have a negative impact on the ride quality and the life expectancy of a pavement. When the centerline joint is uneven, the ride quality of all aircraft is affected negatively. If the unevenness is severe, this rough ride may impose high loads on aircraft landing gear, resulting in a reduced aircraft life and magnified impact loads on the pavement. The next longitudinal construction joint on each side of the centerline may be located near the main gear of larger aircraft. When these joints are uneven, they may have negative impacts on both aircraft and pavement structural integrity.

Traditional pavement design shows the runway cross section with a pointed crown at the center (Figure 1). Most construction drawing also indicate that this crown should be at a longitudinal construction joint. Thus, this joint is subject to all the problems noted. To avoid problems with the quality of this centerline joint, the paving subcontractor for the Clark runway project used a large slip form paver to place a slab 12.2 m (40 ft) wide, centered on the centerline of the runway. The paver had a hinge system, which permitted the center to be constructed as a crown. The contractor also installed a double screed system on the paver, which resulted in a very smooth finished slab. This screed effectively rounded off the centerline "point." The longitudinal centerline joint was then saw cut (Figure 2).

Most aircraft using this runway had main landing gear close to the centerline. The gear rode on the smooth interior portion of the 12.2-m (40 ft) concrete pour. The result of having both the nose wheel and main gears riding on an interior portion of the slab was an extremely smooth aircraft ride. The finished runway received many favorable comments from pilots.

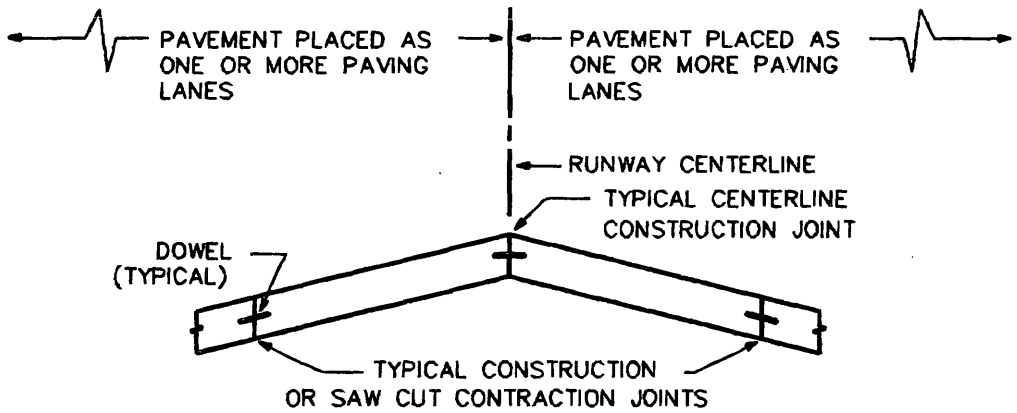

FIGURE 1 Typical runway centerline.

The first longitudinal construction joint was 6.1 m (20 ft) from the centerline of the runway. This joint is therefore close to the location of the heavy main gear on some large aircraft (B–747, KC–10, C–5). It was observed that this joint was fairly smooth, with some minor irregularities. However, when this joint conforms to FAA, military, or International Civil Aviation Organization criteria, it still may have vertical and horizontal deviations, which can induce roughness into the aircraft ride. Also, because the heavy gear of large aircraft are at or near the slab edge, any edge weakness may result in premature distress.

On this project, some of the longitudinal joints constructed under the initial joint venture contract failed to meet alignment and edge slump criteria. This occurred on paving lanes that were 6.1 m (20 ft) wide. Full-depth sawing and removal of the outer .3 m (1 ft) of the centerline paving lane were proposed. This proposal was made to preserve as much of the concrete as possible, while eliminating that section of concrete that contained the most serious deficiencies. Because many other problems existed during the initial paving on this project and the initial contractor was to be terminated, the proposal to remove the outer foot was rejected. Eventually all concrete placed by the original contractor was removed and replaced.

Although saw cutting and removal of a portion of the slab were rejected in this specific case, the concerns for longitudinal joint quality are still valid. It is believed that full depth removal of the outer 0.3 m. (1 ft) of a paving lane is a viable option in meeting the edge slump and smoothness requirements of most paving specifications. The benefits of removal include the following:

- The construction joint would be smooth both longitudinally and vertically because it is an interior portion of the slab.
- The edge of the adjacent pavement slab should also be stronger and smoother at the joint because it will not pick up any unevenness from the first slab.
- The joint quality should be better because the concrete of the first slab should not have any internal weakness due to honeycomb, slumping, or excessive mortar buildup.

It is also believed that paving a lane 12.2 m (40 ft) wide, when combined with saw cutting and removal of the outer .3 m (1 ft) of the lane (Figure 3), can provide a smooth and high-quality runway section. If required for load transfer, dowels can be drilled and grouted into hardened concrete instead of set into plastic concrete.

A question arises about how the missing 0.6 m (2 ft) of the runway is to be made up. Depending on paver width, this might not be a problem, but if no other solution exists, a shoulder .3 m (1 ft) wider might be constructed. It should be noted that runways constructed to international standards of 45 m (147.6 ft) and 60 m

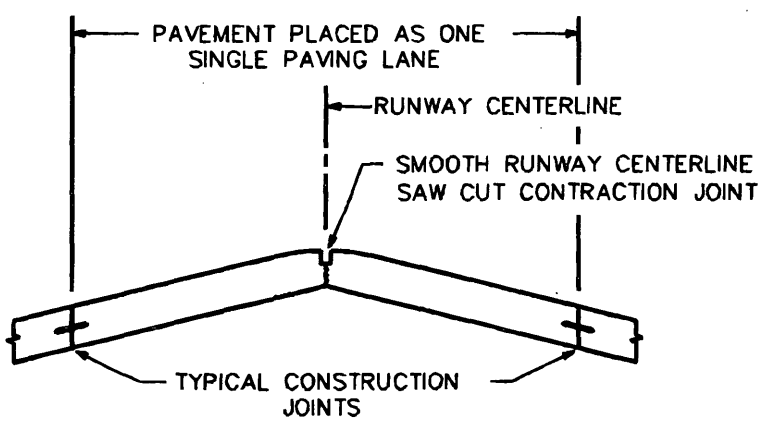

FIGURE 2 Smooth centerline joint constructed as internal saw cut contraction joint.

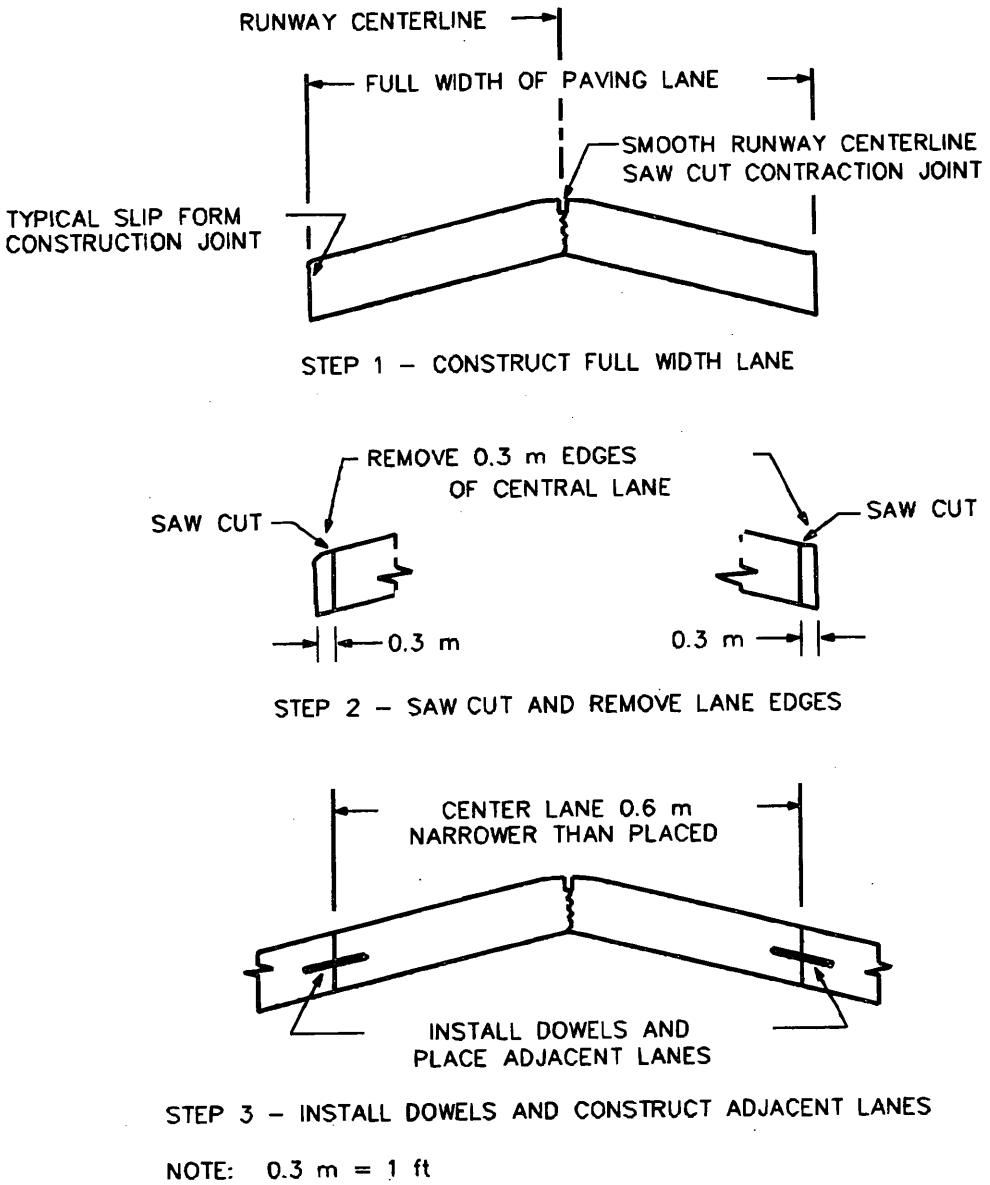

FIGURE 3 Removal of central lane edges.

(196.9 ft) are more than .6 and .9 m (2 and 3 ft) narrower than those designed in the United States. Perhaps no real problem exists.

STANDARDS FOR ACCEPTANCE OF LONGITUDINAL CONSTRUCTION JOINTS

Problems of longitudinal joints have been previously discussed. Current design standards treat all pavements and all joints alike. It is suggested that a high standard, which would allow only minor horizontal and vertical deviations, be applied to the central joints. These high standards should be strictly enforced. Cutting off the edges is a radical suggestion, treating the most critical joints near the center of the runway. Although more costly, it is a clear and enforceable means to ensure a quality joint.

The high cost of this type of joint construction could be partially offset by allowing larger tolerances for the longitudinal construction joints in the outer paving lanes. These outer joints do not have a major impact on the ride and durability of the runway. If transverse drainage is adequate at the joints, a greater degree of unevenness should be acceptable at no loss of serviceability. Sawing, grinding, or building up low spots should not be required, except in extreme cases.

TRANSVERSE CONSTRUCTION JOINTS

Standard runway specifications allow the contractor to decide how to construct transverse construction joints. These joints are built at the end of a paving lane for emergency reasons or end-of-day stoppage. Most designs provide some type of load transfer at these joints

and may include other details. Generally the smoothness requirement, as measured by a straightedge, is applied to this joint as to all other portions of the pavement. At Clark Air Base these construction joints resulted in a "bump" in ride quality. The deviation is usually rectified by grinding down the high portion. However, when an unacceptable spot is low, there is a tendency to attempt a repair either by building up the surface with a partial depth patch or grinding down a large enough area to meet the straightedge test. Despite the effort, these remedies often result in an uneven ride at the joint.

One method to alleviate roughness at transverse construction joints is to pave several feet past the intended joint location. Thus a full pavement section will exist at this location and no fixed forms or other devices need to be used to support the end of the slab. After the concrete is sufficiently cured, it is sawn off at the joint location and the concrete beyond the construction joint removed. If required for load transfer, dowels can be drilled and set with a rapid setting epoxy grout. Paving then continues from this straightedge, with the paver beginning on the existing slab and moving out onto the new, freshly placed concrete.

This construction technique is more costly, and contractors cannot be expected to do this unless it is required. Such a requirement could be incorporated into the specifications for the central lanes of the runway.

RELATIONSHIP BETWEEN LANE WIDTHS AND OTHER FACTORS

Most design criteria specify exact lane width, transverse joint spacing, and required joint details (*1–3*). The choice of lane width and transverse joint spacing is often based on agency experience, amount of reinforcement, load transfer requirement, and some accepted ratio of slab length to width. The size of available pavers should also be a consideration.

Designers should not limit the lane width considerations to locally available machines. Large paving machines are available today, and they can be configured in a range of widths. A large part of mobilizing a paving plant is the setup and breakdown costs. Modern transportation facilities permit moving machines long distances quickly. The extra cost to move larger equipment, even a few thousand miles, is low relative to the other mobilization costs. Because of increased productivity and reductions in length of construction joints, the total cost of the project may be lower if these large paving machines are used.

Another factor considered by designers is the size of the concrete plant specified in contract documents. Plant size is based on the need to deliver an adequate amount of concrete to the paving machine so that it may pave without interruption. The wider the paving lanes specified and the thicker the pavement, the larger the required concrete plant. Designers should be aware that the manufacturer's rated capacity may be for an ideal condition, and actual plant output may be significantly lower. It is suggested that specifications require a manufacturer's rated plant capacity equal to two times the actual volume required to be delivered to the site.

Many typical paving specifications in use today list a range of equipment requirements. Many of these requirements are specific to older paving equipment and may preclude the use of some newer equipment. One factor rarely mentioned is the weight of the slip form paver. When thick concrete runway pavements are constructed, adequate paver weight is critical to achieving required smoothness and quality of the finished pavement.

It is believed that this is an area that requires more input from equipment manufacturers and contractors. Depending on the size of a particular project, specifications should allow the contractor a range of lane widths and transverse joint spacings. Maximum and minimum paving lane widths with a specified transverse joint spacing for each width should be provided. Minimum concrete plant output (volume delivered to the site) for each width should also be specified. Placement of lanes wider than the normal 7.6 m (25 ft) will reduce the number of construction joints and lead to better performing pavements.

For unreinforced concrete pavement, the U.S. Air Force and the U.S. Navy specify maximum slab size of 6.1 by 6.1 m (20 by 20 ft) (*1,2*). The FAA permits up to 7.6 m (25 ft) square slabs (*3*). A generally accepted standard for the ratio of slab length to width is 1.25 maximum. Under a performance specification, selected paving lane width must accommodate these values.

STRAIGHTEDGE TESTING IS UNSATISFACTORY

Traditional surface testing of airfield pavements has been with a straightedge 3.0, 3.7, or 4.9 m (10, 12, or 16 ft) long. Straightedge testing criteria and procedures are not related to aircraft performance and have not been standardized for airports. At Clark Air Base, the specification permitted a 6.4-mm (¼-in.) deviation in the transverse direction and a 3.2-mm (⅛-in.) deviation longitudinally in 3.0 m (10 ft). Most specifications further limit the deviation of the finished pavement elevation from the design elevation to 13 mm (½ in.) or a similar number. These tests are not always adequate to obtain a smooth riding pavement. It is possible, for example, to start at an elevation 13 mm (½ in.) above design grade, dip to 13 mm (½ in.) too low, then rise to the 13-mm (½-in.) high elevation in less than 60 m (200 ft), and completely conform to the straightedge and elevation criteria. Thus a runway having a continuous sine curve can be built and still conform to criteria.

At Clark Air Base, the final runway surface consistently met the specified longitudinal tolerance of 3.2 mm (⅛ in.) in 3.0 m (10 ft). Although not directly quantifiable, the measurements on this project were an accurate assessment of superior ride quality. The only noted failures to meet longitudinal straightedge requirements were across transverse construction joints. Similarly, the only bumps in ride quality were found to coincide with these joints.

At Clark Air Base a condition was also observed in which the smooth riding pavement did not consistently conform to the straightedge test in the transverse direction. On some paving lanes, to prevent edge slump, the paving machine operator used a float attachment that tended to over-build near the edge. This overbuild resulted in a slightly concave upward surface from .3 to 1.0 m (1 to 3 ft) inward from the edge. The 6.4 mm (¼ in.) in 3 m (10 ft) transverse requirement was not always met in these locations. Such a minor deviation in the transverse direction does not affect ride quality and is of no consequence. Overbuilding is preferred to excessive edge slump and shallow patchwork that otherwise might have occurred.

The Air Force and Navy have been experimenting with the use of profilographs for quality control of the longitudinal profile on runways. Future specifications will incorporate these devices. Preliminary, unpublished data, which have been collected by the Army, indicate that a limit of 178 mm (7 in.) per 1.6 km (1 mi) of roughness, using a California-type profilograph, can be achieved for runway construction. This is consistent with many highway

specification requirements (*4*). The FAA continues to support research to determine the response of aircraft to variable profiles. This is a complex problem, given the wide range of aircraft and possible profiles. A means of better specifying acceptance criteria is certainly warranted at this time.

TIED EDGE JOINTS

The joints at the outside of wide pavements are tied to keep outside slabs together when pavement expands and contracts. Constructing tied edge joints presents problems when installing the tie bars and ensuring the pavement does not crack at nearby locations.

The outside lane on the Clark runway project was thinnest at the center of the runway. The two lanes were placed in one 12.2-m (40-ft) wide pass, and the tied joint was created by saw cutting the slab directly above preset tie bars. Cores indicated that most of the joint cracked on the saw cut during the initial shrinkage period. However, in a few locations, a parallel crack developed about 1.5 m (5 ft) inward on the second lane. The cause of this cracking was never conclusively determined. It is believed that either excessive stress built up at this point due to restraint by the tie bars or a cement-stabilized base construction joint caused reflective cracking. This joint in the stabilized base was close to where the cracks occurred.

The value of tied joints is questionable. Ties are normally intended to restrain opening of keyways and prevent loss of load transfer. In the outside paving lanes of runways, only occasional traffic loading is experienced, so load transfer is not a major concern. Although some older pavements may have suffered from outer slab movement, this problem appears less common today. Even if the outside slab moves outward 25 or 50 mm (1 or 2 in.), a point would be reached at which further movement would cease. A widened joint poses no practical problem other than joint seal maintenance. At intersections, where aircraft traverse this portion of the pavement, thicker slabs and load transfer would be provided, and adjacent pavements would serve to inhibit outward movement. It is suggested that the requirement for tied joints in the outside lanes be removed from design criteria.

LOAD TRANSFER AND STABILIZED BASES

Dowels and keyways for load transfer are costly items and may not always be necessary. Dowel and keyway installation can be difficult and, when improperly installed, cause joint spalling and cracking. Repairs to joints containing dowels and keyways is expensive and difficult, and sometimes the attempt to replace the load transfer mechanism results in more damage to the pavement. Joints near the center of the runway can expect direct application of loads. If the pavement design thickness is calculated on the basis of expected load transfer and this transfer does not occur, the life of the pavement may be greatly reduced.

Few airports today can afford to close a runway for long periods for repair. Current thinking by many leaders in airfield pavement technology is to design pavements for a life longer than 20 years. Considering the enormous cost and flight delays as a result of runway repair, a longer design life makes economic sense. Pavement failure often begins at the edges of slabs, which are inherently the weakest feature. Conservative design of the edges would have a favorable impact on pavement life and therefore long-term economic costs. One proposal for improving the quality of the central joints is discussed earlier in this paper. Another means to increase pavement life would be to increase base course quality and concrete thickness in the central portion of the runway and other areas experiencing a high volume of channelized traffic.

Many current design standards call for providing a stabilized base where pavements are designed for large aircraft. This base is usually good quality, intended to prevent loss of fines, improve subgrade support, and provide a stable platform for operating paving equipment. Most designs require the base to be of a uniform thickness, which is usually the thinnest section permitted by design criteria. .

A stronger stabilized or lean concrete base would reduce edge stresses and prevent faulting. Consideration should be given to providing a stronger and thicker base for the central portion of the runway. The outer areas might remain at their reduced dimension. However, providing a stronger base for the full runway width might be a means of ensuring adequate support for thinner pavements at the edge when, on rare occasions, they are traversed by heavy aircraft.

The Navy has designed many airfield pavements with smooth butt-type longitudinal construction joints on high-strength stabilized bases. The high-strength base provides a high subgrade reaction (k-value) and allows the pavement to be designed to accommodate full edge load condition. This design approach requires a moderately thicker slab, but eliminates dowels and keyways. For the relatively light Navy aircraft loads and traffic volume, faulting has not been a problem, and overall performance has been very good.

REFLECTION OF CEMENT-TREATED BASE JOINTS INTO PAVEMENT

As mentioned, reflective cracking from a cement-treated base may occur in the thinner sections of a runway. If even thicker and stronger stabilized bases are to be constructed, this problem may become more severe.

Providing a liberal bond breaker and requirements for a smooth base course surface would help prevent such cracking. However, practical problems arise in maintaining a good quality bond breaker surface during construction, which involves heavy equipment moving about on the surface. At this time, it is recommended that a good bond breaker, such as double applications of curing compound, be used on high-strength cementitious base courses.

CONCLUSIONS

This paper has reviewed recent experience with the construction of a portland cement concrete runway at Clark Air Base in the Philippines. It was found that the use of a wide paver, capable of placing 12.2-m (40-ft) wide lanes, greatly improved the ride quality and the quality of the longitudinal joints. The completed runway was extremely smooth. Transverse construction joints were found to be the only source of bumps in the finished pavement.

Under certain conditions, saw cutting and removal of the outer .3 m (1 ft) of the central interior paving lane when constructing runways are advocated. Removal (and replacement) of the outer .3 m (1 ft) will improve the smoothness and quality of the concrete along the longitudinal construction joints in the heavy traffic areas of the runway.

More flexibility in paving lane and joint design features is also recommended to permit more contractor innovation and use of new and modern paving equipment. Specifications for major runway paving projects should have input from contractor and equipment manufacturers.

Straightedge testing for surface smoothness may be useful as a means of quality control, but it does not relate to aircraft or pavement performance. Better methods of measuring smoothness and profile on airfield pavements are necessary.

It is recommended that tie bars not be placed in keyed longitudinal construction joints and that lean concrete and cement stabilized bases be treated with a heavy bond breaker.

ACKNOWLEDGMENTS

The authors acknowledge the support of the Pacific Division, Naval Facilities Engineering Command, including the contributions of Eric Takai, Design Division Director, and Louis H. Trigg, formerly the Design Engineer in Charge. The authors also thank the many design personnel from the Hawaiian office of the Ralph M. Parsons Co.

REFERENCES

1. *Rigid Pavements For Airfields*. Chap. 3. TM 5–825–3/AFM 88–6. U.S. Departments of the Air Force and the Army, 1988.
2. *Rigid Pavement Design for Airfields*. Military Handbook 1021/4. U.S. Department of the Navy, Naval Facilities Engineering Command, 1987.
3. *Airport Pavement Design and Evaluation*. AC 150/5320–6C. U.S. Department of Transportation, Federal Aviation Administration, 1978.
4. *Measurements, Specifications, and Achievement of Smoothness for Pavement Construction. NCHRP. Synthesis of Highway Practice 167*: TRB, National Research Council, Washington, D.C., 1990, p. 14.

Publication of this paper sponsored by Committee on Portland Cement Concrete Pavement Construction.

Early Strength Testing of Concrete Cores and Cylinders

MICHAEL HALL

During the 1989 construction season in Wisconsin, six projects, which were built by four different concrete paving contractors, were studied to assess the in situ early strength of concrete pavements, the early strength of lightly insulated field-cured concrete cylinders, and the 28-day strength of paving concrete. The projects were also studied to establish the relationship between cylinder and in situ strength typical on paving projects in Wisconsin. The results of testing over 1,500 individual cores and cylinders indicate that most pavements constructed in warm weather attain compressive strengths of 20.7 mPa (3,000 psi) to 24.1 mPa (3,500 psi) in 3 days or less, approximately 95 percent of the paving grade concrete has a 28-day compressive strength of more than 27.9 mPa (4,050 psi), and the compressive strength of lightly insulated cylinders cured in the field provides a reasonable measure of the in situ compressive strength of the pavement as measured in core tests.

Wisconsin Department of Transportation (WisDOT) policy in 1988 required a minimum curing period of 7 days and a minimum compressive strength of 20.7 mPa (3,000 psi) before new concrete pavements could be opened to traffic. The contractors represented by the Wisconsin Concrete Pavement Association (WCPA) requested WisDOT to consider changing this policy to allow traffic on new pavements after the required minimum compressive strength has been achieved or after a shorter minimum time requirement. WCPA believed that, with the widespread use of slipform paving and lower slump concretes, the 7-day requirement was overly restrictive causing unnecessary construction delays. The 7-day requirement also tended to inhibit the implementation of innovative methods such as fast track paving. WisDOT subsequently produced data based on an analysis of the cylinder test records for the 1988 construction season that appeared to indicate that a substantial percentage of test cylinders failed to reach the required level of strength in 7 days.

On review it was pointed out that data for high slump concrete used for purposes other than paving were included. An independent analysis of the same test records showed significantly higher average strengths when only paving concrete was included. In addition, the test cylinders were not given sufficient temperature protection to mimic the thermal mass effect of the material in the pavement slab.

The study described in this report was conducted during the 1989 construction season to address these concerns. Field work was performed by WCPA, Wisconsin Testing, and Twin City Testing Corporation. WisDOT, Wisconsin Testing, and Twin City Testing Corporation performed the laboratory testing.

Wisconsin Concrete Pavement Association, 7609 Elmwood Avenue, Middleton, Wisc. 53562.

The objectives of this study were to

- Assess the typical in situ compressive strength at 3, 5, and 7 days for paving-grade concretes by testing cores cut from the pavement.
- Assess the typical field-cured compressive strength at 3, 5, and 7 days for paving-grade concretes by testing cylinders cured in lightly insulated boxes.
- Assess the typical 28-day compressive strength for paving-grade concretes by testing cylinders fabricated on grade.
- Compare the results of core and cylinder tests to establish a relationship that can be used to predict in situ strength from the compressive strength of field-cured cylinders.

DESCRIPTION

Paving concretes from six separate highway projects built by four contractors were included in this study. These projects are referred to as Beaudoin-45, Cape-190, Vinton-19, Trierweiler-A, and Trierweiler-B for WisDOT grade A–FA concrete, containing fly ash (*1*). A small amount of WisDOT grade A–WR concrete, containing water reducer (*1*), was used on the Beaudoin-45 project and for the entire Vinton-29 project. The WisDOT specified mix component quantities for each grade of paving concrete are shown in Table 1.

Twelve standard 152.4-mm (6-in.) diameter by 304.8-mm (12-in.) long cylinders, in groups of three, were cast each morning for compressive strength testing at 3, 5, 7, and 28 days. A similar set of specimens was produced each afternoon. Except for the Vinton-29 project, the 3-, 5-, and 7-day cylinders were cured on grade in cardboard boxes loosely filled with vermiculite to simulate the thermal condition seen at mid-slab in the pavement. More heavily insulated curing boxes were used on the Vinton-29 project. The 28-day cylinders were cured in the same way for the first 7 days, then stored in a laboratory curing room at 23°C (73.4°F) and 100 percent relative humidity for the rest of the curing period.

Nine 101.6-mm (4 in.) diameter cores, in groups of three, were cut for each day of paving operations and tested for compressive strength at 3, 5, and 7 days. The locations of the cores were matched to a set of cylinder specimens.

The cylinders and cores were prepared and tested in accordance with established ASTM (*2*) procedures for determining the compressive strength of concrete. All the reported core strengths were adjusted for aspect ratio (*L/d*).

All specimen fabrication, curing, and testing was done by Wisconsin Testing for the Beaudoin-45 project, and by Twin City Testing Corporation for the Vinton-29 project. WCPA personnel conducted the field work on the other projects and delivered the cylinders and cores to WisDOT for compression testing. Early

TABLE 1 WisDOT Mix Component Quantities

	WisDOT grade of concrete	
	A-FA	A-WR
Cement (N/m^3)	2,792	3,083
Class C Fly Ash (N/m^3)	640	none
Total Aggregate (N/m^3)	18,207	19,022
Fine Aggregate (% of total aggregate by weight)	30 - 45 %	30 - 45 %
Target Air Content	6%	6%
Typical Water/Cement Ratio	.40 - .45	.40 - .45

* To convert from N/m^3 to lb/yd^3 multiply by 0.172

efforts to break cylinders in the field with a manually actuated portable testing machine were abandoned because of erratic results.

INDIVIDUAL RESULTS BY PROJECT AND GRADE OF CONCRETE

Summaries of the results by project for WisDOT grade A–FA concrete are shown in Table 2 and for WisDOT grade A–WR concrete in Table 3. Each sample point represents the average of three individual test specimens.

COMBINED RESULTS

A summary of the results for the combined grade A–FA data is shown in Table 4. Here the tests from each project are lumped together to form one large sample. The standard deviation given thus includes the differences between the projects as well as the variability inherent in the strength on a given project. This analysis can be used to assess strength on an industrywide basis.

Each sample point represents the average of three individual test specimens. All of the grade A–FA data were used for the core strengths and data for the Trierweiler projects were excluded in the analysis of the cylinder strengths.

Sampling and testing procedures were being refined on these early projects. A portable hand-actuated hydraulic breaker was used to test the cylinders in the field. This equipment gave erratic results, as can be seen from the significantly larger coefficients of variation reported for the Trierweiler-A project (see Table 2). Only laboratory compression testing was conducted on the other projects. The sample size was also very small for both Trierweiler projects, especially Trierweiler-B (see Table 2).

The sample size for grade A–WR concrete was too small to warrant a combined analysis (see Table 3). Most of the A–WR data were from the Vinton-29 project, obtained late in the paving season when the ambient temperature was significantly lower. The cylinders on this project were also cured in more heavily insulated curing boxes, which may have accelerated strength development. This effect can be seen from the significantly higher cylinder strength, relative to core strength, for this project (see Table 3). These results were included for completeness and should not be used to characterize the typical strength of grade A–WR concrete.

POOLED RESULTS

The combined results presented in Table 4 for grade A–FA concrete include the variability between projects. This is appropriate when considering an opening criterion based on curing period alone. This criterion should be applied on an industrywide basis without any on-site testing. This lumping together of data, however, tends to exaggerate the estimate of the variability that can be anticipated on a given project.

The development of opening criteria based on cylinder testing requires an assessment of the strength without the variability between projects. Data used for this purpose should be pooled instead of combined. In the pooling process, variability is determined from the weighted average, by degrees of freedom, of the component project variances. The differences between project mean strengths are thus eliminated from the computed standard deviations.

An estimate of the strength parameters as determined from the pooled results for grade A–FA concrete is shown in Table 5. Note that the standard deviations and resultant coefficients of variation are reduced while the estimated means are unchanged. Each sample point represents the average of three individual test specimens. All of the data were pooled for the core strengths, and the data from the Trierweiler projects were excluded in the analysis of the cylinder strengths for the reasons previously stated. There were not enough data for the grade A–WR concrete to warrant a pooled analysis.

DISCUSSION OF RESULTS

The first objective of this study was to assess the typical in situ compressive strength of paving-grade concretes at 3, 5, and 7 days on an industrywide basis. Review of the core test results for the combined data (Table 4) indicates that most of the surveyed pavements using grade A–FA concrete had attained compressive strengths of 20.7 mPa (3,000 psi) to 24.1 mPa (3,500 psi) after only 3 days.

An estimate of the percentage of pavements that equal or exceed a given strength can be calculated from the mean and standard deviations shown in Table 4. The results of this analysis for strength levels of 20.7 mPa (3,000 psi) and 24.1 mPa (3,500 psi) are given in Table 6.

A picture of both the mean of and the variability in the in situ strength of the grade A–FA pavement on an industrywide basis can

TABLE 2 Summary Statistics for Individual Projects—Grade A–FA

	Average of 3 Cores			Average of 3 Cylinders			
Beaudoin - 45	3-day	5-day	7-day	3-day	5-day	7-day	28-day
Mean (mPa)	29.9	31.9	34.8	23.2	25.3	27.6	33.9
Standard Deviation (mPa)	2.4	3.4	3.2	2.3	2.3	2.6	3.6
Coefficient of Variation	7.9%	10.6%	9.3%	9.7%	8.9%	9.5%	10.6%
Sample Size	10	10	10	17	17	17	17
95% Exceed (mPa)	26.0	26.3	29.4	19.5	21.6	23.3	28.0
	Average of 3 Cores			Average of 3 Cylinders			
Cape - I90	3-day	5-day	7-day	3-day	5-day	7-day	28-day
Mean (mPa)	25.9	28.2	29.3	25.7	27.7	29.0	35.7
Standard Deviation (mPa)	2.2	2.5	3.0	2.2	2.1	1.9	4.0
Coefficient of Variation	8.6%	9.0%	10.1%	8.6%	7.5%	6.6%	11.2%
Sample Size	11	10	10	20	20	19	20
95% Exceed (mPa)	22.3	24.0	24.4	22.1	24.2	25.8	29.1
	Average of 3 Cores			Average of 3 Cylinders			
Vinton - 19	3-day	5-day	7-day	3-day	5-day	7-day	28-day
Mean (mPa)	24.7	24.3	29.7	21.0	22.6	24.3	31.4
Standard Deviation (mPa)	1.9	1.9	2.4	1.3	1.5	1.4	2.0
Coefficient of Variation	7.6%	7.9%	8.2%	6.3%	6.5%	5.6%	6.2%
Sample Size	13	13	13	20	20	20	10
95% Exceed (mPa)	21.6	21.1	25.7	18.8	20.2	22.0	28.2
	Average of 3 Cores			Average of 3 Cylinders [a]			
Trierweiler - A	3-day	5-day	7-day	3-day	5-day	7-day	28-day
Mean (mPa)	23.3	28.7	30.3	22.2	24.9	27.4	34.4
Standard Deviation (mPa)	1.9	2.8	4.4	4.1	3.5	4.1	5.6
Coefficient of Variation	8.0%	9.9%	14.5%	18.6%	14.0%	15.0%	16.3%
Sample Size	3	6	7	10	11	11	9
95% Exceed (mPa)	20.3	24.0	23.1	15.4	19.2	20.6	25.2
	Average of 3 Cores			Average of 3 Cylinders [a]			
Trierweiler - B	3-day	5-day	7-day	3-day	5-day	7-day	28-day
Mean (mPa)	25.1	27.1	28.5	22.1	24.3	26.3	34.5
Standard Deviation (mPa)	3.3	3.9	2.6	1.6	1.2	1.4	1.5
Coefficient of Variation	13.2%	14.2%	9.0%	7.3%	5.0%	5.4%	4.2%
Sample Size	5	4	5	8	8	6	8
95% Exceed (mPa)	19.6	20.7	24.3	19.4	22.3	24.0	32.1

[a] Trierweiler cylinder data contain inconsistencies

* To convert from mPa to psi multiply by 145.14

TABLE 3 Summary Statistics for Individual Projects—Grade A–WR

	Average of 3 Cores			Average of 3 Cylinders			
Beaudoin - 45	3-day	5-day	7-day	3-day	5-day	7-day	28-day
Mean (mPa)	26.3	27.4	31.7	23.3	25.3	26.6	30.6
Standard Deviation (mPa)	1.4	2.0	0.2	0.8	1.2	1.0	1.3
Coefficient of Variation	5.5%	7.1%	0.6%	3.2%	4.6%	3.9%	4.1%
Sample Size	2	2	2	3	3	3	3
95% Exceed (mPa)	23.9	24.2	31.4	22.0	23.4	24.9	28.5
	Average of 3 Cores			Average of 3 Cylinders			
Vinton - 29	3-day	5-day	7-day	3-day	5-day	7-day	28-day
Mean (mPa)	18.6	22.6	26.0	24.2	28.1	29.6	35.2
Standard Deviation (mPa)	3.5	2.5	2.7	4.6	3.6	3.4	3.7
Coefficient of Variation	18.6%	10.8%	10.5%	19.1%	12.8%	11.5%	10.5%
Sample Size	8	8	8	14	14	14	14
95% Exceed (mPa)	12.9	18.6	21.5	16.6	22.2	24.0	29.1

TABLE 4 Summary Statistics for Combined Data—Grade A–FA

	Average of 3 Cores			Average of 3 Cylinders			
	3-day	5-day	7-day	3-day	5-day	7-day	28-day
Mean (mPa)	26.2	27.8	30.7	23.3	25.2	26.9	34.1
Standard Deviation (mPa)	3.1	3.9	3.7	2.8	2.9	2.8	3.8
Coefficient of Variation	11.8%	13.9%	12.2%	11.8%	11.3%	10.5%	11.2%
Sample Size	42	43	45	57	57	56	47
95% Exceed (mPa)	21.1	21.5	24.5	18.8	20.5	22.2	27.9

* To convert from mPa to psi multiply by 145.14

TABLE 5 Estimated Process Parameters for Pooled Data—Grade A–FA

	Average of 3 Cores			Average of 3 Cylinders			
	3-day	5-day	7-day	3-day	5-day	7-day	28-day
Mean (mPa)	26.2	27.8	30.7	23.3	25.2	26.9	34.1
Standard Deviation (mPa)	2.3	2.8	3.1	2.0	2.0	2.0	3.5
Coefficient of Variation	8.7%	9.9%	10.1%	8.4%	7.7%	7.4%	10.3%

* To convert from mPa to psi multiply by 145.14

TABLE 6 Percentage of Pavements Exceeding Given Strength—Grade A–FA

	Age of Pavement		
	3 Days	5 Days	7 Days
Predicted Strength > 20.7 mPa	96%	97%	100%
Predicted Strength > 24.1 mPa	75%	83%	96%

* To convert from mPa to psi multiply by 145.14

be obtained by examining frequency distributions, histograms, for the combined early strength core data. The histogram for the grade A–FA 3-day core strength, (Figure 1) shows the assumed normal distribution and the percentage of the sample within each 500 kPa (72.6 psi) increment.

The second objective of this study was to assess the typical field-cured compressive strength of paving grade concretes at 3, 5, and 7 days for cylinders cured in lightly insulated boxes. Review of the grade A–FA combined cylinder test results (Table 4) shows a lag in strength gain with respect to the cores. It appears that the level of insulation provided was insufficient to recreate the thermal environment of the slab. The histogram for the grade A–FA 3-day cylinder strength from Table 4 is shown in Figure 2.

The third objective of this study was to assess the typical 28-day compressive strength of paving grade concretes on an industrywide basis. Review of the 28-day results for the grade A–FA combined

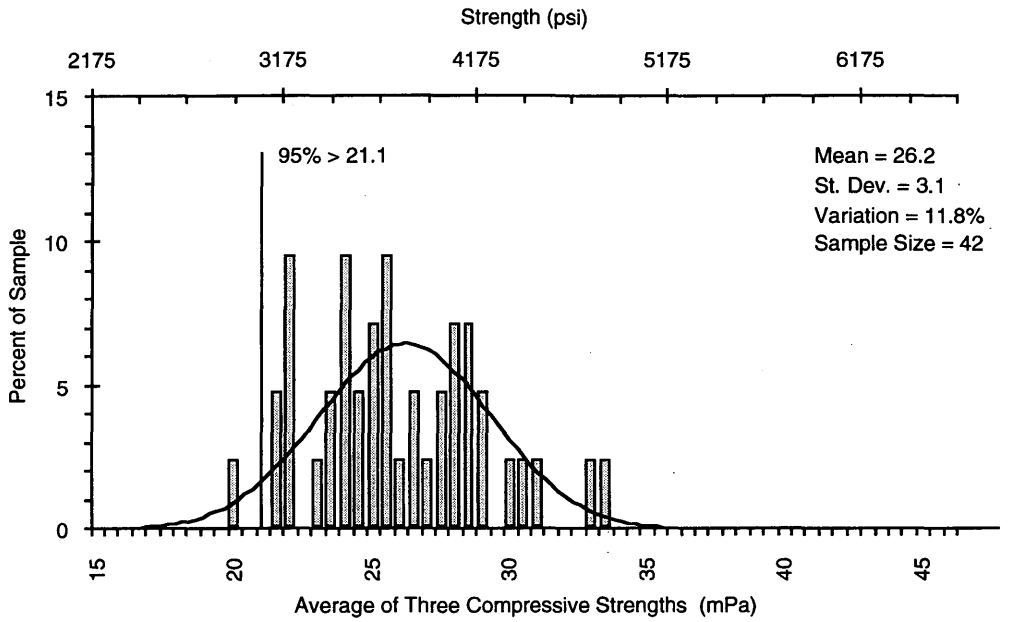

* To convert from mPa to psi multiply by 145.14

FIGURE 1 Histogram of combined data for 3-day cores—Grade A–FA.

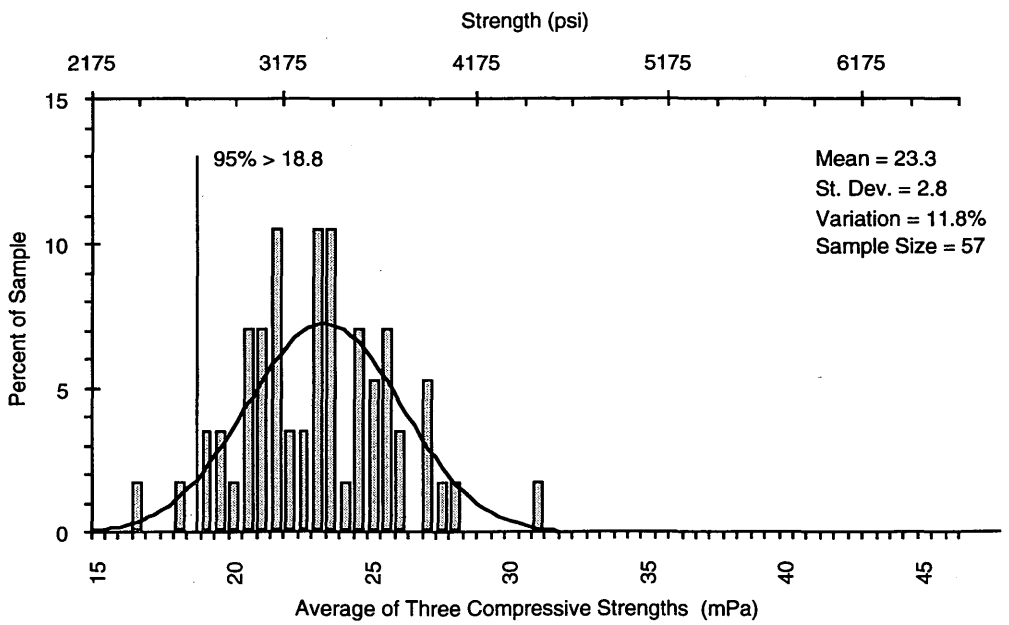

* To convert from mPa to psi multiply by 145.14

FIGURE 2 Histogram of combined data for 3-day cylinders—Grade A–FA.

data (Table 4) indicates that more than 95 percent of the grade A–FA samples exceeds a strength of 27.6 mPa (4,000 psi). The histogram for grade A–FA 28-day cylinder strength from Table 4 is shown in Figure 3.

The final objective of this study was to compare the results of the core and cylinder tests to establish a relationship that can be used to predict in situ strength from the compressive strength of field-cured cylinders.

The grade A–FA core strength is plotted against the cylinder strength in Figure 4. Each pair of values was matched by location to ensure that they represent essentially the same material and curing history.

The 3-, 5-, and 7-day samples from three of the projects are shown. The data from the Trierweiler projects were excluded because of the problems with cylinder strengths previously stated.

Most of the data fall above the line of equality, indicating that core strengths generally exceed cylinder strengths. The scatter in the data, however, makes it difficult to reliably quantify that relationship.

Regression analyses were performed individually for each project and for all the data taken together. The results for grade A–FA concrete are given in Table 7.

The coefficients of determination (R^2) are very low for all cases, as was obvious from Figure 4. Despite the broad scatter, the data appear to be banded, indicating that a relationship exists. Predicting variable core strength in terms of variable cylinder strength with a high level of precision may not be possible. The equation for all the data appears reasonable on physical grounds.

Over the range of cylinder strengths of concern, 17.2 to 31 mPa (2,500 to 4,500 psi), the regression line lies above the line of equality but intersects it at about 31 mPa (4,500 psi). Cores are thus predicted to be stronger than cylinders at about 3 days, while nearly the same strength around 7 days. This makes physical sense, because higher temperatures prevail in the slab for the first day or two, but by 7 days, the relative difference in maturity between the slab and cylinders should be smaller.

Despite the lack of a good statistical fit, the regression equation for all the data can be used to derive a rough estimate of the cylinder strength that should be required. First the mean core strength necessary to equal or exceed the required strength 95 percent of the time can be computed. This value can then be used to compute the mean cylinder strength needed.

For the normal distribution, 95 percent of the strengths exceeds the mean minus 1.645 standard deviations. The average pooled standard deviation for grade A–FA core strength is about 2.7 mPa (397 psi) (see Table 5). The pooled data are used because these opening criteria will be applied on a project-by-project basis. The estimated necessary grade A–FA mean core strengths are

for 20.7 mPa (3,000 psi): $20.7 + (1.645 \times 2.7) = 25.1$ mPa (3,650 psi)

for 24.1 mPa (3,500 psi): $24.1 + (1.645 \times 2.7) = 28.5$ mPa (4,140 psi)

The regression equation from Figure 4 can now be applied to find the required cylinder strengths:

for 20.7 mPa (3,000 psi): $(25.1 - 16.7) \div 0.472 = 17.8$ mPa (2,580 psi)

for 24.1 mPa (3,500 psi): $(28.5 - 16.7) \div 0.472 = 25.0$ mPa (3,630 psi)

This analysis indicates that the resultant grade A–FA cylinder strengths are roughly equivalent to the required strength over the limited range under consideration. Cylinder test results should thus provide reasonable criteria for opening of concrete pavements.

In Wisconsin cylinders for opening are usually cured on grade with no insulation. Although excluded from this analysis, the grade A–WR data from the Vinton-29 project suggest that the level of insulation provided during field-curing is also important.

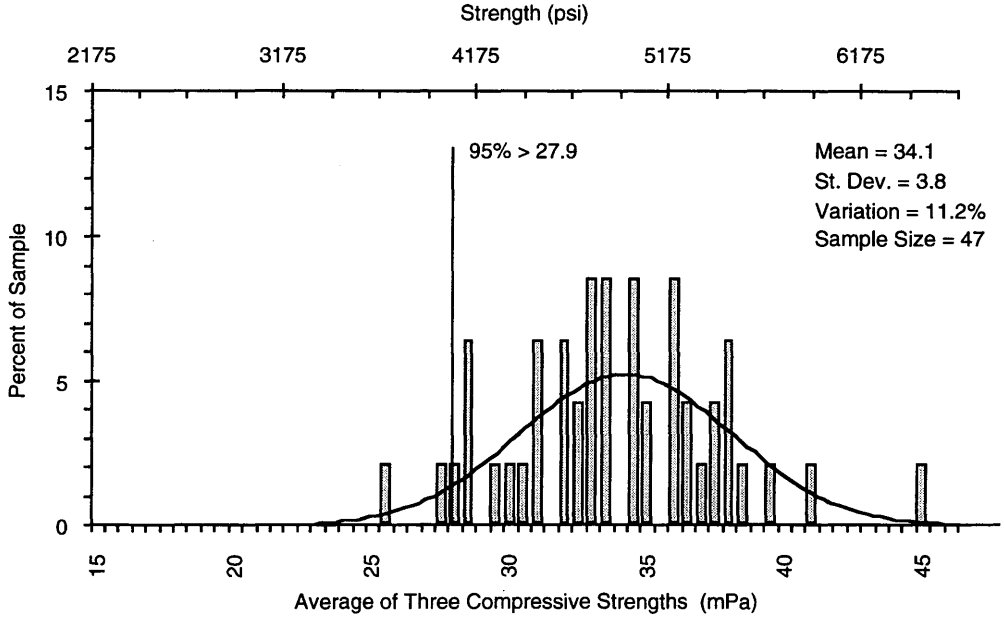

* To convert from mPa to psi multiply by 145.14

FIGURE 3 Histogram of combined data for 28-day cylinders—Grade A–FA.

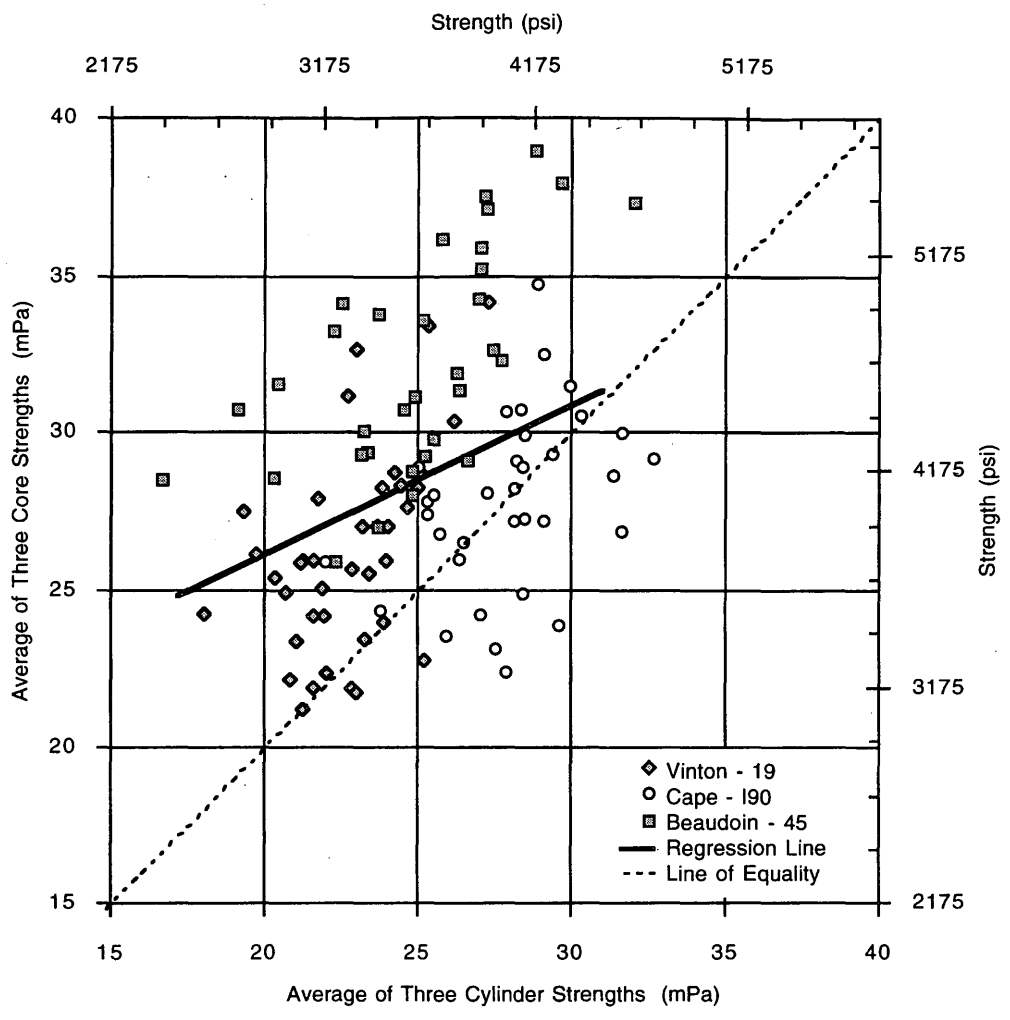

* To convert from mPa to psi multiply by 145.14

** Core Strength = 16.7 + (0.472 x Cylinder Strength)

FIGURE 4 Comparison of core versus cylinder strengths—Grade A–FA.

CONCLUSIONS

The analysis contained in this report is based exclusively on WisDOT grade A–FA concrete placed from June through September. The average daily ambient air temperatures during this period and the construction dates for each project are shown in Figure 5. Any attempt to generalize these results beyond the scope of this analysis should be accompanied by further research. Several variables would likely affect the results to some degree. Cement content, ambient temperature, and the level of insulation or protection afforded to both cylinders and the pavement warrant consideration.

The following conclusions were drawn for WisDOT grade A–FA concrete placed during the typical warm weather portion of the Wisconsin construction season:

- Most WisDOT grade A–FA concrete pavements are attaining strengths of 20.7 mPa (3,000 psi) to 24.1 mPa (3,500 psi) in 3 days or less.

TABLE 7 Core Strength Versus Cylinder Strength Regression Analysis—Grade A–FA

	Data Set			
	Vinton - 19	Cape - I90	Beaudoin - 45	All Data
Coefficient	0.836	0.449	0.693	0.472
Intercept (mPa)	7.22	15.20	14.85	16.70
Coefficient of Determination	.26	.14	.39	.15

* To convert from mPa to psi multiply by 145.14

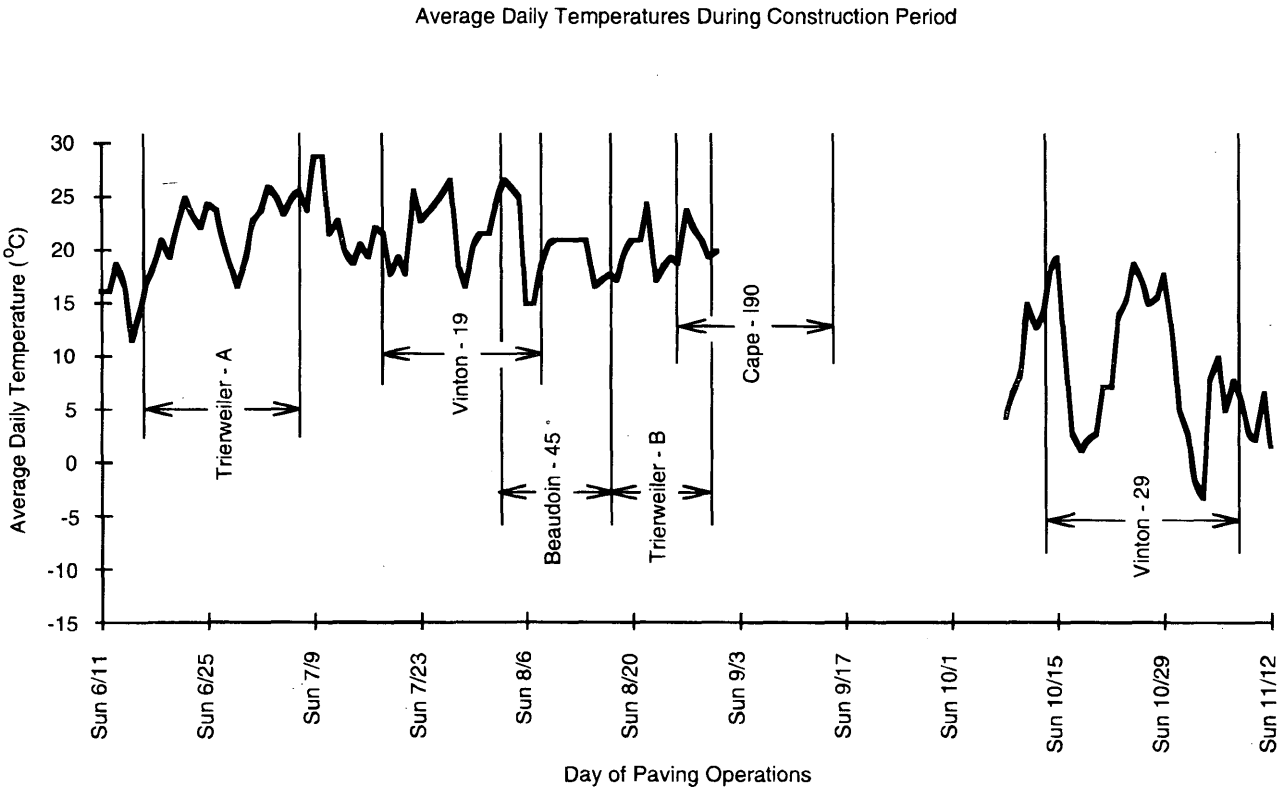

FIGURE 5 Ambient temperatures and project construction dates.

- Approximately 95 percent of WisDOT grade A–FA paving-grade concrete has a 28-day compressive strength in excess of 27.9 mPa (4,050 psi).
- Cylinders cured in the field with light protective insulation provide a reasonable measure of the in situ compressive strength of the pavement.

ACKNOWLEDGMENT

The work presented in this report was cosponsored and cofunded by the Wisconsin Department of Transportation and the Wisconsin Concrete Pavement Association.

REFERENCES

1. Concrete Masonry. *Standard Specifications for Road and Bridge Construction*, Section 501. Wisconsin Department of Transportation, Madison, Wisc., 1989.
2. Concrete and Aggregates. *Annual Book of ASTM Standards*, Vol. 04.02. American Society for Testing and Materials, Philadelphia, Pa., 1989.

Although prepared in cooperation with the Wisconsin Department of Transportation, this report reflects the views of the author who is responsible for the accuracy of the data and the analysis presented.

Publication of this paper sponsored by Committee on Portland Cement Concrete Pavement construction.

Monitoring of European Concrete Pavements

MONTY J. WADE, KURT D. SMITH, H. THOMAS YU, AND MICHAEL I. DARTER

As part of the European Concrete Pavement Evaluation System (COPES) program, 77 concrete pavement sections from France, Italy, the United Kingdom, and Belgium are being monitored and the data evaluated with the objective of providing continual improvements to the design, construction, and maintenance of concrete pavements. An overview of the data collected under the European COPES program is presented, and a general look at overall performance trends is provided. The European sections are all characteristic of the wet-freeze environmental region. Because of higher legal axle weights and longer design periods, European pavements are often exposed to many more equivalent-single-axle-load applications than pavements in the United States. Of the sections evaluated, the most common pavement type is jointed plain concrete pavement. Extensive use of stabilized bases, positive drainage features, and dowel bars is also evident. A qualitative analysis was conducted using present serviceability rating (PSR), age, and traffic as the principal parameters. The use of lean concrete bases and incorporation of a greater number of modernity elements (e.g., dowel bars and positive drainage) were found to improve the performance of the sections. Models predicting the PSR of the pavement sections were also developed.

Under the auspices of the Technical Committee on Concrete Roads of the Permanent International Association of Road Congresses (PIARC), several European countries have been monitoring the performance and behavior of their concrete pavements. The ultimate purpose of this monitoring is to obtain feedback on concrete pavement performance so continual improvements can be made in design, construction, and maintenance.

This interest in monitoring pavement performance parallels a similar interest that has developed in the United States over the last 10 years. For example, the Concrete Pavement Evaluation System (COPES) report, developed at the University of Illinois, not only documented concrete pavement data collection and monitoring procedures but also developed several prediction models for the development of concrete pavement distresses (*1*). Portions of that work served as a building block for the long-term pavement performance studies launched by the Strategic Highway Research Program (SHRP) in 1987 and now being administered by FHWA. In addition, FHWA has sponsored several research studies evaluating the performance of concrete pavements and has shared that data with the European community and with PIARC in particular.

An initial evaluation of performance data from 53 European concrete pavement sections has been conducted, and the results presented at the 19th World Road Congress held in Marrakech in 1991 (*2*). Since that time, additional sections have been incorporated into the study, and further evaluation is being conducted as part of a comprehensive FHWA study on concrete pavement performance, Performance Evaluation of Experimental Rigid Pavements–Data Collection and Analysis. An analysis of the data provides information to PIARC and the participating European countries that may be useful in future concrete pavement design and construction activities. Furthermore, because the European sections contain some unique design features (e.g., widened lanes, thickened slabs, and trapezoidal cross sections), pavement design engineers in the United States may also find this information useful.

ERES Consultants, Inc., 505 West University, Champaign, Ill. 61820.

MONITORING PROGRAM

PIARC has been conducting the pavement monitoring of European concrete pavements in accordance with the aforementioned COPES procedures. It has also included involvement with and cooperation from FHWA and University of Illinois researchers.

Participating Countries

France, Italy, the United Kingdom, Belgium, Switzerland, and Germany are participating in this cooperative study. However, only 77 concrete pavement sections representing four countries are currently available:

- France—29 sections,
- Italy—6 sections,
- United Kingdom—17 sections, and
- Belgium—25 sections.

These sections represent pavements with a range of design features, including widened lanes, trapezoidal cross sections, and nonerodible bases. Roughly one-half of the sections are more than 10 years old, and many are subjected to very heavy traffic loadings. Although most pavement sections are jointed plain concrete pavements (JPCP), several jointed reinforced concrete pavement (JRCP) and continuously reinforced concrete pavement (CRCP) sections are included.

Data Collection

The data collection activities followed the procedures in the original COPES report (*1*). The data can be broadly classified into the following categories:

- Section identification data,
- Pavement design data,
- Distress data,
- Roughness data,
- Patching data,
- Environmental data, and
- Traffic data.

The data were first collected by the participating countries using the International System of Units (SI) and European terminology. Once the data were prepared for entry into an electronic data base, the units were converted to English equivalencies and American terminology to be compatible with the COPES format.

Range of Design Features

The European COPES data base includes a variety of pavement sections in terms of design, age, and traffic. A summary of the design features and performance data for the European COPES sections is given in Table 1. In general, the design practices in Europe do not appear to vary drastically from one country to another, and in many ways, the designs are similar to those in the United States. The following sections illustrate the range of design features encountered in the European COPES sections.

Pavement Type

Of the 29 pavement sections from France, all but one are JPCP designs. The one reinforced pavement section is a JRCP with 0.06 percent longitudinal reinforcing steel. The Italian data consist of four JPCP sections and two JRCP sections with 0.06 percent longitudinal reinforcing steel. One pavement section from the United Kingdom is a JRCP with 0.12 percent longitudinal reinforcing steel, and the other 16 sections are JPCP. The Belgian data consist of 14 JPCP sections and 11 CRCP sections, the latter containing longitudinal reinforcing steel ranging from 0.63 to 0.85 percent of the cross-sectional area.

Overall, the predominant pavement type among the European COPES sections is JPCP. The JPCP sections make up 80 percent of the sections evaluated. The JRCP sections make up only 5 percent of the sections, and the remaining 15 percent are CRCP. All CRCP sections included in the European COPES program are from Belgium.

Joint Spacing

All but two of the JPCP sections from France have joint spacings of either 4.5 or 5.0 m (14.8 or 16.4 ft). Interestingly, the lone JRCP section has a joint spacing of only 5.0 m (16.4 ft). For Italy, the joint spacings are 5.0 m (15.7 ft) for the four JPCP sections and 12.3 m (40.3 ft) for the two JRCP sections. For the United Kingdom, 11 JPCP sections have 5.0-m (16.4-ft) joints spacings and five JPCP

TABLE 1 Summary of Design Features and Performance Data

Country	Project	Highway	Year Built	Slab Design	Lane Width	Joint Spacing	Dowels	Base Type	Reinf Steel	Drainage	Shlder Type	Age	ESALs, x 10^6	PSR
France	55001_01	A6	1981	280 mm JPCP	3.75 m	5.0 m	None	150 mm LCB	None	Edge	AGG	5	26.5	3.5
France	55001_02	A6	1986	280 mm JPCP	3.75 m	5.0 m	20 mm	200 mm PCTB	None	Edge	AGG	3	29.3	2.0
France	55001_03	A6	1980	280 mm JPCP	3.75 m	5.0 m	None	150 mm LCB	None	Edge	AGG	9	52.3	4.0
France	55001_04	A6	1983	250 mm JPCP	3.75 m	5.0 m	None	200 mm LCB	None	None	AGG	6	52.4	4.5
France	55002_01	85	1986	200 mm JPCP	3.5 m	4.8 m	None	120 mm ATB	None	Porous AGG	ST	3	1.5	3.5
France	55002_02	85	1986	230 mm JPCP	3.5 M	4.8 m	None	220 mm ATB	None	Porous AGG	ST	3	2.8	3.5
France	55003_01	N6	1985	200 mm JPCP	3.5 m	4.8 m	None	150 mm ATB	None	Porous AGG	AGG	4	2.2	3.0
France	55003_02	N6	1985	200 mm JPCP	3.5 m	4.0 m	None	150 mm ATB	None	Porous AGG	AGG	4	2.2	3.0
France	55003_03	N6	1985	200 mm JPCP	3.5 m	4.8 m	None	250 mm ATB	None	Porous AGG	AGG	4	2.2	4.0
France	55004_01	N57	1987	370 mm JPCP	3.5 m	10.0 m	None	500 mm AGG	None	Porous PCC	AGG	2	0.9	3.5
France	55004_02	N57	1987	220 mm JPCP	3.5 m	5.0 m	25 mm	150 mm LCB	None	Porous PCC	AGG	2	0.9	3.5
France	55005_01	A42	1983	260 mm JPCP	3.5 m	5.0 m	None	150 mm LCB	None	Porous PCC	AC	6	5.9	3.3
France	55006_01	A1	1977	280 mm JPCP	3.5 m	5.0 m	None	200 mm LCB	None	Porous PCC	AC	9	15.2	3.5
France	55006_02	A1	1977	490 mm JPCP*	3.5 m	5.0 m	None	None	None	Porous PCC	AC	11	43.1	3.5
France	55006_03	A1	1964	275 mm JPCP*	3.5 m	5.0 m	None	200 mm CTB	None	None	AC	22	24.6	2.5
France	55006_04	A1	1976	280 mm JPCP*	3.5 m	5.0 m	None	210 mm CTB	None	None	AC	10	36.3	3.5
France	55007_01	A6a	1960	260 mm JRCP	3.5 m	5.0 m	25 mm	100 mm SC	0.06%	Transverse	AC	26	21.2	1.5
France	55008_01	26	1983	370 mm JPCP	3.5 m	4.5 m	None	250 mm AGG	None	Edge	AC	6	9.2	4.0
France	55008_02	26	1983	370 mm JPCP	3.5 m	4.5 m	None	250 mm AGG	None	Edge	AC	7	5.6	5.0
France	55008_03	26	1981	370 mm JPCP	3.5 m	4.5 m	None	250 mm AGG	None	Edge	AC	9	9.0	4.0
France	55008_04	26	1981	370 mm JPCP	3.5 m	4.5 m	None	250 mm AGG	None	Edge	PCC	9	9.2	5.0
France	55008_05	26	1982	370 mm JPCP	3.5 m	4.5 m	None	250 mm AGG	None	Edge	AC	8	8.4	4.0
France	55008_06	26	1982	370 mm JPCP	3.5 m	4.5 m	None	250 mm AGG	None	Edge	AC	8	8.4	4.0
France	55008_07	26	1985?	370 mm JPCP	3.5 m	4.5 m	None	250 mm AGG	None	Edge	AC	8	4.2	4.0
France	55008_08	26	1985	370 mm JPCP	3.5 m	4.5 m	None	250 mm AGG	None	Yes	AC	5	6.8	4.0
France	55008_09	26	1985	370 mm JPCP	3.5 m	4.5 m	None	250 mm SC	None	Yes	??	5	6.8	??
France	55009_01	4	1976	290 mm JPCP	3.5 m	5.0 m	None	150 mm CTB	None	No	AC	10	3.3	3.5
France	55009_02	4	1976	220 mm JPCP	3.5 m	5.0 m	None	150 mm CTB	None	No	AC	10	3.3	3.5
France	55010_01	A13	1966	250 mm JPCP	3.5 m	5.0 m	None	250 mm CTB	None	No	AC	20	22.5	2.5
Italy	56001_01	SS7	1958	220 mm JRCP	5.25 m	12.3 m	28 mm	250 mm Pozz	0.06%	No	AC	31	62.3	2.5
Italy	56001_02	SS7	1958	220 mm JRCP	5.25 m	12.3 m	28 mm	250 mm Pozz	0.06%	No	AC	31	62.3	2.5
Italy	56002_01	E45	1985	260 mm JPCP	3.5 m	5.0 m	30 mm	150 mm LCB	None	Edge	PCC	4	7.8	2.8
Italy	56002_02	E45	1985	250 mm JPCP	3.5 m	5.0 m	30 mm	200 mm CTB	None	Edge	PCC	4	8.0	2.8
Italy	56002_03	E45	1985	260 mm JPCP	3.5 m	5.0 m	30 mm	150 mm CTB	None	Edge	PCC	4	8.0	2.4
Italy	56003_01	21	1971	240 mm JPCP	3.75 m	5.0 m	None	160 mm CTB	None	None	AC	18	0.9	1.0
UK	57001_01	M20	1972	275 mm JPCP	3.65 m	6.0 m	20 mm	150 mm AGG	None	Edge	AC	16	52.2	2.3
UK	57001_02	M20	1972	275 mm JPCP	3.65 m	6.0 m	20 mm	150 mm AGG	None	Edge	AC	16	52.2	2.3
UK	57002_01	M25	1979	305 mm JPCP	3.65 m	5.0 m	20 mm	225 mm AGG	None	Edge	PCC	9	55.7	2.3
UK	57002_02	M25	1979	305 mm JPCP	3.65 m	5.0 m	20 mm	225 mm AGG	None	Edge	PCC	9	55.7	2.3
UK	57003_01	A2	1973	250 mm JPCP	3.65 m	6.0 m	20 mm	150 mm CTB	None	Edge	AGG	14	40.4	1.2

(continued on next page)

TABLE 1 *(continued)*

Country	Project	Highway	Year Built	Slab Design	Lane Width	Joint Spacing	Dowels	Base Type	Reinf Steel	Drainage	Shlder Type	Age	ESALs, x 10^6	PSR
UK	57003_02	A2	1973	250 mm JPCP	3.65 m	6.0 m	20 mm	150 mm CTB	None	Edge	AGG	14	40.3	1.2
UK	57004_01	A12	1987	280 mm JPCP	3.65 m	5.0 m	20 mm	130 mm CTB	None	Edge	PCC	2	10.8	4.5
UK	57005_01	M25	1976	275 mm JPCP	3.65 m	5.0 m	25 mm	150 mm AGG	None	Edge	PCC	12	106.4	1.2
UK	57005_02	M25	1976	275 mm JPCP	3.65 m	5.0 m	25 mm	75 mm AGG	None	Edge	PCC	12	106.4	1.2
UK	57006_01	M1	1981	300 mm JPCP	3.65 m	5.0 m	20 mm	225 mm LCB	None	Edge	PCC	7	27.3	3.4
UK	57006_02	M1	1982	300 mm JPCP	3.65 m	5.0 m	20 mm	150 mm LCB	None	Edge	PCC	6	24.2	3.4
UK	57007_01	M11	1975	275 mm JPCP	3.65 m	5.0 m	25 mm	150 mm CTB	None	Edge	AC	14	39.7	2.3
UK	57008_01	A12	1971	250 mm JPCP	3.65 m	5.0 m	25 mm	150 mm CTB	None	Edge	??	18	39.5	3.4
UK	57008_02	A12	1971	250 mm JPCP	3.65 m	5.0 m	25 mm	150 mm CTB	None	Edge	??	18	39.5	1.2
UK	57008_03	A12	1969	250 mm JPCP	3.65 m	6.0 m	30 mm	150 mm LCB	None	Edge	??	20	47.8	3.4
UK	57008_04	A12	1965	200 mm JRCP	3.65 m	25.0 m	30 mm	150 mm LCB	0.12%	Edge	??	24	62.0	3.4
UK	57009_01	A120	1982	250 mm JPCP	3.65 m	5.0 m	25 mm	230 mm CTB	None	Edge	??	7	8.3	??
Belgium	58001_01	411	1979	200 mm CRCP	3.75 m	n/a	n/a	150 mm LCB	0.85%	Edge	AC	11	29.5	3.5
Belgium	58001_02	411	1979	200 mm CRCP	3.75 m	n/a	n/a	200 mm LCB	0.85%	Edge	AC	11	29.5	3.5
Belgium	58001_03	411	1973	200 mm CRCP	3.75 m	n/a	n/a	200 mm LCB	0.85%	Edge	AC	17	37.6	3.5
Belgium	58001_04	411	1978	200 mm CRCP	3.75 m	n/a	n/a	200 mm LCB	0.67%	Edge	AC	12	17.9	3.5
Belgium	58001_05	411	1987	200 mm CRCP	3.75 m	n/a	n/a	200 mm LCB	0.67%	Edge	AC	3	6.2	4.5
Belgium	58001_06	411	1988	200 mm CRCP	3.75 m	n/a	n/a	200 mm CTB	0.67%	Edge	AC	2	3.6	4.5
Belgium	58002_01	4	1979	230 mm JPCP	3.75 m	5.0 m	None?	150 mm CTB	None	Edge	AC	10	30.8	3.0
Belgium	58002_02	4	1979	230 mm JPCP	3.75 m	5.0 m	None	150 mm CTB	None	??	AC	10	30.8	3.0
Belgium	58002_03	4	1979	200 mm JPCP	3.75 m	5.0 m	25 mm	150 mm CTB	None	Edge	AC	10	30.8	3.0
Belgium	58002_04	4	1979	200 mm JPCP	3.75 m	5.0 m	25 mm	150 mm CTB	None	Edge	AC	10	30.8	3.0
Belgium	58002_05	4	1979	200 mm JPCP	3.75 m	5.0 m	25 mm	150 mm CTB	None	Edge	AC	10	30.8	3.0
Belgium	58002_06	4	1979	200 mm JPCP	3.75 m	5.0 m	25 mm	150 mm CTB	None	Edge	AGG	10	30.8	3.0
Belgium	58002_07	4	1979	200 mm JPCP	5.0 m	5.0 m	25 mm	150 mm CTB	None	Transverse	AC	10	30.8	3.0
Belgium	58002_08	4	1979	200 mm JPCP	4.0 m	5.0 m	25 mm	150 mm CTB	None	??	AC	10	30.8	3.5
Belgium	58002_09	4	1979	230 mm JPCP	4.0 m	5.0 m	None	150 mm CTB	None	??	AC	10	30.8	3.0
Belgium	58002_10	4	1979	230 mm JPCP	4.0 m	5.0 m	None	150 mm CTB	None	??	AC	10	30.8	3.0
Belgium	58002_11	4	1979	230 mm JPCP	4.0 m	3.5 m	None	150 mm CTB	None	Edge	AC	10	30.8	3.0
Belgium	58002_12	4	1979	200 mm JPCP	4.0 m	5.5 m	25 mm	150 mm CTB	None	??	AC	10	30.8	3.0
Belgium	58002_13	4	1983	200 mm CRCP	3.75 m	n/a	n/a	150 mm CTB	0.63%	Edge	AC	6	21.3	4.0
Belgium	58002_14	4	1979	200 mm CRCP	3.75 m	n/a	n/a	150 mm CTB	0.63%	??	AC	10	30.8	3.5
Belgium	58002_15	4	1985	200 mm JPCP	3.5 m	5.0 m	25 mm	150 mm CTB	None	Edge	AC	5	3.8	4.0
Belgium	58002_16	4	1984	230 mm JPCP	3.5 m	5.0 m	None	150 mm CTB	None	Edge	AC	6	4.4	4.5
Belgium	58003_01	97	1984	200 mm CRCP	3.75 m	n/a	n/a	150 mm CTB	0.85%	Edge	Turf	5	2.9	4.5
Belgium	58003_02	97	1975	200 mm CRCP	3.5 m	n/a	n/a	150 mm CTB	0.85%	Edge	Turf	14	8.0	2.5
Belgium	58003_03	97	1983	200 mm CRCP	3.75 m	n/a	n/a	250 mm CTB	0.85%	Edge	Turf	6	4.5	4.5

* Trapezoidal section

Key: PSI = Present Serviceability Index (0 to 5 scale)
JPCP = Jointed Plain Concrete Pavement
JRCP = Jointed Reinforced Concrete Pavement
AC = Asphalt Concrete
CRCP = Continuously Reinforced Concrete Pavement
PCC = Portland Cement Concrete

1 in = 25.4 mm, 1 ft = 0.305 m
CTB = Cement-Treated Base
ATB = Asphalt-Treated Base
LCB = Lean Concrete Base
AGG = Aggregate
SC = Sand Cement
PCTB = Permeable Cement-Treated Base

sections have 6.0-m (19.7-ft) joint spacings. The one JRCP section has a joint spacing of 25.0 m (82.0 ft). The Belgian sections contain joint spacings ranging from 3.5 to 5.5 m (11.5 to 18.0 ft).

Overall, the joint spacings for the European JPCP sections typically range from 4.5 to 5.0 m (14.8 to 16.4 ft), although one section in France has a joint spacing of 10 m (32.8 ft), and four sections in the United Kingdom have a joint spacing of 6.0 m (19.7 ft). The joint spacings for the JRCP sections range from 5 to 25 m (16.4 to 82.0 ft). The joint spacings for both JPCP and JRCP are similar to those encountered in the United States.

Slab Thickness

Figure 1 illustrates the range of slab thicknesses for the European COPES sections. The French sections have slab thicknesses ranging from less than 200 mm (8 in.) to more than 400 mm (16 in.), although most sections are either between 250 and 300 mm (10 and 12 in.) or between 350 and 400 mm (14 and 16 in.). At least three pavement sections contain trapezoidal cross sections. The slab thicknesses for the Italian sections range from 220 to 260 mm (8.7 to 10.2 in.). The sections from the United Kingdom range in thickness from 200 to 305 mm (8 to 12 in.), although most are between 250 and 280 mm (10 and 11 in.). Of the 25 Belgian sections, 19 sections have a slab thickness of 200 mm (8 in.), and 6 sections have a slab thickness of 230 mm (9 in.).

Overall, the thicknesses range from less than 200 mm (8 in.) to more than 400 mm (16 in.), but most sections fall under three thickness categories: less than 200 mm (8 in.), 200 to 250 mm (8 to 10 in.), and 250 to 300 mm (10 to 12 in.). Considering that a 50 mm (2 in.) difference in the slab thickness can mean an order of magnitude difference in fatigue life of concrete pavements, these slab thicknesses represent a considerable range in structural capacity.

Base Type

A variety of base types are represented in the European COPES sections, as shown in Figure 2. The French sections contain a wide distribution of base types, with thicknesses ranging from 75 to 250 mm

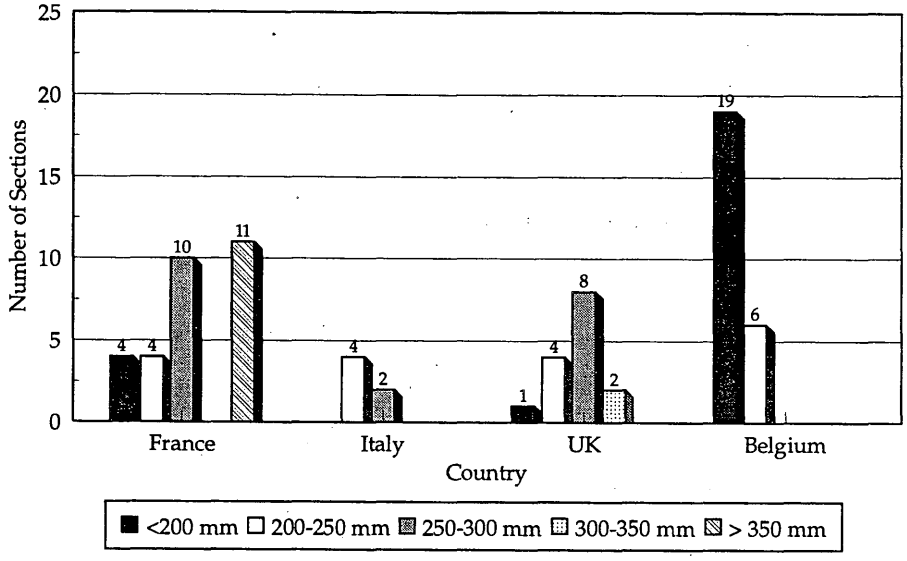

FIGURE 1 Distribution of slab thicknesses.

(3 to 10 in.). The Italian pavement sections contain three different base types—lean concrete base (LCB), cement-treated base (CTB), and pozzolan—with thicknesses ranging from 150 to 250 mm (6 to 10 in.). The pavement sections from the United Kingdom contain three different base types—LCB, aggregate-treated base (AGG), and CTB—with thicknesses ranging from 75 to 225 mm (3 to 9 in.). Five pavement sections from Belgium contain an LCB with a thickness of 200 mm (8 in.), and the remaining 20 sections contain a CTB with thicknesses ranging from 150 to 200 mm (6 to 8 in.). The CRCP sections with 0.85 percent steel have a 60-mm (2.4-in.) bituminous interlayer between the LCB and CRCP.

Overall, stabilized bases are used extensively in the European COPES sections; 80 percent of the sections evaluated have either a stabilized base or a lean concrete base. The most common type of base is the cement-treated base, followed by the lean concrete base, the asphalt-treated base, and the aggregate base.

Dowel Bars

With the exception of the French sections, dowels are provided at transverse joints in nearly all European COPES sections. Dowel diameters range from 20 to 30 mm (0.8 to 1.2 in.). However, only 3 of the 29 French sections contain dowel bars. Although many have experienced high traffic levels, most of the nondoweled French sections are less than 10 years old, making it difficult to judge long-term performance.

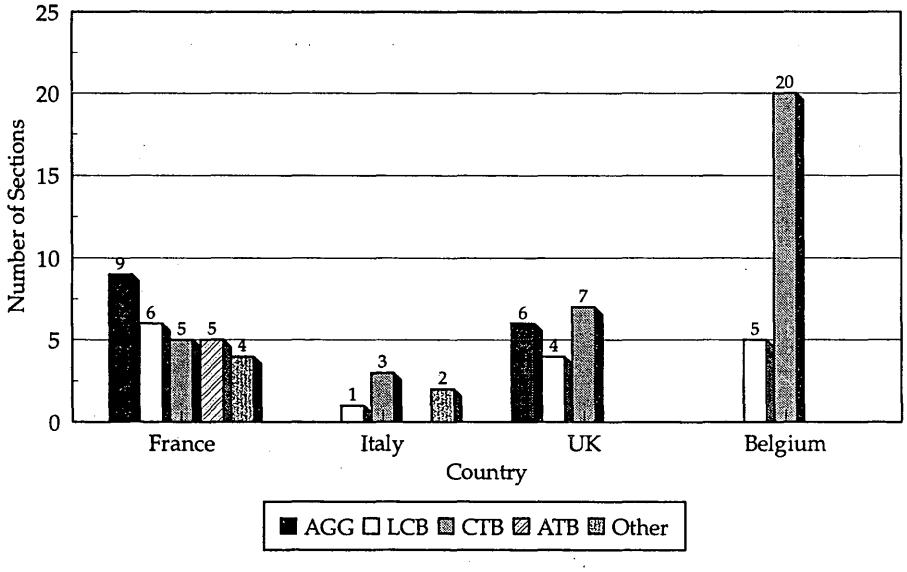

FIGURE 2 Distribution of base types.

Drainage

Nearly all of the European COPES sections were provided with edgedrains or transverse drains. Most of the French sections contain positive drainage features, generally achieved by placing either longitudinal edgedrains or a longitudinal drainage trench of porous aggregate. In addition, one section contains transverse drains, and only six sections contain no positive drainage features. For the Italian sections, three sections have longitudinal edgedrains, and three sections have no drainage system. Every pavement section from the United Kingdom contains longitudinal edge drains. Of the 25 Belgian sections, 18 sections contain longitudinal edgedrains and one section contains transverse drains; drainage information is not available for the remaining six sections.

Shoulder Type

Most of the European COPES sections from France include asphalt concrete (AC) or aggregate shoulders; only one section contains a tied concrete shoulder. Three of the Italian sections contain AC shoulders, and three sections contain porous portland cement concrete (PCC) shoulders. The sections from the United Kingdom consist of three sections with AC shoulders, seven with PCC shoulders, and two with aggregate shoulders. (The type of shoulder is not provided for five pavement sections.) Most of the Belgian sections (21 of 25) contain AC shoulders, one section contains an aggregate shoulder, and three sections contain turf shoulders.

The use of aggregate shoulders appears to be more common in Europe. More than 15 percent of the European sections contain aggregate shoulders, whereas aggregate shoulders are seldom used on higher volume highways in the United States. Concrete shoulders are also used in Europe, but it does not appear to be a common design feature in these sections.

Slab Width

In France, slab widths are either 3.5 m (11.5 ft) or 3.75 m (12.3 ft), whereas the slab widths for the Italian sections are all 5.0 m (16.4 ft). The sections from the United Kingdom are constructed with a slab width of 3.6 m (12 ft). The slab widths from the Belgian sections range from 3.5 to 5.0 m (11.5 to 16.4 ft). The normal slab width for European COPES sections ranges from 3.5 to 3.75 m (11.5 to 12.3 ft), although the use of widened lanes appears to be more common than in the United States.

Pavement Age

Figure 3 shows the distribution of the age of the pavement sections from each country. These are the ages of the pavement from the time they were opened to traffic until the time they were surveyed under the European COPES program. Most of the French pavement sections are less than 10 years old, with an average age of 8.1 years. However, four sections are more than 20 years old. The Italian sections range from 4 to 31 years old, with an average age of 15.3 years. Although this is a wide range of ages, only three different ages are represented—three sections are 4 years old, one is 18 years old, and two are 31 years old. The sections from the United Kingdom range from 2 to 24 years old, with an average age of 12.8 years. The sections from Belgium range from 2 to 17 years old, with an average age of 9.1 years.

The distribution of pavement age at the time of the distress survey is shown in Figure 3. The overall average age of the pavement sections is 10.2 years. This includes five sections that are greater than 20 years old and 18 sections that are less than 5 years old.

Climatic Conditions

Two environmental measures—average annual precipitation and freezing index—can influence concrete pavement performance. The average annual precipitation indicates the amount of free moisture to which the pavement is exposed, although the relative evapotranspiration and the drainage characteristics of the pavement must also be considered (*3*). The freezing index indicates the amount of time throughout the year that the pavement is subjected to temperatures below freezing; it is the summation of the number of degrees that the average daily temperature is below freezing for each day throughout a year (*3*).

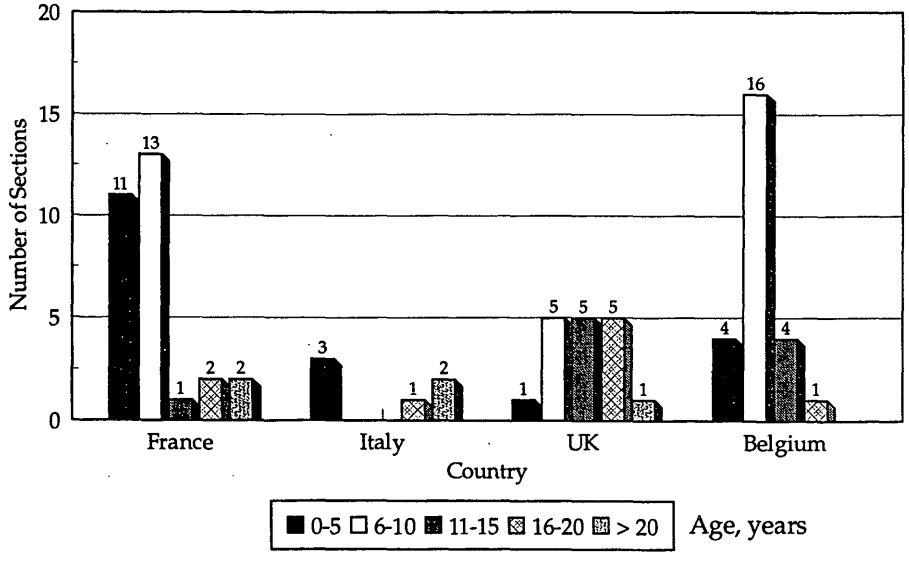

FIGURE 3 Distribution of pavement age.

The environmental conditions for the European sections are characteristic of the wet-freeze environmental region. The annual precipitation for the sections range from about 400 to 875 mm (16 to 34 in.), except for three sections in Italy. The freezing index for the sections range from about 165 to 330°C-days (300 to 600°F-days).

Traffic Loadings

One data item not included in the original European COPES summary tables is the estimated number of 80-kN (18-kip) ESAL applications that the pavement sections had sustained at the time of pavement survey. This factor converts the amount of damage inflicted on the pavement by a given axle load as compared with the amount of damage inflicted by a standard axle load using load equivalency factors developed from the AASHO Road Test (*4*). The European COPES data base contained information on traffic volumes (average daily traffic), truck volumes (percentage of trucks), and truck factors. Because these traffic data were not as complete as desired, several assumptions had to be made, such as assuming an average 4 percent growth rate in traffic volumes and truck factors for years when data were unavailable.

Although the truck volumes are similar to those on major U.S. highways, the axle loads are substantially higher in Europe. The legal load limit for single and tandem axles in Europe ranges from 98 to 128 kN (22 to 28.6 kilopounds) and from 186 to 205 kN (41.9 to 46.3 kilopounds), respectively (*5*). The consequence of the heavy axle loads and the longer design periods used in Europe is extremely high design equivalent single-axle loads (ESALs). Figure 4 shows the distribution of the estimated ESAL applications at the time of survey. Nearly 20 percent of the European sections have sustained more than 40 million ESALs, with over 50 percent of the European sections receiving more than 2 million ESALs per year.

Typical axle load distributions for France are shown in Figure 5 for single and tandem axles. This figure helps explain some of the heavy ESAL applications, because a significant amount of loading is at the higher end of the spectrum. For example, 25 percent of the single axles are greater than 9.1 t (20,000 lb), the legal limit for single axles in the United States. Similarly, 70 percent of all tandem axles are greater than 15.4 t (34,000 lb), the legal limit for tandem axles in the United States. Similar trends are also experienced in other European countries.

Performance Data

Many variables have been collected under the COPES study. The design variables, climatic information, and traffic data have already been discussed. The other major design category is performance data. Unfortunately, complete performance data are not available for all 77 pavement sections included in the evaluation. For example, data on transverse joint faulting, an important measure of concrete pavement performance, are available for only a few sections. Similarly, data on transverse slab cracking, an important indicator of fatigue in jointed plain concrete pavements, are unavailable or inconsistent for many pavement sections. These limitations greatly restrict the extent of the analyses that can be conducted on the pavement sections. The one performance indicator that is present for nearly every section is the present serviceability rating (PSR).

PERFORMANCE EVALUATION

As mentioned, the PSR is the only performance indicator consistently provided for each European section. The pavement serviceability concept, developed at the AASHO Road Test, indicates the ability of the pavement to provide a smooth-riding surface to the traveling public (*4,6*). Using the PSR, it is possible to compare the relative performance of the pavement sections. Presumably, those pavement sections with higher PSR values display less distress. Unfortunately, one drawback of the PSR is that the effect of a specific design feature (e.g., dowel bars) on pavement performance cannot be directly measured; rather, the effect can only be surmised based on whether the design feature reduced any pavement distress that would have otherwise detracted from the serviceability of the pavement.

Another factor complicating the comparison of the performance of the pavement sections is that they were not constructed as experimental sections with the sole purpose of evaluating design features. In addition, many sections within a country are located on the same highway and contain similar (if not the same) design features. Thus,

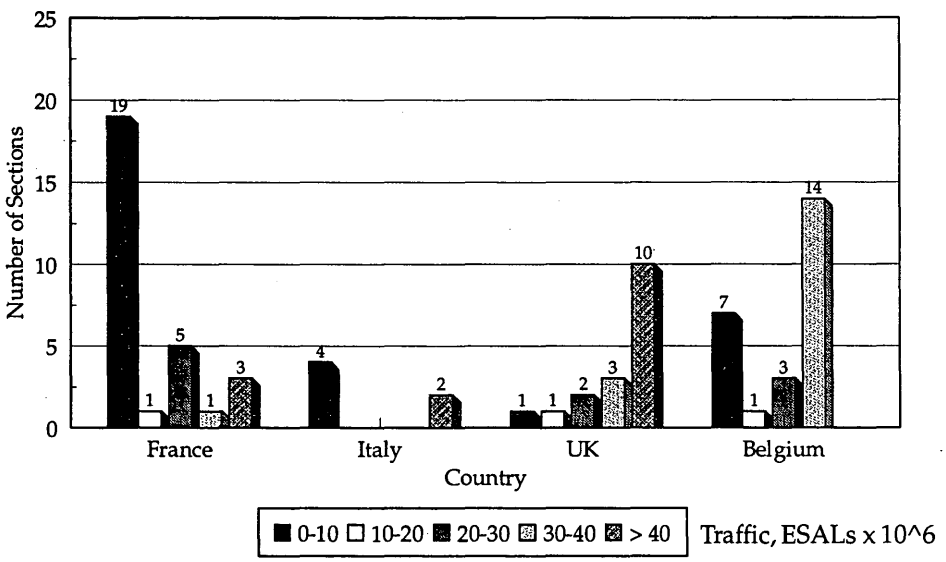

FIGURE 4 Distribution of ESAL applications.

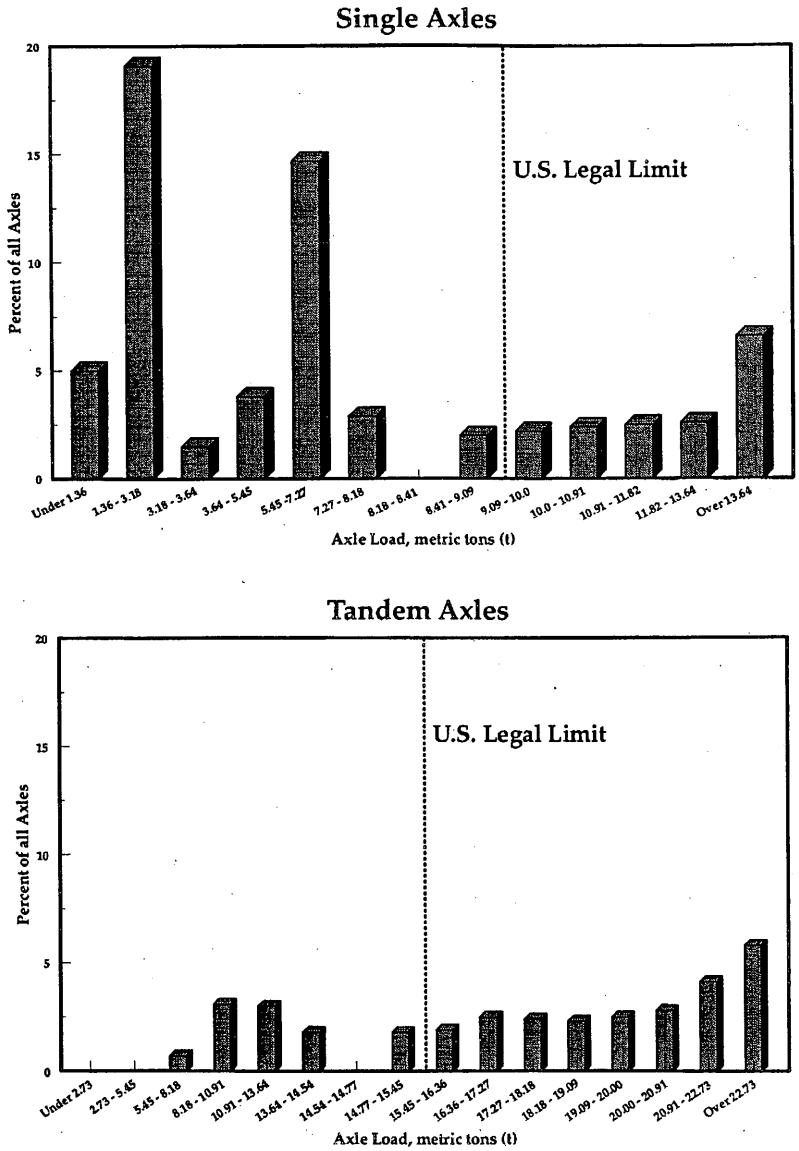

FIGURE 5 Typical axle load distribution from France.

not only are direct performance comparisons infrequent, they are also difficult because of differences in traffic loadings and aging and climatic effects.

Because of the absence of complete performance data and the difficulty in making direct comparisons between pavement sections, a more general evaluation of the performance of the European COPES sections was conducted. The purpose of this type of evaluation was examine the overall performance of the various pavement sections and to identify general performance trends.

PSR Trends

The performance data for the European COPES sections are provided in Table 1. Although only a qualitative analysis was made using three variables as the principal parameters—PSR, age, and traffic—a number of interesting performance trends were observed.

Figures 6 through 8 show the PSR as a function of age, of ESALs, and of the product of age and ESALs, respectively. The latter function, broken out by modernity elements, has been used as a means of analyzing pavement performance (*2*). Because environmental effects and traffic loads are responsible for the deterioration of pavements, in theory, one may expect the pavement condition to deteriorate with increasing age and traffic. Although these figures all show this general trend, considerable scatter is present in the data. Some scatter is expected because the figures include data from all European COPES sections, regardless of the pavement type, slab thickness, or other design feature. Some of these design features are expected to have a significant effect on pavement performance.

The PSR as a function of ESAL applications was also plotted as a function of pavement type, slab thickness, dowels, drainage, and base type. Sufficient data are unavailable to determine the effects of reinforcement or joint spacing. Pavement type does not appear to be a significant factor affecting pavement performance. The only noticeable trend is that CRCP may give better and perhaps more consistent performance than jointed concrete pavements.

The effects of slab thickness, dowels, and drainage were not evident from the data or the graphs. This does not mean that such

important design features do not affect pavement performance; it means only that the effects of these variables on pavement performance could not be determined with the available data.

On the other hand, pavement sections with an LCB seem to perform better than those with other base types. However, further investigation may be warranted to determine the reason that those particular sections performed better. Most European COPES sections containing the LCB are JPCP, and the use of a very stiff base under JPCP requires careful evaluation to avoid cracking due to excessive thermal curling stresses.

Modernity Concept

In the initial evaluation of the European COPES data, the development of the modernity coefficient, or number of modernity elements, is described (*2*). The modernity coefficient is a number from 0 to 4 that indicates the number of specific design features in a pavement section that are expected to contribute to the overall performance of that pavement (*2*). The design features that are expected to contribute to the performance of a pavement are classified in the following four categories:

- Nonerodible base course (specifically, lean concrete base),
- Positive pavement drainage,
- Strengthened structure (thickened slab, dowel bars, or CRCP), and
- Optimization of materials with respect to loading (e.g., widened traffic lanes or trapezoidal cross sections).

For example, a pavement incorporating design elements from each of the categories is assigned a modernity coefficient of 4. Likewise, a pavement containing only dowel bars and positive drainage is assigned a modernity coefficient of 2.

Generally speaking, the pavements in Europe are provided with more features that are expected to promote long-term performance. Many of the European sections (74 percent) have two or more modernity elements. Only 8 percent of the European sections incorporate no modernity elements.

Figure 8 shows the PSR as a function of the product of age and ESALs broken into the number of modernity elements. This figure shows that the sections with three or more modernity elements give better and more consistent performance than other sections. Unfortunately, 14 of the 15 sections having three or more modernity elements also have an LCB. With the available data, it is impossible to determine whether the LCB or the combination of having three or more modernity elements provided the superior performance. Although it is more likely that the latter is the case, this cannot be shown conclusively.

Although the modernity concept provides a useful way of looking at the data, it does not distinguish the difference between the various design features. In addition, it assumes that every modernity element has the same positive effect on pavement performance. Because different design features have different relative effects on pavement performance, the modernity coefficient is only an approximate indicator of the design quality of a concrete pavement.

Prediction Models

Models that predict the PSR of the pavement sections were developed for France, the United Kingdom, and Belgium. (The number of sections was insufficient for developing models for Italy.) The models are based on a limited number of sections and design variables and were developed only as a means of evaluating the effect of the various design features on PCC pavement performance. In addition, the models are only accurate within the range of variables incorporated in the sections in which they were developed. Therefore, the prediction models should not be used for design purposes.

The models were developed using the least-square regression technique with the available data. The terms used in the equations are described as follows:

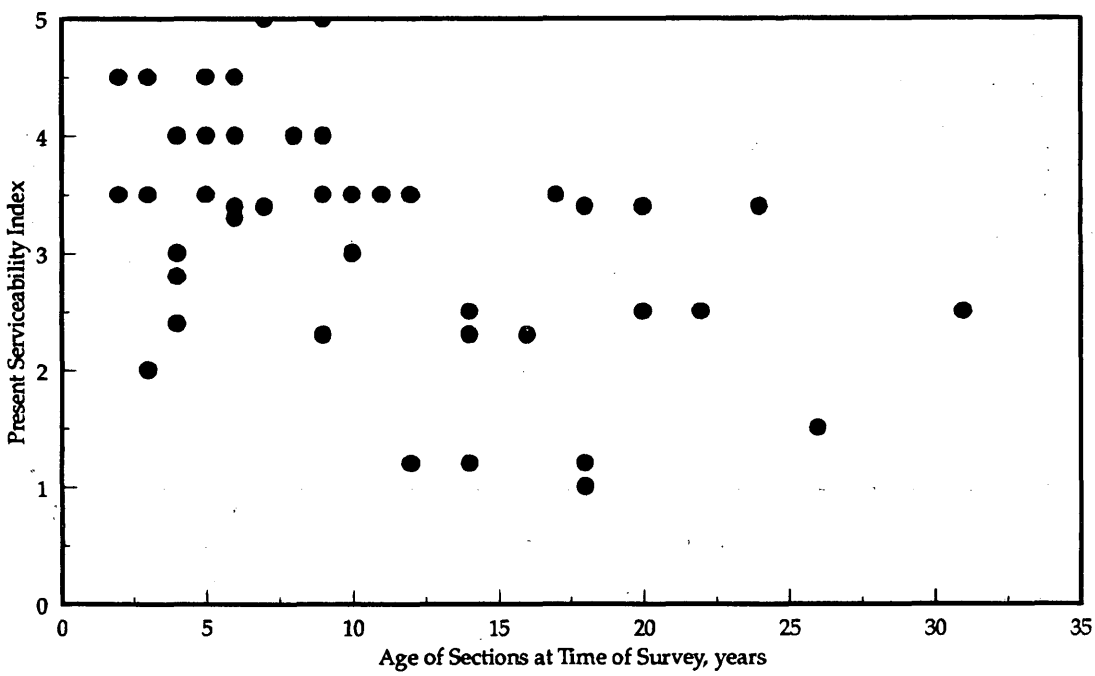

FIGURE 6 PSR versus age for European COPES sections.

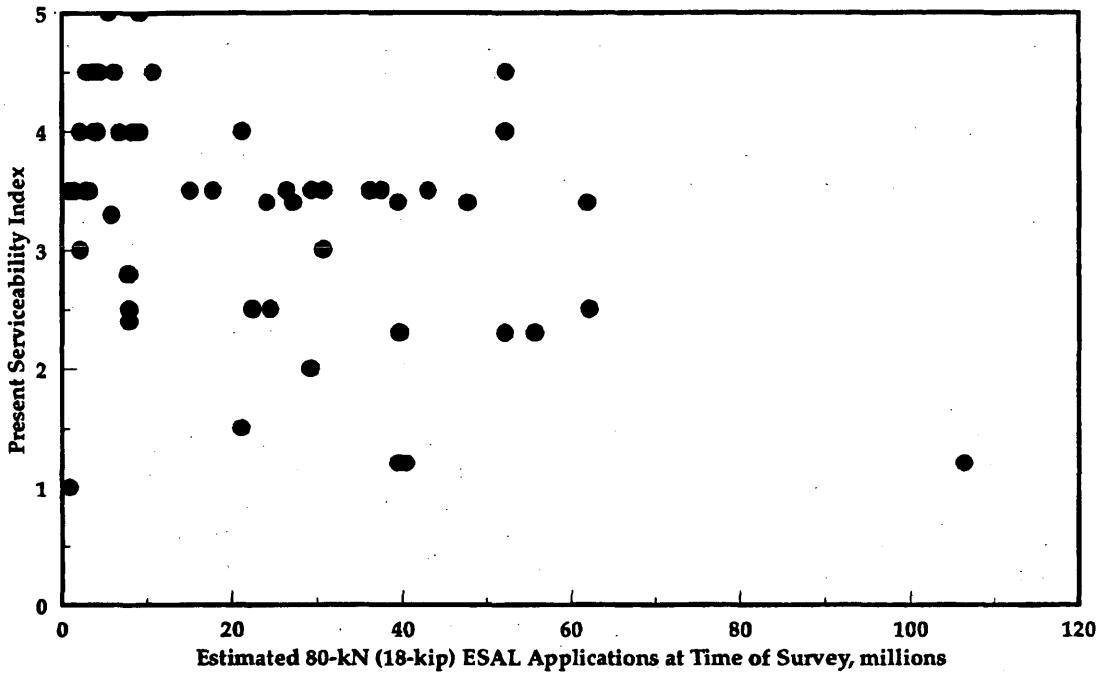

FIGURE 7 PSR versus ESALs for European COPES sections.

- PSR = present serviceability rating,
- AGE = time since construction (in years),
- ESAL = estimated 80-kN (18-kilopounds) ESALs (in millions),
- THICK = PCC slab thickness (in mm),
- DRAIN = dummy variable for drainage design (1 for edgedrains, 0 for none), and
- PTYPE = dummy variable for pavement type (0 for JPCP, 1 for CRCP).

France

The prediction model developed for the French sections is shown in the following equation:

$$PSR = 3.0803 - 0.00043\ AGE^2ESAL^{0.5} + 0.00159\ THICK + 0.4945\ DRAIN \quad (1)$$

$R^2 = 0.75$ $R^2adj = 0.71$ SEE = 0.28 N = 24

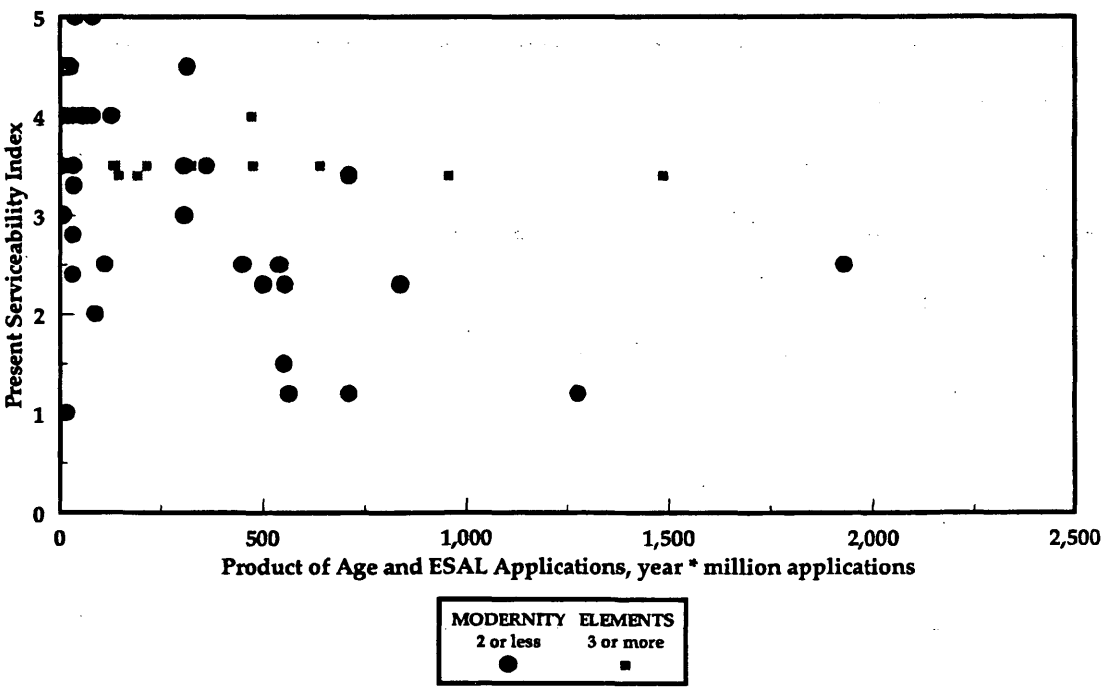

FIGURE 8 PSR versus age*ESALs for European COPES sections.

This model applies only to JPCP without dowel bars and is limited to the range of design features and conditions of the available sections. The model is sensitive to age and ESALs, especially after about 15 years. The use of edgedrains results in a PSR increase of about 0.5 (evident by the coefficient on the drainage variable). The model is not overly sensitive to changes in slab thickness.

United Kingdom

The PSR model for the United Kingdom is only applicable to JPCP sections with longitudinal edge drains and dowel bars. The model is also limited to variables used to develop the equation. The following model was developed:

$$PSR = 4.2561 - 0.0264\,ESAL - 2.460\left(\frac{AGE}{THICK}\right) \quad (2)$$

$R^2 = 0.78$ $R^2adj = 0.74$ $SEE = 0.44$ $N = 13$

The model is more sensitive to ESALs than to age, which indicates that heavy loads damage the pavement more than the environment. Slab thickness is not a significant variable in the model.

Belgium

The Belgian model was developed for both JPCP and CRCP sections and includes a dummy variable to distinguish the pavement type. The following model was developed for Belgium:

$$PSR = 4.1826 - 0.1134\,AGE - 0.00862\,ESAL + 0.00152\,THICK + 0.4763\,PTYPE \quad (3)$$

$R^2 = 0.76$ $R^2adj = 0.71$ $SEE = 0.33$ $N = 25$

Age is the most significant variable in the equation, whereas thickness and ESALs affect the model to a much lesser extent. CRCP sections have performed better than the JPCP sections, which is also evident in the model.

SUMMARY

This paper presents an evaluation of the performance of concrete pavement sections included in the European COPES program. Under this program, several European countries—France, Italy, the United Kingdom, and Belgium—have been collecting performance data on their concrete pavement sections. The overall objective of this program is to obtain feedback information on the behavior and performance of the European concrete pavements so improvements to their design and construction can continually be made. Such improvements may include the identification of particular design features (e.g., dowel bars) or combinations of design features (e.g., dowel bars and positive drainage) that greatly increase the performance capabilities of concrete pavements.

A qualitative analysis was conducted using the PSR, age, and traffic as the principal parameters. The following presents a summary of the observations from the European COPES data and the results of the analysis:

- The most common type of concrete pavement in Europe appears to be JPCP. The JPCP sections made up 80 percent of the European COPES sections.
- Stabilized bases are used extensively in Europe; 80 percent of the sections evaluated have either a stabilized base or an LCB.
- Nearly all European COPES sections are provided with positive drainage. With the exception of those in France, most sections are also provided with dowel bars at transverse joints.
- A much greater proportion of the European sections have two or more modernity elements as compared with the U.S. sections (74 percent for Europe versus 25 percent for United States).
- The European COPES sections are subjected to climatic conditions that are characteristic of a wet-freeze environmental region.
- The European highways are subjected to very high traffic loads. The high design ESALs are a result of the legal heavy-axle loads and long design life (30 to 40 years) that are common in Europe.
- The base type was found to have significant effect on pavement performance. Sections with LCB performed better than those provided with other base types.
- Pavement sections with three modernity elements performed better than those with two or fewer.
- PSR prediction models were developed and were found to accurately predict PSR for the limited number of design variables.

These observations and conclusions were made on the basis of a qualitative analysis conducted on limited data. Further investigations may be needed to verify some of the above findings.

ACKNOWLEDGMENTS

This paper is based on work conducted under FHWA Contract DTFH61–91–C–00053, Performance Evaluation of Experimental Rigid Pavements—Data Collection and Analysis. The authors appreciate the efforts of Jim Sherwood and Roger Larson of FHWA for arranging for the analysis of the European COPES data and in guiding the overall work. In addition, the authors acknowledge the support provided by the Technical Committee on Concrete Roads of PIARC and, in particular, the assistance of J.P. Christory.

REFERENCES

1. Darter, M.I., J.M. Becker, M.B. Snyder, and R.E. Smith. *NCHRP Report No. 277: Portland Cement Concrete Pavement Evaluation System (COPES)*. TRB, National Research Council, Washington, D.C., 1985.
2. Christory, J.P. COPES System, Europe–USA Cooperation. *Proc., 12th World Road Congress*, Vol. 190.7.B, Sept. 22–28, 1991.
3. Carpenter, S.H., M.I. Darter, and B. J. Dempsey. *A Pavement Moisture Accelerated Distress (MAD) Identification System—Volume I.* Report FHWA/RD–81/079. FHWA, U.S. Department of Transportation, Washington, D.C., Sept. 1981.
4. *Special Report 61E: The AASHO Road Test.* HRB, National Research Council, Washington, D.C., 1962.
5. *Report on the 1992 U.S. Tour of European Concrete Highways.* Report FHWA–SA–93–012, FHWA, U.S. Department of Transportation, Washington, D.C., 1993.
6. Carey, W.N., Jr., and P.E. Irick. The Pavement Serviceability-Performance Concept. *Bulletin 250*, HRB, National Research Council, Washington, D.C., 1960.

Publication of this paper sponsored by Committee on Portland Cement Concrete Pavement Construction.

Effect of Optimized Total Aggregate Gradation on Portland Cement Concrete for Wisconsin Pavements

STEVEN M. CRAMER, MICHAEL HALL, AND JAMES PARRY

Most state paving specifications for portland cement concrete pavement allow a broad range of total aggregate gradation for concrete mixes. It has long been debated whether special efforts to control total aggregate gradation provide concrete improvements that justify potential increased costs. The results of an investigation examining the effect of optimizing total aggregate gradation on the properties of concrete used for paving in Wisconsin are reported. The investigation used concepts presented by Shilstone to optimize gradations consisting of carefully selected proportions of locally available aggregate. Unit weight, shrinkage, change in the water-to-cement ratio (w-c) at constant slump, change in slump at a constant w-c ratio, compressive strength, and possible segregation under vibration were measured in field test sections and laboratory mixes. This investigation showed that use of optimized total aggregate gradations instead of near-gap-graded gradations in pavement resulted in an increase in compressive strength of 10 to 20 percent, reduced water demand by up to 15 percent to achieve comparable slump, air contents achieved with 20 to 30 percent reductions in air entraining agent, potentially higher spacing factors in the air void system of hardened concrete, and reduced segregation following extended vibration (1 to 3 min). Not all efforts at gradation optimization in this study yielded measurable improvements in performance and the availability of local aggregates may still limit, to varying degrees, the ability to optimize. However a reasonable effort to optimize gradation can lead to significant mix benefits.

Most state paving specifications for portland cement concrete pavement allow a broad range of total aggregate gradation for concrete mixes. This is consistent with traditional mix design philosophy allowing wide variation in aggregate gradation such that economy can be maintained by allowing naturally occurring aggregates to be used from one locality to the next. The topic of total aggregate gradation has been debated repeatedly, and while acceptable concrete can be made with a range of total aggregate gradations, recent work by Shilstone (*1*) has suggested that concrete performance can be improved by optimizing total aggregate gradation. The use of aggregate classified into two categories as coarse and fine can lead to gradations where intermediate-sized particles are scarce or absent, and this in turn can lead to harsh, unworkable concrete. The research reported here explored the possible benefits of controlling total aggregate gradation for different Wisconsin pavement mixes by monitoring unit weight, shrinkage, change in the water-to-cement ratio (w-c) at constant slump, change in slump at a constant w-c ratio, compressive strength, and possible segregation under vibration. Research was conducted in the laboratory and in field pavement test sections.

S.M. Cramer, University of Wisconsin-Madison, 1415 Johnson Drive, Madison, Wisc. 53706. M. Hall, Wisconsin Concrete Pavement Association, 7609 Elmwood Avenue, Middleton, Wisc. 53562. J. Parry, Wisconsin Department of Transportation, 3502 Kinsman Boulevard, Madison, Wisc. 53704.

It has long been debated whether gap gradings produce better concrete than continuous gradings (*2*). It appears clear that there is no one answer to this question and that application as well as local conditions play roles in providing an answer for each situation (*3*). Other literature concerning the effect of aggregate gradation consists of case studies and anecdotal evidence by experienced concrete practitioners. Such reports include the work by Sehgal (*4*) that described the important linkage between aggregate gradation and concrete performance. Equations for theoretically ideal grading curves are found in a work by Popovics (*3*). Popovics points out that it is unrealistic to expect a single grading curve to be ideal for all concrete properties simultaneously and the expense of complying with a grading specification can increase rapidly as the number of specified details increase.

In this study, an *ideal gradation* is defined as a precise mix of particle sizes that leads to the most workable, durable, and strongest concrete possible from given aggregate sources. In contrast, an *optimized gradation* is defined as one where practical and economic constraints are combined with attempts to obtain and use a mix of aggregate particles sizes that will lead to improved workability, durability, and strength. The subjective nature of the later definition recognizes the give-and-take as well as common sense that must be applied in optimizing aggregate gradations.

The primary motivation for this investigation originated from concepts presented in a work by Shilstone (*1*). Logic and case histories have been presented suggesting that optimizing total aggregate gradation improves mix workability and mix durability and provides a more reliable basis for mix design. The methodology is based on (a) aggregate particle size distribution, (b) a coarseness factor, (c) a workability factor, and (d) a mortar factor. A definite formula for particle-size distribution has not been presented, but it appears that the examples of optimized particle distribution presented hold some similarities to the 0.45 power curve (*5*). The *coarseness factor* (*1*) is defined as the percentage of material larger than the No. 8 sieve retained on or above the 9.5 mm (3/8 in.) sieve. The *workability factor* is the percentage of material passing the No. 8 sieve. The *mortar factor* is the percentage of mortar as defined by the fine aggregate passing the No. 8 sieve plus the paste portion. The coarseness and workability factors are assessed together in a coarseness factor chart presented elsewhere (*1*). This chart reflects the need to balance the fine aggregate portion with larger particles. Too much aggregate passing the No. 8 sieve will lead to a sticky mix with a high water demand. Too little sand will create a harsh mix with other finishing problems. By using Shilstone's method and a third aggregate to achieve a more optimal particle size distribution,

the Colorado Department of Transportation reported a 5 percent reduction in water demand and a 10 percent increase in strength on a bridge deck project (*6*).

FIELD AND LABORATORY INVESTIGATION

The investigation involved both field testing of concrete using two 0.8 km (½ mi) highway test sections and laboratory mixing and testing. Concrete using a gradation that approached a gap-graded condition (near gap-graded) was contrasted with concrete containing an optimized gradation (optimized). All gradations and mix proportions met the requirements of Wisconsin Standard Specifications for Road and Bridge Construction (*7*). The mix proportions used in the field are shown in Table 1. The laboratory mixes contained similar proportions except for the aggregate where a specified gradation was remanufactured from local aggregate.

The near-gap-graded and optimized gradations are shown in Figures 1 and 2. The aggregate sources were the same for each gradation and consisted of a local sand, an AASHTO No. 67 stone and an AASHTO No. 4 stone derived from crushed limestone. For the optimized mix, the sand was reprocessed through a classifier to remove fine material to better achieve the target gradation. This resulted in some waste material and additional handling cost beyond that associated with a more typical gradation. The optimized UW Laboratory gradation was selected to follow the centerline of the project specification. Later these gradations were evaluated according to Shilstone's coarseness factor chart. According to Shilstone (*1*), the most desirable gradations will lie close or within the bands on the chart. As shown in the chart (Figure 3), the optimized laboratory gradation is further from the preferred gradation bands than the near-gap-graded gradations.

Primary measurements of the fresh mixes were slump, air content, unit weight, and aggregate gradations established from fresh concrete mixes. A procedure was developed such that collected samples of fresh concrete were subjected to a washing process where all material larger than the No. 200 sieve was retained. The washed samples were taken to the laboratory where they were oven-

TABLE 1 Mix Proportions

Constituent	Proportions in kg/m³			
	Near-Gap-Graded Field Mix		Optimized Field Mix	
Cement	281		284	
Fly Ash	110		110	
Sand	759	41% of total aggregate	757	40% of total aggregate
AASHTO #67 Stone	471	26%	675	36%
AASHTO #4 Stone	619	33%	457	24%
Free Water	143		122	
AE Agent (ml)	434		302	

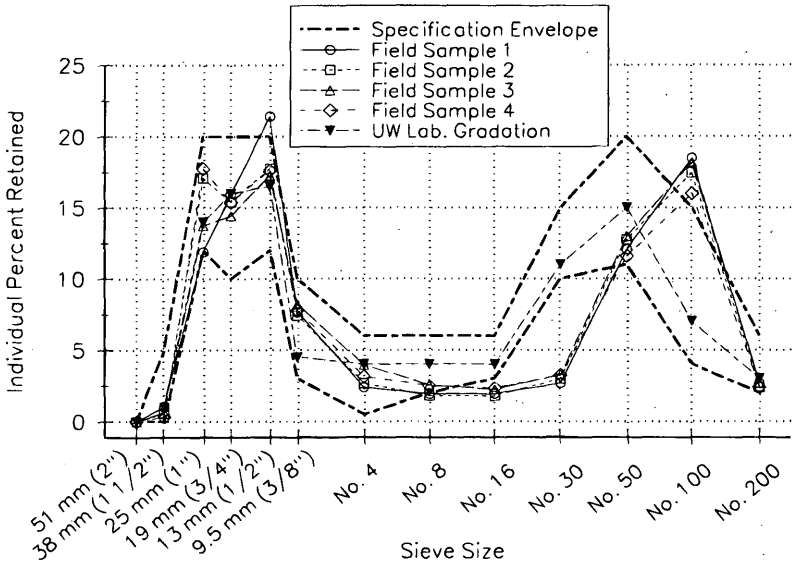

FIGURE 1 Near-gap-graded field and laboratory gradations for pavement mixes.

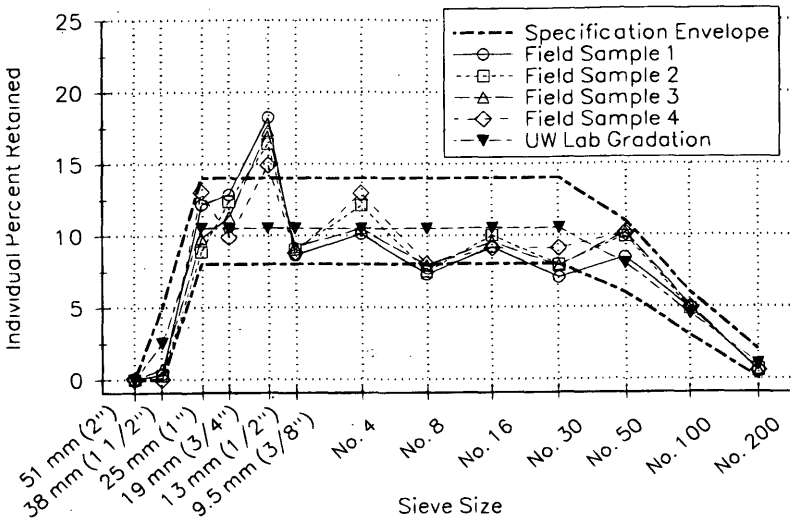

FIGURE 2 Optimized field and laboratory gradations for pavement mixes.

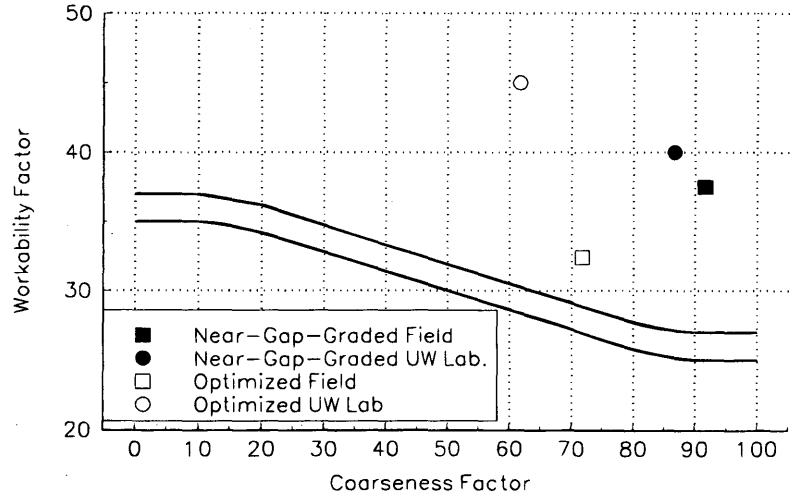

FIGURE 3 Coarseness factor chart for field and laboratory pavement mix gradations.

dried and then subjected to the standard dry sieve analysis. Primary measurements of the hardened mix were compressive strengths at 7 and 28 days, shrinkage, and air-void analysis of cores obtained from the pavement test sections. Test specimens are summarized in Table 2.

Compressive strength results taken at age 28 days are summarized in Table 3. All results were adjusted to a common air content of 6 percent by decreasing strength 1,378 kPa (200 psi) for every percent increase in air content. This adjustment is based on experience with similar paving mixes and is consistent with recommendations (*8*). Strength gains achieved with the optimized mixes ranged from 11 to 22 percent with 95 percent confidence intervals suggesting that the strength gains are statistically meaningful.

Average data resulting from pavement cores are presented in Table 4. These values show that near-gap-graded mixes contained an air-void spacing factor less than the optimized mix, although the near-gap-graded mixes also averaged a slightly lower air content. Generally, a spacing factor of 0.20 mm (0.008 in.) or less indicates sufficient freeze-thaw resistance. The durability characteristics of these mixes must be further analyzed before this finding can be considered significant.

Other collected data suggested that unit weights were no more than 1 percent greater with the optimized mixes. Differences in shrinkage measurements between the two mixes were inconclusive.

Figure 4 shows the average slump and free water content for the mixes. The optimized mixes in the field required an average of 15 percent less water compared with the near-gap-graded mixes in achieving comparable slumps. The same water reduction was not realized in the laboratory mixes, but it can be reasoned that the higher-than-optimal fine particle content (see Figure 3) is the rea-

TABLE 2 Test Specimens Made at Each Test Site for the Pavement Investigation

Mix Site	US Hwy 51 Field Site		Univ. of Wisc. Materials Laboratory		
Mix Type	Near Gap-Graded	Optimized Constant Slump	Near-Gap-Graded	Optimized Constant Slump	Optimized Constant Water
No. of Batches Sampled	4	4	2	2	2
No. of Strength Cylinders	24	24	12	12	12
No. of Shrinkage Prisms	4	4	3	3	3
No. of Core Samples	4	12	NA	NA	NA

TABLE 3 28-Day Cylinder Compression Summary

Mix Type	Location	Air Content, Percent	28 Day Compr. Strength, kPa	95 Percent Confidence Interval, kPa	Optimized/Near-Gap-Graded, Percent
Near-Gap-Graded	Field	6.0	26,300	2,140	NA
Optimized	Field	6.0	29,900	965	114
Near-Gap-Graded	UW Lab	6.0	23,000	1,100	NA
Optimized/ Constant Slump	UW Lab	6.0	28,200	895	122
Optimized / Constant Water	UW Lab	6.0	25,600	1,860	111

TABLE 4 Core Air Void Analysis

Core Identification	Air Content %	Spacing Factor mm	Apparent Specific Gravity	Volume of Permeable Voids %
Near-Gap-Graded Section				
Core 1	6.5	0.15	2.54	12.3
Core 2	5.1	0.18	2.53	13.1
Core 3	6.1	0.15	2.53	12.5
Core 4	6.7	0.18	2.55	12.6
Average of 4 Cores	6.1	0.17	2.54	12.6
Optimized Section				
Core 1	5.8	0.25	2.49	12.6
Core 2	7.1	0.13	2.57	12.5
Core 3	4.9	0.28	2.60	12.3
Core 4	4.7	0.28	2.62	12.8
Average of 4 Cores	5.6	0.23	2.57	12.6

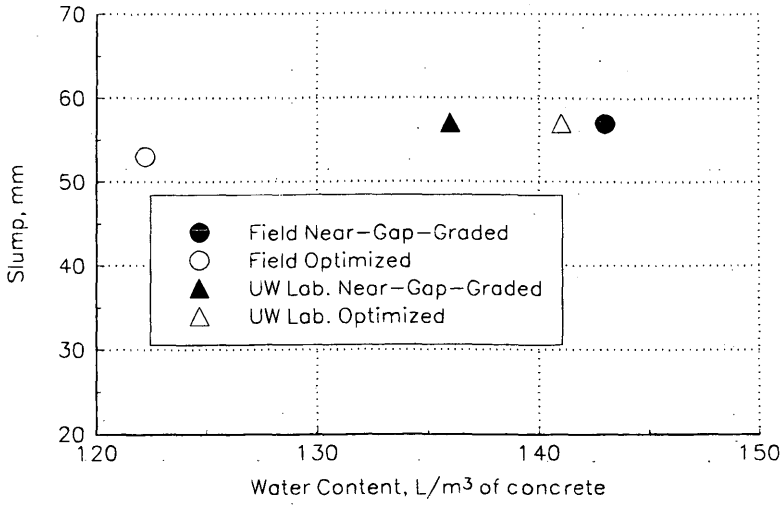

FIGURE 4 Average slump and free water content/m³ of concrete for all mixes.

son for the higher water demand. In addition, 30 percent less air entraining agent was needed to entrain the same amount of air in the field optimized mix (Figure 5), but as indicated in Table 4 an increase in the spacing factor was subsequently observed in the air-void analysis. For the laboratory optimized mix, 20 percent less air entraining agent was needed.

PARTICLE SIZE REDISTRIBUTION UNDER VIBRATION

The redistribution of particle sizes following vibration was studied by establishing the gradation of individual layers of a larger volume of concrete. A test cylinder consisting of a 560-mm (22-in.) section of a PVC pipe 390 mm (15¼ in.) in diameter was fabricated. The test pipe could separate into four layers. A total volume of approximately 0.05 m³ (1.7 ft³) was placed in the test device, with each of the four layers rodded 50 times. A field vibrator was placed in a fixed position in the middle of the test pipe and allowed to vibrate at 10,000 vibrations per minute for a specified time. Both the UW laboratory near-gap-graded mix and the laboratory optimized mix were subject to 20 sec, 1 min, and 3 min of vibration. The washing method described earlier was used for each layer leading to a dry sieve analysis. For 20 sec and 1 min of vibration, each mix retained approximately the same particle distribution in all four layers of the test pipe. At 3 min of vibration, the near-gap-graded mix underwent large redistribution (segregation) of particle sizes while the optimized gradation tended to retain its original distribution in all four layers. The resulting particle distributions from the 3 min tests are shown in Figures 6 and 7.

OTHER EXPERIENCE WITH OPTIMIZING TOTAL AGGREGATE GRADATION

A bridge deck project was also used to explore the effect of total aggregate gradation before the investigation with the paving mixes. As in the pavement study, field test sections and laboratory test

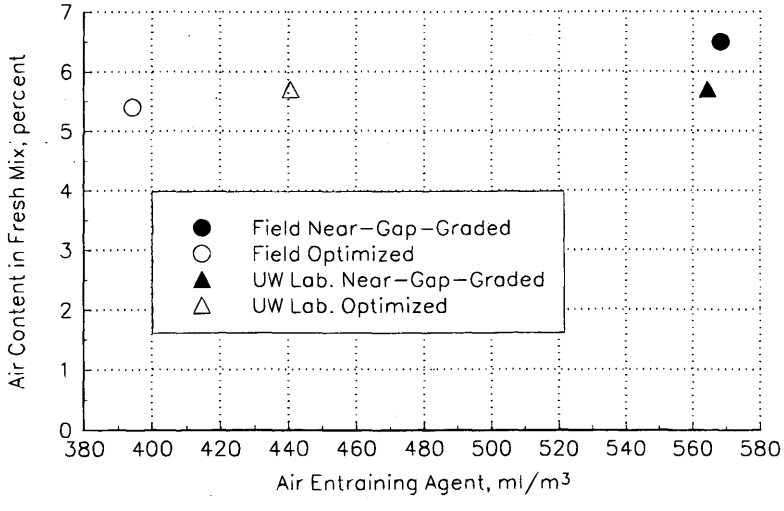

FIGURE 5 Average air content and amount of air entrainment for all mixes.

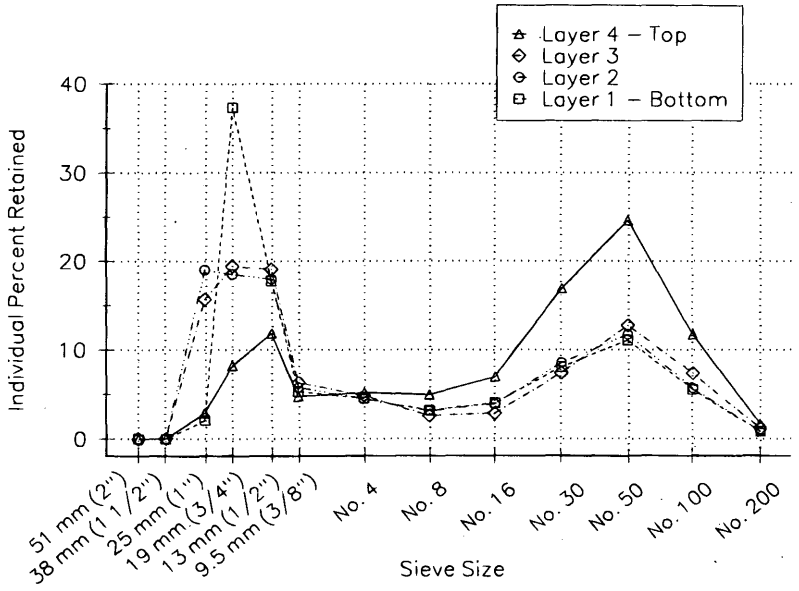

FIGURE 6 Particle redistribution in laboratory near-gap-graded mix subject to 3 min vibration.

mixes were investigated using locally available aggregates. The near-gap-graded and slightly optimized gradations that could be achieved with local aggregates were not as distinctive as in the pavement investigation. Figure 8 shows the near-gap-graded and slightly optimized gradations used in the field portion of the bridge deck project. Laboratory gradations were only slightly more distinctive than those used in the field. In designing these gradations, the coarseness factor chart was ignored and subsequent computation suggested that the slightly optimized mix did not represent an improvement over the near-gap-graded mix.

The results obtained from the bridge deck investigation were not as conclusive as in the pavement study described earlier. In the field and the laboratory, the slightly optimized mixes again required less water than the near-gap-graded mixes to achieve similar slump, but these water reductions were not as large as in the pavement study and ranged from 1 to 7 percent. Strength comparisons ranged from a 13 percent increase in strength in laboratory work to a 6 percent decrease in strength in the field work when the slightly optimized mix was compared with a near-gap-graded mix. Shrinkage and unit weight measurements again showed no difference between the two gradations.

The bridge deck investigation provided several cautionary footnotes to the favorable findings observed in the pavement study. First, available aggregates and economics may limit the optimization that can reasonably be obtained in many projects. Second, minor attempts to mitigate a near-gap-graded gradation by simply

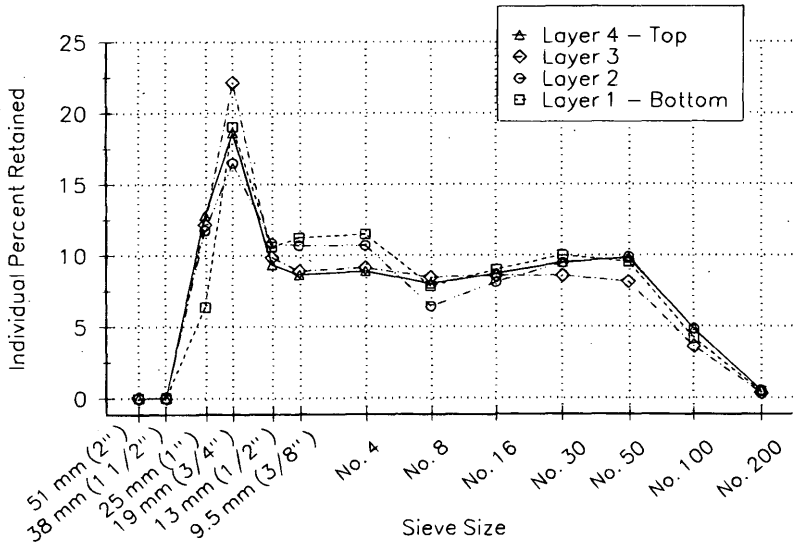

FIGURE 7 Particle redistribution in laboratory optimized mix subject to 3 min vibration.

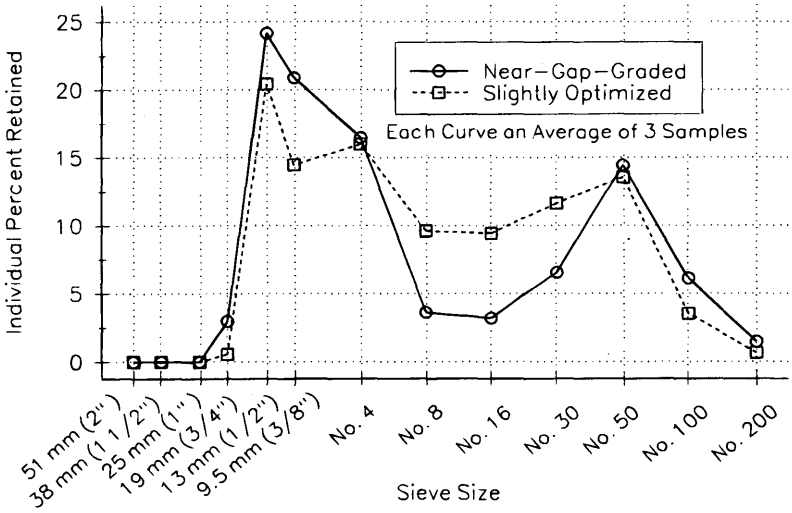

FIGURE 8 Near-gap-graded and slightly optimized bridge deck mix field gradations.

adding some intermediate-sized particles that are scarce do not guarantee an identifiable improvement in concrete strength or workability. Attention to the concept of the coarseness factor chart appears to hold some importance besides simply filling in scarce intermediate-sized particles.

SUMMARY AND CONCLUSIONS

This pilot study examined the differences in portland cement concrete performance for pavement mixes containing near-gap-graded total aggregate gradations and those using an optimized total aggregate gradation. Optimized gradations were established on the basis of a methodology (*1*) by which a continuous particle-size distribution was achieved. Field and laboratory investigations were directed toward evaluating unit weight, shrinkage, change in the w-c ratio at constant slump, change in slump at a constant w-c ratio, compressive strength, and possible segregation under vibration.

This investigation showed that use of optimized total aggregate gradations in place of near-gap-graded gradations in pavement resulted in

- An increase in compressive strength of 10 to 20 percent,
- Reduced water demand by up to 15 percent to achieve comparable slump,
- Air contents achieved with 20 to 30 percent reductions in air entraining agent,
- Potentially higher spacing factors in the air-void system of hardened concrete, and
- Reduced segregation following extended vibration (1 to 3 min).

Not all efforts at gradation optimization guarantee measurable improvements in performance, and the availability of local aggregates may still limit to varying degrees the ability to optimize. Further investigation into the effect of total aggregate gradation on durability is planned and is needed before widespread use of total gradation optimization will be considered in Wisconsin. This study suggests, however, that reasonable effort to optimize gradation can lead to significant mix benefits.

ACKNOWLEDGMENTS

The authors acknowledge the sponsorship of this research by the Wisconsin Department of Transportation. The contributions of Paul Bakke of the University of Wisconsin are appreciated. American Petrographic Services, Inc., assisted in the air-void analysis of the core samples.

REFERENCES

1. Shilstone, J.M. Sr. Concrete Mixture Optimization. *Concrete International*, June 1990, pp. 33–39.
2. Li, S.T. Selected Bibliography on Gap Grading and Gap-Graded Concrete. *ACI Journal, Proc., Vol. 67. No. 7*, 1970.
3. Popovics S. *Concrete Materials*, 2nd ed., Noyes Publications, 1992.
4. Seghal, J.P. Good Concrete Does Not Just Happen. *Concrete*, Vol. 47, No. 10, Feb. 1984, pp. 30–36.
5. Fuller W.B., and S.E. Thompson. The Laws of Proportioning Concrete. *Transactions*, Vol. 59, ASCE, 1907, pp. 67–143.
6. Doing More with Less: Optimizing Concrete Mix. *Better Roads*, Vol. 60, No. 8, Aug. 1990, pp. 18–25.
7. *State of Wisconsin Standard Specifications for Road and Bridge Construction*, 1989 ed. Wisconsin Department of Transportation, 1989.
8. Kosmatka S., and W. Panarese. *Design and Control of Concrete Mixtures*, 13th ed., Portland Cement Association, 1988, pp 205.

Publication of this paper sponsored by Committee on Portland Cement Concrete Pavement Construction.